Brassica carinata MEAL ISSUED FROM AVIATION FUEL PRODUCTION, A RENEWABLE RESOURCE OF VALUABLE CHEMICALS

By

VINH PHUC THINH NGUYEN

A DISSERTATION PRESENTED TO THE GRADUATE SCHOOL
OF THE UNIVERSITY OF FLORIDA IN PARTIAL FULFILLMENT
OF THE REQUIREMENTS FOR THE DEGREE OF
DOCTOR OF PHILOSOPHY

UNIVERSITY OF FLORIDA

2021

“To my beloved wife Camille and our family”

ACKNOWLEDGMENTS

First and foremost, I would like to acknowledge my advisors Dr. Jon Stewart and Dr. Florent Allais for their guidance. I am grateful for the given opportunity to do research in both countries USA and France. It was such a pleasure to work on research projects which I enjoyed doing in the labs. I would like to acknowledge the opportunity given by Dr. Stewart to work with the SPARC project. I would like to acknowledge the opportunity given by Dr. Allais to be co-chairing the inaugural Gordon Research Seminar, which was such a great experience to get involved in the international scientific community. I would like to acknowledge the University of Florida and AgroParisTech. I would like to acknowledge all of the members of the SPARC project. I would like to acknowledge the USDA-NIFA (award number 2016-11231) for funding this research project and the Fondation Paris-Reims and the Department of Chemistry (University of Florida) for funding this joint Ph.D. program.

I would like to acknowledge my UF committee members Dr. Nicole Horenstein, Dr. Stephen Miller, Dr. Steven Bruner, Dr. Robert McKenna, Dr. Nicolas DiLorenzo; and, my AgroParisTech committee members Dr. Arnaud Haudrechy (Univ Reims), Dr. Richard Daniellou (Univ Orleans), Dr. Florian Seebeck (Univ Basel).

I would like to acknowledge all of the current and former members of the Stewart's crew Dr. Sarah Beaudoin, Dr. Huynjun Choe, Dr. Louis Mouterde, Richard Watkins, Ahram Kim, Jarrad Padza, Rukshana Uddin, and Minsun Cha for their support throughout my stay at UF. I really enjoyed the time that we have spent in the lab, as well as outside the lab.

I would like to acknowledge all of the current and former members of URD ABI. I am thankful to Dr. Irina Ioannou for her guidance and her help on the recovery of

secondary metabolite project. I would like to thank Nour Zaiter, Dr. Amandine Flourat and Dr. Sami Fadlallah for carrying out the DMNA project during my absence. I would like to acknowledge the URD ABI analytical team. I would like to acknowledge Dr. Louis Mouterde for his help during my stay. I would like to acknowledge all PhD students who shared the office with me, especially now Dr. Florian Diot-Néant for his enthusiastic aid.

I would like to thank the limitless support from my parents, my brother and his family, without whom I cannot get myself to this point. I would like to dedicate all of this work to my dad, who passed away while I was abroad for my study. Finally, I would like to thank my wife Camille for her love and pronounced encouragement during this journey.

TABLE OF CONTENTS

page

LIST OF TABLES

LIST OF FIGURES

LIST OF ABBREVIATIONS

%EtOH	Ethanol concentration in mixture ethanol/MilliQ-water
2FG	2-Deoxy-2-fluoroglucosinolate
4CL	4-Coumaroyl CoA-ligase
AE	Aqueous ethanol
$AgNO_3$	Silver (I) nitrate
ANOVA	Analysis of variance
AOAC	The Association of Official Analytical Chemists
Arg	Arginine
ASE	Accelerated solvent extraction
Asx	Asparagine/Aspartate
ATP	Adenosine triphosphate
BCAT	Branched-chain amino acid aminotransferase
Btu	British thermal units
C4H	Cinnamate 4-hydroxylase
Ca	Calcium
CCR	Cinnamoyl-CoA reductase
CMOT	Caffeic acid *O*-methyltransferase
CoA	Coenzyme A
CRU	Cruciferin
Cu(I)	Copper (I)
CYP	Cytochrome-P450 dependent monooxygenase
Cys	Cysteine
Da	Dalton
DAHP	3-Deoxy-D-heptulosonate 7-phosphate

DBM	Diamondback moth
desGSL	Desulfated glucosinolates
DHQ	3-Dehydroquinate
DM	Dry matter
DMNA	6-Hydroxy-5,7-dimethoxy-2-naphthoic acid
DNA	Deoxyribonucleic acid
$DPPH^{\bullet}$	2,2-Diphenyl-1-picrylhydrazyl radical
DTT	Dithiothreitol
EAI	Emulsifying activity index
EDTA	Ethylenediaminetetraacetic acid
EI	Extractability index
EPSP	5-Enolpyruvylshikimate 3-phosphate
ER	Endoplasmic Reticulum
ES	Emulsifying stability
EtOH	Ethanol
F5H	Ferulate 5-hydroxylase
FA	Foaming activity
FAO	The Food and Agriculture Organization of the United Nations
FDA	The Food and Drug Administration
$FeCl_3$	Iron (III) chloride
FGE	Formylglycine generating enzyme
fGly	Formylglycine
FS	Foaming stability
gDM	Gram of dry matter
GSH	Glutathione

GSL	Glucosinolates
GSS	Glucosinolate sulfatase
Glx	Glutamine/Glutamate
Gly	Glycine
HCl	Hydrochloric acid
HCT	*p*-Hydrocinnamoyltransferase
HPLC	High-performance liquid chromatography
HSCCC	High speed counter-current chromatography
IEA	The International Energy Agency
IPMP	Isopropylmalate isomerase
IPM-DH	Isopropylmalatedehydrogenase
IPTG	Isopropyl β-D-1-thiogalactopyranoside
IR	Infra-red
ITC	Isothiocyanates
KOH	Potassium hydroxide
LB	Lysogeny Broth
Leu	Leucine
LTP	Lipid transfer proteins
Lys	Lysine
MALDI	Matrix-assisted laser desorption/ionization
MAM	Methylthioalkylmalate synthase
MIO	3,5-Dihydro-5-methyldiene-4H-imidazol-4-one
MS	Mass spectrometry
MS-MS	Tandem mass spectrometry
MW	Molecular weight

MYR	Myrosinase
NADP	Nicotinamide adenine dinucleotide phosphate
NADPH	Reduced nicotinamide adenine dinucleotide phosphate
NaOH	Sodium hydroxide
NAP	Napin
NMR	Nuclear magnetic resonance
OG	Protecting group
ONU	The United Nations
PAL	Phenylalanine ammonia lyase
PC	Phenolic compounds
PDB	The Protein Data Bank
PEP	Phosphoenolpyruvate
Phe	Phenylalanine
ppm	parts per million
Pro	Proline
QTL	Quantitative trait locus
REF1	Reduced epidermal fluorescence 1 aldehyde dehydrogenase
rpm	Round per minute
RSM	Response surface methodology
S-GT	*S*-glucosyltransferases
Sc-CO_2	Supercritical carbon dioxide
SDS	Sodium dodecyl sulfate
SDS-PAGE	Sodium dodecyl sulfate - polyacrylate gel electrophorese
Ser	Serine
SinA	Sinapic acid

SinE	Sinapoyl esters
SinG	Sinapoyl glucose
SinM	Sinapoyl malate
SinP	Sinapine
SMT	Sinapoylglucose:malate sinapoyltransferase
SPARC	The Southeast Partnership for Advanced Renewables from Carinata
TA	Thomasidioic acid
T_e	Extraction temperature
TFA	Trifluoroacetic acid
Thr	Threonine
ToF	Time of flight
Trp	Tryptophan
UHPLC	Ultra-performance liquid chromatography
USDA	The United States Department of Agriculture
US	The United States of America
UV	Ultraviolet
WHO	The World Health Organization
Wo	Weight to molar quantity

Abstract of Dissertation Presented to the Graduate School
of the University of Florida in Partial Fulfillment of the
Requirements for the Degree of Doctor of Philosophy

BRASSICA CARINATA MEAL ISSUED FROM AVIATION FUEL PRODUCTION, A RENEWABLE RESOURCE OF VALUABLE CHEMICALS

By

Vinh Phuc Thinh Nguyen

August 2021

Chair: Jon D. Stewart
Major: Chemistry

Brassica carinata is cultivated in the Southeast of the United States as a winter crop for aviation fuel and other valuable co-products. The proteins extracted from the *B. carinata* meal (referred as Carinata meal) are not yet considered nutritionally safe due to their high content of glucosinolates and erucic acid. Furthermore, the presence of additional antinutrients and other metabolites reduces the usability of these valuable proteins for which applications might otherwise be found in the food industry thanks to their functional properties. The removal of these secondary metabolites prior to protein extraction is, therefore, required in order to allow a full valorization of the latter. Secondary metabolites in Carinata meal are particularly of interest as bioactive reagents thanks to their biological activities. Taken together, a potential valorization of proteins and secondary metabolites will enhance the added value of Carinata meal.

In this dissertation, information related to structure, composition, and natural occurrence of *Brassica carinata* proteins will be first discussed along with the current extraction and purification methods. Next, the natural occurrence, biosynthesis, accessibility of main secondary metabolites will be reviewed. Literature evidence related

to biological activities of these secondary metabolites will also be discussed in order to confirm the potential use of these molecules.

The sustainable recovery of secondary metabolites from *Brassica* agro-industrial products often involves the use of high concentrations of ethanol and/or high temperatures. Therefore, the effects of an optimized extraction process using aqueous ethanol as the extraction solvent were studied and are reported in this document. The outcomes resulted in an optimal protein extraction process from Carinata meal with minimized effects on protein extractability and functional properties.

Phenolic compounds are of particular particularly thanks to their functionalizable structures. In order to further valorize these valuable biobased compounds, chemical modifications are often required. Such transformations can give access to a novel family of high-value biobased monomers.

Upon tissue damages, toxic breakdown products of glucosinolates are released by myrosinase-mediated hydrolysis. In order to reduce the toxicity of these secondary metabolites in Carinata meal, a biochemical approach by mimicking the feeding pattern of a *Brassica* specialist will be established.

CHAPTER 1
INTRODUCTION TO *Brassica carinata*

Background

The production of energy has continually grown to meet increasing global demand due to population growth. The International Energy Agency (IEA) reported that global energy demand increased by 0.9% in 2019 to 120 million tons of oil equivalent.[1] In recent years, interest in energy production from renewable sources has increased significantly, with a global growth of 3.7% in 2019. In the same year, renewable energy made up to 11% of primary energy consumed in the United States, which is equivalent to 2.25 billion barrels of petroleum, or 500 million tons of coal.[2] Energy from biomass, which makes up 43% of the total energy consumed in the U.S. from renewable sources (Figure 1-1), is counted among low-carbon energy sources.[1,2] Renewable energy from biomass has been mainly produced from oilseeds by pyrolysis.[3] The most popular oilseeds include soybean, palm, rape, and sunflower. Rapeseed crops are popular as its oil is easily and cheaply available on the international market.[4] Compared to palm, rapeseed crops are more advantageous for being seasonal crops. According to a report of United States Department of Agriculture (USDA) in December 2019, rapeseed is the third most abundant oil, and over 27 million metric tons have been produced worldwide in 2019, just behind palm and soybean (Figure 1-2).[5] Taken together, rapeseed has increasingly drawn attention as a profitable oilseed crop.

The Southeast Partnership for Advanced Renewables from Carinata (SPARC) promotes the cultivation of *Brasssica carinata*, a close relative of rapeseed, as a non-food, winter oilseed crop in the Southeast United States of America.[6] These plantations will be economically and ecologically beneficial for local farmers, as cultivating *B.*

carinata preserves local ecosystems by improving the conservation of the soil nutrient and moisture during winter seasons.[7] While the main purpose of these cultivation is geared toward renewable bio-fuel production, the residual meal has been demonstrated to be suitable for cattle feeding.[8] Additionally, bio-product and co-product feedstock will enhance value across the supply chain.

***Brassica carinata*, a Valuable Oilseed Crop**

Historically cultivated in Ethiopian highlands and adjoining areas of East Africa and Mediterranean regions, *Brassica carinata*—Ethiopian mustard or Abyssinian mustard—is an oilseed crop with high content in oil (up to 48% of seed weight). Naturally occurring *B. carinata* is a genetic hybrid between *B. nigra* and *B. olearacea*.[9]

First consumed as food by Ethiopians, *B. carinata* has recently become a feedstock for biofuel production.[10] Rich in erucic acid (which makes up > 40% of total oil content) and containing a low content of saturated fatty acids (< 7%), the oil fraction of *B. carinata* is desirable for aviation bio-fuel production thanks to its attractive oil profile (higher molecular weight than other seed oils; a higher relative concentration of very long chain fatty acid versus long chain and saturated fatty acids, which requires minimal processing during the refining.[7,11]

Compared to other mustard species, *B. carinata* is a potential candidate for dedicated biofuel production in warmer regions thanks to its high seed yield, high oil content, heat resistance, and low seed shattering yield.[12] *B. carinata* seeds harvested across the Southeast U.S in 2015-2017 season showed high seed yield with high oil content, and up to 3161 kg/ha and 47.8% of seed weight, respectively, have been documented.[12] The oil quality was determined to be high in erucic acid, making up to 42.9% of seed oil fraction. Moreover, the cultivation of *B. carinata* as a winter crop has

proven to be economically profitable while providing ecosystem services by bringing under-utilized fallow land under cultivation.[12]

Whereas the main purpose of *B. carinata* cultivation is to provide raw materials for biofuel production, the residual meal contains a high protein content that has been approved as a cattle feed supplement.[7] The nutritional information for *B. carinata* protein from meal remaining after biofuel and bio-oil production was reported by Xin and Yu.[13] These authors also confirmed the viability of using *B. carinata* as a high-protein supplement source for cattle feeding. These conclusions were in agreement with the observation reported by Schulmeister and co-workers who fed beef cattle with *B. carinata* meal as a daily protein supplement.[8] Based on the performance among different selected meals, the authors suggested that *B. carinata* meal is a potential alternative to commonly used protein supplements like cottonseed and soybean meals.

Canola—*Brassica napus*—has been designated by the Food and Drug Administration (FDA) to be safe for human consumption.[14] In addition, canola meal proteins are balanced in all essential amino acids, with a better amino acid profile than soybean protein.[15] Canola proteins are also less lipidemic and atherogenic than casein by comparing the lysine/arginine ratio, a determinant of the cholesterolaemic and atherogenic effects, in both protein isolates. *B. carinata*, as a close relative to *B. napus*, is expected to deliver similar nutritional performance than that of its relative. Protein isolate from *B. carinata* meal also exhibits desirable functional properties for the food industry, such as foaming and emulsifying.[16] Taken together, existing data indicates that *B. carinata* proteins are well-suited to human consumption, either as a protein supplement or as a food additive.

Secondary metabolites present in *B. carinata* meal include phenolic compounds (PCs), mainly tannins and sinapine, glucosinolates (GSLs), and phytic acid. Negative effects of these metabolites on canola proteins are often mentioned.[17–19] For example, with its six phosphate groups and twelve dissociable protons, phytic acid behaves as a precipitating agent.[18] Phytic acid is also considered to be an antinutrient due to its ability to bind essential dietary minerals, thereby reducing their bioavailability. PCs are present in *B. carinata*, along with condensed tannins, in both the free and esterified forms with sinapic acid (SinA). Deteriorated functional performance has been observed when phenolic compounds are bound to canola protein gel.[20] Additionally, PCs are believed to contribute to the dark color and astringent taste of the protein isolate solution.[21] GSLs are a family of sulfur-containing molecules and over 130 different GSL structures have been discovered to date.[22] The pungent, mustardy flavor and odor of *B. carinata* is related to degraded metabolites from hydrolysis of GSLs.[21] When high concentrations are consumed, these degraded metabolites are deleterious to animal health.[23] The structures of common secondary metabolites present in *B. carinata* meal are shown in Figure 1-3.

Despite the aforementioned antinutritional effects, these secondary metabolites display interesting characteristics, which might allow them to be transformed into value-added products for non-food applications. For example, phytic acid is beneficial for cancer prevention.[24–26] Furthermore, the effects of phytic acid on multiple common pathological conditions such as Alzheimers, diabetes, and high cholesterol have been documented.[27] PCs, on the other hand, exhibit strong antioxidant properties.[28,29] In addition, cardio-protective, anti-cancer, anti-diabetic, and anti-aging effects have been

documented, as well as many other beneficial biological activities of these metabolites.[30] Although intact GSLs are biologically inactive, their breakdown products possess therapeutic activities including anti-cancer[31] and anti-bacterial[32,33].

Dissertation Overview

We believe that cultivating *B. carinata* can be profitable in the southeastern US thanks to its high oil content and suitable quality, which makes *B. carinata* oil an ideal feedstock for bio-fuel production. Residual meal issued from bio-fuel production, on the other hand, could be used as a protein supplement for beef cattle feed and secondary metabolites such as GSLs and PCs could be employed for downstream applications in the pharmaceutical and cosmetic industries.

In order to provide sufficient knowledge of the main compounds in *B. carinata* meal, the next three chapters will sequentially focus on seed storage proteins, PCs, and GSLs. In Chapter 2, the origin, structural information, and applications of seed storage proteins in *B. carinata* are discussed along with other minor proteins such as oleosin and trypsin inhibitor peptides. The innate occurrence, biosynthesis, accessibility via chemical synthesis or biomass extraction, and biological activities of sinapic acid and its derivatives, and glucosinolates will be discussed in Chapters 3 and Chapter 4. As the recovery of secondary metabolites from agro-industrial wastes have nowadays drawn more attention, the effects of optimal aqueous ethanol extraction will be discussed in Chapter 5. Chapters 6 and 7 will focus on the valorization of PC, more specifically a sinapic acid-derived phenolic acids as a novel biobased monomer; and development of GSL detoxification methodology employing enzymes, respectively. Chapter 8 summarizes the information described throughout this document and discusses potential future work in this area.

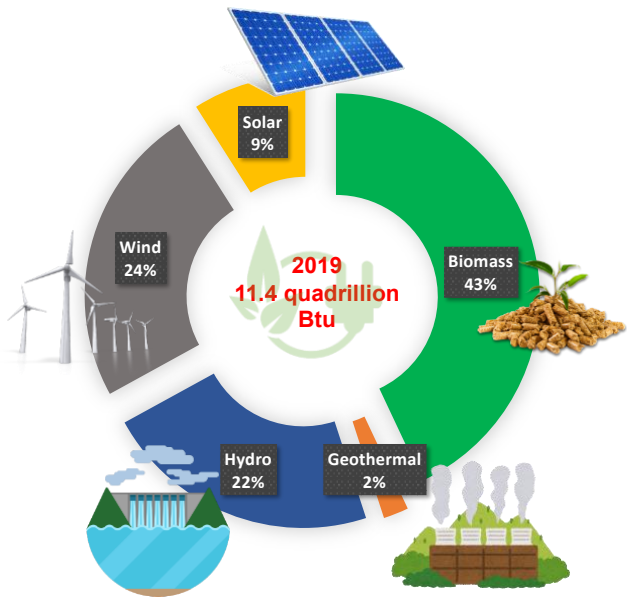

Figure 1-1. Distribution of U.S. domestic consumption of renewable energy in 2019. Btu = British thermal units.

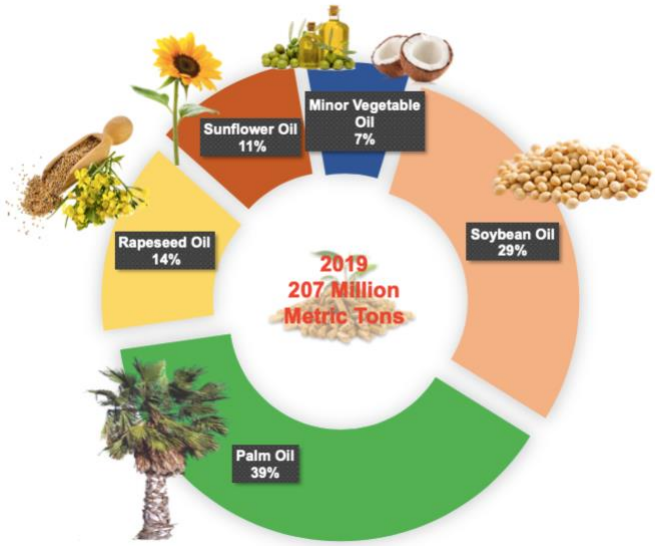

Figure 1-2. Distribution of worldwide production of vegetable oil reported by USDA in December 2019.

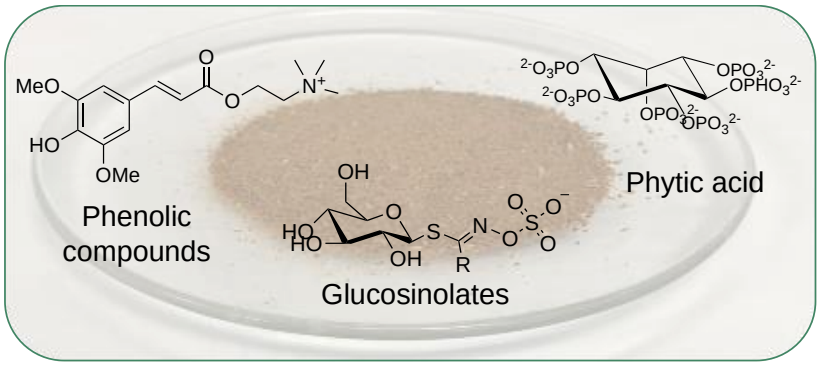

Figure 1-3. Structures of common secondary metabolites presented in *B. carinata* meal.

CHAPTER 2
PROTEINS IN *Brassica*

Introduction

The *B. carinata* meal residue from oil extraction contains a number of valuable co-products including proteins, phytic acid, PCs, and GSLs. Among these co-products, proteins make up over 40% of the biomass[a].[7,12] The functional properties of these plant based proteins are of interest to the food industry thanks to their excellent emulsifying, liquid retention, and foam stabilization abilities.[18]

The defatted *B. carinata* meal also constitutes an important protein source, which is considered well-balanced for human nutrition.[15,18,34] According to the study reported by Pedroche et al., proteins make up to 38.9% of *B. carinata* defatted meal derived from hexane extraction.[16] The amino acid composition of *B. carinata* isolates was also determined by the authors. The sulfur-containing amino acid amount in the protein isolate is approximately 2.9 g / 100 g of protein, which exceeds the daily requirement for children and adults proposed by the FAO.[35] Moreover, this sulfur content in *B. carinata* proteins is comparable to that of soybean proteins and casein.[15] The content of other essential amino acid such as leucine, isoleucine, and valine in *B. carinata* meal also exceeds the recommendation of the FAO. Although the lysine content was reduced during alkaline extraction, protein isolates generated under these conditions contained of up to 4.5 g of Lysine / 100 g protein, which approaches the required value of 5.8 g / 100 g protein recommended by the FAO.[34] Taken together, it is reasonable to suggest that *Brassica* proteins are potential protein supplements for human nutrition.

[a] The protein content was calculated based on nitrogen content determined by Kjeldahl method and multiplied by a predefined factor (×6.25)

The nutritional value of *B. carinata* proteins is clearly comparable to that of casein, and even better than other plant proteins such as soy, sunflower, pea and wheat proteins, as stated Pedroche et al.[16] *B. carinata* proteins and *Brassica* proteins are, therefore, potential plant based proteins to replace animal proteins in daily diets.[18,34]

This chapter presents an overview of these valuable seed storage proteins with regard to their structures, current isolation and purification strategies, and biological activities. Other minor proteins found in the meal are also of interest. Oleosins, lipid body associated proteins, exhibit excellent emulsifying and micellar stabilization properties.[36] Peptides belonging to the napin (NAP) family in defatted canola meal act as potential inhibitors against angiotensin I-converting enzymes, one of the major causative factors of cardiovascular disease.[37] For this reason, minor seed proteins in *Brassica* will also be discussed in this chapter.

Major Seed Proteins in *Brassica*

Seed storage proteins in *B. carinata* are mainly composed of cruciferin (CRU) and napin (NAP). Both of these proteins are biosynthesized during the expansion phase of embryo development of the plant and are stockpiled within the mature seed.[38] These major seed proteins are used for long-term storage of amino acids and are mobilized as carbon and nitrogen sources during seed growth. The amino acid composition of mature CRU and NAP dictates their potential end uses.[39] For instance, meal with low content of Lys, Thr, and Trp would not be suitable as feed for monogastric animals. It is therefore important to understand the structural information, the composition and the maturation of CRU and NAP to achieve a better understanding of these proteins in seeds, which is critical for their downstream applications.

Structural Information, Composition and Maturation

Cruciferin

Cruciferin makes up approximately 60% of total protein in mature seed.[18] Based on the overall structure of proCRU from *B. napus*, the native structure of 12S seed protein CRU exhibits the most structural similarity to 11S soy glycinin.[40] ProCRU is a hexamer, which is formed from two non-covalently linked trimer units. Each trimer is composed of three protomers linked by disulfide bridges. The primary structure of these protomers ranges between 465 to 509 amino acid residues depending on the gene involved in expression.[40] Each protomer unit is constituted of a heavy *α*- (approximate molecular weight (MW) = 32 kDa) and a light *β*- (approximate MW = 22 kDa) polypeptide chain linked by disulfide bonds.[41] Although a structure for mature CRU has been proposed and the protein profile of CRU can be easily visualized by gel electrophoretic analysis, the actual, detailed three-dimensional structure of mature CRU remains unknown because of the molecular heterogeneity of this protein. The structure of proCRU (Figure 2-1) is the only available structure that provides guidance as to the structure of mature CRU.[40]

The behavior of pure CRU obtained *via* chromatography was investigated at different pH values by Perera et al.[42] An unfolded structure of CRU was observed at pH 3, while minimal or no-structural change was observed at pH 7 and 10. These results confirmed that acid-induced unfolding leads to aggregation of CRU at low pH values. When aggregation occurs, the native hexameric CRU dissociated into two trimeric CRU units. Further dissociation of trimeric CRU eventually occurs, resulting in six unfolded protomers. These dissociations were reported to be reversible.[43] In weakly alkaline water, the native hexameric structure of CRU could be reconstituted either from trimers

or from protomers. The structural change of CRU with increasing temperature, however, was determined to be irreversible.[42]

The polypeptide profiles of *B. napus* proteins under reducing and non-reducing conditions are shown in Figure 2-2. Under reducing conditions, CRU exhibited a polypeptide profile ranging from ca. 18 to 60 kDa on a typical 1D SDS-PAGE analysis (Lane-R, Figure 2-2). The polypeptide band appearing around 67 kDa was attributed to the protomer of CRU. Perera et al. have suggested that a complex mixture of heterogeneous protomer units of CRU exists within the mature seed, which explained the multiple bands around 60 kDa.[42] The dissociated polypeptides of CRU that were not covalently linked were also visible under non reducing conditions (lane NR, Figure 2-2). Under reducing conditions, the protomer band representing the protomer of CRU around 60 kDa disappeared, which was an evidence of the protomer dissociation upon the reduction of disulfide bridges. The reduced CRU protomer dissociated to shorter *α*- and *β*- polypeptide chains, which corresponded to polypeptides ranging from 22 to 32 kDa (Lane R, Figure 2-2).

The amino acid composition of *Brassica* is balanced in essential amino acids. *Brassica*'s CRU isolate is mainly composed of Asx , Glx, Leu and Arg, and the sum of these amino acids is 46.2-48.6 % of protein weight.[16,44] It is noteworthy that the content of Leu in *Brassica*'s isolates exceeded the daily intake for adults recommended by FAO/WHO/ONU.[35] Sulfur-containing amino acids in *Brassica* isolates (2.8-3.9 %) also exceed the recommended daily intake for adults.[16,45] In addition, the Lys content in CRU isolates (ca. 4.5%) is comparable to animal proteins.[46] Taken together, *Brassica*

proteins can be considered well balanced as a protein supplement for animal and human nutrition.

The general CRU biosynthetic pathway was described by Shewry et al. in their review.[39] CRU is originally synthesized as a secretory protein. Once the required structure is assembled, the protein is cleaved and translocated into the lumen of the endoplasmic reticulum (ER), where maturation of CRU and other seed storage proteins occurs. It has been mentioned that three types of ER lumenal proteins likely assist in this maturation process.[39] These proteins include molecular chaperones of the HSP70/BiP family, the peptidyl-prolyl *cis-trans* isomerases and *N*-linked glycosylases. Molecular chaperones located in the ER aid folding of CRU and prevent the formation of incorrect inter- or intramolecular interactions. The function of lumenal isomerases is to assist folding by accelerating the isomerization of Xaa-Pro[b] peptide bonds. The post-translational modification of CRU is then carried out by *N*-glycosylases. Ultimately, mature storage proteins are transported to the vacuole by the Golgi apparatus and stored there until required during germination.

Napin

The small albumin NAP was observed and isolated for the first time from mature rapeseed seed by Bhatty et al.[47] NAP constitutes approximately of 20% of total storage proteins in mature seeds and plays an important role in the nitrogen and sulfur supply of the seed during germination.[18,42]

The 2S albumin NAP is described as a small, compact protein composed of two polypeptide-chains: a large (ca 9 kDa) and a small chain (ca 7 kDa), linked by disulfide

[b] Xaa-Pro is peptide bond between any amino acid with Pro

bridges.[48,49] The overall structure is a combination of five right-handed helices (Figure 2-2). [42,50] The small polypeptide forms two short helices (Helix Ia and Ib), and the large polypeptide forms 3 helices (Helix II, III and IV). The polypeptide profile of NAP under non-reducing and reducing conditions is also depicted in Figure 2-1. Under non-reducing conditions, NAP appears as a single band around 16 kDa. This dissociates into two polypeptide bands of ca 9 and ca 7 kDa, which correspond to the long and short polypeptide chains of reduced NAP, respectively (R, Figure 2-3).

Slight acid-induced structural changes of NAP were observed by Perera and co-authors.[42] These structural changes, however, were not as extensive as was observed in CRU. No significant structural changes were observed at neutral and alkaline pH for NAP. The pH stability of NAP can also explain the high extractability of NAP at different pH values. The presence of NAP in *B. napus* extracts performed at different pH values (reported by Fetzer et al.) has confirmed the previous conclusions.[45]

The denaturation temperature of NAP remains to be elucidated. In their study, Perera and co-workers reported that the degradation signal was only observed when the temperature reached over 100 °C, while other evidence has shown that heat denaturation of NAP occurs at lower temperatures.[51,52] Although the thermal denaturation requires further study, it is clear that NAP possesses a thermostable structure that is less affected by medium pH as compared to CRU.[42]

The amino acid composition of NAP isolated from *B. napus* revealed that Asx, Glx, Leu, and Arg make up 5.1, 30.4, 8.5 and 8.6% of the total amino acid composition, respectively.[44] This pattern is quite similar to that of the CRU isolate, where these amino acids make up to over 45% of the total amino acid composition. The level of sulfur-

containing amino acids in NAP (ca 0.6%), was reported to be lower than in the CRU isolate,[44] although it should be noted that the CRU isolate in this study had lower sulfur content compared to other studies.[16] This dissimilarity can be explained by differences in the source materials including the origin, growth environment, and processing methodology.

The biosynthesis and maturation of NAP has been documented by Byczynska and Barciszewski in their review.[53] Originally synthesized as a preproprotein on membrane-bound ribosomes, the precursor of NAP is translocated into the lumen of the ER where the maturation of NAP occurs upon formation of inter- and intramolecular disulfide chain bonds. Subsequently, mature NAP is transported from the ER to the vacuole where post-translation modifications of NAP occur. Fully developed NAP is then stored together with CRU and other minor seed proteins within the vacuole until seed germination.

Isolation and Purification

Isolation

Seed storage proteins can be easily extracted based on their solubilities: CRUs are globulins—proteins soluble in salt solutions—and NAPs are albumins—proteins soluble in water. A simple maceration of the raw materials with aqueous solution provides an efficient recovery of these major seed proteins.[16,42,45,54]

Akbari and Wu have reported that the protein contents of extracts made from hexane-defatted *B. napus* meal increased at increasing pH from 8 to 12.5.[54] Several parameters including salt concentration, detergent concentration, meal/solvent ratio, extraction duration, and various pH values from 8 to 12.5 were studied by the authors. The alkaline extraction at pH 12.5 yielded the most protein. It was also reported that the

extraction yield was reduced with increasing concentrations of salt, which is due to the salting-out effect on the extracted proteins prompted by adding salt under alkaline conditions. On the other hand, adding detergents such as sodium dodecyl sulphate (SDS), increased the extraction yield, but led to lower protein content in the extract due to the binding of SDS to non-protein compounds. Based on the results, optimal extraction conditions were determined to involve pH 12.5 in the absence of additional salt and detergent. These optimized conditions were consistent with the results reported by Pedroche et al., where the defatted *B. carinata* meal was also extracted most efficiently at pH 12.[16]

The recovery of seed proteins from *Brassica* defatted meal mainly relies on alkaline extraction. The recovery yield can vary depending on the extraction conditions of the meal. A strong negative impact on protein solubility by high temperatures during conventional processing, which is directly related to the recovery yield of desired proteins, was observed by Fetzer et al.[45] The processing of the biomass prior to alkaline extraction often impacts the solubility of *Brassica* proteins, which is directly related to the functional properties of isolated proteins. The solubility of *B. carinata* protein isolate is also altered during meal processing. The nitrogen solubility of protein isolate extracted at acidic pH was indeed reported to be lower than in that of the meal.[16]

Enzymatic assistance has proven useful in enhancing protein recovery from rapeseed raw materials and several successful extraction strategies have been devised and documented.[45,55,56] In general, the enzyme-mediated extraction is designed to liberate proteins from the meal matrix by degrading the cell wall, which facilitates the recovery of these proteins by the extraction solvent.[45] Furthermore, it was proven that

the recovery yield was enhanced by ultrasound assistance.[56] Unfortunately, this synergy also resulted in partial denaturation of the recovered proteins, which might alter their functional properties.

Reversed micelles have been used for extracting proteins from *B. carinata* and *B. juncea* meals.[57] This method takes advantage of spheroidal aggregates formed by an amphiphilic surfactant in organic solvent. The micelles facilitate the simultaneous recovery of oil, proteins, and GSLs from raw materials. The recovery yield was proportional to the molar ratio between water and surfactant which is expressed in Wo. Based on the value of Wo, seed proteins can be selectively recovered. For instance, low Wo levels selectively isolated hydrophobic proteins, while higher Wo levels enabled isolation of all seed proteins. In addition to yielding the main seed storage proteins such as CRU and NAP, the reverse micelle method also allows the recovery of Myrosinase (MYR), a thioglycosidase which plays an important role in the defense system of *Brassica* plants.

Purification

To meet the requirements for nutritional uses, *Brassica* proteins must be separated from non-protein components and chromatography is often employed for this purpose.[42,58] Both size exclusion and ion exchange chromatographies have been used. Firstly, a protein extract obtained under slightly alkaline conditions is desalted by gel filtration. Different protein fractions can be identified by gel electrophoresis. CRU-rich fractions are next separated from NAP by employing cation exchange. The separated CRU and NAP fractions can be further purified by size exclusion and hydrophobic interaction chromatography, respectively. This method was used to isolate pure CRU and NAP from *B. napus* defatted meal on a gram scale. [58] By employing this strategy,

200 g of pure CRU and 42 g of pure NAP were obtained from 3.5 kg of defatted *B. napus* meal. Additionally, 5 g of pure lipid transfer protein—oleosin—was also isolated. However, this method exhibits low time- and cost efficiency, which discourages scale-up.

Compared to the previous method based on chromatography, a precipitation strategy employed by Akbari and Wu appears to be more advantageous.[54] This method was successfully removed the undesirable antinutrient phytic acid while yielding protein concentrates of NAP and CRU. This method involved an acidic wash of the defatted meal prior to alkaline extraction. The alkaline extract was then adjusted to pH 4 to precipitate CRU. The crude CRU fraction was then washed with acid and freeze-dried to afford the protein isolate. The acidic extracts from the previous steps were then combined, ultra-filtered, and dia-filtered to afford a NAP protein concentrate (82% protein content). Although the functional properties of CRU and NAP were conserved throughout the purification process, the protein precipitation method did not yield proteins with comparable purity to that obtained via the chromatographic method.

We suggest that, in order to establish an efficient production of protein isolates from *Brassica* biomass, the purity of protein isolates should be carefully studied with regard to the downstream purposes. Additionally, a combination of acid-precipitation and one-step chromatography should be a solution to yield higher purity of protein isolate to while reducing the extensive effort and time of multistep chromatography approach.

Functional Properties

Wu and Muir reported that emulsions prepared with CRU showed the highest specific surface and the lowest mean particle size in oil, which results in excellent

emulsifying stability.[59] According to the authors, NAP possesses a lower emulsifying ability due to an abundance of basic amino acids, which are not favorable for hydrophobic groups of oil phase. The presence of NAP, therefore, diminishes the emulsifying properties of CRU.[54] In contrast, the foaming capacity and foaming stability of NAP were higher than that of CRU.[44,54] The excellent functional properties of NAP isolate are related to the high surface activity in stabilizing oil-water interfaces by these albumins.[18]

Taking advantage of the excellent emulsifying and foaming properties of CRU, a number of different types of CRU nanoparticles were synthesized for encapsulating bioactive compounds.[60,61] In general, CRU nano particles were synthesized from protein isolates of CRU complexed with either chitosan[60,61] or calcium[62]. In their study, Akbari et al. showed that both CRU/Ca and CRU/Chitosan nanoparticles exhibited potential mucus-penetrating property in non-digestion, while mucoadhesive property after digestion in the gastrointestinal tract of CRU/Chitosan particles was demonstrated.[60] Basing on these results, the potential use of edible CRU-based particles as oral drug or vaccine delivery systems was confirmed.

Gelling capacity is a significant factor in judging the quality of protein isolates, and this is related to the protein structure.[18] Plant-based protein products possess excellent gelation properties and are often used for improving product quality and reducing production costs in the food industry.[63] Heat-induced gelation of both CRU and NAP proteins isolated from *B. napus* were investigated by Schwenke et al.[64] Their results showed that the gelation temperature of CRU is lower than that of NAP. Interestingly, the gelation temperature of NAP drastically decreased with increasing pH

while that of CRU was insensitive to pH. These observations indicated that the gelation temperature and gel strength of *B. napus* protein isolates are essentially determined by CRU, whereas NAP causes poor gelling properties.[64]

The incorporation of *Brassica* proteins in our diet to replace meat proteins and lipids has been demonstrated. Besides been used as food additives, combining these plant-based proteins with other biopolymer matrices such as chitosan might allow applications in drug delivery and other areas.

Biological Activities

Although biological activities of CRU have not been widely reported, peptides bearing the primary CRU sequences may show interesting activities such as antihypertensive, antioxidative, and others according to an *in silico* study.[18] By employing immunoblotting and enzyme-linked immunosorbent assays, Palomares et al. have identified a major allergen related to CRU.[65] This finding might lead to further allergenicity evaluation related to CRUs of the *Brassica* family.

NAP has been classified as one of three major groups of allergenic proteins of the prolamine superfamily found in *Brassicaceae* seeds.[18] A number of clinical studies have confirmed allergenicity related to mustard NAP.[66] NAP also exhibits significant antifungal properties.[67,68] The synergy between NAP and thionins—abundant endosperm proteins which possess antifungal and antibacterial activities—tremendously affects the permeability of fungal membranes.[67] More specifically, NAP and thionins enhance antagonist activity against fungal calmodulin, which inhibits fungal growth.[67] It is noteworthy that these calmodulin antagonist activities disappear during seed germination in order to avoid interference.[69]

The biological activities of *Brassica* seed proteins have been well studied. Besides routine amino acid storage functions, they also enhance the environmental adaptation of the plant by enhancing antagonist activity against environmental insults, such as specialist insects, bacteria or fungi.

Other Minor *Brassica* Proteins

Other minor proteins present in *Brassica* mature seeds include oleosins and trypsin inhibitors.[18] Oleosins reside in the phospholipid membrane, and act as oil body stabilizers.[70] The expression level of oleosins directly impact the oil composition of the seed.[71] Serine protease inhibitors ubiquitous in the plant kingdom as they are part of their defense mechanism.[72] These peptides bind specifically to the protein binding sites of predator proteinases, which reduces plant digestibility. The regulation of this protein class in *Brassica* is often understudied, because of the emphasis on GSLs.[73]

Structural Information and Origins

Oleosin

The accumulation of neutral lipids within the seed is required for seedling development.[70] These lipids are stored in spherical compartments (referred to as lipid droplets), whose diameters range between 0.2-2.5 μm.[74] During the final stage of germination, the cytoplasm compresses and the lipid droplets are forced into contact with one another. By covering their surfaces with lipid transfer proteins (LTPs, oleosins), these organelles resist coalescence and remain as small individual units.[75]

Oleosins are ubiquitously present in oilseed crops. These proteins are of low molecular mass (15-26 kDa) and are often associated with lipid droplets, making up 1-4% of the lipid droplet body.[76] These LTPs possess short amphipathic *N*- and *C*-terminal peptides oriented horizontally on or extending from the lipid droplet surface.[74] A

hairpin constituted mostly nonpolar amino acid residues enables oleosins to be anchored on the surface of lipid droplets. A loop of twelve conserved residues constitutes the head of the anchor. The four most conserved residues are located in the middle of the central hydrophobic domain of oleosin and this is indicated in red in Figure 2-4.[77]

Oleosins are involved in the ontogeny of lipid droplets during seed development, the stabilization of lipid droplets during seed desiccation, and the mobilization of lipid droplets after seed germination.[77] The mechanism of stabilization of lipid droplets by oleosins was described by Huang.[76] The hairpin, which is 5 to 6 nm long, penetrates the triacylglycerol core of the lipid droplet and stabilizes the whole compartment. In addition, Murphy has suggested that accumulation of seed oleosin occurred during the later phase of embryo development, regulating storage lipid biogenesis.[77] Taken together, it is suggested that lipid bodies are initially formed on the endoplasmic reticulum followed by the accumulation of mature seed oleosins for later seed growth processes.

Serine protease inhibitors

In *Brassica*, serine protease inhibitors are a defense against natural enemies.[72] The production of these inhibitors is often associated with other classes of defense proteins and induced upon tissue damage. Environmental, developmental, and genotypic factors can affect the expression of protease inhibitors.[73]

Serine protease inhibitors belong to the low molecular mass trypsin inhibitor class.[18] Three distinct classes of inhibitors have been identified in *B. napus*: two thermolabile proteins, whose molecular masses are approximately 19 kDa and one thermostable, with an approximate molecular mass of 6.5 kDa. These peptides consist of a single polypetide chain with four intra-chain disulfilde bonds.[68] The structures of *B.*

napus serine protease inhibitors are highly similar to NAP,[18] although evidence reported by Svendsen et al. has demonstrated the difference between NAP and these minor peptides.[78] Whereas crude seed storage protein extracts showed no inhibitory activities, isolated peptides with molecular weights within the NAP range exhibited reversible, competitive inhibition with trypsin using N^{α}-benzoyl-L-arginine 4-nitroanilide as substrate. A comparison of the amino acid sequence conducted by the authors clearly indicated that the isolated peptides belong to the NAP family. The biological function of these proteins, however, differs from that of NAP.

Isolation and Purification

Bérot et al. have devised an isolation strategy for oleosins and other seed proteins from rapeseed meal by employing a chromatographic method.[58] The authors successfully isolated 5 g of LTP from 3.5 kg of rapeseed meal. Rapeseed defatted meal was extracted with Tris-HCl buffer pH 8.5 to recover LTP along with other seed storage proteins like CRU and NAP. The extract was next purified by cation exchange chromatography pH 8.5. The eluate was recovered, desalted by gel filtration and then separated a second time by cation exchange chromatography at pH 5.3. The effluent was recovered and dialyzed. Pure LTP was obtained after a final polishing step using reversed phase chromatography. The molecular weight of the isolated protein was found to be 9423.7 ± 1.6 Da, which corresponded to the expected value for oleosins. To the best of our knowledge, this is the first process that successfully isolated oleosin from *B. napus* on a gram scale. Unfortunately, the extensive use of chromatography makes the method labor- and time-intensive and as well as costly.

D'Andrea et al. reported a one-step extraction of oleosins from seeds of recombinant *Arabidopsis thaliana* oleosins using organic solvents.[79] In their method, *A.*

thaliana seeds were first pulverized in 50 mM sodium carbonate buffer at pH 11. Oleosins were then recovered from the aqueous phase by extracting with 9 volumes of a 5/4 chloroform/methanol mixture. They also found that chloroform/methanol ratios higher than 5/4 yielded biphasic mixtures in which the oleosins were mainly found at the interface. The authors did not purify the olesins further after the extraction step and the proteins were quantified by dot-blot or immunoblot. Although it was not rigorously determined, the recovery efficiency of this method was estimated to be >60%, with over 91% of other seed proteins also extracted. This method was therefore judged to be faster, simpler and cheaper than the previous chromatographic approach.

Proteinase inhibitors have been isolated from *B. napus* using conventional solvent extraction followed by an additional purification step.[78,80] In general, the peptides are recovered from the biomass by extracting with an appropriate buffer, then inhibitory proteins are obtained either by chromatography[78] or ammonium sulfate fractionation.[80] Both methods were reported to yield inhibitors with satisfactory activities against selected proteolytic enzymes. Fractionation with ammonium sulfate appeared to be advantageous over chromatography with regard to time- and cost- efficiencies. Nevertheless, chromatography is often required in order to obtain proteins with higher purities.[81] Taken together, an efficient and straightforward isolation remains to be devised.

Applications of Minor Seed Proteins

The main industrial applications of oleosin were reviewed by Huang.[74] It is considered to be a natural and safe emulsifying agent that possesses unique functional properties and oleosin-lipid droplets have been used as to prepare micelles for drug

delivery.[36] Adding oleosin can also enhance food stability, textures, and preserve nutrients in different soybean extracts.[74]

Recombinant oleosins expressed in bacteria have been used as a production platform for protein surfactants with regards to their biological activity.[82] Introducing oleosin/lipid droplets as protectants or metabolic sinks could result in higher oil contents and new lipid droplets in seed and yeast cells.[74] Nevertheless, Huang suggested that the plant growth rate penalty caused by oleosins must be evaluated, since oil overproduction by the plant will divert more energy that could have otherwise been devoted to plant to growth. [74]

Protease inhibitors are useful in biofumigation. A study showed that protease inhibitors co-induced with GSL in *B. napus* treated with jasmonic acid inhibited the growth of *P. xylostella* larvae fed on these plants.[83] The expression of protease inhibitors in *B. napus* leaves was induced along with GSL by foliar application with jasmonic acid. Another study conducted by Dastranj et al. involved feeding *P. xyllostella* and *Pieris rapae* with *B. rapa* subsp. *pekinensis* leaves dipped in extracts containing protease inhibitors. This inhibited the growth of both specialists and decreased the weights at both the fourth larval instar and pupa stages.[80] In addition, the survival rates of *P. xylostella* also declined when fed treated leaves compared to untreated ones. Taken together, there is good potential to use protease inhibitors from *Brassica* as pest control methods that would replace organic pesticides with high environmental impacts.

Conclusion and Future Work

Seed proteins are still hiding within the hulls, thus masking their tremendous potentials. Major seed proteins NAP and CRU are potential plant-based proteins that could be potential alternatives to animal proteins for animal and human consumption

thanks to their favorable amino acid compositions. Additionally, these proteins might also find applications in the pharmaceutical and material industries because of their interesting functional properties that include foaming, emulsification, and gel formation. Minor proteins like oleosins and serine protease inhibitors could also become more attractive thanks to their physical and biological functions.

On the other hand, there are several drawbacks that must be circumvented before that these seed proteins can be employed routinely. Although extracting seed proteins is straightforward, purification of the individual proteins remains challenging due to reliance on chromatography. Solving this problem requires that the targeted proteins and their end uses must be determined prior to developing extraction methods in order to successfully establish an isolation process that meets the targets for time and cost efficiency. It must always be borne in mind that the functional and biological properties of the isolated proteins can be altered by the processing methods employed and this can create another challenge for protein isolation. Hence, establishment of an efficient extraction process requires careful consideration regarding the processing method applied to the feedstock.

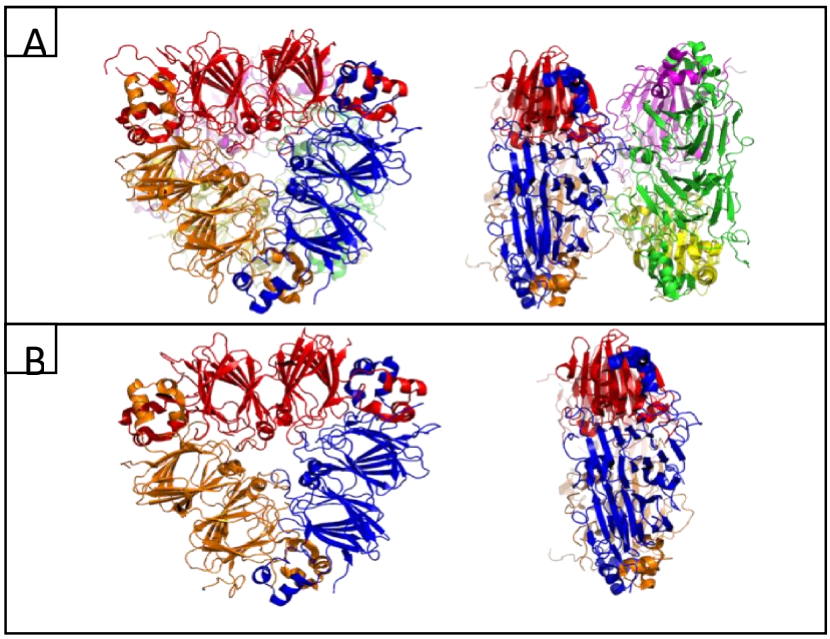

Figure 2-1. Overall structure of proCRU (PDB accession number: 3KLG) (A) The overall structure of hexameric proCRU in facial and side view. (B): the overall structure of trimeric proCRU in facial and side view. The structures were generated using PyMol.

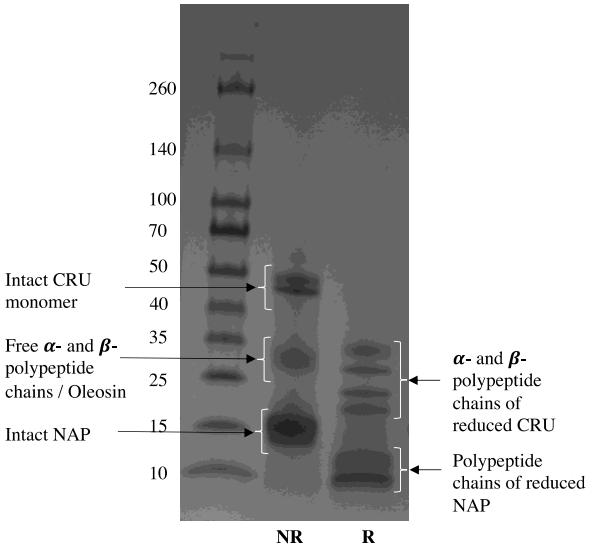

Figure 2-2. Polypeptide profiles of B. carinata extract under reducing (R) and non-reducing (NR) conditions

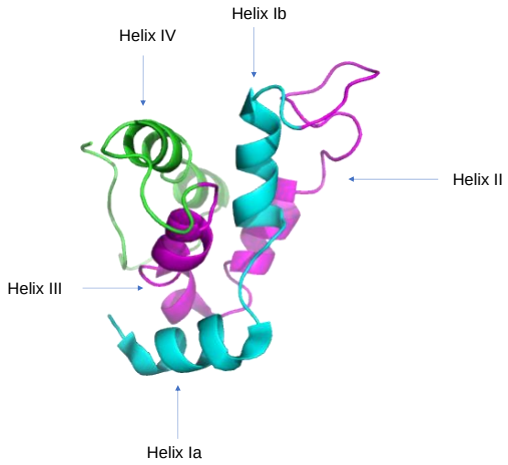

Figure 2-3. Crystallographic structure of NAP. The structure was generated using PyMol. (PDB Accession number 1SM7).

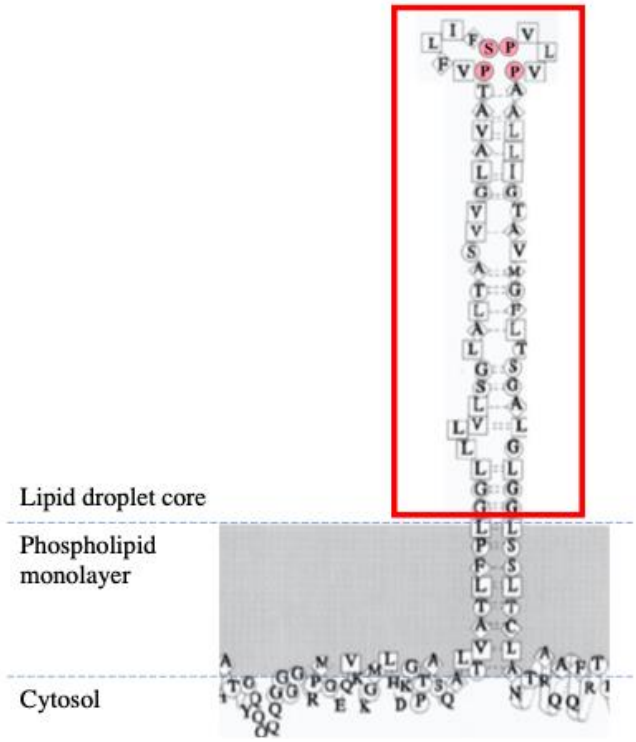

Figure 2-4. Illustration of oleosins anchored on the surface of lipid droplet. Red box indicates the hydrophobic anchor of oleosins. Blue dashed lines indicate the separation between cytosol, phospholipid monolayer, and lipid droplet core. (Reprinted from Huang, 2018)

CHAPTER 3
SINAPIC ACID AND DERIVATIVES IN *Brassica*: INNATE ACCUMULATION, BIOSYNTHESIS, ACCESSIBILITY, AND BIOLOGICAL ACTIVITIES[a]

Introduction

p-Hydroxycinnamic acids represent one of the most widely distributed chemicals in the plant kingdom, along with other phenylpropanoids such as flavonoids, stilbenes, and lignans. *p*-Hydroxycinnamic acids occur in fruits, vegetables, cereals, and beverages and are involved in plant tissue development and response to external stress.[84,85]

Primary roles of *p*-hydroxycinnamic acids in different parts of plants include coloration of flowers that attract pollinating animals, protection from injurious UV radiation, natural aromas and tastes that defend against predators, resistances to pathogens, and enhancing the host plants by affecting the growth of other, neighboring plants.[85]

Sinapoyl esters (SinEs) are the most important *p*-hydroxycinnamoyl esters present in plants of the *Brassicaceae* species.[29] SinEs possess an aromatic phenyl moiety with two methoxy substituents. Many SinEs have been found in plants, such as sinapoyl choline, also known as sinapine (SinP), sinapoyl glucose (SinG), and sinapoyl malate (SinM). The structure of SinA and its major corresponding esters are illustrated in Figure 3-1.

[a] This chapter has been reproduced with permission from V. P. Thinh NGUYEN, Jon STEWART, Irina IOANNOU and Florent ALLAIS; Sinapic Acid and Sinapate Esters in Brassica: Innate Accumulation, Biosynthesis, Accessibility via Chemical Synthesis or Recovery from Biomass, and Biological Activities. *Frontiers in Chemistry* **9**, 664602. (2021) (DOI: 10.3389/fchem.2021.664602)[386]

SinEs have various biological properties such as antimicrobial[86,87], anti-inflammatory[88,89], anticancer[89–91], and anti-anxiety activities.[92] Moreover, it is suggested that SinEs could be used as food and cosmetic additives, as well as bioactive compounds in the pharmaceutical industry.[29] Sinapic acid (SinA), the carboxylic acid form of SinE, could be employed as a building block for the design of renewable monomers and polymers.[93–95]

Here, we review the innate accumulation of *p*-hydroxycinnamic acid and its derivatives in *Brassica* plants, mainly focused on SinA and SinEs. As well, this chapter discusses biosynthesis, accessibility via chemical synthesis or direct extraction and biological activities.

Innate Accumulation of Sinapic Acid and Derivatives in *Brassica*

Phenylpropanoids are omnipresent in the plant kingdom and have been identified in a multitude of edible plants including fruits, vegetables, cereals, and spices. The concentrations of SinA and its derivatives varies from one species to another. For instance, strawberries, *Fragaria ananassa* L. was reported to possess the highest concentration of SinEs (up to 450.30 *μ*g per gram of biomass), while the lowest concentration was determined in rye *Secale cereale L.* (a few *μ*g per gram of biomass).[29] The review by Niciforovic and Abramovic provides a detailed report on the natural occurrence of these PCs.[29]

Within the *Brassicaceae* vegetables, SinA and its derivatives are ubiquitously present in both free and esterified forms. Many SinEs have been identified in different species from *Brassica* family.[96,97] Generally, the concentration of natural-occurring SinA appears to be lower than its choline ester, SinP. The concentrations of SinEs, mainly

SinP, range from 8 to 10.4 mg/g of biomass, whereas SinA ranges from 0.49 to 2.49 mg/g of biomass.[98–100]

The accumulation of phenolic compounds has been probed within different parts of *Brassica* plants. Many SinEs have been identified in edible parts such as leaves, stems, flower buds, and roots.[101] Malate derivatives were determined to be the main *p*-hydroxycinnamic esters presented in the leaves of pak choi *Brassica campestris* L subsp. *chinensis* and Chinese mustard *Brassica juncea* Coss.[102] SinA and its derivative esters have also been found in large amounts within rapeseed seeds and in their defatted residues. In their study of rapeseed meal, Laguna et al. reported that the SinA concentration in non-industrial and industrial meals, after alkaline hydrolysis, was up to 14.0 and 10.5 mg per gram of dry matter, respectively.[103] Another study on sinapine (SinE) concentration in aqueous ethanol extracts from mustard bran (*B. juncea*) was up to 8.7 mg per gram of dry matter.[100]

The accumulation of SinA and its derivatives, along with other phenylpropanoids, is believed to favor the adaptation process in plants under environmental stresses. By soaking *B. juncea* seeds prior to germination in 24-epibrassinolide, Sharma et al. observed enhanced accumulation of phenolic compounds in soaked seedling grown in the presence of imidacloprid.[104] The levels of SinA and its derivatives in seedlings that grew from soaked seeds were increased by over 100% compared to seedlings derived from untreated seeds. The accumulation of SinA and its derivatives also occurred under biotic stress including insect attack and pathogen infection. Gunnaiah et al. observed that the up-regulation of phenylpropanoid biosynthesis occurred in wheat infested with *Fusarium graminearum*, a fungal plant pathogen.[105] An increased cell wall thickness

prompted an excessive accumulation of SinA and its derivatives in infested plants, which is thought to be a physiological response to biotic stress. It was furthermore suggested that *Brassica* plants accumulate phenolics and other metabolites to enhance survival rates against environmental stresses, which is in agreement with the suggestion of Beckman et al. [85]

The involvement of these secondary metabolites in response to environmental stresses, however, exacts a cost to the plants with regard to the energy devoted to accumulating phenolic compounds, which leads to lower growth rates. In the study conducted by Moreno et al., chinese cabbage (*Brassica rapa L.* subsp. *Pekinenesis*) grown under sub-optimal conditions accumulated higher phenolic concentrations than those grown under optimal conditions.[106] The weights of plants grown under sub-optimal conditions were, as a result, lower than those grown under optimal conditions.

The accumulation of SinA and its derivatives varies with the growth environment since these modulate the physiological state of the plants. We therefore suggest that adverse environmental factors should be included in future studies in order to anticipate potential over-accumulation of these secondary metabolites. The concentration of SinA and its derivatives in plant can also be used as an indicator to monitor plant growth and the effects of growth conditions on plant development.

Biosynthesis of Sinapic Acid and Derivatives

Plant growth depends on environmental conditions and accumulating phenolics enables plants to survive under sub-optimal growth conditions.[107,108] SinA and its derivatives, along with other secondary metabolites, are biosynthesized by plants *via* a set of chemical reactions.[109] Studying these pathways within plants will therefore allow us to understand how environmental stresses affect phenolic accumulation generally,

and more specifically, SinA and SinEs in *Brassica* plants. In recent years, the biosynthesis of these secondary metabolites has been extensively studied thanks to the advanced development of model plants including *Arabidopsis thaliana*, a member of the *Brassica* family.[109,110]

The biosynthesis of SinA derivatives involves the phenylpropanoid pathway, which is composed of three sequential stages: (1) Formation of Phe via the shikimate pathway; (2) Non-oxidative deamination of Phenylalanine (Phe) followed by oxygenation to yield activated *p*-coumaroyl CoA; (3) further reactions of *p*-coumaroyl CoA to afford a broad range of SinEs.[109] As an example, the biosynthesis of SinE from erythrose 4-phosphate and phosphoenolpyruvate (PEP) is shown in Figure 3-2.

Formation of Phenylalanine Following Shikimate Pathway (1)

As depicted in Figure 3-3, the formation of Phe starts with the 3-deoxy-D-heptulosonate 7-phosphate (DAHP) synthase-catalyzed condensation of PEP and erythrose 4-phosphate to afford DAHP.[111] This latter is then transformed by 3-dehydroquinate synthase into 3-dehydroquinate (DHQ) that is subsequently dehydrogenated and reduced by 3-dehydroquinate dehydratase and the shikimate:nicotinamide adenine dinucleotide phosphate (NADP) oxidoreductase, respectively, to afford shikimate.

The multi-step conversion of shikimate to Phe occurs requires its transformation into chorismate. Shikimate is phosphorylated by shikimate kinase to yield shikimate 3-phosphate. 5-Enolpyruvylshikimate 3-phosphate (EPSP) synthase then installs a phosphoenolpyruvate group at the 5-position. Chorismate synthase eliminates the phosphate group to afford chorismate.

Chorismate is converted to prephenate *via* a chorismate mutase-catalyzed Claisen rearrangement of the enolpyruvyl side chain. Prephenate aminotransferase installs the amino group to yield arogenate, then this is simultaneously decarboxylated and dehydrated by arogenate dehydratase to yield Phe.

The formation of aromatic amino acids from PEP and erythrose 4-phosphate has been well studied and many of these enzymes have been isolated and characterized.[112,113] Detailed discussions of regulation and mechanisms for each of the enzymes involved in the shikimate pathway can be found in a number of previously-published reviews.[111–113]

Formation of 4-Coumaroyl CoA (2)

The conversion of Phe to 4-coumaroyl CoA requires consecutive modifications by phenylalanine ammonia lyase (PAL), cinnamate 4-hydroxylase (C4H), and 4-coumaroyl CoA-Ligase (4CL).[109] The conversion of 4-coumaroyl CoA to its CoA-linked ester is illustrated in Figure 3-4.

The first step of this pathway involves the non-oxidative deamination of Phe catalyzed by PAL.[114] The proposed mechanism of PAL is similar to that of histidine ammonia lyase.[115] Although no exogenous cofactor is required, an electrophile is still needed for the deamination; hence, the enzyme contains a 3,5-dihydro-5-methyldiene-4H-imidazol-4-one (MIO) moiety, formed by the cyclization and elimination of water from the inner tripeptide Ala-Ser-Gly.[116] The mechanism of this conversion is shown in Figure 3-5.

C4H belongs to the CYP73A family of P450 enzymes and catalyzes the hydroxylation of cinnamic acid at the 4-position, yielding *p*-coumaric acid. This transformation requires NADPH-cytochrome P450 reductase, which acts as an electron

donor.[117] The crystal structure of C4H from *Sorghum bicolor* (PDB accession number 6VBY) was recently solved and provides critical structural insights into the substrate specificity of this enzyme.[118] The mechanism of the C4H-catalyzed transformation of cinnamic acid into *p*-coumaric acid is described in Figure 3-6.

The final step of this biosynthetic pathway involves the 4CL-mediated conversion of *p*-coumaric acid into the corresponding Coenzyme-A thioester. A reaction mechanism has been proposed by Knobloch and Hahlbrock.[119] As depicted in Figure 3-4, the activation of *p*-coumaric acid requires ATP and a CoA unit. The substrate specificity of 4CL has been well studied by Lindermayr et al[120] and these authors have reported that recombinant 4CL can utilize several different *p*-hydroxycinnamic acids besides *p*-coumaric acid including caffeic acid, ferulic acid, and SinA to afford the corresponding CoA-linked thioesters. The recently published crystal structure of 4CL provided further insight into this enzyme with regard to its substrate specificity.[121] It is noteworthy that 4CL isoforms also contribute to the biosynthesis of lignin and other secondary metabolites in addition to its involvement in the biosynthesis of sinapoyl esters.[122,123]

Formation of Sinapic Acids and Derivatives (3)

Rational enzyme-catalyzed conversions of *p*-coumaroyl-CoA to other phenolic-CoA esters following pathway of phenylpropanoid biosynthesis was suggested (Figure 3-7).[124] The first step of this biosynthetic pathway involves adding a hydroxyl group at the 3-position, which converts *p*-coumaroyl-CoA to caffeoyl-CoA (Figure 3-8). Interestingly, this modification is catalyzed by *p*-hydroxycinnamoyl-CoA: quinate shikimate *p*-hydrocinnamoyltransferase (HCT), which also catalyzes a condensation of *p*-coumaroyl-CoA with shikimate to form the corresponding *p*-coumaroyl-shikimate ester.[125] A hydroxyl group is then added by CYP98A3 to afford the caffeoyl-shikimate

ester. The transformation of caffeoyl-shikimate ester to caffeoyl-CoA is also catalyzed by HCT.

Caffeoyl CoA is next converted into feruloyl-CoA *via* methylation of the 3-hydroxyl by caffeic acid *O*-methyltransferase (CMOT). It is noted that this enzyme also contributes to the defense systems in plants besides in addition to its involvement in phenylpropanoid biosynthesis.[126] The resulting feruloyl-CoA is furthermore transformed by cinnamoyl-CoA reductase (CCR) to afford coniferaldehyde. Ferulate 5-hydroxylase (F5H) then adds a hydroxyl group onto the coniferaldehyde at the 5-position to provide 5-hydroxyconiferaldehyde. The 5-hydroxyl is then methylated by CMOT to yield sinapaldehyde. Finally, sinapate is formed from sinapaldehyde in the presence of reduced epidermal fluorescence 1 aldehyde dehydrogenase (REF).[127]

Further modifications of sinapate yield three main sinapoyl esters including sinapoyl glucose, sinapoyl malate, and SinP (Figure 3-9). It has been suggested that sinapoylglucose:malate sinapoyltransferase (SMT) is also responsible for the conversion of sinapate to sinapoyl glucose (SinG).[128] 1-*O*-Sinapoylglucose:choline sinapoyltransferase (also known as sinapine synthase) converts sinapoyl glucose (SinG) to sinapine.[129] Sinapoycholine esterase can also convert SinP back to SinA in order to provide the required amount of choline during the seedling stage.[130] On the other hand, replacing the glucose moiety of sinapoyl glucose by malate is catalyzed by sinapoylglucose:malate sinapoyltransferase (SMT), producing sinapoyl malate (SinM).[128] By using these three sinapoyl esters as the main building blocks, plants produce a broad range of SinEs that are involved in many different biological processes.[29]

Chemical Synthetic Pathway of Sinapic Acids and Derivatives

Sinapic Acid

SinA can be readily synthesized chemically *via* a Knoevenagel-Doebner condensation of syringaldehyde and malonic acid in piperidine (Figure 3-10).[131] Several improved approaches involving microwave activation[132] or L-proline as a catalyst in ethanol[133] have been developed in order to reduce the use of hazardous base and to enhance the overall yield and greenness of the synthetic process. Nevertheless, these improvements also have their own limitations. For example, substituting L-Pro for piperidine in ethanol requires an extra purification step by chromatography[133] whereas using piperidine as the catalyst requires only a simple acidic washing to afford pure SinA.[131] Taken together, the current protocols are straightforward and provide access to SinA; however further improvements should be made in order to enhance the greenness of the process.

Sinapate Esters

Sinapoyl choline or sinapine (SinP)

SinP is omnipresent in Brassica plants. The first synthetic approach to SinP was reported by Clausen et al. (Figure 3-11).[134,135] Using SinA isolated from *Sinapis Alba* L., and $AgNO_3$, the corresponding SinA-Ag complex was reacted with bromocholine bromide to afford the pure product after chromatographic purification. Although pure SinP was obtained, there were several drawbacks to this approach including low overall yield, toxic reagents and waste-generating purification steps.

Mouterde et al. have recently reported a more straightforward multigram-scale synthetic process for SinP.[136] Their approach relies on the well-established Knoevenagel-Doebner condensation of syringaldehyde and choline malonate. This two-

step strategy gives access to SinP in a decent overall yield, while avoiding the use of toxic reagents. This enhances both the cost-efficiency and the environmental friendliness of the process. Moreover, this method was reported to be applicable to other naturally occurring *p*-hydroxycinnamic acids such as *p*-coumaric, caffeic, and feruloyl acids. We believe that this approach is, to date, the most cost- and time-efficient protocol as well as the most attractive in the context of green chemistry.

Sinapoyl glucose (SinG)

SinG is the precursor of sinapoyl malate (SinM) in SinE biosynthesis (Figure 3-9). The enzymatic conversion of *p*-hydroxycinnamic acid into the corresponding glucose derivative using recombinant *Gomphrena globosa* sinapate glucosyltransferase was studied by Matsuba et al.[137] This biochemical approach was applicable to most naturally occurring *p*-hydroxycinnamic acids such as ferulic acid, caffeic acid, 4-coumaric acid, and sinapic acid. Unfortunately, the reported yield was low for sinapoyl and feruloyl glucose.

Zhu et al. devised another synthetic strategy to overcome the limitations of the previous method.[138] The authors carried out a stereoselective glycosylation between a protected glycosyl donor and 4-*O*-chloroacetylated *p*-hydroxycinnamic acids (either ferulic or sinapic acids) (Figure 3-13). The subsequent cleavage of the chloroacetyl groups was then performed under mild conditions to yield desired sinapoyl or feruloyl glucose derivatives. This method successfully afforded the target molecules with high yields. To the best of our knowledge, this synthetic strategy remains the most efficient way to obtain SinG. One drawback is that this synthesis requires multiple protection/deprotection steps for both the sugar and the *p*-hydroxycinnamic moieties.

Sinapoyl malate (SinM)

Biosynthesized from SinG *in planta*, SinM is crucial for regulating lignin biosynthetic enzymes in plants.[122] A total synthesis of SinM was reported by Allais et al.[139] This strategy employed a convergent approach from SinA and the corresponding protected malate moiety to afford the desired SinM (Figure 3-14).

Although pure final product was obtained with a decent yield, the extensive use of toxic solvents along with multiple protection/deprotection steps throughout the pathway will likely hinder of the application of this approach at multigram-scales. With this in mind, Peyrot et al. have devised a more sustainable and straightforward, protecting group-free procedure based on the Knoevenagel-Doebner condensation of syringaldehyde and malic monomalonate ester (Figure 3-15).[140] SinM and analogues were thereby obtained in higher yields. In addition, the method is more environmentally friendly as it avoids toxic solvents and reagents as well as waste-generating protection/deprotection steps.

Other sinapoyl esters

Other SinEs are of great interest with regard to their photophysical and biological properties.[141–143] Most SinEs are obtained via Knoevenagel-Doebner condensations.[142,143] This route is more advantageous than direct acid-catalyzed esterification of SinA, as it enables access to a larger range of SinEs while remaining simple and ecologically attractive (e.g., no protection/deprotection sequences). Some structural examples are shown in Figure 3-16.

Recovery of Sinapic Acid and Derivatives from Biomass

Conventional Solid-Liquid Extraction Using Water/Alcohol

The extraction of bioactive molecules from agro-industrial wastes has drawn increasing attention.[144,145] The recovery of sinapic acids and derivatives mainly relies on solid-liquid extraction where water/alcohol mixtures are often used as the extraction solvent.[100,103,146,147] Despite its popularity, there has been little attention paid to optimizing the extraction process by this approach. One exception was the study of Flourat et al., who were optimizing the recovery of SinP from mustard bran.[147] Response surface methodology was employed and alcohol concentration, extraction temperature, and liquid/solid ratio were the varied parameters. The results showed that high alcohol concentration (66%) and high extraction temperatures were best (55 ◦C), respectively. These extraction conditions were similar to those reported by Reungoat et al (70% and 75 ◦C).[100] The alcohol concentration and temperature were varied between 60 to 80% and from 50 °C to the solvent boiling point in order to recover SinA and derivatives from *Brassica* biomass. Although aqueous methanol has been conventionally used to recover phenolics from processed biomass[96,146,148], aqueous ethanol mixtures are more attractive thanks to the low toxicity of ethanol over the more hazardous methanol.[100,147]

Additional purification is often necessary in order to recover metabolites of interest at the necessary levels of purity and adsorption chromatography has often been used for this purpose.[98,99,146,148] Crude products were then adjusted to acid pH values prior to loading onto preparative ion exchange columns. Bound SinA was then eluted with an aqueous alcohol solution. Moreno-Gonzalez et al. have improved the binding capacity by studying a large range of anionic resins.[149] The authors further showed that, compared to the batch adsorption method, the column adsorption approach afforded

higher selectivity towards SinA, which led to a higher recovery rate. Although the adsorption/desorption approach allows an efficient recovery of SinA on preparative scales, SinP was not recovered in its native ester form, as this method takes advantage of charge differences between SinP and SinA.

An innovative recovery of SinA and accompanying SinEs in their corresponding alkyl ester forms using different alcohols has been reported by Li and Guo.[150] Base-catalyzed alcohol extraction of rapeseed meal was conducted, then this was followed by column chromatography with silica as the stationary phase. The recovery of SinE (methyl sinapate) was reported to be up to 7.2 mg/g of rapeseed meal. Several alkyl SinEs (including ethyl, propyl butyl, hexyl, octyl, decyl and dodecyl) were obtained through this method; however, their purification proved difficult due to the similar polarity of the alcohol and the corresponding alkyl sinapate ester. It is worth mentioning that the subsequent valorization of carbohydrates and residual meal was included in the extraction process. In summary, this method allows one to simultaneously isolate the desired phenolic compounds in their ester forms along with other valuable components from rapeseed meal.

Solid-liquid extraction using water/alcohol mixtures remains the conventional method to recover phenolic compounds from *Brassica* biomass thanks to its simplicity, time, and cost efficiency. This method, however, requires an additional purification step, as the use of mixture alcohol/water also extracts other non-phenolic compounds such as proteins, glucosinolates, carbohydrates and many other water soluble chemicals. A more selective and straightforward recovery method of these secondary metabolites remains to be established.

Intensified Recovery of Sinapic Acid and Derivatives Using Physical Accelerators

Intensified water/alcohol extraction techniques enhance the recovery of secondary metabolites from various *Brassica* biomass samples.[151–154] These advanced technologies are more time- and energy-efficient as compared to conventional extraction methods since they reduce both the extraction temperature and the amount of extraction solvent required. This avoids the need for high alcohol concentrations and extended extraction durations. In this context, we provide in this section relevant examples of intensified SinA and derivative recovery from many that have reported in the literature.

Physical accelerators, such as ultrasound, have been employed in a number of studies.[151,155,156] Dubie et al. reported that low-frequency, high-intensity ultrasound treatment (20 kHz and 0.5 W/mL) of *B. juncea* meal improved the aqueous ethanol extraction. Several parameters, i.e., extraction temperature, ethanol concentration, sonication duration, and solvent/material ratio were subjected to a one-factor-at-a-time optimizations.[151] The results showed that the extraction of SinA and derivatives under mild conditions (70% EtOH/water for 30 min at 25 °C) yielded comparable results to the conventional water/ethanol extraction that required an extended extraction time (70% EtOH for 7 days at room temperature). These results furthermore confirmed the potential utility of this intensification strategy.

Microwave assistance enhances the extraction of bioactive molecules by increasing the motion of free water molecules within the plant tissue which then releases the target metabolites.[152] This extraction method is believed to be advantageous compared to the conventional method.[157–160]Jokic et al. reported a recovery of phenolics from broccoli using microwave treatment along with aqueous

methanol under optimal conditions.[157] Microwave irradiation reduced extraction time while enhancing the phenolic concentration in the extracts. Unfortunately, the relatively high cost of the microwave apparatus, along with undesired chemical reactions provoked during the extraction hinders wider use of this method, despite its benefits.[161]

Accelerated solvent extraction (ASE) is a technique carried out under high pressure and an inert atmosphere with a range of extraction temperatures from 35 to 200 °C. This intensification method has been applied to recover secondary metabolites from *Brassica* biomass[22,162,163], including SinA and its derivatives.[153,164] Aqueous alcoholic extraction of phenolics at high temperature (140-180 °C), and high pressure resulted in better extraction yield than conventional methods.[153] On the other hand, it was also reported that, under similar extraction conditions (200 °C, 20 min), SinA was degraded into canolol by decarboxylation.[164] The relatively high cost of the accelerated solvent extractor apparatus must also be considered a drawback.

Nowadays, supercritical carbon dioxide (Sc-CO_2) has become attractive as an environmentally friendly extraction solvent. The advantages of using Sc-CO_2 for phenolic extraction over conventional methods from canola press cake was reported by Li et al.[154] Their results showed that Sc-CO_2 extraction using ethanol as a co-solvent enhanced the recovery of phenolics, and approximately 10 mg of phenolics were obtained per gram of dry matter. In addition, this extraction method appears to avoid the conversion of SinP into SinA during the extraction process. The major drawback is the need for very specific technical expertise as well as material costs.

Advanced extraction techniques such as ultrasound-accelerated extraction, microwave-assisted extraction, Sc-CO_2, or ASE exhibit many advantages in terms of

time, solvent consumption, and energy efficiency. Nevertheless, these processes still have an unfavorable cost/benefit ratio for industry.

Enzyme-Assisted Recovery of Sinapic Acid and Derivatives

Carbohydrase (Viscozyme L) and pectinase (Rapidase) were used to assist the recovery of phenolics from cauliflower (*B. oleracea* L var. *botrytis*) outer leaves by disrupting linkages between phenolics and cell-wall polymers.[165] In this study, cauliflower leaves were pretreated with either carbohydrase or pectinase prior to aqueous alcohol extraction of phenolics. Multiple extraction parameters related to the enzyme pretreatment step including type of enzyme, concentration, incubation temperature, pH, and time were studied. As a result, enhanced recovery yields were observed in enzyme pretreated samples.

Another study employing enzyme-assisted extraction of rapeseed meal was also disclosed by Laguna et al.[103] Recombinant cinnamoyl or feruloyl esterase from *Aspergillus niger* was applied to the methanolic extract of rapeseed meal in order to hydrolyze ester linkages between *p*-hydroxycinnamic acids and carbohydrates. This enhanced the specific recovery of SinA.

Enzyme-assisted recovery becomes an attractive and environmentally friendly method to recover SinA and its derivatives from biomass. This approach is straightforward and accessible thanks to the convenient operating conditions. Nevertheless, the substrate specificity and the high cost of using enzymes limit the wide use of this methodology.

Biological Activities

Along with other ubiquitous *p*-hydroxycinnamic acids in the plant kingdom, SinA and its derivatives have been extensively studied regarding their biological

activities.[166,167] Their most important biological property of these metabolites is their antioxidant activity. The radical scavenging activity of SinA for 2,2-diphenyl-1-picrylhydrazyl (DPPH$^{\bullet}$) was determined to be 33.2% and 88.4% at a molar ratio of SinA to DPPH$^{\bullet}$ of 0.2 and 0.5, respectively.[168,169] SinP, on the other hand, exhibited even higher antioxidant activity than SinA.[170] The free radical scavenging activity of SinA and derivatives towards other free radical molecules such as superoxide anion radicals, hydroperoxyl radical, hypochlorite, and nitric oxide were documented by Niciforovič and Abramovič.[29]

SinA and its derivatives also exhibit high photo-stabilities, which is useful for their use as potential UV-filter reagents.[143,171] Unfortunately, there are also several limitations, including their absorption thresholds[131,142] and the genotoxicity of *cis*-isomers.[172] A variety of synthetic SinEs have therefore been synthesized to overcome these obstacles.[144,172] SinA and derivatives are thus potential biobased UV-filter reagents with antioxidant activities that could replace current UV-filters that are flagged as human- and eco-toxic.[173,174]

The antimicrobial activities of SinA and its derivatives have also been well studied. For instance, Lyon and McGill reported on the antimicrobial activity of SinA against *Erwinia carotovora* subsp. *carotovora*, which causes foodborne illness in root vegetables.[175] Inhibition of a broad range of Gram-negative and Gram-positive bacteria have been demonstrated using a SinA fraction isolated from the ethanolic extract of rapeseed.[176] The antimicrobial activities of SinP[136] and other SinEs[140] against *Escherichia coli* have also been recently reported. These literature reports strongly suggest that SinA and its derivatives are potential biobased antimicrobial reagents.

Many human health benefits of SinA and derivatives have been reported, and these include anti-inflammatory[88,177], anticancer[90,91], anti-diabetic[178,179], and antihypertensive[180] activities as well as their protections of the nervous, respiratory, and digestive systems.[167] For further details on the health benefits of these metabolites, we highly recommend the reviews by Sova and Saso[167] and by Neelam et al.[166]

As mentioned above, SinA and its derivatives exhibit many useful properties for human health beyond their well-known antioxidant and antibacterial activities.[29] Their photo-physical properties are also important for applications as biobased UV-filters.[143,171] As a result, these bioactive molecules represent attractive ingredients in the pharmaceutical, cosmetic and food industries.

Conclusion

The therapeutic and biological benefits of SinA and its derivatives have been extensively studied. Although the use of advanced extract techniques to recover these metabolites remains limited, mainly due to their relatively high cost, the accessibility of these metabolites from biomass extraction has been improved. Meanwhile, chemical synthesis of natural and non-natural SinEs through sustainable approaches have been devised that enhance access to these molecules while taking into account the environmental impacts of the processes. Biochemical studies of SinA and its derivatives have also been extended to provide crucial information concerning their innate accumulation and their important biological roles in plants. Taken together, we believe that SinA and its derivatives represent potential multifunctional chemicals with a bright future that deserves to be further investigated and developed.

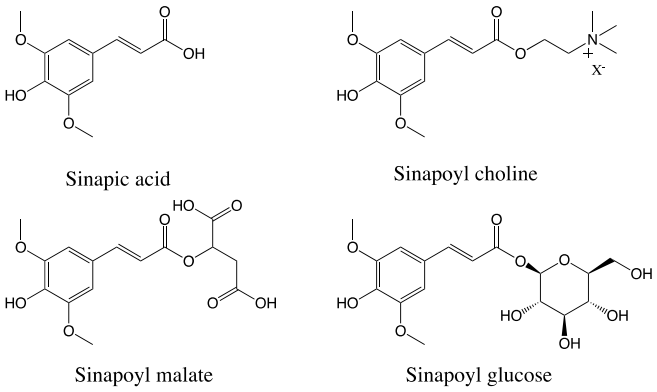

Figure 3-1. Structures of sinapic acids and its main corresponding esters.

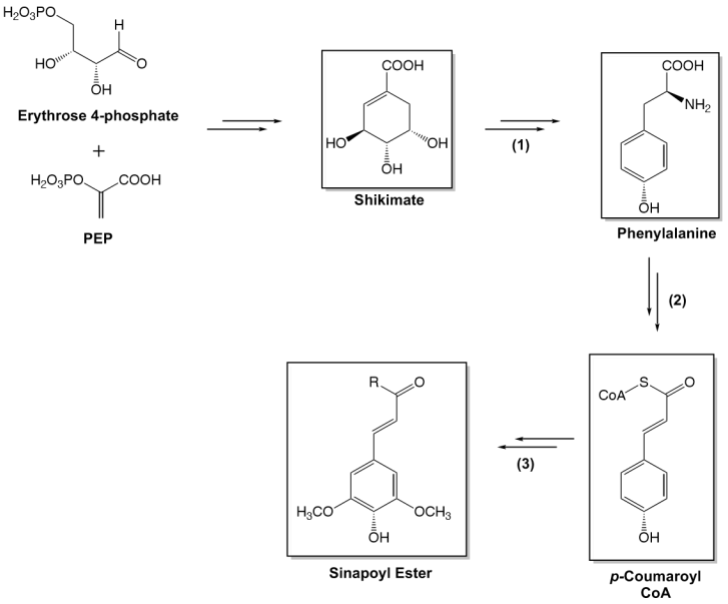

Figure 3-2. Three main stages of SinE biosynthesis: (1): Formation of Phe; (2): Formation 4-coumaroyl CoA intermediate; (3) Formation of sinapoyl esters.

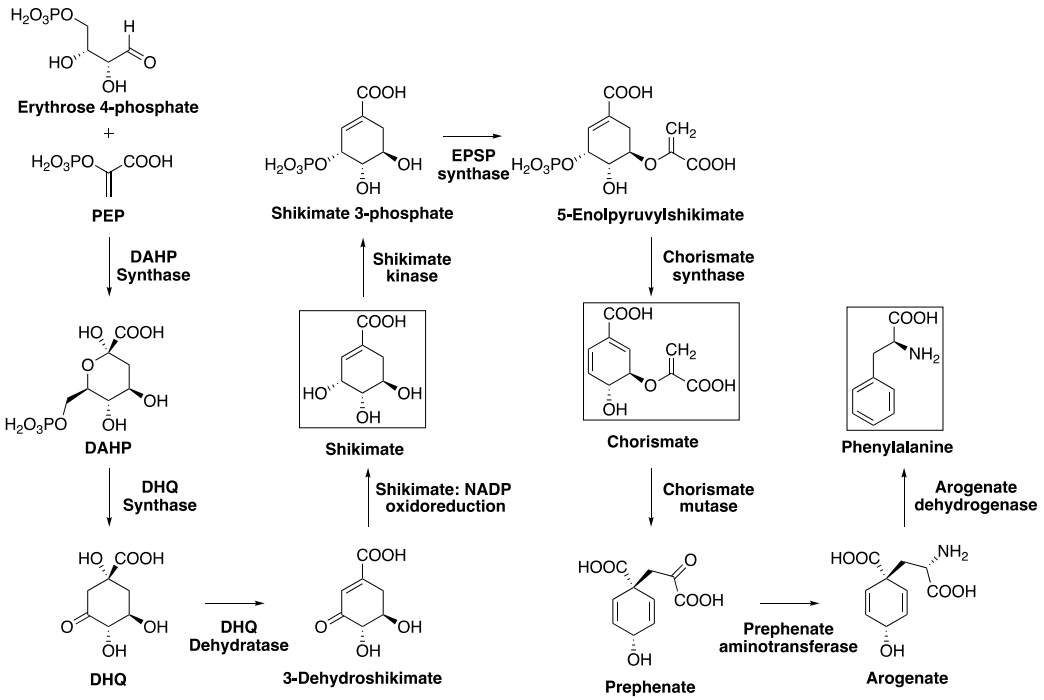

Figure 3-3. Formation of Phe following the shikimate pathway. Square boxes indicate relevant intermediates.

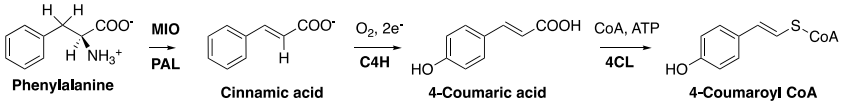

Figure 3-4. The formation of 4-coumaroyl CoA .

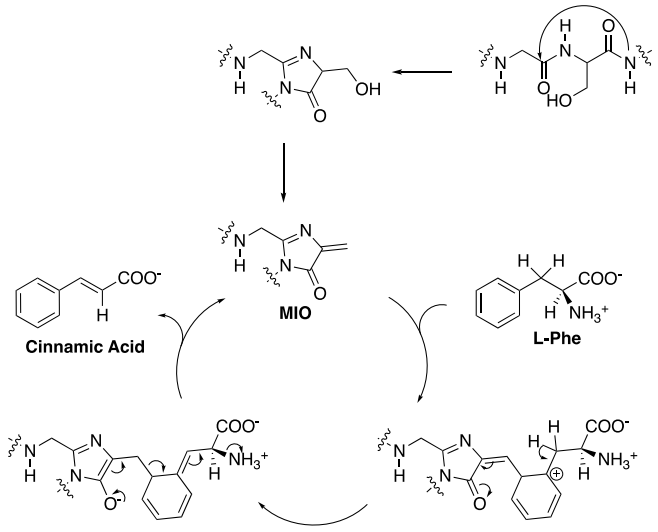

Figure 3-5. Mechanism of the deamination of Phe catalyzed by PAL.

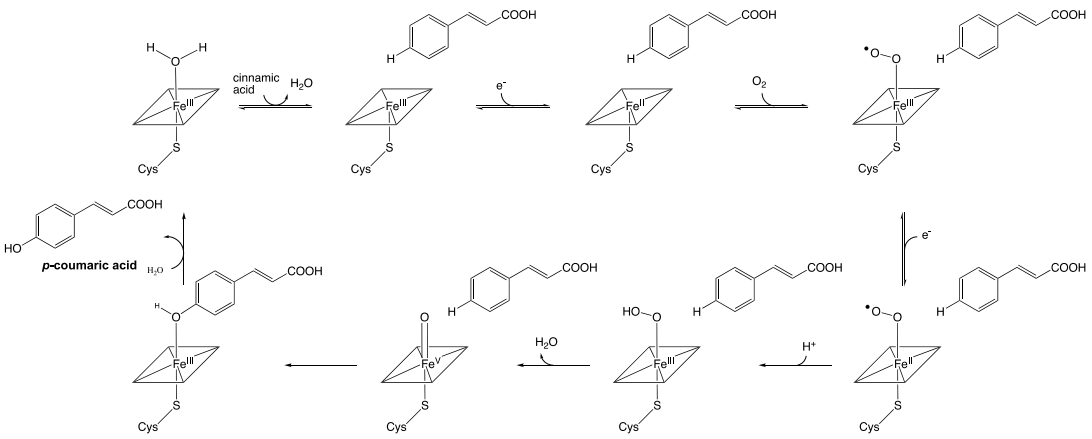

Figure 3-6. Mechanism of the formation of *p*-coumaric acid catalyzed by C4H.

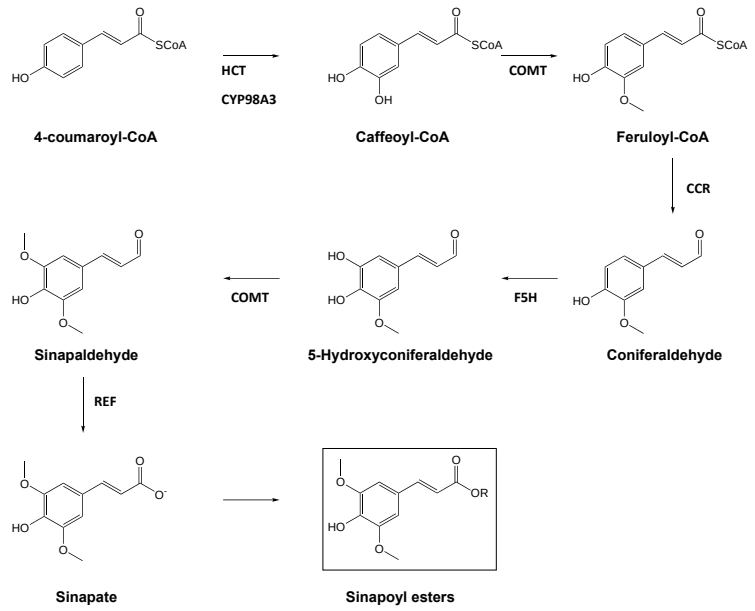

Figure 3-7. Biosynthesis of sinapoyl esters. HCT: *p*-Hydroxycinnamoyl-CoA: quinate shikimate *p*-hydrocinnamoyltransferase; COMT: Caffeic acid *O*-methyltransferase; CCR: Cinnamoyl-CoA reductase; F5H: Ferulate 5-hydroxylase; REF: Reduced Epidermal Fluorescence Aldehyde Dehydrogenase.

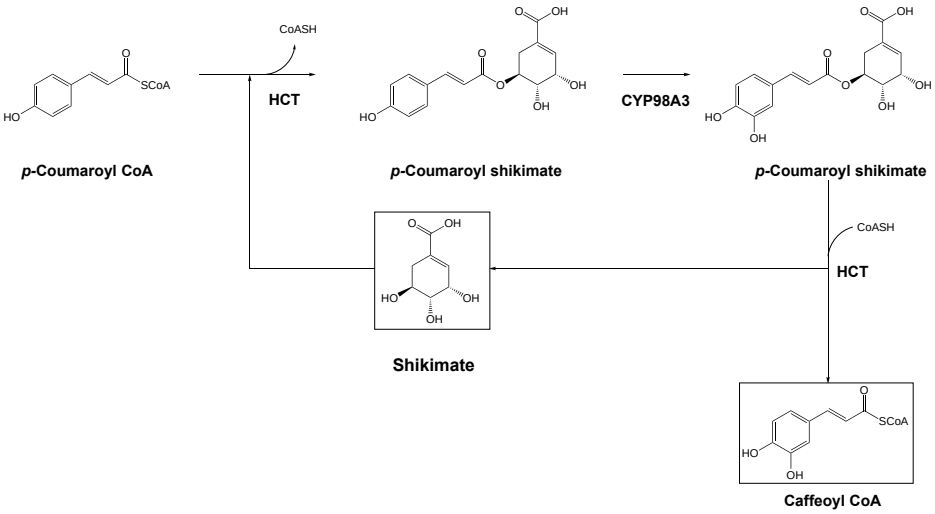

Figure 3-8. Transformation of *p*-coumaric acid into caffeoyl CoA.

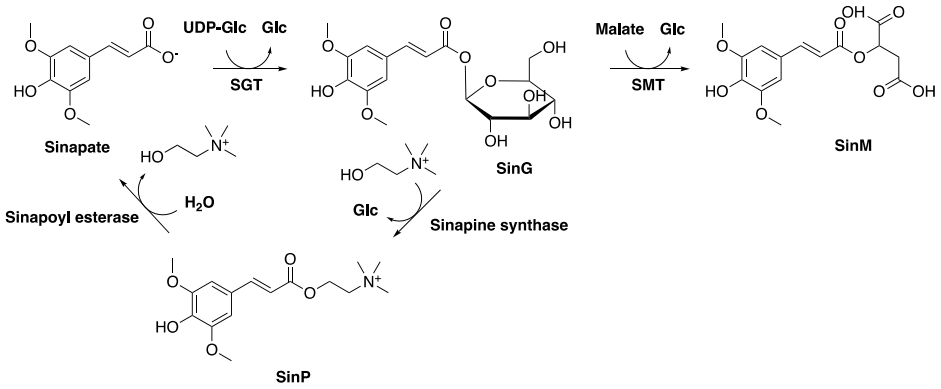

Figure 3-9. Biosynthetic modification of sinapate to afford three main SinE in plants.

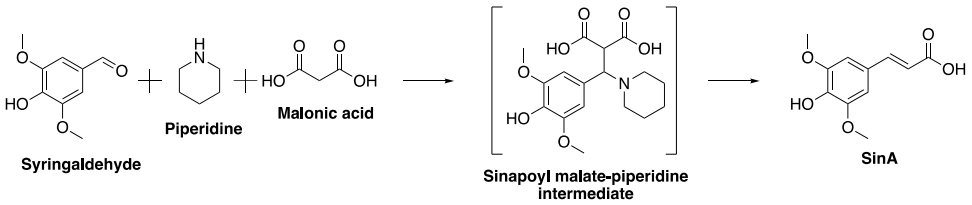

Figure 3-10. Synthesis of SinA via a sinapoyl malate-piperidine intermediate following the Knoevenagel-Doebner condensation approach.

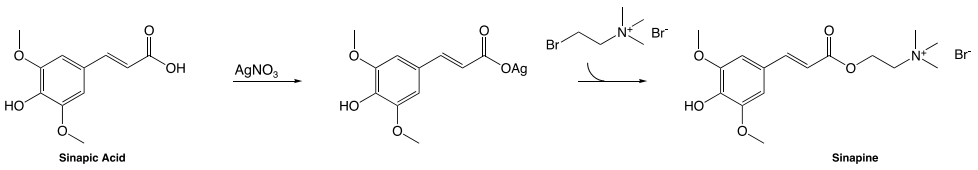

Figure 3-11. Synthesis of SinP described by Clausen et al.

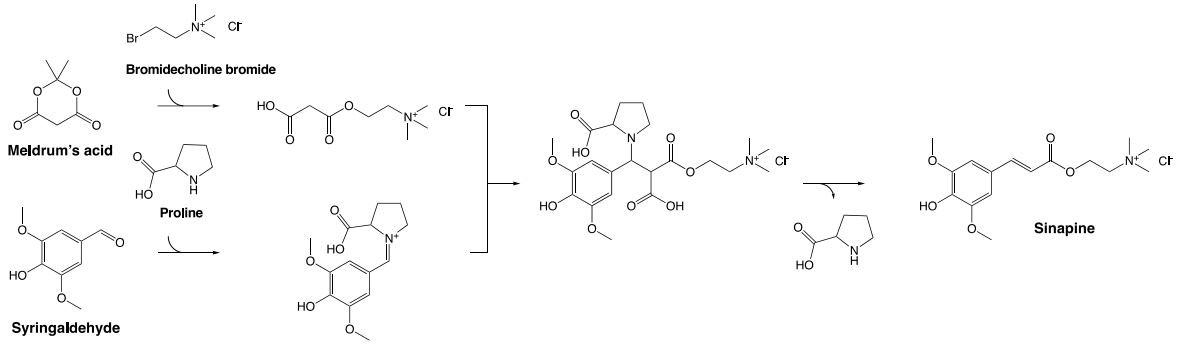

Figure 3-12. Synthesis of SinP described by Mouterde et al.

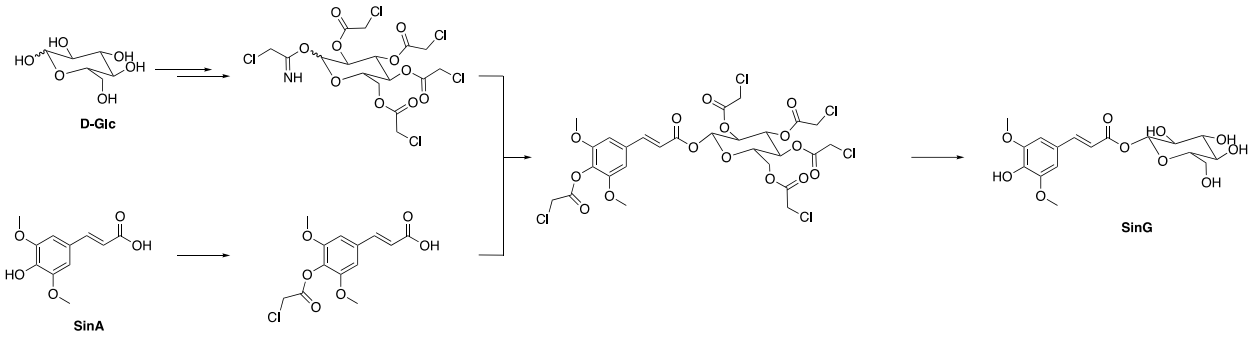

Figure 3-13. Synthesis of SinG described by Zhu et al.

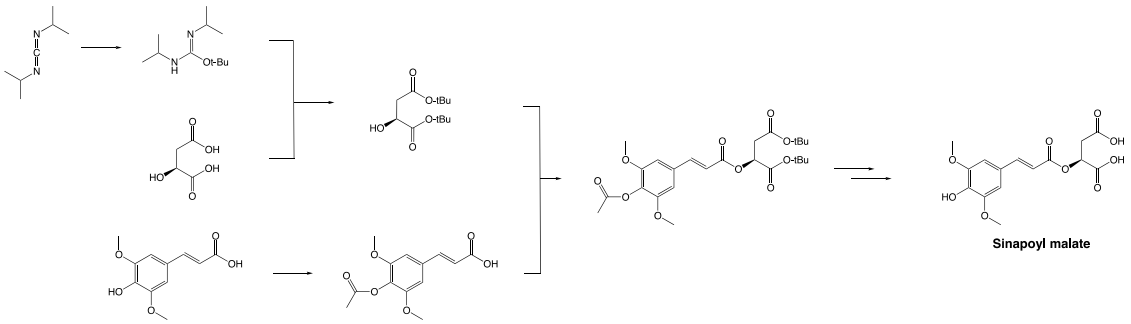

Figure 3-14. Synthesis of sinapoyl malate described by Allais et al.

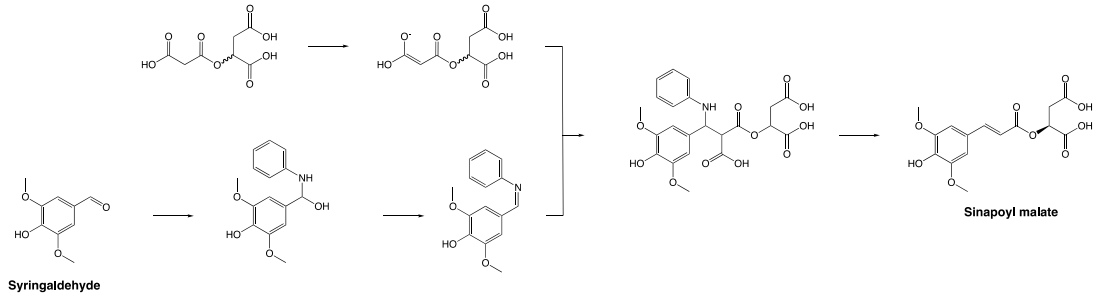

Figure 3-15. Synthesis of sinapoyl malate described by Peyrot et al.

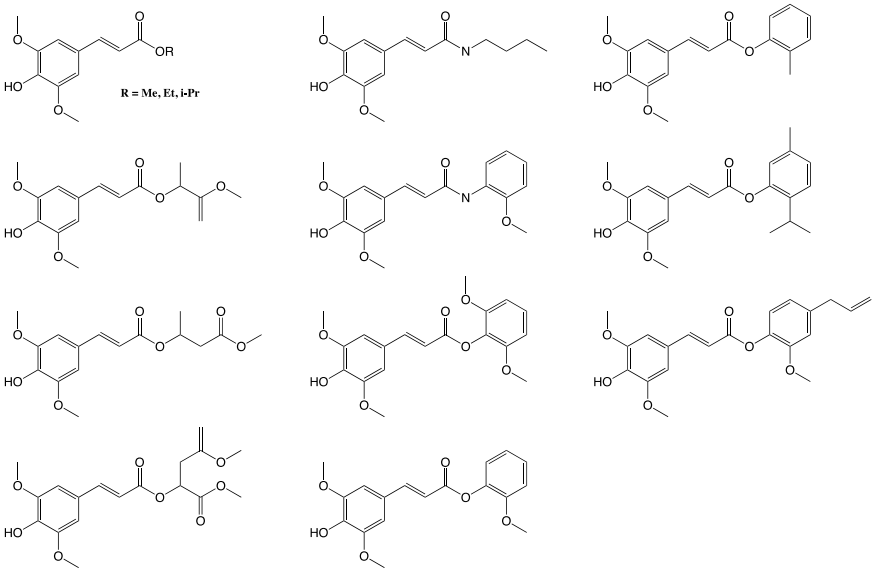

Figure 3-16. Several structural examples of other sinapate esters.

CHAPTER 4
GLUCOSINOLATES: NATURAL OCCURRENCE, BIOSYNTHESIS, ACCESSIBILITY, ISOLATION, STRUCTURES, AND BIOLOGICAL ACTIVITIES[a]

Introduction

Amino acid-derived glucosinolates (GSLs) are secondary plant metabolites that contain a sulfate and a thioglucose moiety and that play biological important roles in the *Brassicaceae* family defense system, crops of great relevance to agriculture.[181] The coexistent thioglucosidase myrosinase (MYR) (EC 3.2.1.147) originally segregated within plants[182], comes into contact with GSLs upon tissue disruption. Consequently, the enzymatic hydrolysis of GSLs occurs to form glucose, and an unstable aglucone that undergoes degradation to afford various of active components in response to environmental stresses (Figure 4-1). Along with the aforementioned role in the *Brassicaceae* defense system, GSLs are also likely involved in the survival system of this family. In a study of *A. thaliana* under abiotic stress, e.g., high salt, overproduction of short-chain aliphatic GSLs and underproduction of indolic GSLs occurred in leaves[183], suggesting adaptation of the plant in response to environmental stresses. This is a clear evidence that showed the biological importance of GSL in *Brassicaceae* survival system, along with their prominent role involved in the defense mechanism.

Over 130 GSL structures have been discovered and validated to date[22], and the variations GSL side-chains (R group in Figure 4-1) imply different biological activities. While sinigrin, the most abundant aliphatic GSL in Brassicaceae, is directly implicated in

[a] This chapter has been reproduced with permission from V. P. Thinh NGUYEN, Jon STEWART, Michel LOPEZ, Irina IOANNOU and Florent ALLAIS; Glucosinolates: Natural Occurrence, Biosynthesis, Accessibility, Isolation, Structures, and Biological Activities *Molecules*, **25**, 19, 4537. (2020) DOI: 10.3390/molecules25194537.[162]

controlling soil-borne plant pests[184], indolic GSLs are likely involved in insect-deterring functions.[185] Understanding the biosynthetic pathways and regulation of different groups of GSLs should lead to an understanding of the structural diversity of GSLs.

Synthetic approaches to GSLs have been devised to support studies of their involvement in different biological processes in plants as well as their health benefits.[32,184] Several natural GSLs such as sinigrin[186] and glucobrassicin have been obtained[187], along with a number of artificial GSLs.[188] These syntheses appear to be straightforward and easily accessible. Nevertheless, the stereoselectivity challenge prompted by certain natural GSLs remains to be circumvented.[188] As a result, isolation of natural GSL from biomass is often the method of choice to complement the limitations of synthetic approaches.

As natural GSLs are water-soluble components[33], these secondary metabolites can be extracted from various biomass starting materials by simple maceration.[189] The effect of extraction method on their biological activities, the stabilities of extracted GSLs and their concentrations determine the success of the extraction process. We, therefore, suggest that the stability and storage method of GSLs must be included in extraction processes in order to provide a thorough insight into the extraction strategy. For instance, it is often mentioned that high temperature prompt GSL degradation.[190,191] Therefore, extraction at lower temperature will fully recover GSL without altering their structures and corresponding biological activities.

The characterization of GSLs has been well developed.[192] Extracted GSLs can be purified by liquid chromatography followed by characterization either by mass spectrometry or UV absorption. Additionally, NMR analysis can be used to confirm the

structure of GSLs. In the case of GSLs extracted from a complex matrix, an extra desulfation step using sulfatase is needed to yield the correspond desulfated GSL (desGSLs) prior to characterization. Although robust compounds, the analysis of desGSLs is time consuming as the incubation of sulfatases with GSLs requires approximately 24h prior to the characterization.

The classification of GSL structures has also been well studied. Several systems have been proposed based on different criteria such as the GLS precursors, distinctions between “aliphatic”, “aromatic”, and “indole”[193,194], and, the most recent criterion suggested by Blazevic and coworkers, the presence or absence of aromatic motif. [22]

GSLs are omnipresent in *Brassicaceae* plants and their processed products.[23] Upon assimilation, both positive and negative effects of GSLs remaining in processed products have been probed in animal nutrition.[23,195] For human nutrition, negative effects of GSL remain to be determined due to a lack of studies in this area; however, the health benefits of consuming vegetables containing GSLs (e.g., broccoli, cabbage, etc.) are often mentioned, including antibacterial, anticancer, antioxidant, and anti-inflammatory functions.[33,196]

The aim of this chapter is to provide an overview of the chemical and biochemical aspects of GSLs. The biosynthesis as well as current chemical synthetic strategies of GSLs will also be discussed. In addition, extraction strategies, along with purification and characterization methods of GSL will also be explored in order to complement the limitation of chemical syntheses. We will also include in this chapter the most recent classification of GSLs, based on their side chain structures as proposed by Blazevi˘c´ et al.[22] Additional topic include the stability of extracted GSLs and isolation methods will

also be explored to emphasize the potential use of these natural molecules as bioactive compounds. The detailed mechanism of MYR-mediated hydrolysis, the fate of the GSL aglucone, and its health benefits will also be covered in this chapter.

Natural Occurrence of Glucosinolates

Their abundant presence in *Brassicaceae* vegetables and condiments makes GSLs of interest to human society. To date, the therapeutic benefits of GSLs[33] have prompted more attention to this class of secondary metabolites, alongside with their original food purposes. Although several synthetic approaches have been documented[188], most of the more than 130 different GSLs have been identified and validated after isolation from plants.[22,194]

GSL concentrations are unequally distributed throughout plant body. For instance, in *Brassica napus*, the GSL concentration in seed is greater than that in leaves.[197] This variation appears to be more relevant to root vegetable crops (family *Moringacea*) than that in oilseed crops (family *Brassicaceae*). Moreover, the GSL profile varies depending on the tissue type. Although aliphatic GSLs predominate both in leaves and in seeds, indole GLSs are more abundant in leaves than in seeds.[198] This difference may be related to functional differences of these plant tissues. A study of Troufflard et al.[199] showing that *A. thaliana* accumulated more GSL in the roots than in the shoots in response to abiotic stress is a clear evidence supporting the last suggestion. For further information on plant response to abiotic stress involving GSL accumulation, we recommend the review of Martinez-Ballesta et al.[200]

Breeding approaches are often employed to obtain crops with low GSL content for food or feed purposes[201–203], while those with high GSL content remain of interest for non-food applications. Therefore, the choice of species should be carefully considered

with regards to the downstream purposes of raw materials. We also suggest that growth conditions should be carefully chosen in order to adapt the chosen crops to their cultivating environment.

The occurrence of GSLs varies among different species within the same order (Table A-1). These variations occur even for the same crop in different years. For instance, Ishida et al reported that the amount of GSLs in the same crops of Japanese radish varied between 2005 and 2009.[204] It was assumed that the accumulation of GSLs within plants highly depends on changeable environmental factors such as the weather, thus directly impacting the GSL contents of the crops. Therefore, the GSL content of the same drops must be kept updated annually, or more frequently if needed.

Glucosinolates: Biosynthetic and Chemical Synthetic Pathways

Biosynthesis of Glucosinolates in Plants

GSL biosynthesis in plants has been studied extensively.[205,206] As depicted in Figure 4-2, this pathway is composed of three separate phases: (1) chain elongation that involves the insertion of a methylene group into the side chain of aliphatic amino acids, (2) metabolic reconfiguration of the amino acid moiety to afford the core structure of a GSL, and (3) the modification of the core structure to yield GSLs bearing various aglucone structures.

Side chain elongation of amino acid

In an early study of GSL biosynthesis in the 1960s, Chrisholm and Wetter used radio-labeled methionine as an aglucone precursor to provide first evidence for side chain elongation phase.[207] More recent studies by Graser and coworkers confirmed the existence of the chain elongation process by characterizing the extension of 2-oxo acid

using radioisotope and tandem mass spectrometry with stable isotope coupling analysis.[208,209]

The chain elongation phase is initiated by deamination by branched-chain amino acid aminotransferase (BCAT) that transforms the parent amino acids into the corresponding 2-oxo acids (Step (i), Figure 4-2). The next stage consists of a three-step transformation cycle where *(1)* the resulting 2-oxo acid is condensed with acetyl-CoA by a methylthioalkylmalate synthase (MAM) to form a 2-malate derivative (Step (ii), Figure 4-2), *(2) the* 2-malate is then isomerized to a 3-malate derivative by an isopropylmalate isomerase (IPMP) (Step (iii), Figure 4-2) followed by *(3)* a decarboxylation by an isopropylmalatedehydrogenase (IPM-DH) to yield an intermediate elongated 2-oxo acid (Step (iv), Figure 4-2).[210] This intermediate can either undergo a transamination to provide an extended amino acid for the next phase (Step (v-i)); or, reenter into the transformation cycle for further elongation (Step (v-ii), Figure 4-2).[193]

Reconfiguration of amino acid to glucosinolate core

The conversion of amino acid to aldoximes.

Amino acid reconfiguration begins with the oxidation to the corresponding aldoximes (Step (vi), Figure 4-2). The oxidation is catalyzed by three different enzyme systems: a cytochrome-P450 (CYP79) dependent monooxygenase, a flavin-containing monooxygenase and a peroxidase.[205] The involvement of each enzyme system depends on the nature of the amino acid precursors[181]: GSLs from Tyr or Phe precursors are oxidized by cytochrome-P450 dependent monooxygenase while those containing homophenylalanine or elongated methionine GSLs are oxidized by cytochrome P450-independent monooxygenases, respectively; while plasma membrane-bound peroxidases produce GSL from Trp.

The conversion of aldoximes to thiohydroximic acids.

CYP83 cytochrome monooxygenases activate the aldoxime resulting from amino acid oxidation to give the corresponding thiohydroxymate (Step (vii-a), Figure 4-3). The activated aldoxime is then conjugated to glutathione (GSH), which acts as a sulfur-donor[183] to yield the corresponding thiohydroximate intermediate (Step (vii-b), Figure 4-3). The newly formed *S*-alkyl-thiohydroximate intermediate is then cleaved by a C-S lyase: SUR1 to provide the corresponding thiohydroximates[185] (Step (vii-c), Figure 4-3). An experiment conducted by Czerniawski and Bednarker while studying biosynthesis of indolic GSL showed the formation of intermediate GSH-conjugates, which suggests the involvement of GSH within the biosynthesis of GSLs.[211]

The formation of the glucosinolate core.

Thiohydroximates are subsequently transformed by UDP-glucose: thiohydroximic acid *S*-glucosyltransferases (S-GT) (Step (viii), Figure 4-2), and desulfoglucosinolate sulfotransferases to afford GSL core structures with the corresponding side-chains (Step (ix), Figure 4-2). Transferases involve in the formation of the GSL core have been identified and reported in the literature.[212,213] This identification clarifies how the GSL core has been formed via the transfer of glucose and sulfate moieties by corresponding transferases.

Natural side chain modification of glucosinolates

Side chain modifications of newly-formed GSL core structure are frequently encountered.[22,214] Chemical transformations of GSL side-chains occur *in vivo* via enzyme-catalyzed oxidations, eliminations, alkylations, and esterifications.[215] Most reported side chain modification are related to methionine-derived GSL.[216]

These side chain decorations have drawn increasing interest with regard to their influence on the direction of MYR-catalyzed hydrolysis as well as the resulting activities of the hydrolysis products.[206] Moreover, these modifications contribute to the structural diversity of this class of molecules. As a result of the diversity of side-chains, a number of GSLs with more complex side chains results in multiple biological activities in plants.[210]

Regulation of glucosinolate biosynthesis

Studies of the regulatory system that controls GSL biosynthesis in the model plant *A. thaliana* by employing a genetic approach along with structure profiling has provided further information about the analogous route in *Brassica* plants. A Quantitative Trait Locus (QTL) is a region of DNA (Deoxyribonucleic acid) that influences a quantitative phenotype trait.[217] Analyzing the expression of phenotypic traits, in this case, GSLs , in *A. thaliana* allows one to identify new functional loci.[210] *GS-ELONG, GS-OX, GS-AOP*, and *GS-OH* have all been identified as associated with side-chain variability of aliphatic GSLs.[218] In the case of indolic GSLs, QTL mapping has been combined with transcript profiling, and subsequent *cis*-expression of a QTL to identify the regulatory gene for 4-methoxy indolyl-3-methyl glucosinolate in *A. thaliana*.[219] Wentzell et al. have successfully identified a locus that regulates the expression of aliphatic and indole glucosinolates by mapping the expression QTL with the expression phenotype traits in *A. thaliana*.[220] For further genomic insights, review of Sønderby et al. is highly recommended.[210]

The regulatory system of GSL biosynthesis in plant is complex. In spite of the extensive studies on GSL biosynthesis[221–223], some aspects of the genetic and biochemical nature of their regulation remain to be elucidated. Further investigation

should be conducted to examine the biosynthesis of GSLs, which can lead to a deeper understanding of the biological role of GSLs under environmental stresses as the regulation of these metabolites is tightly coupled to the survival of the plants.

Chemical Synthesis of Glucosinolates

Chemical synthesis can be an efficient way to produce pure naturally occurring and artificial GSLs. Two synthetic strategies have been proposed based on two disconnections between the glucose and aglucone moieties: the anomeric disconnection, and the hydroximate disconnection (Figure 4-4).[188]

Anomeric disconnection

The anomeric disconnection strategy involves a standard electrophilic glucosyl donor and a thiohydroxamic acid acceptor. The method was established by Ettlinger and Ludden.[224] Figure 4-5 illustrates the synthesis of GSL following this method.

The synthesis starts with the addition of benzyl magnesium chloride to carbon disulfide. The reaction was then treated with aqueous hydroxylamine hydrochloride at 0 °C to form *in situ* nucleophile a in equilibrium with the desired nucleophile b (c.a. 33%). The latter is then reacted with protected *α*-bromoglucose under basic conditions to provide the corresponding glucosyl thiohydroximate. The next step relies on reacting glucosyl thiohydroximate with sulfur trioxide pyridine. The resulting peracetylated glucotropaeolate anion is then crystallized as either the potassium or tetramethylammonium salt. Ultimately, glucotropaeolin undergoes purification by cation exchange chromatography. This method results in low-yield, probably due to the formation of the unstable alkylthiohydroxamic acid intermediate. The moderate efficiency of the nucleophilic displacement at the anomeric position of the glucosyl halide counterpart is another drawback that contributes to the unpopularity of this

approach. To the best of our knowledge, this synthetic procedure has never been optimized further since its original disclosure.[188] For this reason, most of GSL synthetic studies follow the alternative hydroximate disconnection described below.

Hydroximate disconnection

This methodology involves 1,3-addition of a protected thio-*β*-D-glucopyranose to a highly labile nitrile oxide. This route is the most popular methodology for GSL synthesis. One disadvantage is that the nitrile oxide must be generated *in situ* from the corresponding hydroximoyl precursor.[22] Multiple approaches have, therefore, been developed to access to this labile precursor starting from aldoximes, from aliphatic nitronates, or from nitrovinyl derivatives.

The Aldoxime pathway.

In the early 1960's, M.H. Benn devised the first synthesis of GSL that employs the aldoxime pathway (Figure 4-6).[225] The hydroxinamic chloride was prepared by chlorinating of the aldoxime precursor, then reacted *in situ* with a base to yield the unstable corresponding nitrile oxide. This was then reacted with protected glucosyl thiol to give the corresponding glucosylthiohydroxamate that, upon subsequent sulfonation, afforded the desired protected GSL. Final deprotection yielded the desired GSL in its salt form. Although the aldoxime pathway remains a popular method for synthesizing GSLs, the halogenation tolerance of side-chain aldoximes limits the scope of this method.[188] As a result, alternative approaches employing nitronate and nitrovinyl pathways have been investigated.

The nitronate and nitrovinyl pathway.

In the previous methodology, the low tolerance of many vinyl and aryl aldoxime precursors under the halogenation reaction conditions was a significant drawback. To

overcome this limitation, an alternative method for generating the key hydroximoyl chloride intermediate via the formation of a nitronate was established first time by Benn and Ettlinger.[186] In their study, sinigrin was successfully synthesized from but-3-enyl bromide employing the nitronate pathway (Figure 4-7).

The synthesis starts with the conversion of but-3-enyl bromide to the corresponding nitronate anion. The medium containing the newly formed nitronate is chilled to 0 °C, then lithium chloride-hydrochloric acid is added, which yields the corresponding but-3-enohydroxamoyl chloride. The latter then undergoes the same established pathway as that of aldoxime by reacting with tetraacetyl-*β*-D-glucopyranosyl mercaptan to afford the corresponding thiohydroximic acid, which is then transformed to desired sinigrin as depicted in the last step of Figure 4-7.

The nitrovinyl pathway is based on the discovery of a one-step conversion of nitroalkenes to hydroximoyl chlorides.[226] As depicted in Figure 4-8 for the synthesis of indolic GSL, the conversion of nitroalkenes relies on their reaction of nitrovinyl derivatives with triethylsilane (a hydride source) in the presence of a Lewis acid to provide substituted acethyhydroximol chlorides.[187] This hydroximoyl intermediate then follows the same pathway as in aldoxime and nitronate strategies to afford the desired GSL.

Many successful syntheses of vinyl, aryl, and indole GSLs using the nitronate and nitrovinyl pathways have been performed and reported.[22,188] However, one exception[227] has shown that the nitronate pathway is less efficient than the aldoxime one for certain aryl GSLs. In addition, there is a lack of stereoselectivity in previously-

established pathway.[188,228] Based on these considerations, higher stereoselective synthetic methodologies remain to be designed to tackle these challenges.

Extraction, Purification and Characterization of Glucosinolates

Extraction of Glucosinolates

Glucosinolates are water soluble components with very low octanol-water partition coefficients, owing to their ionized sulfate and hydrophilic thioglucose moeities.[33] Therefore, extracting these metabolites from plant materials mainly relies on solid-liquid extraction with boiling water[189,229] or aqueous organic solvent mixtures as extraction solvents.[162,230–232]

Various modifications of the extraction parameters including solvent composition, temperature, and tissue disruption method have been investigated in order to optimize the extraction process. Doheny-Adams et al. studied effects of these parameters on the extraction of GSLs from several *Brassica* plants.[233] Boiling water and mixtures of methanol/water were tested as extraction solvents. Tissue disruption prior to GSL extractions was also carefully investigated. One result of these studies was the elimination of freeze drying for short term storage of plant tissue samples. Freeze drying, however, is still advised for long term storage in order to maintain the GSL recovery yield of the established process. Using cold 80/20 methanol/water as the extraction solvent instead of boiling mixture 70/30 methanol/water appears to be advantageous for industrial scales due to the reduction in the number of steps in the process while also being less hazardous and offering improved or comparable GSL recovery rates.

Originally established by Thies[234], the isolation of intact GSLs has recently been improved by Forster et al.[235] This process started by extracting GSLs from *Moringa*

oleifera leaves with 70% methanol/water at 80 °C. The extract was then purified by chromatography to yield a purified GSL fraction. Additional recrystallization steps were needed to afford the final, pure GSL mixture. This method was reported to yield up to 600 *μ*mol of GSL per gram of dry material. With regards to the amount of GSL amount isolated from *M. oleifera* leaves, this strategy appears to be both efficient and accessible. On the other hand, employing hot extraction with methanol might lead to the partial degradation of GSLs, which can be seen from the authors' observation of the formation of artifact GSLs and loss of the acetylated GSLs. Therefore, the extraction at high temperature should be carefully weighed against the potential for GSL degradation. Besides extracting intact GSLs, Forster et al. also employed a desulfation strategy in order to isolate GSL from M. oleifera leaves.[235] This strategy followed the same protocol as for intact GSLs. However, rather than being directly eluted, bound GSLs were treated with a cleaned-up *Helix pomatia* sulfatase solution in order to remove the sulfate group of GSLs. After overnight incubation, desulfated GSLs were easily eluted by flushing the column with ultra-pure water. Despite the qualitative difference between the desulfation and the intact extraction, the resulting total amount of GSL resulting from both methods were reported to be similar. Nevertheless, the formation of artifacts and loss of acetylated GSL observed while employing desulfation approach for isolating *M. oleifera*'s GSLs suggests that the desulfation method is not appropriate for recovering GSLs from plant materials.

The use of physical accelerators to intensify the extraction, such as ultrasound, has been explored in order to enhance the extraction yield.[236] Ultrasound was applied during the extraction step, which improved the GSL recovery rate and time efficiency,

and also reduced the amount of extraction solvent required. Taken together, ultrasound significantly enhaced productivity over the conventional extraction method, by eliminating the outer pectinous materials, which facilitates the recovery of GSLs from plant materials.

Supercritical carbon dioxide has drawn increasing attention as an alternative, and environmentally friendly technique for solvent extraction. The advantages of using Sc-CO_2 for GSL extraction from *Eruca sativa* leaves over conventional methods have been recently reported.[237] A mixture of Sc-CO_2 and water allowed efficient extraction of GSLs from the plant materials, with a recovery of 64% of the total GSL amount originally present. The recovery yield remained stable at the temperatures ranging from 45 to 75 °C at a constant pressure of 30 MPa. Moreover, the substrate selectivity of the extraction could also be controlled. For instance, by increasing the pressure from 15 to 30 MPa, GSLs were selectively recovered over the polyphenols, which were more favorably extracted at lower pressures. Despite the lower extraction yield compared to the conventional method using boiling water, Sc-CO_2 selectively extracted GSLs from other secondary metabolites while preserving their bioactivities.

Accelerated solvent extraction is a technique carried out under pressure and an inert atmosphere that allows a range of extraction temperatures from 35 to 200 °C. It has been shown that ASE quantitatively enhanced the recovery yields of hydrocarbons from reference materials.[238] This technique has also been applied to recover GSLs from *Isatis tinctoria* leaves.[162] The extraction conditions were optimized with respect to raw material particle size (0.5 mm), temperature (50 °C), extraction solvent (70 % methanol in water), and extraction time (three 5 min. extraction cycles). The recovery yield of the

study was reported to be over 97 %, although it was noted that GSL degradation was observed when the extraction temperature exceeded 50 °C. This information underscores the thermal sensitivities of GSLs during the extraction process. ASE was also employed to extract GSLs from *Lepidium sativum*.[239] In this study, however, the method did not show any recovered yield advantage as compared to the conventional maceration extraction technique. Moreover, the recovered GSLs appeared to be less efficient in reducing the bacterial growth compared to those obtained by other extraction techniques. This observation suggested that the partial degradation of GSLs occurred during the extraction process, which led to lower biological activities.

As GSLs are recovered along with other water-soluble components from the biomass such as proteins and phenolic compounds, a selective GSL extraction method is desirable in order to isolate these metabolites efficiently. Conventional solvent extraction using water-alcohol mixtures is often used due to its simplicity, speed and cost-efficiency, as well as a high recovery rate of GSLs; however, the extract must often be subject to downstream purification chromatographic processes, which is time-consuming and costly. Performing the extraction using intensified techniques such as ultrasound accelerated extraction, Sc-CO_2, or ASE has been found to be advantageous over conventional method in terms of time, solvent consumption, and energy efficiency. In addition, the selectivity of these extraction methods with respect to GSLs are high and enable GSLs to be efficiently isolated from other components of the biomass. Unfortunately, these intensified processes still are too costly for common use in industry.

Purification and Separation of Glucosinolates

Isolation of GSLs from the aqueous extracts described above can be arduous as these metabolites are extremely hydrophilic. An early reported isolation of sinigrin from rapeseed devised by Thies took advantage of the ionic nature of GSLs.[234] Targeted GSLs were adsorbed onto a weak anion-exchange resin (DEAE Sephadex A25). The bound GSLs were then eluted by adding a high concentration of potassium sulfate solution. The eluate was concentrated under vacuum, and then further purified using a weak cation-exchange resin (CM Sephadex C25). The eluate obtained from the second purification was subsequently concentrated and recrystallized to afford a pure, solid GSL fraction. Sinigrin and glucotropaeolin with high purity have been isolated on gram scales by employing this method and it was recently employed by Wang et al.[240] The adsorption/desorption of negatively charged GSLs was performed on macroporous ion-exchange resins. The process successfully recovered sinigrin, the main GSL in *Brassica juncea* L., with 58% purity and a recovery rate near 80%.

Most GSL separation methods rely on chromatographic techniques. Charpentier et al. have separately isolated progoitrin and gluconapin using chromatography on alumina.[241] The recovery yields have been reported to be 96% and 98% from the aqueous extract for progoitrin and gluconapin, respectively. By employing preparative scale HPLC, Rochfort and coworkers have developed an isolation process that provided 17.6 mg of pure glucoraphanin from 3 g of broccoli seeds.[242]

High speed counter-current chromatography (HSCCC) is a hybrid technique that combines liquid chromatography and liquid-liquid counter-current distribution in conjunction with the use of centrifugal force.[243] Fahey et al. have successfully separated different GSLs from broccoli seed extract by employing this technique.[244] The partition

coefficients of the immiscible solvents are crucial in order to successfully separate similar GSLs. The optimal solvent system was determined to be 1-propanol / acetonitrile / saturated aqueous ammonium sulfate / water in a ratio of 1 / 0.5 / 1.2 / 1. Separation of different GSLs in the extract was achieved along with high recoveries (over 88 % of recovered yields).

Although conventional techniques employing liquid chromatography enable the isolation of individual GSLs with high purities, these processes demand precise and high-cost instruments, operating systems, columns, and a large amount of high-salt and high-polar solvents along with high energy and time commitments. By contrast, batch adsorption onto an ion-exchanger resin allows a straightforward purification of total GSL that is rapid and can be performed on an industrial scale. The drawnback is that this method does not allow for a facile separation between different GSLs residing in the extract. When selecting a purification method, the downstream applications of the isolated GSLs must be carefully considered.

Characterization of Glucosinolates

Glucosinolates, once recovered and purified from plant materials, can be characterized. Their qualitative characterization is mainly conducted using liquid chromatography tandem mass spectrometry.[22,241,245] NMR spectrometry is often used as the ultimate confirmation since its allows for unambiguous determination of GSL structures.[22,246] Other characterization techniques have also been used to complement these analytical methods. Crystallization enabled the structure determinations for both glucoiberin[247] and sinigrin[248] by X-ray analysis. These are the only GSL crystal structures that have been documented, to the best of our knowledge. Fourier-transform

infrared spectroscopy analysis is often used to confirm the presence of the sugar moiety, which is considered to be a characteristic of these metabolites.[245,249]

A desulfation procedure is often employed to determine glucosinolate structures.[230,233] The intact GSL is initially immobilized on an anion exchange resin by interactions with negatively charged sulfate group. Applying *Helix pomatia* sulfatase directly to the resin removes the sulfate groups localized on aglucone moiety of bound GSLs. The desGSLs are then released from the anion ion resin and eluted by flushing the cartridge with ultra pure water. Analysis of the desGSL derivatives permits one to deduce the corresponding original GSL structures.

While the desulfation procedure can to distinguish between different isomers of several GSLs[250], it is not a universal approach for characterizing GSLs. Some desGSLs are less stable, which leads to analytical difficulties.[194] Also, GSLs with negatively charged side chains cannot be characterized by the desulfation procedure as it is impossible to elute these desGSLs from the anion exchange resin due the remaining negative charge on the side chain.[22] Despite these disadvantages, this method is still employed and approved by current reviewers.[230]

For complete characterization, spectral data should include at least ^{1}H NMR, MS, IR. Additional spectroscopic data, such as ^{13}C NMR, MS-MS, and elemental analysis are also highly useful. Although the desulfation procedure followed by conventional analysis remains the typical method for GSL identification, this approach still has limitations regarding the stability of the desulfated products and other issues involving the diversity of GSL side chains. Moreover, desulfation is time consuming. It would

therefore be useful to be develop new analytical tools to expand our scientific understanding of these metabolites.

Structure and Classification of Glucosinolates

GSLs are anions composed of thiohydroxymates carrying an S-linked *β*-glucopyranosyl residue and an *N*-linked sulfate bearing an amino acid derived side chain, which is referred as “R group” in the general structure Figure 4-1. This side chain is subject to broad structural variation, which is likely associated with variations in biological functions[22]

GSLs are frequently classified into three main families based on the nature of these amino acid components, namely “aliphatic”, “aromatic” and “indole”.[210] However, that classification is thought to have little biological and chemical significance according to the recent review by Blazeviˇc and coauthors.[22] These authors introduced a classification system based on amino acid precursors. In their review, over 130 identified and validated GSLs have been classified into 9 panels from A to I, depending on three main criteria: 1) the amino acid precursor, 2) the type of degradation product, either volatile or non-volatile Isothiocyanates (ITC) or oxazolidine-2-thione; and 3) the presence and absence of an aromatic moiety in the GSL. Table A-2 gives an example to how GSLs are classified according to these criteria.

The newly proposed criteria offer a reliable system for GSL classification based on chemical and biochemical properties of GSLs and their degradation products while conserving the information related to their amino acid precursor. The criterion concerning the presence or absence of an aromatic moiety in the GSL is meaningful as it allows one to quickly separate a large amount of GSLs while using UV detectors. The usefulness of this criterion was demonstrated by the authors by separating GSLs for

which Phe, Tyr, and Trp are precursors, from other non-aromatic groups. A further subgrouping within aromatic group that separates indolic GSL from other phenylalkyl and less common aromatic GSLs appears to be useful.

Stability of Glucosinolates

Effects of Processing Methods on Glucosinolate Profile

Beside chemical degradation involving the MYR-catalyzed hydrolysis, the thermal degradation of GSLs also occurs.[190,191,251] As a result, GSL profiles of cooked *Brassica* vegetables are altered at different levels depending on the culinary techniques employed, such as cooking, steaming, and microwaving. Reduction of red cabbage (*Brassica oleracea*) indolic GSL during the cooking process has examined.[253] The content of glucobrassicin (Structure shown in Figure 4-9) and its homologs drastically declined during cooking below 120 °C. On the other hand, aliphatic GSLs appeared to be more stable, and only a slight degradation has been observed under the same cooking conditions. The degradation became drastic for all GSLs under canning conditions, where the processing temperature exceeds 120 °C. The total amount of GSLs was reduced by over 70% under these harsh conditions. These observations allow some conclusions with regards to differences between the thermal stabilities of aliphatic and indolic GSLs.

A study conducted by Song and Thornalley also investigated the thermal degradation of GSLs due to domestic processing of *Brassica* vegetables, such Brussel sprouts, broccoli, cauliflowers, and green cabbage.[252] Moreover, the effects of cooking methods such as microwaving, steaming, and stir-frying on GSL amounts were also investigated. Cooking by these methods did not significantly decrease GSLs, in contrast to boiling, which showed significant losses by leaching of GSLs into the cooking waters

at high temperatures.[190] Thus, boiling *Brassica* should be avoided in order to preserve intact GSLs in raw materials.

A recent study on the roasting process of rapeseed seed showed that industrial scale post-harvest treatments, which are often necessary to produce higher quality oil related products, impact the GSL profile of the plant materials.[251] Up to 29% of the original GSL amount in plant materials were lost during the roasting process. The industrial scale roasting processes reduces the GSL content mainly by thermal degradation, and up one third of GSL are degraded by this route.

Based on the information described above, we suggest that, with regards to downstream purposes, the selection of plant material should rely on the processing method. Although thermal treatments of plant materials reduce the GSL content, these are also beneficial for food and feed applications. If GSLs are desired for non-food purposes, thermal treatments should be avoided. We highly recommend the review by Hanschen and coauthors[253] for further information concerning the reactivities and stabilities of GSLs and their breakdown products in food.

Degradation of Glucosinolates in Solution

The stabilities of GSLs and desGSLs from *Moringa oleifera* in solution were investigated with the presence and absence of buffers.[235] The GSLs extracted from plant materials, either desulfated or intact, were dissolved in ultra-pure water and stored at room temperature or -20 °C. After 9 days of storage, the GSL profiles of the extracts were analyzed. The results showed that GLSs were stable at low temperature with little isomeric conversion or degradation.

By contrast, GLS solutions stored at room temperature showed significant conversion among acetylated GSL isomers. Furthermore, degradation of GSLs has

been reported to be up to 32 % of the original level. At room temperature, buffered solutions of GSL appear to be more stable than those in pure water, with a reduction of 20 % of the total amount of GSL recorded over 9 days. There was no significant difference between unbuffered and buffered GSLs stored at low temperature. Based on these results, we suggest storing GSL solutions under buffered conditions and at low temperatures (preferably -20 °C) in order to safely preserve the original GSL profile. It should be noted that GSLs are even more stable when stored as solid salt forms.

Biological Activities of Glucosinolates

Mechanism of Myrosinase

Glucosinolates play an important role in the defense mechanism of *Brassica* plants. Upon tissue disruption, catabolites released by myrosinase-catalyzed hydrolysis are frequently responsible for the toxicity of the parent GSLs whose intact forms, by contrast, are biologically inactive.[254,255] This mechanism of prevention against herbivory feeding suggested that this is the main function of GSLs in plant defense systems.[206]

Intact GSLs are stored separately from the thioglycosidase MYR. The latter catalyzes the hydrolysis of GSL upon plant tissue disruption. As described in Figure 4-1, an unstable aglucone moiety is released along with the glucose during hydrolysis. The aglucone moiety then undergoes further transformation to yield a number of metabolites.

MYR belongs to the Glycosidase family (EC 3.2.1.-). Although it catalyzes *S*-glycosylation, the deduced amino acid sequences of MYR reveal strong similarities with several *O*-glycosidases.[256] Furthermore, MYR displays a retaining mechanism which is similar to that of family 1 *O*-glycosidases.[257] In order to elucidate the mechanism of MYR, Burmeister *et al.* has studied the crystal structure of MYR.[256,258] A substrate

analog complex was prepared by soaking the MYR crystals with 2-deoxy-2-fluoroglucosinolate (2FG) (Structure shown in Figure 4-9c). The results clearly showed that the 2-fluoroglucose moiety, released from the substrate upon myrosinase attack, was covalently bound to Glu 409 within the active site (Figure 4-9a). The crystal structure of the 2FG-MYR complex confirmed that MYRs are retaining glycosyl hydrolases.

Like most retaining glycosyl hydrolases, MYRs follow a conventional two-step mechanism: 1) formation of a covalent enzyme-substrate intermediate; and 2) the release of glucose via hydrolysis of the previously formed intermediate. The mechanism of the glucose hydrolysis step is described in Figure 4-10. The glycosylation begins with the introduction of GSL into the active site of MYR. The residue Glu 406 then binds to the glucose moiety of the substrate at the anomeric position, releasing aglucone moiety.

Ascorbic acid was identified as a coenzyme for MYR by Ettlinger et al.[259] Although nonessential for the catalyzed GSL hydrolysis[258], its presence enhances up to the glycosylation of MYR by up to 400-fold.[259] The ultimate step consists in the release of both ascorbic acid and glucose from the active site to yield the enzyme in its native conformation (Figure 4-11).

Hypothetical recognition role of sulfate group.

Although characteristic of GSL structures, the sulfate group in the aglucone moiety exhibits an unclear function with respect to MYRs. A distorted conformation of GSL due to the interaction of the sulfate group with an active site amino acid side chain of MYR within its active site has been noted.[258] Based on these results, it was hypothesized that myrosinase recognizes GSL substrates via the sulfate group.

Attempts have been made to rationalize the role of the sulfate group in GSL recognition by MYR based on the feeding pattern of crucifer specialist insects. The investigation on the feeding pattern of *Plutella xylostella* larvae by Ratzka et al. suggested that the removal of the sulfate group rendered GSLs invisible to MYR.[260] Furthermore, several studies have shown that removing the sulfate group of GSL allows specialist insects to feed on crucifer plants.[261–263]

These observations support our hypothesis regarding the recognition role of sulfate group within the defense system in crucifer plants. However, there is, to date, no further research article investigating on the sulfate group of GSL since the publication of the crystal structure of *Sinapis alba* MYR by Burmeister et al.[256,258] Further investigation on the substrate recognition mechanism of MYRs will likely confirm the role of the sulfate group.

Reconfiguration of unstable aglucone

As described previously, an unstable aglucone moiety of GSL is released along with a glucose unit upon MYR-catalyzed hydrolysis. A number of biologically active compounds are obtained further reactions of this unstable aglucone.[190] ITC, the most studied among GSL catabolites, is formed via a spontaneous Lossen rearrangement of the corresponding aglucone under physiological conditions (Figure 4-10).

An additional range of bioactive non-ITC catabolites from MYR-catalyzed hydrolysis have also been identified.[190,264] Sinigrin is the only known GSL that can form an ITC along with other products such as nitriles, epithionitriles and thiocyanates (Figure 4-10). Their formation is dependent on the allyl structure of the aglucone, as well as by protein specifiers.[265] It is noteworthy that these catabolites are also formed in *in vitro* at low pH in the presence of ferrous ions but in the absence of specifier-proteins,

albeit in low yields.[264] These finding highlight the pH dependence of catabolite formation in downstream reactions of GSL aglucones.[22]

Biological Activities of Glucosinolates and their Catabolites

Negative effects of GSLs on domestic animals have been documented by Tripathi and Mishra in their review.[23] These effects usually occur upon assimilation of GSLs at high concentrations. Among relevant symptoms, reduction of feed intake which causes growth depression, and induction of iodine deficiency are often reported.[266,267] Moreover, high GSL diets eventually result in higher mortality in pig, rat, and rabbits.[23] As such, an intake limit of GSLs should be defined in order to avoid the occurrence of unexpected negative effects.

To the best of our knowledge, there is no clear evidence in the literature that documents a negative effect of GSL assimilation on human health. Indeed, GSL catabolites such as ITCs, and nitriles have been proved to provide attractive therapeutic effects such as inducing of phase II enzymes.[195] Increased tissue levels of the phase II detoxification enzymes is associated with decreased susceptibility to chemical carcinogenesis.[31] In their study, Munday and Munday observed an increase in phase II detoxification enzymes, such as quinone reductase and glutathione *S*-transferase in rat tissues by daily oral-assimilation of different ITC compounds.[195] These authors therefore suggested that chemoprotective effects are common to ITC.

GSL catabolites are potent inhibitors of bacterial activity.[33] Although intact GSLs are usually bio-inactive[23], allyl ITCs exhibit antimicrobial activities. By studying the effect of allyl ITCs on *Staphylococcus aureus*, a methicillin-resistant bacteria which causes purulent skin and soft tissue infections, Dias and coworkers concluded that these

molecules derived from GSL hydrolysis possess strong antimicrobial activity against these specific bacteria.[32]

Biofumigation is a process where plants are used as natural “pesticides” to reduce soil-borne pests and pathogens. The biofumigation properties of GSLs and their breakdown products have been investigated by Haschen and coworkers.[268] In their study, the cultivation of *B. juncea* produced a significant amount of GSLs and their hydrolysis products, such as ITCs, and nitriles, and released them into the cultivating soil. Consequently, growth of bacterial community was inhibited. These results confirmed the fumigation properties of GSL, and their breakdown products.

In other circumstances, GSLs are catalytically hydrolyzed *in vivo* by supplementary proteins known as specifier proteins.[269] These promote the formation of non-ITC catabolites such as nitriles, epithionitriles and thiocyanates whose biological roles have been reviewed.[264] The coexistence of specifier proteins along with MYR suggests the adaptation of plants to circumvent the presence of natural enemies. For instance, favoring production of simple nitriles over ITCs upon herbivore damage may enable a better defense of *A. thaliana* against the specialist herbivores.[270]

Conclusion

Recently, GSLs and their breakdown products have been studied extensively with regards to their therapeutic and agricultural benefits. The diversity of side chains, with over 130 GLS structures discovered to date, along with their abundance presence in *Brassica* plants, makes these metabolites interesting for natural product chemistry, biochemistry and biology.

Despite the advanced development of synthetic approaches, extracting naturally occurring GSLs from corresponding plant materials remains the method of choice to

obtain many molecules of interest. On the other hand, extraction approaches have several drawbacks that must be overcome before they can be employed routinely at the industrial scales. The high hydrophilicity of GSLs makes their separation from the aqueous extract difficult by conventional extraction method. In addition, the purification and characterization of individual GSLs often requires advanced chromatography techniques which exact a high cost in time and labor. As a result, a more straightforward, accessible, and sustainable extraction method should be developed.

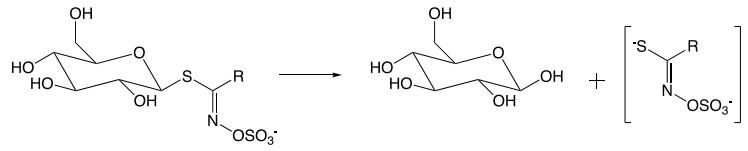

Figure 4-1. Hydrolysis of GSL by MYR upon tissue disruption. (R = alkyl, aryl, indole).

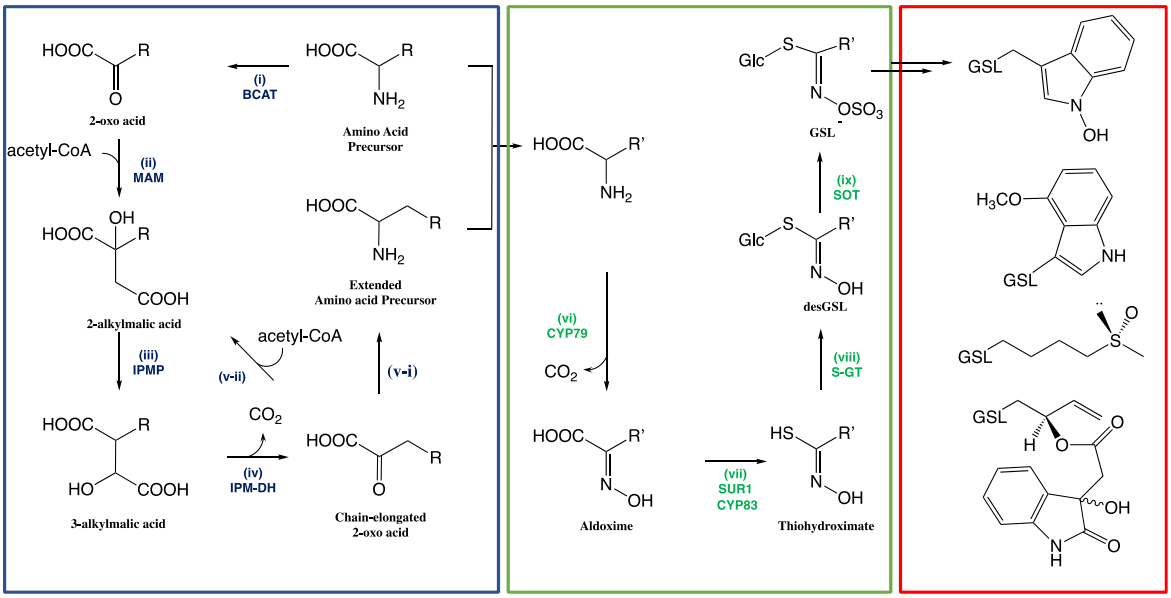

Figure 4-2. Three separate phases of glucosinolate biosynthesis: R indicates the variable amino acid precursors, and R' indicates either original or extended amino acid. The blue box indicates the chain elongation phase, the green box indicates the reconfiguration phase yielding the core structure of glucosinolate, and the red box indicates the glucosinolate side chain modification phase of the glucosinolate core structure with some structural examples from Table A-2. The figure was adapted from the biosynthesis of GSL proposed by Graser and coworkers.

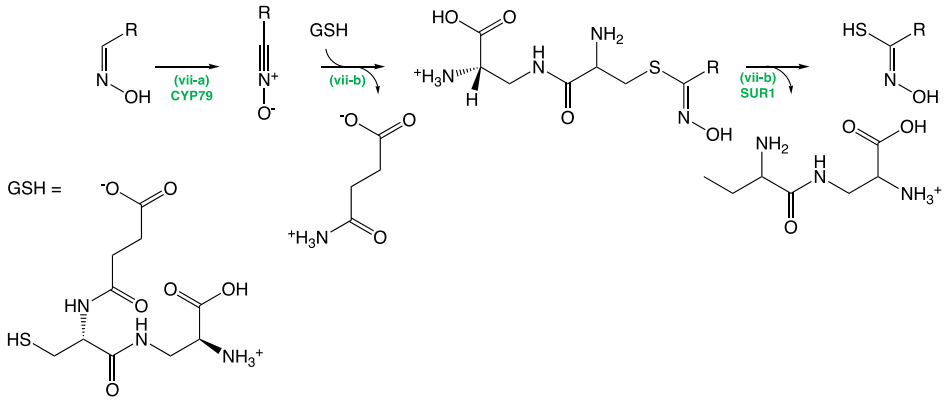

Figure 4-3. Conversion of aldoximes to thiohydroximic acids. GSH: Glutathione.

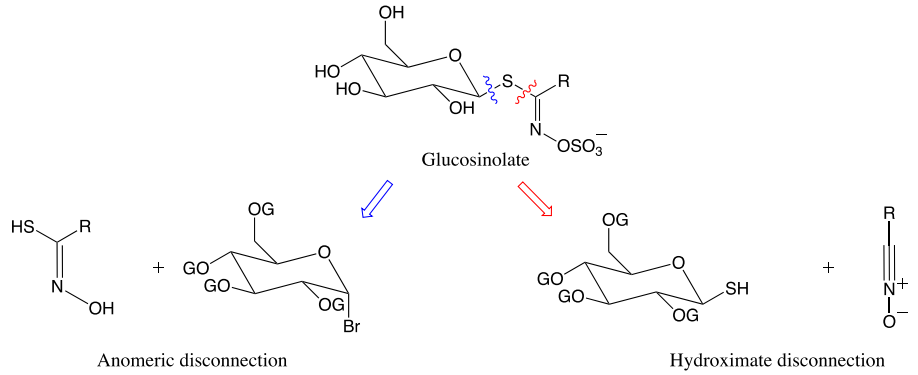

Figure 4-4. Retrosynthesis approach to GSL synthesis: anomeric disconnection (blue), hydroximate disconnection (red). OG represent suitable protecting group.

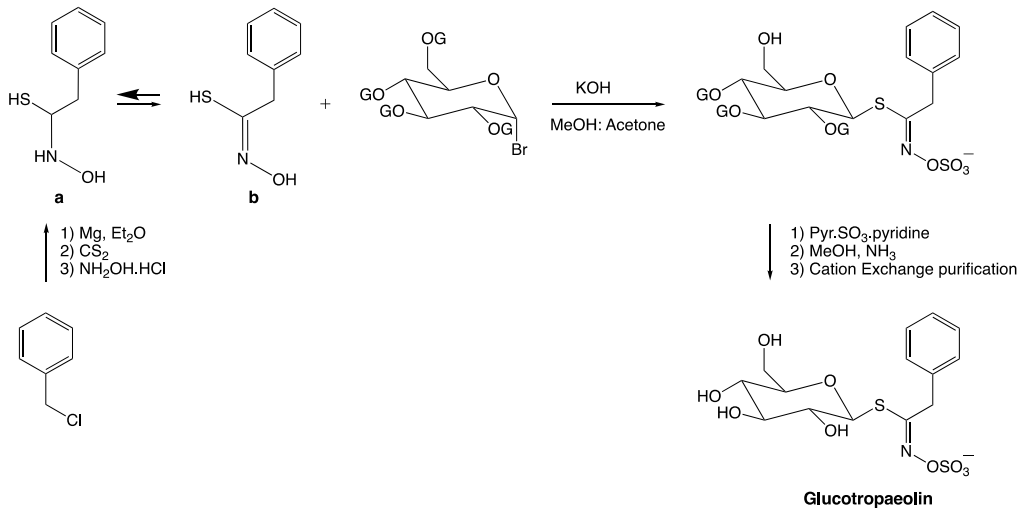

Figure 4-5. Synthesis of glucotropaeolin. OG represent suitable protecting group.

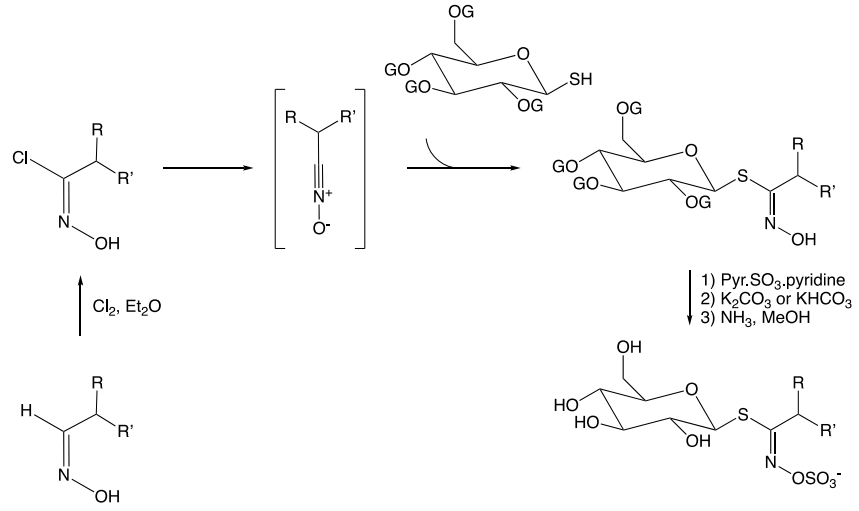

Figure 4-6. Synthesis of GSL following the aldoxime pathway. (R, R' = H, alkyl and aryl)

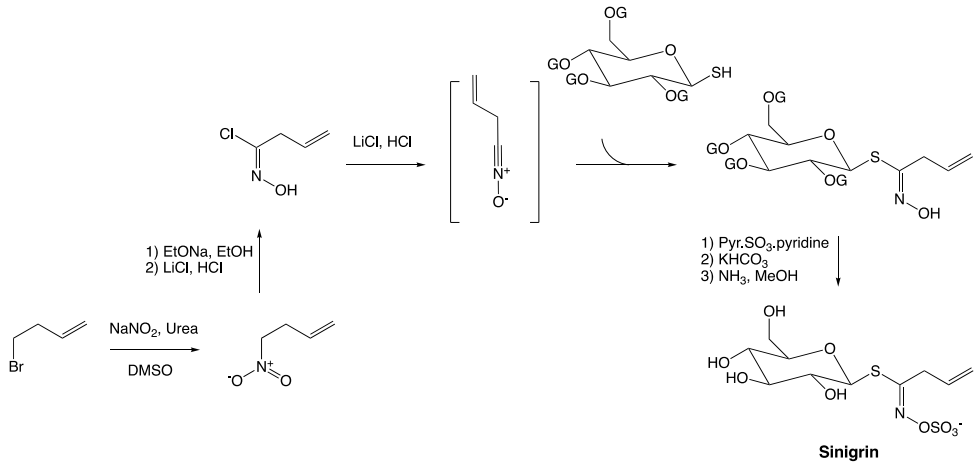

Figure 4-7. Synthesis of sinigrin employing nitronate pathway.

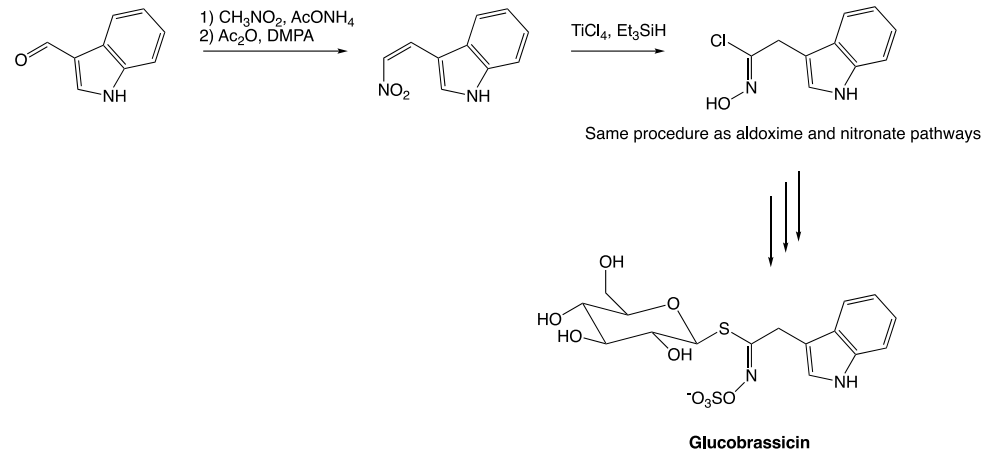

Figure 4-8. Synthesis of glucobrassicin.

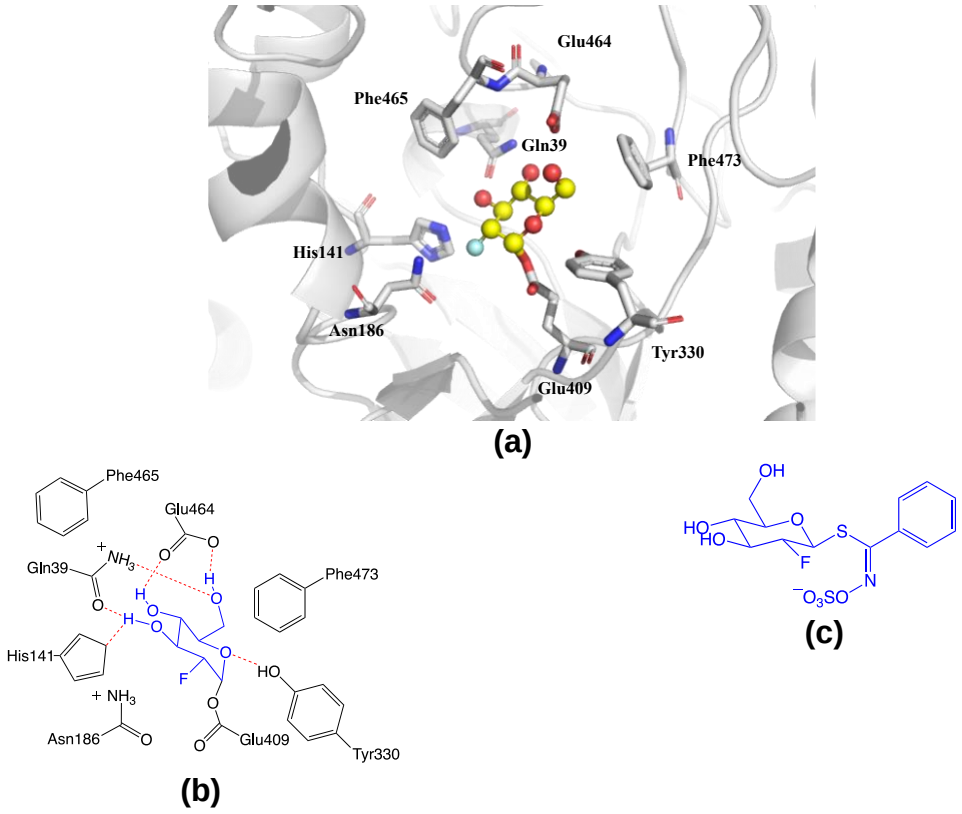

Figure 4-9. Overview of the active site of *Sinapis alba* Myrosinase showing interactions between residues and the 2-deoxy-2-fluoroglucosinolate (2FG) as substrate (PDB accession number 1E70, resolution: 1.65 A). Red dashed lines show hydrogen bonding interactions between the substrate and MYR residues within the active site. *(a)* PyMOL representation. *(b)* Chemical structure representation of the MYR-2FG. *(c)* Structure of 2-deoxy-2-fluoroglucosinolate.

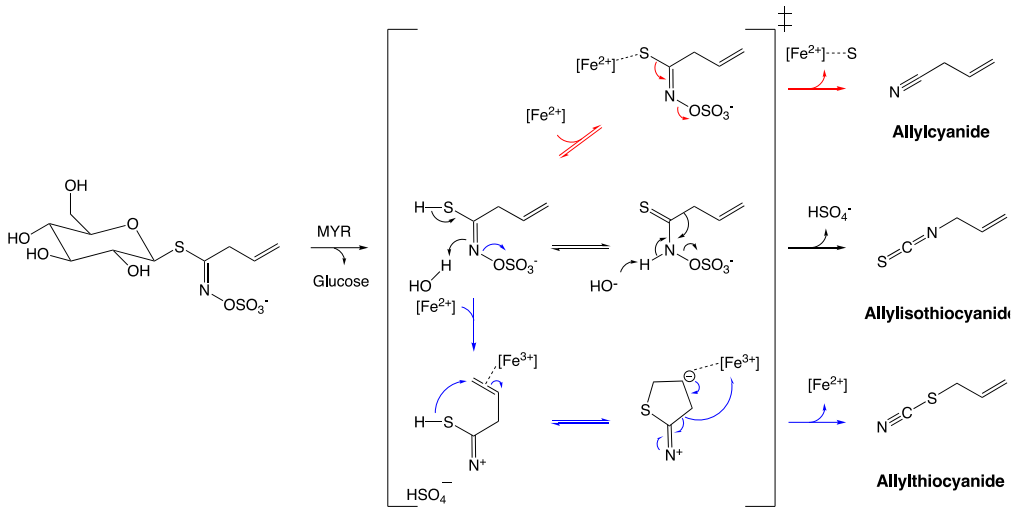

Figure 4-10. Reconfiguration of unstable allylglucosinolate aglucone upon myrosinase-catalyzed hydrolysis. Black arrow pathway shows the formation of allylisothiocyanates employing spontaneous Lossen arrangement. Blue arrow pathway shows the formation of allylthiocyanate assisted by protein specifier. Red arrow pathway indicates the formation of allylcyanide assisted by protein specifier.

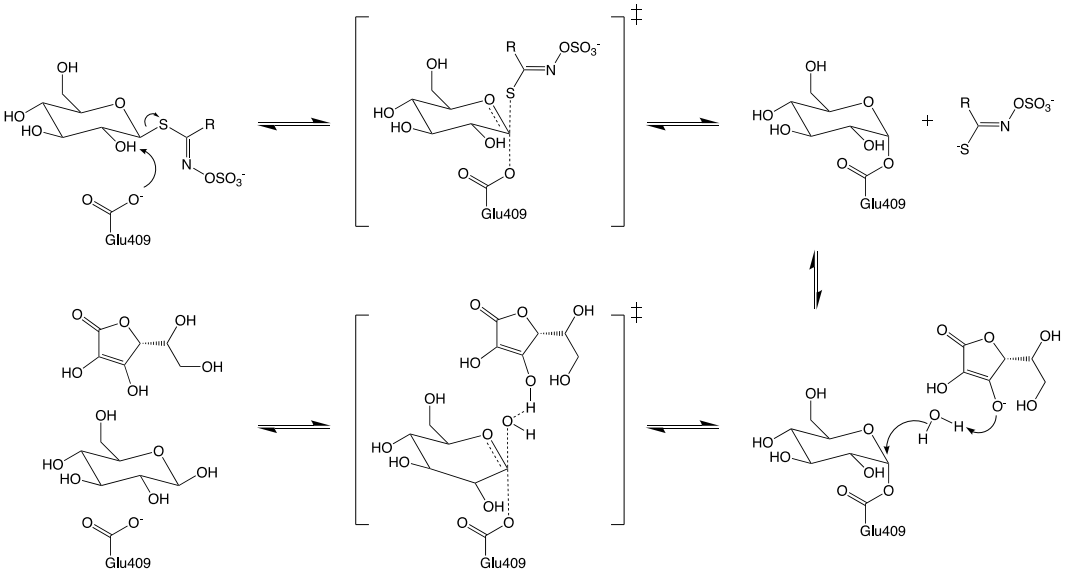

Figure 4-11. Schematic reaction mechanism of Myrosinase in the presence of ascorbic acid.

CHAPTER 5
ISOLATION OF PROTEINS AND SECONDARY METABOLITES

Introduction

Historically cultivated in the Ethiopian highlands and adjoining areas of East Africa and in Mediterranean regions, *Brassica carinata* (referred as Carinata) is a nonfood oilseed crop with high oil content rich in erucic acid, which is suitable for aviation biofuel production.[271] Cultivating Carinata in the southeast regions of the USA is believed to be economically and ecologically beneficial for local farmers by improving the soil nutrient and moisture conservation during winter seasons.[6] Although the main purpose of such cultivations is to support bio-fuel production, the residual meal still contains valuable components such as proteins and secondary metabolites.[7,16]

The defatted Carinata meal obtained after oil extraction could constitute an important protein source. The nutritional value of Carinata is similar to that of rapeseed (*B. napus*), which is considered to be well-balanced for human nutrition.[15,18,34] The nutritional value of Carinata is furthermore comparable to that of other plant-based proteins (soybean, sunflower), and even certain animal based proteins (casein).[16] It should be noted that these proteins also have functional properties of great interest[54,59], for many applications.[60,61] The secondary metabolites of Carinata meal are mainly phytic acid, PCs, and GSLs.[18,272] Although therapeutic benefits of these molecules have often been mentioned[18,24,29,33], they also exhibit anti-nutritional activities at high concentrations, and thereby decrease the nutritional value of meal or protein extracts.[17,18] An additional separation step is, therefore, required to remove secondary metabolites from protein extracts. This process must have a high separation efficiency

without altering the biological activities and functional properties of each category of the molecules.

Sustainable and environmentally friendly recovery of bioactive molecules from biomass is attracting ever-increasing attention.[144] The recovery of these metabolites from agro-industrial wastes using aqueous alcohol extraction has become popular.[100,147,150,272,273] Although aqueous methanol has traditionally been used to recover phenolic compounds from biomass[96,103], aqueous ethanol (AE) has become more attractive because of its low toxicity.[100,147] Nevertheless, such an extraction process often involves the use of alcohol at high concentrations and/or the use of high temperatures, which can partially alter the solubility and functional properties of proteins due to structural changes.[42,274] To our knowledge, very few studies have focused on the extractability and functional properties of the proteins contained in the meal after an AE extraction. Indeed, only one study on rapeseed meal has been reported.[274] The effect of AE extraction was studied under defined conditions (70% EtOH/ultrapure water, room temperature), and this produced an 11% decrease in protein extractability. Hence, the originality of our approach is to propose an enhanced study on the effects of AE extraction on the proteins of Carinata meal according to operating conditions using the Response Surface Methodology (RSM).

In the context of double valorization of Carinata meal, our approach is based on a 2-step fractionation: an AE extraction to recover secondary metabolites followed by an alkaline extraction to obtain protein extracts. The first part of our approach focuses on optimizing the AE extraction to recover secondary metabolites from Carinata meal (sinapine and sinapic acid as PCs, and sinigrin as GSLs) using RSM. The effects of AE

extraction on protein extractability were then investigated, focusing on the protein concentration obtainable and the polypeptide profile of the extracts. Finally, optimizing the operating conditions for the AE extraction process made it possible to obtain not only high concentrations of PC, but also highly extractable proteins. These operating conditions were a compromise in order to maximize each of the three criteria. The effect of these conditions were evaluated with respect to the functional properties of the proteins extracts.

Materials and Methods

Chemicals

Sinigrin hydrate and sinapic acid used as external standards were purchased from Sigma-Aldrich. Pure synthetic sinapine chloride was synthesized in our laboratory and used as standard for HPLC analyzes.[100,136] The ethanol solution used for extraction was purchased from ThermoFisher. Formic acid and acetonitrile (both LC-MS grade) for HPLC analysis were purchased from ThermoFisher. MilliQ water was produced by Milli-Q Direct 8 from Merck Millipore (Burlington, USA).

Carinata Meal Samples and Their Characterization

Hexane-solvent extracted Carinata meal was provided by Dr.Nicolas DiLorenzo (IFAS/UF). The meal was ground, passed through a 30-mesh screen (500 microns), and stored at -20 °C until use. The water content of the meal was determined to be 88.8 ± 0.38 mg/g of Carinata meal using a standard moisture analyzer (MB35-OHAUS™). Ash and protein contents were determined to be 72.0 ± 0.2 mg/g of dry matter (mg/g_{DM}) and 499.1 ± 1.7 mg/g_{DM}, respectively, using AOAC approved methods.[275] Soluble carbohydrates corresponded to 74.7 ± 3.7 mg/g_{DM} using the protocol described by Dubois et al.[276] The concentration of phytic acid was 7.6 ± 0.4 mg/g_{DM} using the

colorimetric method described by Reichwald and Hatzack.[277] The remaining mass corresponds to fibers and secondary metabolites, including PCs and GSLs. These chemical compositions are similar to those of defatted Carinata meal reported by other studies.[13,16]

Fractionation Process of Carinata Meal

The fractionation process involves two successive extractions as shown in Figure 5-1.

Five grams of defatted *B. carinata* meal was extracted with 50 mL of a mixture of EtOH/MilliQ water for 1 h at 300 rpm. The EtOH concentration and the extraction temperature varied according to the design of experiments presented below. The slurry was centrifuged for 20 min at 4000 rpm and 25 °C (Allegra X15-R from Beckman Coulter). After centrifugation, the supernatant (henceforth referred as the AE extract) and the residual meal (pellet) were recovered. The AE extract was evaporated under vacuum to remove EtOH. The concentrated liquid was freeze-dried, weighed, and stored at room temperature. The concentrations of sinapine and sinigrin in the AE extracts were determined along with the nitrogen solubility and the polypeptide profile. The residual meal was air-dried overnight (referred as treated Carinata meal), and then stored at 4 °C for a maximum of 2 days prior to alkaline extraction.

Alkaline extraction was performed by following the method of Pedroche with slight modifications.[16] In brief, treated Carinata meal was extracted with 50 mL of 0.1 M KOH at 300 rpm for 30 min. The slurry was centrifuged for 20 min at 4000 rpm and 25 °C. After centrifugation, the supernatant (protein extract) and the pellet (exhausted meal) were recovered. The protein extract was freeze-dried, weighed, and stored at room temperature. The same analysis used previously for the AE extracts was also

carried out on the protein extracts. The control is represented by protein extract obtained from the original Carinata meal by alkaline extraction (with no prior AE step).

Determination of Phenolic Compound and Glucosinolate Concentrations

HPLC quantification of PCs was performed as previously described[100] on a UHPLD-DAD system (Ultimate 3000, Dionex, ThermoFisher) equipped with a quadratic pump, auto sampler, column furnace and diode array detector. Data were analyzed with Chromeleon software (Version 6.8).

The GSL content was determined following procedure described by Grosser and van Dam with some modifications.[230] Samples were diluted ten times prior to the desulfation step. One millileter of sample was loaded onto a glass pipette preconditioned with 0.5 mL of Sephadex A25 0.1 mg /mL in MilliQ-water. 2 × 1 mL of MilliQ-water was used for washing. The column was next washed with 2 × 1 mL of acetate buffer (40 mM, pH 5.5). Twenty microliters of cleaned-up *Helix pomatia* sulfatase solution (Sigma-Aldrich, S9626) was added onto the column following by flushing with 50 μL of acetate buffer. The column was incubated at room temperature prior to eluting with 2 × 1 mL of MilliQ-water. The eluted fraction was then analyzed by HPLC.

Determination of Protein Concentration of AE Extracts

The protein concentrations of AE extracts were calculated based on the nitrogen solubility according to the AOAC approved method and is shown in Equation 5-1.[275] Nitrogen solubility (%N) of freeze-dried AE and protein extracts were determined using the Dumas method and performed by UMR 614 Institut National de la Recherche Agronomique - Université de Reims Champagne-Ardennes (INRA-URCA) as a commercial service.

$$C_{protein} = \frac{\%N \times 6.25 \times m_{\text{lyoph extract}}}{m_{DM}} \quad (5\text{-}1)$$

Where %N is the nitrogen concentration of freeze-fried extracts determined by combustion following the Dumas method (%). $m_{\text{lyoph extract}}$ is the mass of freeze-dried supernatant (g), m_{DM} is the mass of dry matter in Carinata meal (g).

Analysis of Polypeptide Profile

The polypeptide profile of AE and alkaline extracts was analyzed using electrophoresis. Sodium dodecyl sulfate polyacrylamide gel electrophoresis (SDS-PAGE) was carried following standard procedure under non-reducing conditions. In brief, around 10 mg of freeze-dried supernatant were dissolved in 1 mL of MilliQ-water, with vortex mixing to resuspend the solid. Fifteen microliters of this solution were mixed with 5 μL of 4 × Laemmli Sample Buffer (Biorad). The mixture was boiled for 15 min and cooled at room temperature for 30 min. Twenty microliter aliquots were then loaded onto the precast gradient gels (MiniProtein TGX 4-15% Strain Free, Biorad) along with15 μL of standard proteins (Spectra^{TM} Multicolor Broadrange, Thermo Fisher) was loaded onto the gel. Separation of samples was done for 1h at 20mA per gel.

Optimization of the AE Extraction of Secondary Metabolites

A D-optimal design was used to optimize the operating conditions of the AE extraction of secondary metabolites with a total of 13 experiments including a triplicate at the central point (Table 5-1). The independent variables used in this optimization were the concentration of ethanol (*%EtOH*, X_1) and extraction temperature (T_e, X_2). The significant contributions of *%EtOH* and T_e to the recovery yield of secondary metabolites were recently reported.[100,147] As a result, *%EtOH* and T_e were varied at four different levels (25, 45, 70 and 90%) and three different levels (25, 50 and 75 °C), respectively.

The limit was set at 75 °C in order to avoid loss of solvent by evaporation. Other solid-liquid extraction parameters including extraction time, solvent-solid ratio, extraction time and extracting materials particle size remain constant as these are thought to be non-significant in the context of our study.

Three responses were optimized: the phenolic compound concentration (Y_1), the sinigrin concentration (Y_2) and the extractability index of proteins (Y_3) of the AE extracts.

For some conditions, sinapine can be hydrolyzed to SinA. These two molecules correspond to the two main phenolic compounds in the Carinata meal. Thus, the PC measure included both the sinapine and the sinapic acid contributions. Y_1 is expressed according to the dry matter and calculated as shown in Equation 5-2:

$$Y_1 = \frac{\left(C_{\text{sinapine}} + C_{\text{sinapic acid}}\right) \times \left(m_{\text{extract}} \times d\right)}{m_{DM}} \quad (5\text{-}2)$$

Where C_{sinapine} is the concentration of sinapine in AE extract (in mg/mL), $C_{\text{sinapic acid}}$ the concentration of sinapic acid in AE extract (in mg/mL), m_{extract} the mass of extract (in g), d the volumetric mass density (g/mL), m_{DM} the mass of dry matter in Carinata meal.

The GSL concentration of AE extracts (Y_2) is expressed according to the dry matter and calculated as shown in Equation 5-3:

$$Y_2 = \frac{C_{GSL} \times \left(m_{\text{extract}} \times d\right)}{m_{DM}} \quad (5\text{-}3)$$

Where C_{GSL} is the concentration of GSL (as sinigrin) in AE extract (µmol/mL), m_{extract} is the mass of the extract (g), *d* is the volumetric mass density (g/mL) and m_{DM} the mass of dry matter in Carinata meal.

The impact of AE extraction on proteins mainly concerns their extractability (Y_3) in this optimization study. The protein concentration of the different extracts was

calculated according to Equation 5-1. By taking the protein concentration of the control (alkaline extracts from untreated Carinata meal) as the maximum concentration that can be extracted, we can define an index of extractability as described in Equation 5-4.

$$Y_3 = \frac{C_{protein} \times m_{extract}}{C_{protein\ control} \times m_{control}} \times 100\% \quad (5\text{-}4)$$

Where $C_{protein}$ is the protein concentration of alkaline extract from residual meal upon AE extraction (mg/g_{DM}), $m_{extract}$ is the mass of the extract (g), $C_{protein\ control}$ is the protein concentration of the alkaline extract from the control Carinata meal (mg/g_{DM}) and m_{DM} the mass of the control Carinata meal (g).

The experimental data were fitted using a second-order polynomial equation (Equation 5-5):

$$Y_q = \beta_0 + \sum_{i=1}^{2} \beta_i X_i + \sum_{i=1}^{2} \beta_{ii} X_i^2 + \sum \sum_{i<j=1}^{2} \beta_{ij} X_i X_j + \varepsilon_{residues\ q} \quad (5\text{-}5)$$

Y_q: the different responses (q = 1 - 3); β_0, β_i, β_{ij}, β_{ii}: regression coefficients for the mean, linear, interaction, and quadratic terms, respectively; X_i and X_j: independent variables. $\varepsilon_{residues\ q}$: the differences between the observed and the predicted values.

Experimental design and analysis were performed using the software MODDE v.12.0 (Umetrics AB, Sweden). An analysis of variance (ANOVA) with 95% confidence level was carried out for each response in order to test the model significance and adequacy. Effect plots presented the effect of each factor studied.

Determination of Optimal Operating Conditions

A software optimizer tool based on the Nelder-Mead simplex method was used to optimize recovery of secondary metabolites. On the other hand, the operating

conditions leading to a good compromise between the recovery of secondary metabolites and the protein extractability were estimated manually using Microsoft Excel (Version 16.43). Indeed, the Y_1, Y_2, and Y_3 responses varied antagonistically, and the MODDE optimizer tool was defeated. We have plotted graphs where Y_1, Y_2, and Y_3 values were calculated using prediction models according to the *%EtOH* and a fixed extraction temperature. Thus, six graphs were plotted for extraction temperatures ranging from 25 to 50°C in steps of 5. T_e was limited at 50 °C to avoid the dissociation of certain proteins such as cruciferin. The optimum zone, corresponding to the meeting points of the 3 models, was determined for each graph. The operating conditions corresponding to the compromise result from the fusion of all these optimum zones.

Functional Properties

Preparation of acid-precipitated isoelectric protein isolates

The protocol of Aluko and McIntosh was used to produce acid-precipitated isoelectric protein isolate for functional property analyses.[278] In brief, Carinata meal was extracted with 10 volumes of 0.1 M NaOH for 30 min at 300 rpm and room temperature. The slurry was then centrifuged for 20 min at 4000 rpm and 25 °C. The supernatant was then separated from the residue, then gradually adjusted to pH 4 using 1 M HCl. The precipitate was then recovered by centrifugation, washed twice with 10 volumes of MilliQ-water. The washed precipitate was next freeze-dried, weighed and stored at -20 °C until further analyses.

Emulsifying activity index

The emulsifying activity index (EAI) was determined following the protocol described by Aluko and McIntosh.[278] Protein solutions (1% w/v) were prepared in 0.01 M phosphate buffer (pH 7.0), and 5 mL was added to 1 mL of pure commercial canola

oil. The protein solution and oil phase were homogenized at 16000 rpm for 1 min using a T25 digital Ultra-Turrax (IKA-Works, Inc., Cincinnati, OH). Ten microliters of the emulsion were immediately diluted to 5 mL with 0.1% (w/v) SDS solution (0.1 g/ 100 mL), and the absorbance at 500 nm was measured using the 0.1% SDS solution as a blank. The EAI ($m^2.g^{-1}$) was calculated as described in Equation 5-6 according to the Pearce and Kinsella method.[279] The emulsions were allowed to stand at room temperature for 30 min, and the EAI was determined and expressed as a percentage of the initial EAI to obtain emulsion stability (ES).

$$\mathrm{EAI} = \frac{2 \times 2.303 \times \mathrm{A} \times \mathrm{N}}{\mathrm{C} \times \varphi \times 10000} \qquad (5\text{-}6)$$

Where A is the absorbance recorded at 500 nm, N is the dilution factor (×500), C the protein concentration before the formation of the emulsion (g/mL) and φ, the volume fraction of the oil (mL).

Foam expansion (FE) and foam stability (FS)

FE was determined according to the protocol described by Aluko and McItosh.[278] Ten milliliters of protein solution (1% w/v) prepared in 0.01 M sodium phosphate buffer (pH 7.0) were homogenized at 16000 rpm for 30s. The volume of foam obtained was expressed as a percentage of the initial volume of protein solution. FS was determined by measuring the volume of foam that remained after standing at room temperature for 30 min and then expressed as a percentage of the initial foam volume.

Statistical Analysis

Each analysis was done in duplicate. Results correspond to the mean associated to its standard deviation. Student's t-test, ANOVA, and post-hoc analysis using Tukey's test were carried out using RStudio (Version 3.6.1).

Results and Discussion

In a successful double valorization of Carinata meal, the extraction of secondary metabolites, carried out in the first step, must have a slight impact on the extractability and functional properties of the proteins obtained in the second extraction. In order to verify this impact, the extraction process of PC and GSL was optimized and the impact on proteins then studied.

Optimization of Aqueous Ethanol Extraction Using Response Surface Methodology

A D-optimal design was used to optimize the operating conditions for the AE extraction from Carinata defatted meal based on the secondary metabolite concentrations. Two independent variables *%EtOH* with four levels (25, 45, 70 and 90%) and T_e with three levels (25, 50 and 75 °C) were selected as factors. The responses upon optimization were Y_1 the PC concentrations, Y_2 the GSL concentration and Y_3, the extractability index of proteins.

Model adequacy

The D-optimal design constituted 13 extractions and multiple regression using polynomial second order were obtained for the responses. Analysis of variance (ANOVA) was conducted to determine the regression coefficients of each model. Table 5-2 summarizes the statistical parameters obtained in this study.

Coefficients were considered as significant for $p < 0.05$. Non-significant coefficients were removed to obtain reduced models. The coefficients of determination of the three prediction models indicated good model accuracy ($R^2 > 0.8$). The adjusted determination coefficients furthermore confirmed the adequacy of our established models (R^2 adjusted > 0.75). The orthogonality of all models was determined to be

good, as the condition numbers were inferior to 10. With good reproducibility values (> 0.8), the relationships between the variables and the responses were well described by these models.

Phenolic compound concentration in aqueous ethanol extracts (Y_1)

The concentration of phenolic compounds includes the concentration of PCs as described in Equation 5-2. Variations of Y_1 were found among the experiments of the D-optimal design and ranged from 7.26 to 11.33 mg/g_{DM}.

The model predicting the phenolic compound concentration with unscaled coefficients is shown in Equation 5-7.

$$\begin{aligned}\mathrm{Log}(Y_1) = {} & 0.6028 + 0.0090\ \%\boldsymbol{EtOH} + 0.0069\ \boldsymbol{T_e} \\ & - (6.3289 \times 10^{-5})\ \%\boldsymbol{EtOH^2} \\ & - (4.0226 \times 10^{-5})\ \boldsymbol{T_e^2} \\ & - (4.3260 \times 10^{-5})\ \%\boldsymbol{EtOH\ T_e}\end{aligned} \qquad (5\text{-}7)$$

The most significant terms in the model equation are the quadratic term for the ethanol concentration (*%EtOH*%EtOH*) and the interaction between the ethanol concentration and temperature (*%EtOH*T_e), which have a negative impact on the recovery of phenolic compounds (Table 5-2). These results are consistent with other studies. [100,146] Reungoat et al. showed that *%EtOH*%EtOH* leads to a negative effect on AE extraction of sinapine from mustard bran (-3 mg/g $_{DM}$).[100] In contrast to other studies[100,146], the quadratic term for T_e in this study is not significant. The use of different types of biomasses for the AE extraction was suggested to account for the difference observed. The effect of the linear term, T_e, on the other hand, is in agreement with the other studies.

The prediction model enabled us to determine that the highest concentration of phenolic compounds (over 10.2 mg/g_{DM}) is reached for a *%EtOH* varying from 40 to 70 %. In contrast, the recovery deteriorates for an extraction carried out with a %EtOH less than 40 % or greater 70%. A decrease of 1 mg/g_{DM} in phenolic compounds was noticed at these concentrations, as depicted in Figure 5-2.

Glucosinolate concentration in aqueous ethanol extracts (Y_2)

The concentration of sinigrin in the AE extract was a determinant factor for the outcome of the optimization. The model predicting the GSL concentration with unscaled coefficients is shown in Equation 5-8.

$$Log(Y_2) = 1.7708 + 0.0073\ \%\boldsymbol{EtOH} + 0.0028\ \boldsymbol{T_e} - (1.1128 \times 10^{-4})\ \%\boldsymbol{EtOH^2} - (3.2136 \times 10^{-5})\ \boldsymbol{T_e^2} - (2.6154 \times 10^{-5})\ \boldsymbol{EtOH\ T_e} \quad (5\text{-}8)$$

The quadratic term of ethanol concentration (*%EtOH*%EtOH*) had a negative effect on sinigrin recovery, whereas other parameters related to T_e did not significantly contribute to the recovery of this metabolite.

The GSL concentration followed the same trend as Y_1. Increasing T_e from 25 to 50 °C enhanced the recovery of sinigrin, increasing its concentration from 88 to 93 μmol/g_{DM} as depicted in Figure 5-2. These results were expected due to the use of a conventional sinigrin recovery process. Indeed, the latter being very hydrophilic because of the ionized sulfate and hydrophilic thioglucose moieties, a solid-liquid extraction with an alcohol/water mixture is adequate.[163,230] However, the GSL concentration appeared to be more sensitive to the change in *%EtOH* than the PC

concentration, with more than half the amount of GSL was reduced by increasing the *%EtOH* from 40% to 90%. The highly hydrophilic nature of GSL is responsible for this reduction of concentration in AE extracts.

Determination of the optimal conditions of aqueous ethanol extraction and validation of the prediction models

These results suggested that by AE extraction, PC and GSL can be simultaneously and optimally recovered from defatted Carinata meal. The optimal conditions, suggested by the MODDE software basing on the previously established models, were %EtOH = 47 % and T_e = 62 °C. Under these conditions, concentrations of PC and GSL were determined to be 11.74 ± 1.26 mg/g_{DM} and 103.61 ± 16.2 µmol/g_{DM} µmol/g_{DM}, respectively. These values are not statistically different from the observed values (10.87 ± 0.54 mg/g_{DM} and 98.96 ± 4.9 for the PC and GSL, respectively). Thus, the models developed to predict Y_1 and Y_2 can be considered valid.

Effects of Optimal Aqueous Ethanol Extraction on Carinata Proteins

Extractability of proteins resided in Carinata treated meal (Y_3)

Considering the characteristics of the proteins, their extractability can be influenced by the processes involved upstream from their extraction.[148] Thus, the effect of the AE extraction process of secondary metabolites on the extractability of proteins (Y_3) was studied and quantified using RSM. The model predicting the extractability index with unscaled coefficients is shown in Equation 5-9.

$$-Log(100 - Y_3) = -1.5924 - 0.0053\ \%\boldsymbol{EtOH} + 0.0042\ \boldsymbol{T_e} - (1.0742 \times 10^{-4})\%\boldsymbol{EtOH^2} - (1.3123 \times 10^{-4})\ \%\boldsymbol{EtOH\ T_e} \quad (5\text{-}9)$$

The quadratic term of ethanol concentration (*%EtOH*%EtOH*) had a positive effect on the protein extractability, whereas other parameters showed negative effects. Optimal zones to obtain a high extractability index of proteins are shown in Figure 5-3.

The prior AE extraction of the secondary metabolites decreased the extractability of proteins during the alkaline extraction, regardless of the operating conditions. The prediction model suggested that the AE extraction of secondary metabolites performed with a high *%EtOH* (> 80%) at low T_e (< 35 °C) allowed retaining a high extractability of the proteins (%). In order to better understand these results, the polypeptide profile of alkaline extracts was studied by SDS-PAGE analysis under non-reducing conditions (Figure 5-4). The main Carinata proteins included albumin (napin), and globulin (cruciferin), which are attributed to the bands at 15 kDa and 50 kDa, respectively.[18] The bands at 30 kDa correspond to free polypeptide chains dissociated from cruciferin.

Effects of optimal aqueous ethanol extraction on Carinata protein profile

The most important difference between the profiles of alkaline extracts obtained during the experimental design and the control was the change of the 50 kDa bands (cruciferins). At an extraction temperature of 75 °C, loss of these bands was observed (lanes 6, 12 and 13, Figure 5-4). Hence, cruciferin was either completely removed during the recovery of secondary metabolites or was dissociated when exposed to high temperatures during the EA extraction process.[96]

The optimum conditions for the AE extraction process, suggested by the MODDE software based on Equation 5-9, were *%EtOH* = 90% and T_e = 25 °C. Under these conditions, the EI of proteins during alkaline extraction was the highest and reached 76 ± 3.8%. No significant difference was found between the values predicted and observed (78.8 ± 0.7%.). Thus, the model predicting the EI of proteins is validated.

Unfortunately, these conditions were antagonistic for the recovery of secondary metabolites. Reaching a compromise leading to a high recovery of secondary metabolites while maintaining high protein EI is therefore discussed in the next section.

Determination of Operating Conditions for the Optimization of Y_1, Y_2 and Y_3

A 3D graph representing the responses (Y_1, Y_2 and Y_3) as a function of *%EtOH* and T_e was drawn in order to visualize the areas for which the recovery of secondary metabolites was maximal with minimal loss of protein extractability (Figure 5-5). The prediction model indicated a decline of protein extractability (Y_3) when a moderate *%EtOH* (40-60%) and moderate T_e (30-50 °C) were employed. This was due to the high recovery rate of proteins along with secondary metabolites during the AE step, which resulted in lower protein availability in the treated meal upon these operating conditions. The SDS-PAGE profile of AE extracts indeed supported this explanation (Figure B-6).

From the response surface plot generated by the experimental design software, it was difficult to define the precise operating conditions that would enable the best compromise between the three responses. This was due to complex antagonistic effects between the recovery of secondary metabolites and the protein extractability, as depicted in (a), Figure 5-5. However, a more precise evaluation could be done by working from 2D graphs. Consequently, the graphs representing the three responses according to the *%EtOH* varying from 20 to 90 % were plotted with fixed values of T_e. All graphs are available in Figure B-1. Figure 5-5b presents the evolution of Y_1, Y_2 and Y_3, for T_e = 50°C and *%EtOH* that ranged between 20 and 90%. For instance, optimal conditions for AE extraction were determined to use 20% EtOH. The responses under

these conditions were then calculated at different T_e ranged from 25 to 50 °C and reported in Table 5-3.

The optimal *%EtOH* and T_e determined on each graph were as expected ranging from 21% to 29% and from 25 to 50 °C, respectively. No significant differences were noticed for Y_2. However, for Y_1 and Y_3, the highest values were reached at 50 °C. Therefore, the operating conditions to simultaneously reach optimal values of the three responses were proposed (*%EtOH* = 21% and T_e = 50 °C). Extractions under these conditions were thus carried out to confirm our prediction and the results were as follows: Y_1 = 9.12 ± 0.05 (mg/g_{DM}), Y_2 = 86.54 ± 3.18 ($\mu mol/g_{DM}$), Y_3 = 59.8.X ± 2.1%. These results showed there was no significant differences between the predicted and observed values and hence validating our prediction model

Effect of the New Operating Conditions on Functional Properties of Carinata Proteins upon Aqueous Ethanol Extraction

Functional properties such as the foaming and emulsifying capacities of *Brassica* proteins are of great interest[45,54] and directly depend on their 3D structures.[18] According to the literature, these functional properties can be considered as significant indicators to determine the effect of AE extraction on proteins. The emulsifying activity index (EAI), emulsifying stability (ES), foaming activity (FA), and foaming stability (FS) of protein isolates from original meal and treated meal upon the selected extraction conditions previously (21% EtOH at 50 °C) are shown in Table 5-4.

EAI and FS values of protein isolates from both original and treated Carinata meal were not significantly different, according to the Student's t-test. Although the ES of original meal was significantly higher than that of the treated meal, this loss remained low considering the value of ES. Our results were consistent with the functional

properties of Carinata protein isolate pH 12 reported Pedroche et al.[16] The ES value, on the other hand, corresponded to that of a protein isolate prepared at pH 10 reported by other authors. These differences might be due to the difference between the analytical methods employed.

The FA of treated meal was higher than that of original meal, whereas the FS of both protein isolates were similar, which are also comparable to protein isolate from defatted canola meal.[54] These results suggested that the removal of secondary metabolites had modified the composition and, eventually the structure of proteins, which led to higher foaming capacity of protein isolate from treated meal.

Taken together; these results revealed that the functional properties of treated meal upon AE extraction of Carinata meal with 21% EtOH at 50 °C showed improved foaming activity while preserving other functional properties of protein isolates.

Conclusion

Optimization of AE extraction resulted in validated models based on selected factors and responses. These models predicted that extraction with low *%EtOH* at moderate T_e compromised the best balance between the efficiency of metabolites recovery from Carinata meal and the protein extractability of treated meals upon AE extraction, while preserving the functional properties of protein isolates. Although metabolites recovered from Carinata meal have not been individually separated in this study, preparative chromatography can be employed for this purpose.[272,273] Future work will, therefore, address the individual isolation of these bioactive molecules from AE extracts. Moreover, further study on Carinata proteins is ongoing in order to elucidate the structural changes caused by AE extraction.

Table 5-1.D-optimal experimental design.

Experiments	*%EtOH* (%) X_1	T_e (°C) X_2
0	0	25
1	70	50
2	20	25
3	70	50
4	20	50
5	45	50
6	20	75
7	70	25
8	70	50
9	90	25
10	20	25
11	90	50
12	45	75
13	70	75

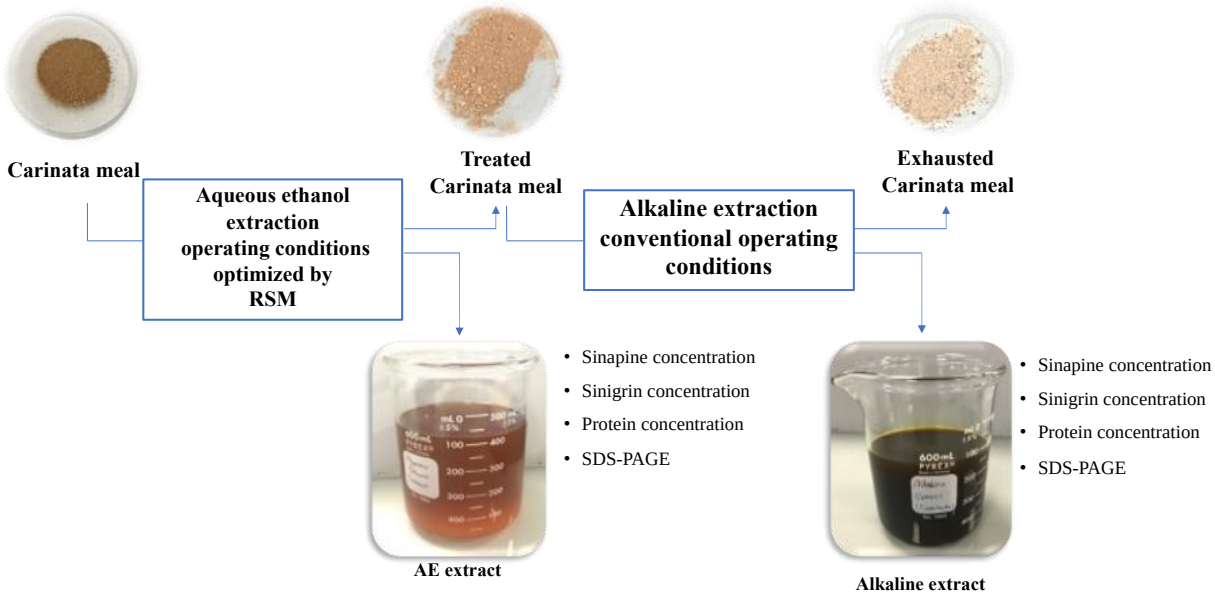

Figure 5-1. Fractionation of Carinata meal.

Table 5-2. Model equation coefficients and statistical parameters.

Factors	Coefficient values		
	PC concentration Y_1	GSL concentration Y_2	Extractability Index Y_3
Constant	1.0333	1.9744	-1.7016
%EtOH	0.0028^{NS}	-0.0864	-0.0080 ^{NS}
T_e	0.0144^{NS}	0.0221^{NS}	-0.0529
%EtOH%EtOH*	-0.0457	-0.0847	0.0818
*Te*Te*	-0.0145^{NS}	-0.0126^{NS}	
%EtOH Te*	-0.0220^{NS}	0.0143^{NS}	-0.0717
R^2	0.869	0.929	0.849
R^2 adjusted	0.775	0.870	0.763
Regression (*p*-value)	5.413E-3	2.1682E-3	5.2646E-3
Lack of fit	0.324	0.708	0.273
Reproducibility	0.847	0.820	0.900
Condition number	4.654	4.683	3.605

NS: non-significant

(a) (b)

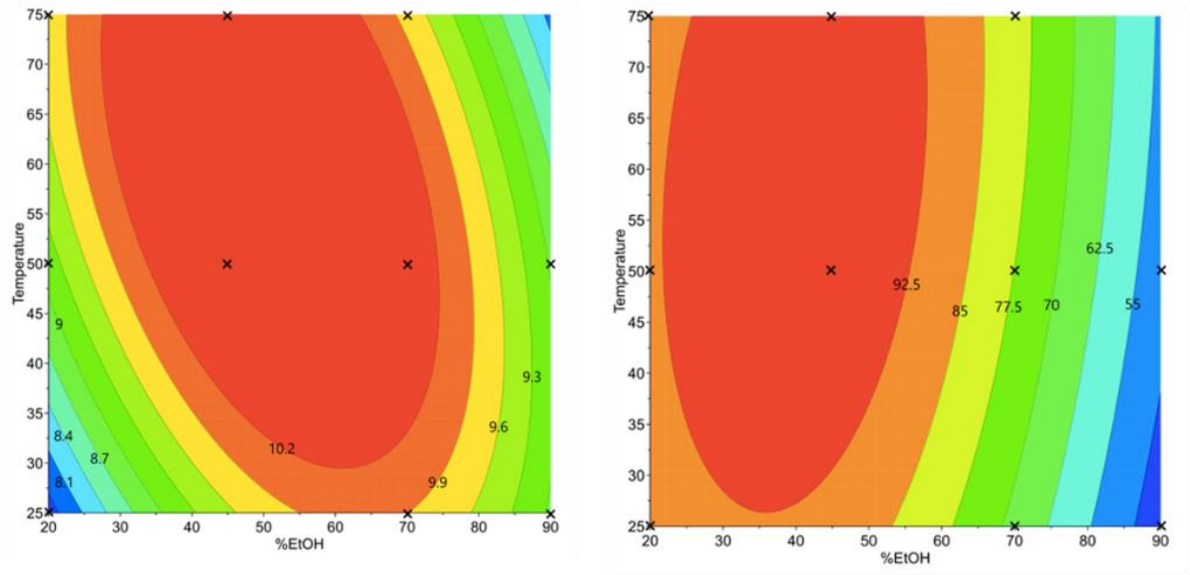

Figure 5-2. Contour plots for the prediction of phenolic compounds (mg/g_{DM}) (**a**) and glucosinolate concentrations (**b**) (µmol/g_{DM}). The crosses indicate data points that were fitted for plot building.

Table 5-3. Values of PC and GSL concentrations (Y_1 and Y_2) and EI (Y_3) associated to each % EtOH optimum according to T_e.

T_e (°C)	Optimal *%EtOH*	Y_1 (mg/g_{DM})	Y_2 (µmol/g_{DM})	Y_3 (%)
25	29%	$8.47^{b} \pm 0.08$	90.83 ± 0.90	$55.85^{c} \pm 0.56$
30	27%	$8.65^{b} \pm 0.08$	91.96 ± 0.92	$56.70^{b,c} \pm 0.57$
35	25%	$8.80^{a,b} \pm 0.09$	92.46 ± 0.92	$57.88^{b,c} \pm 0.58$
40	24%	$8.92^{a,b} \pm 0.09$	92.98 ± 0.93	$58.83^{a,b,c} \pm 0.59$
45	23%	$9.18^{a} \pm 0.09$	93.05 ± 0.93	$59.90^{a,b} \pm 0.60$
50	21%	$9.24^{a} \pm 0.09$	91.87 ± 0.93	$61.73^{a} \pm 0.61$

Letters associated to the means correspond to equivalent values according to the Tukey's test.

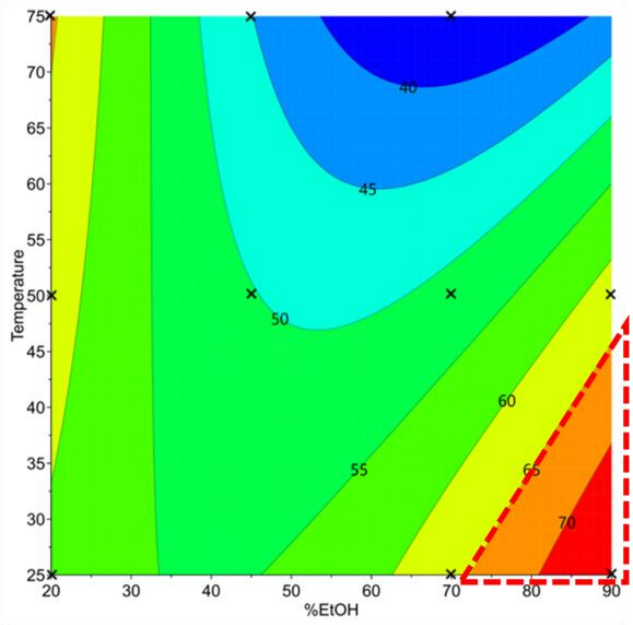

Figure 5-3.Contour plot for the prediction of extractability index (%) of proteins. Dashed black triangle indicates optimal zone of protein extractability index.

Table 5-4. Protein concentration and functional properties of Carinata protein isolates of original and treated meal.

Type of meal	EAI ($m^2.g^{-1}$)	ES (%)	FA (%)	FS (%)
Original meal	10.7 ± 1.4	63.5 ± 0.2	123.8 ± 1.8	94.9 ± 1.5
Treated meal	10.0 ± 0.6	61.4 ± 1.1	147.3 ± 3.2	94.2 ±1.6
Student's test (p-value)	0.5706	0.035	4.07E-12	0.4665

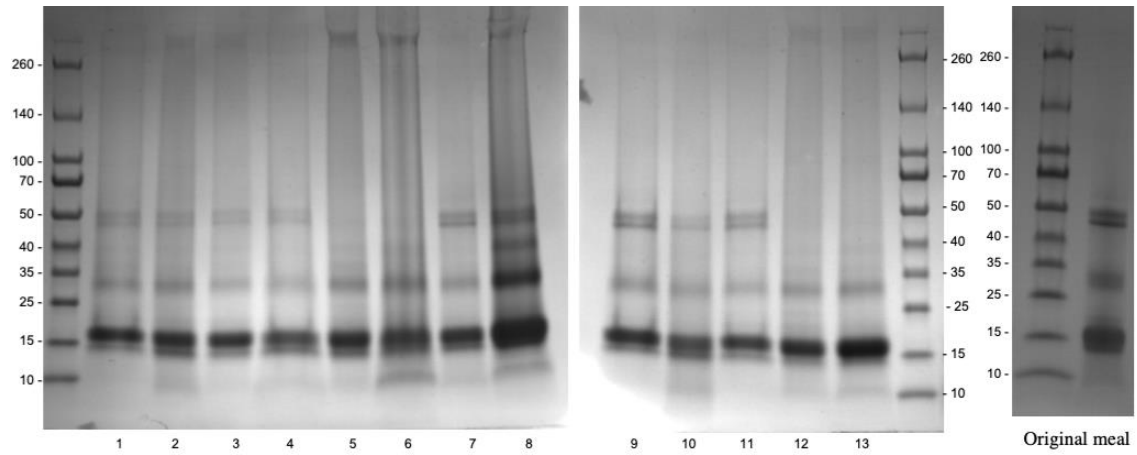

Figure 5-4. Polypeptide profiles of alkaline extracts from residual Carinata meal upon aqueous ethanol extraction. The numbers below indicate the experiments of the D-optimal design described Table 5-1.

(a)

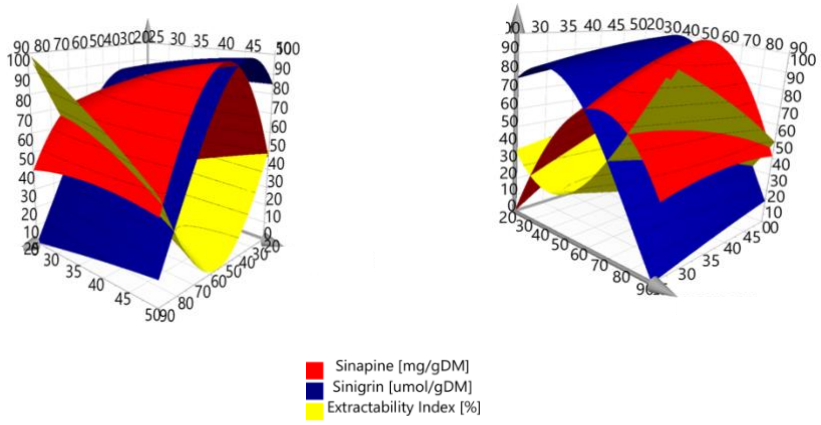

(b)

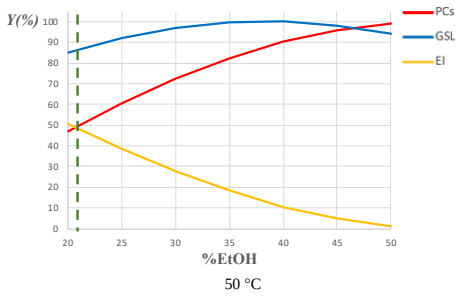

Figure 5-5. (**a**) Response surface plot of three main factors (PC concentration, GSL concentration, and EI) to reach the compromise between the recovery of secondary metabolites and protein extractability upon AE treatment. The response values were scaled where the minima and the maxima were set at 0 and 100%, respectively; (**b**) Plotting chart to determine the desired compromise at 50 °C. The X axis was limited to 50% to visualize the reached compromise between selected responses.

CHAPTER 6
SYNTHESIS OF RENEWABLE HIGH VALUE-ADDED BUILDING BLOCK FROM SINAPIC ACID[a]

Introduction

p-Hydroxycinnamic acids represent one of the most widely distributed chemicals in the plant kingdom, along with other phenylpropanoids such as flavonoids, stilbenes, and lignans. SinA and its analogues are among the most important *p*-hydroxycinnamic acids present in *B. carinata* meal. 6-Hydroxy-5,7-dimethoxy-2-naphtoic acid (DMNA) was first assumed to be a natural product in the alkaline extract of the heartwood of *Ulmus thomasii Sarg*;[280] however, the natural origin of this compound is questionable according to Charlton and Lee, who suggested that DMNA was actually an oxidized product of SinA under strong alkaline conditions.[281] The structure of DMNA (Figure 6-1) is similar to that of 6-hydroxy-2-nathoic acid, which is derived from petroleum resource and is commonly used to produce high value-added polymer (e.g., Vectra®).[282–284] This structural resemblance suggests that DMNA could be further valorized as a potential renewable building block for biobased material. Further therapeutic applications of this renewable chemical can also be suggested with regards to biological properties of several analogues of this latter.[285,286]

Synthetic approaches have been sought in order to deliver DMNA on a decent scale for further valorization of this renewable building block. It is known that DMNA is the product of secondary oxidation of thomasidioic acid (ThoA) which is formed via a *β*-*β* dimerization of SinA[287,288], a naturally occurring phenylpropanoid (Figure 6-1).[29] In

[a] Nota bene: the original idea described in this chapter was proposed by V.P.Thinh Nguyen; nevertheless, due to a bike accident which led to 5-month absence of V.P.Thinh Nguyen, a portion of the experimental material presented in this chapter was carried out by Nour Zaiter who was supervised by Dr. Amandine Flourat and Dr. Sami Fadlallah at URD ABI AgroParisTech (France).

order to favor the formation of DMNA, the *β*-*β* dimerization pathway should be favored over other dimerization possibilities for SinA.[93,288] Rubino et al. have shown that adding $FeCl_3$ favors the *β*-*β* oxidative dimerization of sinapic acid to afford ThoA.[289,290] The latter subsequently undergoes a secondary oxidation under strongly alkaline conditions to yield DMNA.[287] A more direct approach to synthesize DMNA from SinA was described by Lee.[287] Although multiple studies have employed this protocol to obtain DMNA on milligram scales[291,292], a preparative scale synthesis via this approach remains unachievable. We believe that the utilization of a large amount of solvent (20 mL of 0.1M KOH for 0.263 mmoles of SinA) disfavors the scale-up feasibility of this method. Moreover, multiple undesired polymerization might also occur under these conditions.[292] Therefore, further improvement should be established in order to reduce the amount of solvent, as well as favoring the desired *β*-*β* dimerization of SinA to efficiently afford desired DMNA. A synthetic approach to obtain DMNA was devised by Fuganti and Serra from syringaldehyde, a *p*-hydroxybenzaldehyde obtained from the oxidation of hard-wood lignins.[293] Unfortunately, this method employs a multi-step route using hazardous reagents such as ethyl chloroformate. In order to fully valorize DMNA, a preparative synthesis of this latter should be established, ideally avoiding hazardous reagents to reduce the environmental impacts of the synthesis process. Keeping this in mind, we herein propose a straightforward and accessible method to obtain DMNA from SinA.

Our first approach is to employ an oxidizing agent, $FeCl_3$, in order to favor the formation of dehydrosinapic acid intermediate (Figure 6-2) prior to its oxidation to DMNA under alkaline conditions. Moreover, favoring the formation of ThoA by adding an

oxidizing agent will also reduce the amount of solvent in the synthesis of DMNA, which appears to be an advantage over to the protocols reported in previous studies.[287,291,292] In addition, a laccase-mediated transformation of SinA is proposed to afford bislactone intermediate (Structure shown in Figure 6-1) based on previous work reported in the literature.[93,294] This latter is believed to yield desired DMNA under alkaline conditions.[287]

Compared to earlier synthetic strategies[293], our approaches avoid the use of hazardous reagents while reducing the number of synthetic steps. Although proof-of-concept has relied on commercially-obtained syringaldehyde, the SinA used in this study can eventually be replaced by that isolated from plant-based products.[100,147] Taken together, this method exhibits plausible advantage as a straightforward and accessible synthetic pathway to obtain a new renewable building block (i.e., DMNA) for biobased chemicals and materials.

Materials and Methods

Materials

Chemicals were purchased from Sigma-Aldrich. NMR solvents including deuterated acetone and deuterated dimethyl sulfoxide were purchased from Cambridge Isotope Laboratories.

Characterization

^{1}H NMR spectra of samples were recorded at 300 MHz (DMSO-d_6 and Acetone-d_6 residual signal at 2.50 and 2.05 ppm, respectively). ^{13}C NMR spectra of samples were recorded at 300 MHz (DMSO-d_6 and Acetone- d_6 residual signal at 39.5 and 29.8, respectively). Chemical shifts are reported in parts per million (ppm). Multiplicities are reported using the following abbreviations: s, singlet; d, doublet.

Synthesis of sinapic acid

Sinapic acid was obtained following the protocol described by Horbury et al with some modification.[131] In brief, 25 g of syringaldehyde (137.5 mmol) was dissolved in 35 mL of piperidine. 21.5 g of malonic acid (206 mmol) and aniline (1.25 mL, 13.8 mmol) were added, and the mixture was stirred overnight at 60 °C. The mixture was cooled to room temperature and then poured into 500 mL of ice-cold deionized water. The mixture was rigorously stirred and adjusted to pH 2 with 3M HCl. The precipitate was recovered by gravity filtration, washed several times until the effluent reached neutral pH. The precipitate was dried under vacuum overnight to afford a light yellow solid (22 g, 71%). The final product was sufficiently pure for use directly in the next step. ^{1}H NMR (Acetone-d_6) δ_H (ppm) 3.93 (s, 6H), 6.38-6.47 (d, J = 15.9 Hz ,1H), 7.02 (s, 2H), 7.52-7.61 (d, J = 15.6 Hz, 1H). ^{13}C NMR (Acetone-d_6) δ_C (ppm) 56.7 (2CH_3), 106.8 (CH), 116.3 (CH), 126.3 (C), 139.4 (C), 146.3 (C), 148.9 (C), 168.1 (CO).

Synthesis of thomasidoic acid

One gram of SinA (4 mmol) was stirred overnight in Tris-buffer pH 9 at 37 °C. The solution became dark brown. The solution was adjusted to pH 2 with 3 M HCl and extracted with 3 × 50 mL AcOEt. The organic layers were combined, washed twice with 50 mL brine solution, dried with anhydrous $MgSO_4$, and evaporated under vacuum to afford a brown residue. Chromatography of the residue on silica gel with 30/70 AcOEt/Cyclohexane gave a white solid (0.133 g, 0.3 mmol, 15%). ^{1}H NMR (DMSO-d_6) δ_H 3.48 (s, 3H), 3.60 (s, 6H), 3.75 (s, H), 3.82 (s, 3H), 4.81 (s, H). 6.20 (s, 2H), 6.99 (s, 1H), 7.55 (s, 1H), 8.22 (s, 1H), 9.18 (s, 1H), 12.39 (s, 1H).^{13}C NMR (Acetone-d_6) δ_C 53.2 (3CH_3), 62.51 (CH_3), 105.8 (CH), 109.23 (CH), 123.5 (CH), 124.2 (C), 134.0 (C), 135.21 (CH), 142.3 (C), 146.3 (C), 148.5 (C), 174.0 (CO).

Synthesis of 6-hydroxy-5,7-dimethoxy-2-naphthoic acid from Sinapic Acid *via* $FeCl_3$-mediated dimerization

The synthesis of DMNA was performed following the protocol described by Lee with some modification.[287] In brief, 1 g of SinA (4 mmol) and different amount of $FeCl_3$ were stirred in 5 mL EtOH for 30 min at room temperature. Forty-five milliliters of deionized water were added. The solution immediately became pink. The mixture was vigorously stirred for 5 h at room temperature. The mixture was adjusted to pH 12 using 3M NaOH and stirred overnight at 60 °C. The solution then became dark brown. The solution was adjusted to pH 2 with 3 M HCl and extracted with 3 × 50 mL AcOEt. The organic layers were combined, washed twice with 50 mL brine solution, dried with anhydrous $MgSO_4$ and evaporated under vacuum to afford a brown residue. Chromatography of the on silica gel with 30/70 AcOEt/Cyclohexane gave a light yellow solid (0.165 g, 0.6 mmol, 30%). ^{1}H NMR (Acetone-d_6) δ_H 3.99 (s, 6H), 7.31 (s, H), 7.90-7.93 (d, J = 10.4 Hz H), 8.00-8.03 (d, J = 8.8 Hz, H), 8.49 (s, H). ^{13}C NMR (Acetone-d_6) δ_C 56.4 (CH_3), 60.8 (CH_3), 104.0 (CH), 121.5 (CH), 124.1 (CH), 126.5 (C), 127.2 (C), 128.2 (C), 130.5 (CH), 141.0 (C), 141.2 (C), 150.8 (C), 167.7 (CO).

Synthesis of 6-hydroxy-5,7-dimethoxy-2-naphthoic acid from Sinapic Acid *via* Bislactone intermediate dimerization

Synthesis of Bislactone Intermediate

One gram of SinA (4.46 mmol) was dissolved in acetone nitrile (ACN) (12%, 3.7 mL). Forty-one milliliters of McIlvaine buffer (Na_2HPO_4/Citric acid) and laccase (6.6 mg, 21 U.mmol^{-1}) were added. The solution immediately became pink after the addition of the enzyme. The whole mixture was vigorously stirred for 1.5 h at room temperature. The mixture was then extracted twice with 50 mL of ethyl acetate. The organic layers were combined, washed twice with 50 mL brine solution, dried with anhydrous $MgSO_4$

and evaporated under vacuum to afford a pink solid (0.9 g, 1.9 mmol, 85% yield). No further purification was required according to the NMR results. ^{1}H NMR (Acetone-d_6) δ_H 3.84 (s, 12H), 4.13 (s, 1H), 5.76 (s, 2H), 6.74 (s, 4H), 7.52 (s, 2H). ^{13}C NMR (Acetone-d_6) δ_C 48.2 (2CH), 55.8 (4CH_3), 82.5 (2CH), 104.3 (4CH), 128.9 (2C), 136.5(2C), 148.13 (4C), 175.2 (CO).

Synthesis of 6-hydroxy-5,7-dimethoxy-2-naphthoic acid from bislactone intermediate

One gram of bislactone (2.1 mmol) was dissolved in ACN/NaOH (1 M) mixture (1:1) (12%, 3.7 mL) and the whole mixture was vigorously stirred overnight at room temperature. The initial solution pink became dark brown after one night. The mixture was then extracted twice with 50 mL of ethyl acetate. The organic layers were combined, washed twice with 50 mL brine solution, dried with anhydrous $MgSO_4$ and evaporated under vacuum to afford a light yellow solid (0.47 g, mmol, 90%). No further purification was required according to the NMR results. ^{1}H NMR (Acetone-d_6) δ_H 3.84 (s, 7H), 4.13 (s, 2H), 5.76 (s, 2H), 6.74 (s, 4H), 7.52 (s, 2H). ^{13}C NMR (Acetone-d_6) δ_C 56.4 (CH_3), 60.8 (CH_3), 104.0 (CH), 121.5 (CH), 124.1 (CH), 126.5 (C), 127.2 (C), 128.2 (C), 130.5 (CH), 141.0 (C), 141.2 (C), 150.8 (C), 167.7 (CO).

Synthesis of Ethyl-6-hydroxy-5,7-dimethoxy-2-napthoate

DMNA (100 mg, 0.4 mmol) was stirred in 100 mL EtOH for 30 min at 4 °C. Five drops of concentrated sulfuric acid were added and the whole mixture was then stirred for 3 days at reflux. The reaction was stopped by evaporating the mixture to dryness under vacuum. Fifty milliliters of saturated sodium bicarbonate solution were added to the residue. The aqueous solution was extracted twice with 50 mL of ethyl acetate. The organic layers were combined, washed twice with 50 mL brine solution, dried with

anhydrous $MgSO_4$ and evaporated under vacuum to afford a light yellow solid (67 mg, 0.24 mmol, 60% yield). No further purification was required according to the NMR results. ^{1}H NMR (Acetone-d_6) δ_H 1.29 (s, 2H), 4.0 (s, 6H), 7.33 (s, 1H), 7.90-7.91 (d, J = 8.7 Hz, 1H), 8.00-8.02 (d, J = 8.8 Hz, 1H), 8.49 (s, 1H). ^{13}C NMR (Acetone-d_6) δ_C 27.0 (CH_2), 55.9 (CH_3), 60.4 (CH_3), 103.6 (CH), 121.0 (CH), 123.7 (CH), 126.1 (C), 127.3 (C), 127.7 (C), 130.1 (CH), 140.6 (C), 140.7 (C), 150.3 (C), 167.5 (CO).

Results and Discussion

The first step of this work consisted in the SinA synthesis using our in-house optimized Knoevenagel-Doebner condensation of syringaldehyde and malonic acid.[131] This approach allowed to avoid extended purification, as only a simple washing with acid solution was required to afford pure SinA. By employing this route, we have successfully obtained SinA with quantitative conversion yield from syringaldehyde on a multigram-scale.

Lee has shown that DMNA can be obtained via a direct oxidation of SinA under alkaline conditions on milligram scale.[287] We therefore attempted to convert SinA into DMNA following these conditions (Table 6-1). Unfortunately, in our hands, oxidation under alkaline conditions only resulted in uncomplete conversion of SinA on gram scale. Another approach was therefore required in order to obtain DMNA.

Rubino et al. reported the conversion of SinA into ThoA using $FeCl_3$ as oxidizing agent with moderate yields. [289] ThoA can be converted to DMNA through decarboxylation.[287] We thus devised an one pot approach to obtain DMNA via the $FeCl_3$-mediated dimerization of SinA (Table 6-2). We have successfully optimized this conversion, with only 0.5 equiv of $FeCl_3$ required to yield a complete conversion of SinA. Unfortunately, all attempts to conduct this reaction on larger scales (over 1 g of SinA)

led to significant decreases in overall yield. In addition, the isolation of DMNA and ThoA required an extensive and tedious purification on silica gel (cyclohexane-ethyl acetate as eluant) and the isolated yield remained low (<40%). We therefore decided to devise another approach to obtain DMNA from SinA on a larger scale.

Laccase has been used to catalyze the transformation of SinA to a bislactone intermediate[294], which can be subsequently oxidized under alkaline conditions to obtain DMNA (Figure 6-3).[287] Nevertheless, the operating conditions appears to be unfavorable from both an economic and green chemistry standpoint, requiring highly diluted media (0.45 μmol.L^{-1}) and excessive amounts of enzyme (> 300 U.mmol^{-1}).[294] We therefore improved this protocol to address both of these problems. Our revised conditions successfully provided the bis-lactone intermediate and these results encouraged us to optimize this step further to achieve complete conversion of SinA to the bislactone intermediate (Table 6-3). We observed that longer reaction times result in oligomerization of the desired bislactone, thereby decreasing the yield in SinA. On the other hand, insufficient amounts of enzyme resulted in incomplete conversion of SinA, which complicated the downstream purification of DMNA. Our results showed that, when a proper balance between reaction time (1.5 h) and enzyme amount (21 U.mmol^{-1}) was reached, a quantitative amount of bislactone was obtained without further purification, with 90% of SinA converted to desired intermediate. We also observed that the addition of acetonitrile into the laccase buffer improved the reaction while providing a more pure bislactone.

The next step was to convert the bislactone intermediate to DMNA. This transformation was achieved by adding an alkaline mixture of NaOH 1 M and ACN,

which resulted in complete conversion of DMNA with high purity. The results showed quantitative conversion of bislactone intermediate to DMNA (90% of yield).

With a successful route to DMNA in hand, we envisage different approaches towards DMNA-based polymesr in order to valorize this novel biobased monomer (Figure 6-4). As a preliminary step, DMNA was esterified using ethanol as solvent, providing a decent conversion to the corresponding ethyl ester (60%).

Summary and Future Work

Although $FeCl_3$, an oxidizing reagent, facilitates the conversion of SinA to DMNA, this approach did not deliver the desired results on multi-gram scales. By contrast, our optimized synthetic approach proved successful and provided good conversion of SinA to DMNA via laccase-mediated formation of the bislactone intermediate. The operating conditions for the laccase-mediated SinA conversion had to be further improved in order to deliver DMNA on larger scales. We therefore developed a one-pot synthesis of DMNA via the bislactone intermediate.

DMNA and its corresponding ethyl ester are now available in high purity and on a multi-gram scale. This will allow work on their polymerizations via a solvent-free free radical polymerization to access novel polymers that will be thoroughly characterized.

Finally, biological activities of DMNA such as antioxidant, antibacterial will be further evaluated to enhance the value of Carinata meal.

Table 6-1. Optimization of the direct conversion of SinA to DMNA under alkaline conditions.

Entries	SinA (g)	Base	Base volume (ml)	Time (h)	Temperature (°C)	Results
1	5	KOH 1M	100	16h	80	Only ThoA
2	0.5	KOH 1M	100	24	25	Traced ThoA, no DMNA
3	0.5	NaOH 1M	50	24	25	Traced ThoA, No DMNA
4	1	KOH 1M	20	16	60	DMNA formed but remaining SinA
5	1	KOH 0.1 M	200	20	60	DMNA formed but remaining SinA

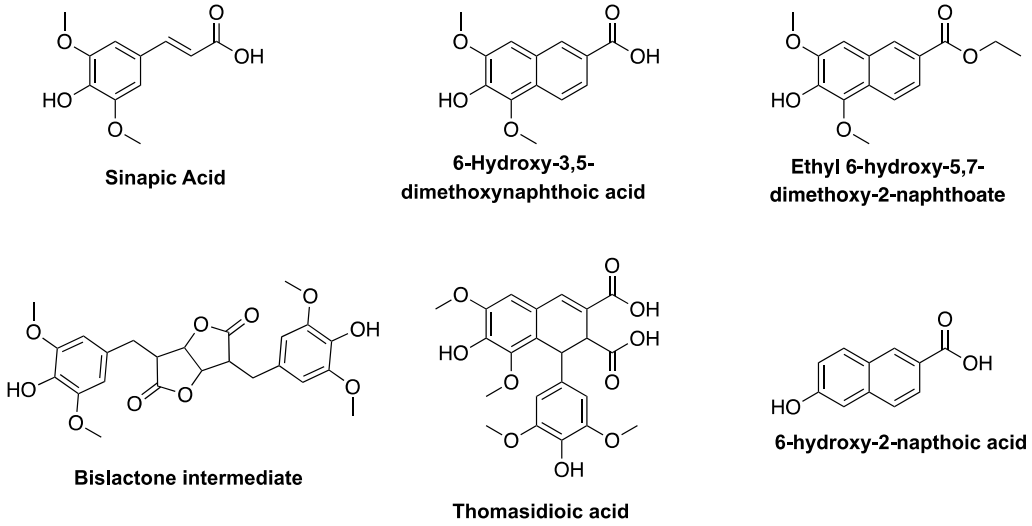

Figure 6-1. Structure of sinapic acid and its oxidative derivatives, 6-hydroxy-2-naphthoic acid, DMNA, and ethyl-DMNA

Table 6-2. Optimization of conversion of SinA to DMNA via $FeCl_3$-mediated dimerization.

Entries	m_{SinA} (g)	$FeCl_3$ (equiv)	Conversion of SinA to DMNA (%)	Yield (%)
1	1	3	100	3
2	1	1	100	30
3	1	0.5	100	30

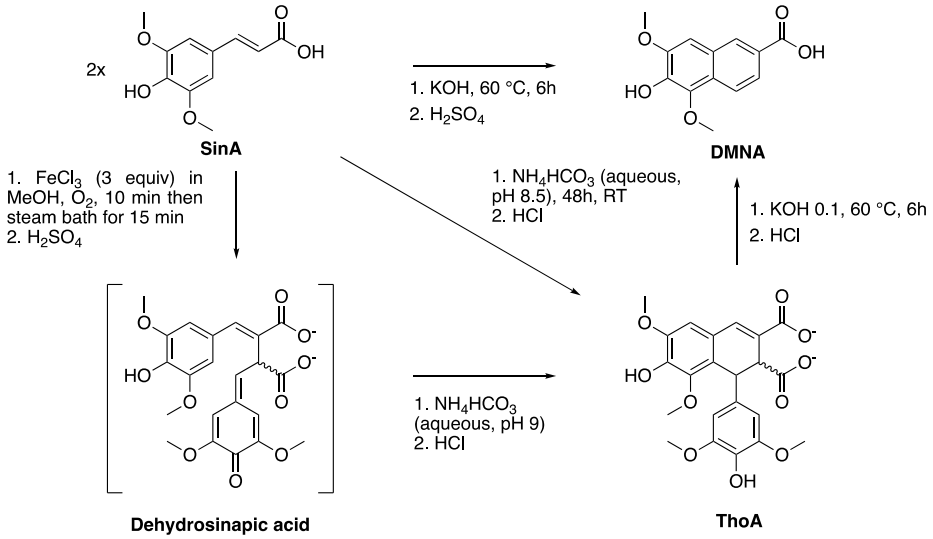

Figure 6-2. Oxidative *β-β* dimerization of SinA to afford ThoA and DMNA via the dehydrosinapic acid intermediate.

Table 6-3. Optimization of conversion of SinA to bislactone intermediate via laccase-mediated dimerization

Entries	SinA (g)	Bislactone (g)	Time (h)	Amount of laccase* (mg)	Yield (%)
1	1	0.2	16	5	20
2	1	0.3	1.5	10	30
3	1	0.4	2	8	40
4	1	0.4	2	7.8	40
5	1	0.45	2	6.6	45
6	1	0.9	1.5	6.75	90

* Laccase activity: 21 $U.mol^{-1}$

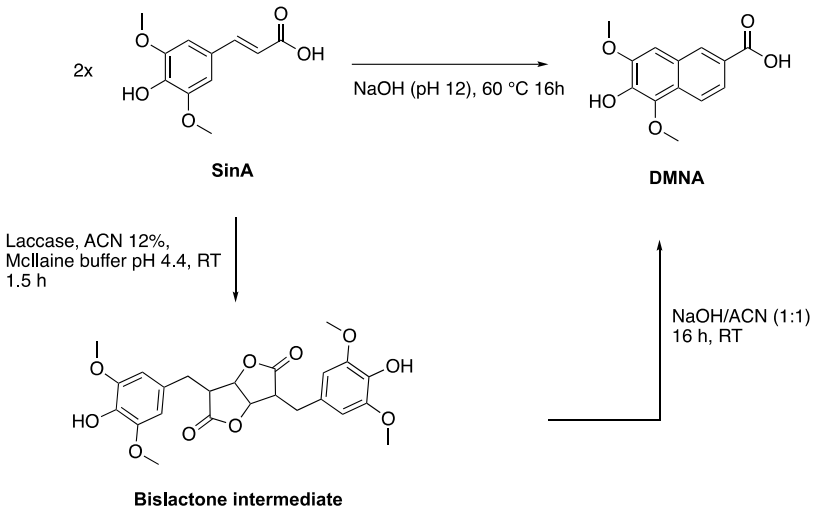

Figure 6-3. Proposed strategy to synthesize DMNA from SinA via bislactone intermediate.

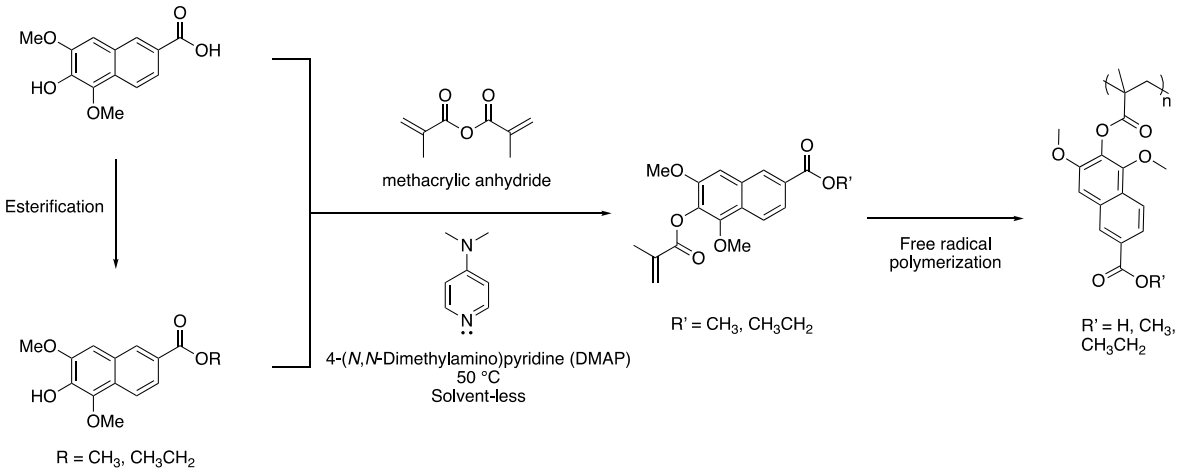

Figure 6-4. Proposed polymerization of DMNA.

CHAPTER 7
ACTIVATION OF *Plutella Xylostella* SULFATASE USING FORMYL GLYCINE ENZYME

Introduction

Diamondback moth (DBM), *Plutella xylostella* L. is known to be the most destructive insect for cruciferous plants. The feeding pattern of DBM on cruciferous plants has been studied by Ratzka et al.[260] The glucosinolate sulfatase (GSS) that is secreted into the gut lumen of the DBM larvae enables them to feed on cruciferous plants while avoiding toxic effects of GSL breakdown products. GSS removes the sulfate moiety from GSL, which makes them non-substrates for MYR. The mechanism of the sulfate group removal is described by an addition-hydrolysis or by transesterification-elimination mechanisms (Figure 7-1).[295] However, the real mechanism has remained elusive due to lack of a well characterized sulfatase.

Our approach to reduce the GSL's breakdown product amounts in Carinata meal is based on the feeding pattern of DBM on Cruciferae plants (Figure 7-2). This approach entails removing the sulfate part of GSLs before the glucose thioester and MYR can come into contact with one another during seed processing. Consequently, no ITCs or other toxic breakdown products would be produced. Furthermore, the desulfated GSLs are considered bioinactive and would have negligible impacts on other downstream uses. This approach could also lead to improved bioavailability of Carinata meal which increases its bio-value.

The most challenging part of this proposal is the activation of GSS. Ratzka and coworkers reported that GSS heterologously expressed by *Escherichia coli* was inactive due to lack of an essential post-translational modification.[260] The sulfatase needs to be activated by formylglycine generating enzyme (FGE) in order to become catalytically

competent. The transformation of a Cys or Ser side chain into a formylglycine (fGly) motif by FGE is required for sulfatase activity.[296] The generation of fGly by FGE is highly selective and guided by the highly conserved amino acid sequence of sulfatase: (C/S)XPXRXXXLTG. The mechanism of this transformation is described in Figure 7-3. The sulfatase proteomic sequence of GSS showed existence of this amino acid sequence (Figure 7-4)Therefore, the activation of GSS could be achieved by FGE.

The heterologous expression of FGE from *Thermosporal curvata* has been reported by Knop et al.[297] The recombinant FGE exhibited acceptable enzyme activity (k_{cat}/K_M = 100 $M^{-1}.min^{-1}$) as well as a with high expression level, up to 10 mg of purified FGE per culture liter. This enzyme activity can be improved through mutagenesis and using Cu (I) solution as catalyst. Based on these results, we have decided to clone and to overexpress FGE from *T. curvata* to activate GSS. FGE from *T. curvata* was obtained and the GSS was cloned and heterologously expressed by *E. coli*. Further investigations were performed and reported here in order to evaluate the feasibility of our strategy.

Materials and Methods

Materials

Restriction enzymes were purchased from NEB (New England, US). Electroporation was carried out with a BioRad GenePulser apparatus using 0.1 cm cuvettes. DNA primers were synthesized by Integrated DNA Technologies, Inc (Coralville, IA) and Sanger DNA sequencing was performed by Genewiz (South Plainfield, NJ). Mass spectrometry analysis was carried out with a Bruker Autoflex LRF MALDI-TOF at the Mass Spectrometry Research and Education Center (Department of Chemistry, University of Florida).

Cloning

A synthetic gene encoding FGE from *Thermomonosporal curvata* was obtained from Genescript (Pistacaway, NJ) and amplified by PCR using two primers (5'-TTATTTCATATGATGGTGGCCATCCC - 3' and 5' - TAATTGGGATCCATACTCGAGCTACAG-3'). The gel purified amplification product was digested with restriction enzymes *Nde*I and *Bam*HI, and then ligated between these sites in pEt15b. The ligation mixture was used to transform *Escherichia coli* strain ElectroTen Blue competent cell using electroporation, then spread on LB agar plates supplemented with 50 µg/mL ampicillin and grown overnight at 37 °C. Randomly-chosen colonies were cultured overnight in LB medium supplemented 100 µg per mL of ampicillin at 37 °C. Plasmids were recovered using the Promega Wizard® Plus SV Miniprep DNA purification system kit. One plasmid was analyzed by Sanger sequencing using T7 and T7ter primers and shown to have the desired structure. This plasmid was designated pNVPT1

The synthetic gene encoding *Plutella xylostella* glucosinolate sulfatase was synthesized by Genescript (Pistacaway, NJ) and amplified by PCR using the cloning primers 5'-ATAGTACATATGGCGATTCTGCATCAAG-3' and 5'-CATACTATTCGG AGTCGGAGTAGGG-3'. The gel purified amplification product was digested with *Nde*I and *Bam*HI, and then ligated between these sites in pEt15b. The ligation mixture was used to transform *Escherichia coli* strain ElectroTen Blue competent cell using electroporation, then spread on LB agar plates supplemented with 50 µg/mL ampicillin and grown overnight at 37 °C. Randomly-chosen colonies were cultured overnight in LB medium supplemented 100 µg per mL of ampicillin at 37 °C. Plasmids were recovered

using the Promega Wizard® Plus SV Miniprep DNA purification system kit. One plasmid was analyzed by Sanger sequencing using T7 and T7ter primers and shown to have the desired structure. This plasmid was designated pNVPT2

Protein Production

Plasmid pNVPT1 was used to transform *E. coli* strain BL21(DE3)-Gold using the electroporation method. The transformed cell aliquot was spread on LB agar-plates supplemented with 50 μg per mL of ampicillin and grown overnight at 37°C. A single colony of the appropriate strain was used to inoculate 10 mL of LB medium supplemented 100 μg per mL of ampicillin and the culture was shaken overnight at 37 °C. The saturated aliquot was then transferred into 1 L of LB medium supplemented 100 μg per mL of ampicillin. The culture was grown at 37 °C with stirring at 250 rpm until the OD_{600} reached 0.5 – 0.6. Protein overexpression was induced by addition of 0.1 or 0.5 mM IPTG at 37 °C for 4 h. Cells were harvested by centrifuging at 4000 RPM at 4 °C, resuspended in 20 mM KP_i, 0.5 M NaCl, 20 mM imidazole 50 mM EDTA pH 7.4 and lysed using BugBuster® HT Protein Extraction solution (Merck). An aliquot was centrifuged and purified using a Hitrap His-tag equilibrated in buffer 20 mM KP_i, 0.5 M NaCl, 20 mM imidazole 50 mM EDTA pH 7.4. The bound protein was eluted with buffer containing 20 mM KP_i, 0.5 M NaCl, 500 mM imidazole 50 mM EDTA pH 7.4. The purified protein was analyzed using SDS-PAGE under Laemmli conditions.[298] The final yield of FGE was 3.7 mg/L culture volume. Glycerol was added to a final concentration of 20% and the concentrated protein (1.37 mg/mL) was stored in aliquots at –20 °C until further use.

FGE Assay

The assay was performed according to Knop et al.[297] The substrate (Polypeptide sequence: ALCSPARTAVLTG) was synthesized by ABclonal Science (Woburn, MA) with a purity up to 95.5%. The reaction mixture was prepared by adding 50 μM of substrate, 2 mM of DTT, 50 mM of NaCl and 50 mM EDTA to Tris-Cl, pH 8.0. The addition of 1 μM of TcFGE initialized the reaction. One equivalent of $CuSO_4$ was added as a cofactor. The reaction was stopped after 1 h by adding 1 equivalent of 1% aqueous TFA to the reaction media. The product was then analyzed using MALDI-TOF-MS as the detection method with α-cyano-4-hydroxycinnamic acid in 50% 1% aqueous TFA / 50% methanol as matrix.

Results and Discussion

Recombinant TcFGE has been successfully overexpressed from *E. coli* with a 3.7 mg per culture liter protein yield, lower than that described by Knop et al.[297] Hence, the protein expression (several expression parameters including type of media, type of induction, and expression temperature) must be further optimized in order to reach the expected expression rate of desired FGE.

An enzymatic assay was conducted to determine the activity of our enzyme as described by Knop et al. [297] The results showed the formation of desired peptides with and without Cu(I) addition (Appendix D). Meanwhile, the measuring the reaction rate remains to be performed.

Although different host strains (BL21(DE3)-Gold versus Rosetta-gami2(DE3)) were used for enzyme overexpression, recombinant PxGSS was poorly expressed in *E. coli*, with apparent early termination of translation leading to bands at lower molecular

weights (Appendix D). We believe that a co-expression of GSS and FGE will result in better expression rate of functional GSS, as mentioned by Jonas et al. A new plasmid including both GSS and FGE was therefore designed and will be employed to confirm this hypothesis (pNVPT4-Appendix D).[299]

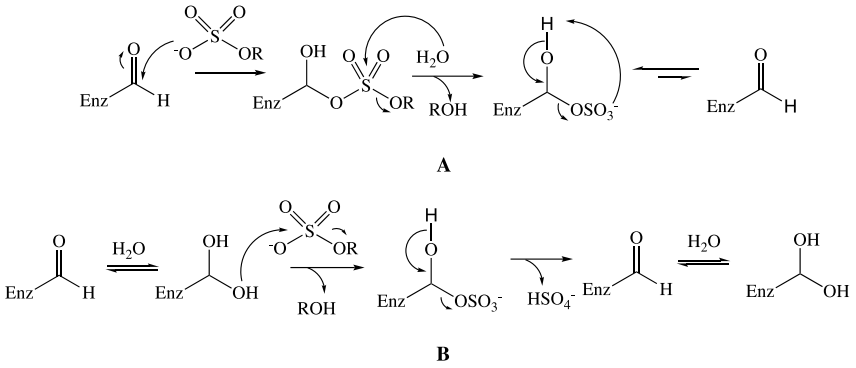

Figure 7-1.Proposed mechanism for the hydrolysis of sulfate esters by sulfatase. (A) Mechanism of addition hydrolysis removing sulfate group. (B) Mechanism of transesterification-elimination mechanism.

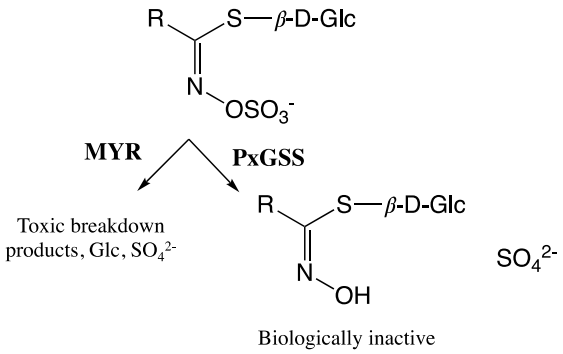

Figure 7-2. Schematization of proposed approach to remove sulphate group from GSL proposed.

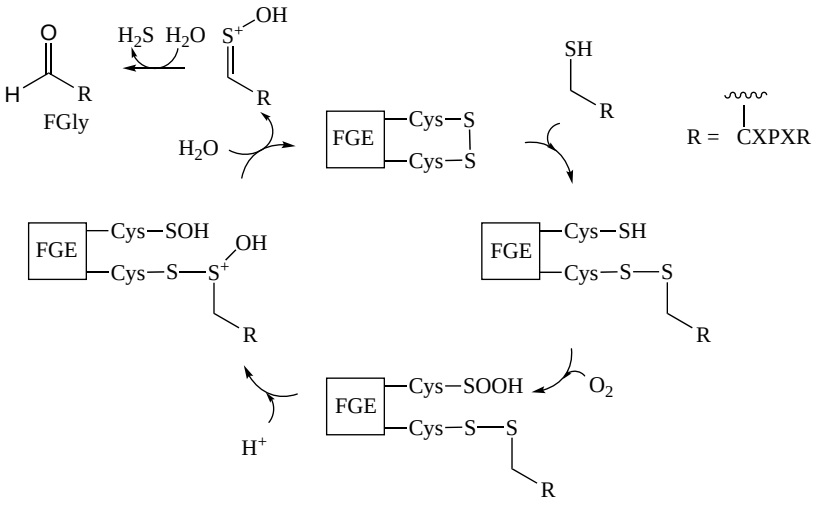

Figure 7-3. The proposed mechanism of the transformation Cys or Ser by FGE into fGly.

*MAILHQAVVLLGAALCVSA*ATKPHVIMIMADDMGW**DD**TSTHGSKSVL

TPNLDVLTRSGVSLHRYYTHAL**C**SPARTAVLTGKYAHTVGMQGMPLS

NAEERGIPLEERLISQYLQDAGYRTQMVG**K**WHVGHAFFEQLPTYRGF

ENHFGVRGGFIDYYEYNAQEQLDGRPVTGLCLFDDLQPDWTTEGYIT

DVYTEKSTTIIENHNVSEPLYLLLTHHAP**H**NGNEDASLQAPPEEVRA

QRHVELHPRRIFAAMVKKLDDSIGEIVATLEKKGMLENTIITFST**DN**

GAPTVGLGANSGSNYPLRGV**K**KSPWEGGIRGNAMIWAGPEVAPGNAW

RGKVYDGNMHAADWVPTLLEAIGEKIPAGLDGIPMWSHIIENKPSPR

TEIFEIDDYFNHSSVTLGRHKLVKGTIDESLSKHYGEDLRGIIGTPP

DYKQKLRDSKAWESLETIGIPLDADVMADRDEAIVTCGNVVPKPCSP

SAESWCLYDIIEDPCELRDLSEELPQLAQILLYRLEQEEAKIIPREG

QYVADPKSAPKYFNYTWDAYLSVEPYSDSE

Figure 7-4. Proteomic sequence of GSS. The target sequence of FGE was highlighted with the target Cys pointed out.

CHAPTER 8
CONCLUSION

Renewable energy from biomass makes up over a third of renewable energy in 2019, and rapeseed and its related crops, including *B. carinata*, are the third most abundant oil. Carinata meal, a co-product of renewable aviation fuel production from *B. carinata* cultivated in the southeast USA, can be further valorized. Indeed, proteins remaining in the meal have been demonstrated to be suitable for cattle feed. Furthermore, Carinata proteins are of particular interest thanks to their biological activities and interesting functional properties (reviewed in Chapter 2). On the other hand, many studies have demonstrated that secondary metabolites including *p*-hydroxycinnamic acids, mainly sinapic acid in its choline ester form, and glucosinolates also found in Carinata meal represent potential multifunctional chemicals for which applications can be found in the pharmaceutical, cosmetic and food industries (reviewed in Chapter 3 and Chapter 4).

The recovery of secondary metabolites from agro-industrial wastes employing sustainable and environmentally friendly strategies have nowadays drawn more attention, particularly methods based on solid-liquid extraction using aqueous alcohol as solvent. Although several studies have reported the successful recovery of sinapine from biomass, high temperatures and high concentrations of alcohol were often used. Consequently, we probed the effects of the extraction process on the remaining protein. Applying Response Surface Methodology to aqueous ethanol extraction followed by protein extraction, we have reported in Chapter 5 that a compromise could be reached. In summary, we have established a process where an efficient recovery of valuable secondary metabolites, including PCs and GSLs, has occurred while preserving the

extractability along with functional properties of residual proteins. In addition, the valorization of SinA as biobased monomer (Chapter 6), as well as an environmentally friendly detoxification of GSLs employing biochemical approaches (Chapter 7) are being investigated and could further enhance the economic and ecologic value of Carinata meal.

APPENDIX A
SUPPLEMENTARY INFORMATION FOR CHAPTER 4

Table A-1. Occurrence of GSL in plants of order Brassicales. GSL concentration expressed as minimum - maximum in µmol/g of dry material.

Family	Species	Tissue	GSL Content	Reference
Brassicaceae	*Camelina sativa*	Seed	15.8–19.4	[300]
	Camelina rumelica subsp. *rumelica*	Seed	18.6–21.7	
	Camelina macrocarpa	Seed	8.0–19.1	
	Brassica napus	Leaf	0.6–6.9	[197,301,302]
		Seed	10.8–57.9	
	Brassica carinata A Braun	Seed	35–170	[201,202]
	Brassica juncea	Leaf	4.3–129.9	[303]
		Seed	15.7–127.6	
	Brassica oleracea L. var *capitata*	Leaf	2.3–11.5	[304]
	Brassica oleracea L. var *italica*	Floret	8.2–19.5	[305]
	Brassica oleracea L. convar *capitata* var *alba*	Petiole	0.5–31.7	[306]
	Brassica rapa	Leaf	17.3	[301]
		Seed	39.4–81.3	
	Arabidopsis thaliana	Leaf	5.0–30.7	[307]
	Raphannus sativus L.	Root	1.0–145.5	[204,308]
Moringacea	*Moringa oleifera* Lam.	Leaf	4.7–217	[203,309]
		Seed	112–354.4	[235,272]
	Moringa stenopetala L.	Leaf	33.9–59.4	[310,311]
		Seed	256–282	

Table A-2. Classification of some GSL structural examples.

No	Class	Index	Semi systematic Name	Trivial Name	Characterization Methods	Reference
1	Ala	A	Methyl GSL	Glucocapparin	MS, NMR of GSL; MS of desGSL	312,313
2	Val	A	1-Methylethyl GSL	Glucoputranjivin	UV, IR, MS, NMR of GSL	249
3	Val	A	(1*R*)-Methyl-2-hydroxyethyl GSL	Glucosisymbrin	MS, NMR of desGSL	246,250
4	Val	B	(1*R*)-2-Bezoyloxt-1-methylethyl GSL	Glucobenzosisymbrin	UV, IR of ITC	314
5	Glu	A	3-Carboxypropyl GSL		Deducted from ITC structure	315
6	Glu	A	3-Methoxycarbonyl - propyl GSL	Glucoerypestrin	Partial NMR of GSL	316
7	?	A	Ethyl GSL	Glucolepidiin	Thiourea-type, IR compared to GSL structure	317
8	?	A	*n*-Butyl GSL		Thiourea-type method compared to GSL and MS from ITC	318,319
9	?	A	*n*-Pentyl GSL		MS of ITC	320
10	?	A	*n*-Hexyl GSL		MS of ITC	319
11	?	A	4-Oxoheptyl GSL	Glucocapangulin	Deducted from IR and 5-oxooctanoic acid	321
12	?	A	5-Oxoheptyl GSL	Gluconorcappasalin	Thiourea-type, IR compared to GSL; MS from ITC	322
13	?	A	5-Oxooctyl GSL	Glucocappasalin	UV, IR of GSL and desGSL; partial NMR of desGSL	323
14	?	A	4,5,6,7-Tetrahydroxydecyl GSL		UV, IR, NMR of ITC	324
15	?	B	Phenyl GSL		MS of GSL	319
16	?	B	2-(4-Methoxyphenyl)-2,2-dimethyl ethyl GSL		IR, MS, NMR of ITC	325
17	Leu	A	2-Methylpropyl GSL		MS, NMR of GSL and desGSL	250,326
18	Leu	A	2-Hydroxy-2-methylpropyl GSL	Glucoconringiin	MS, NMR	327
19	Leu	A	3-Methylbutyl GSL		MS of ITC	320

Table A-2. Continued

No	Class	Index	Semi systematic Name	Trivial Name	Characterization Methods	Reference
20	Leu	A	3-Methylbut-3-eyl GSL		IR, MS, NMR of ITC	328
21	Leu	A	4-Methylpentyl GSL		MS of ITC	329
22	Ile	A	(1*S*)-1-Methylpropyl GSL	Glucococchlearin	MS, NMR of GSL and desGSL	250,330
23	Ile	A	(1*R*)-1-(Hydroxymethyl)-propyl GSL	Glucosisaustricin	MS, NMR of desGSL	250
24	Ile	B	(1*R*)-1-(Benzoyloxymethyl)-propylGSL	Glucobenzsisaustricin	Thiourease-type, IR compared to GSL	331
25	Ile	A	(2*S*)-2-Methylbutyl GSL	Glucojiaputin	UV, IR, MS, NMR of GSL and des GSL	249,250
26	Ile	A	(2*S*)-2-Hydroxy-2-methylbutyl GSL	Glucocleomin	NMR of desGSL	246
27	Ile	A	3-Methylpentyl GSL		UV, IR, MS, NMR of GSL; MS, NMR of desGSL	249,250
28	Ile	A	3-(Hydroxymethyl)pentyl GSL		NMR of GSL	332
29	Ile	A	2-Hydroxy-3-methylpenyl GSL		MS, NMR of desGSL	250,332
30	Trp	C	4-Methoxyindol-3-yl GSL	Glucorapassicin A	UV, IR, MS, NMR of synthesized GSL	333
31	Trp	C	Indol-3-ymethyl GSL	Glucobrassicin	UV, IR, MS, NMR of GSL and desGSL	249,250
32	Trp	C	1-Hydroxyindol-3ylmethyl GSL		MS of GSL; UV, MS of desGSL	334
33	Trp	C	4-Hydroxyindol-3-ylmethyl GSL	4-Hydroxy-glucobrassicin	MS of GSL; UV, MS, NMR of desGSL	334–336
34	Trp	C	4-Methoxyindol-3-ylmethyl GSL	4-Methoxy-glucobrassicin	UV, MS, MS, NMR of GSL and desGSL	249,336
35	Trp	C	1-Methoxyindol-3-ylmethyl GSL	Neoglucobrassicin	UV, IR MS, NMR of GSL; MS, NMR of desGSL	249,250,334
36	Trp	C	1,4-Dimethoxyindol-3-ymethyl GSL	1,4-Dimethoxy-glucobrassicin	UV, MS, NMR of desGSL	250,332

Table A-2. Continued

No	Class	Index	Semi systematic Name	Trivial Name	Characterization Methods	Reference
37	Trp	C	1-Acetylindol-3-ymethyl GSL	N-Acetyl-glucobrassicin	MS of desGSL	337
38	Trp	C	1-Sulfoindol-3-ylmethyl GSL	N-Sulfo-glucobrassicin	UV, IR, MS, NMR of GSL	327,338
39	Trp	C	6′-Isoferuloylindol-3-ylmethyl GSL	6′-Isoferuloyl-glucobrassicin	MS of GSL; UV, MS, NMR of desGSL	339,340
40	Phe	B	Benzyl GSL	Glucotropaeolin	MS, NMR of GSL; UV, MS, NMR of desGSL	246,341,342
41	Phe	B	3-Hydroxybenzyl GSL	Glucolepigramin	MS of GSL; MS, NMR of desGSL	327,343
42	Phe	B	3-Methoxybenzyl GSL	Glucolimnanthin	MS, NMR of GSL; UV, MS, NMR of desGSL	246,344
43	Phe/Trp	B	4-Hydroxybenzyl GSL	Glucosinalbin	UV, MS, NMR of GSL and desGSL	233,246,327
44	Phe/Trp	B	4-Methoxybenzyl GSL	Glucoaubrietin	MS of GSL; UV, MS, NMR of desGSL	250,327,345
45	Phe/Trp	B	3,4-Dihydroxybenzyl GSL	Glucomatronalin	MS of GSL	327
46	Phe/Tyr	B	4-Hydroxy-3-methoxybenzyl GSL	3-Methoxysinalbin	UV, MS, NMR of desGSL	343
47	Phe/Tyr	B	3-Hydroxy-4-methoxybenzyl GSL	Glucobretschneiderin	UV, IR, MS, NMR of GSL	346
48	Phe/Tyr	B	3,4-Dimethoxybenzyl GSL		UV, MS, NMR of desGSL	343
49	Phe/Tyr	B	4-Hydroxy-3,5-dimethoxybenzyl GSL	3,5-Dimethoxy-sinalbin	UV, MS, NMR of desGSL	343
50	Phe/Tyr	B	3,4,5-Trimethoxybenzyl GSL		MS of GSL; UV, MS, NMR of desGSL	342,343
51	Phe	B	2-Phenylethyl GSL	Gluconasturtiin	NMR of GSL; UV, MS, NMR of desGSL	246,327
52	Phe	B	(2*S*)-2-hydroxy-2-phenylethyl GSL	Glucobarbarin	MS, NMR of GSL and desGSL	250,327,336
53	Phe	B	(2*R*)-2-Hydroxy-2-phenylethyl GSL	Epiglucobarbarin	MS, NMR of GSL and des GSL	327,339,347

Table A-2. Continued

No	Class	Index	Semi systematic Name	Trivial Name	Characterization Methods	Reference
54	Phe	B	2-(3-Hydroxy-phenyl)ethyl GSL		UV, MS, NMR of desGSL	347
55	Phe	B	2-(4-Hydroxy-phenyl)ethyl GSL	Homosinalbin	MS, NMR of GSL; UV, MS, NMR of desGSL	327,348
56	Phe	B	(2*R*)-2-Hydroxy-2-(3-hydroxyphenyl)ethyl GSL	*m*-Hydroxy-epiglucobarbarin	UV, MS, NMR of GSL and desGSL	194
57	Phe	B	3-Phenylpropyl GSL		MS of ITC	349
58	Phe	B	4-Phenylbutyl GSL		MS of ITC	349
59	Phe	B	5-Phenylpentyl GSL	Glucoarmoracin	MS of ITC	349
60	Phe/Tyr	B	2-(4-Methoxy-phenyl)ethyl GSL		NMR of GSL, MS, NMR of desGSL	327,332,345
61	Phe/Tyr	B	(2*R*)-2-Hydroxy-2-(4-hydroxyphenyl)ethyl GSL	*p*-Hydroxy-epiglucobarbarin	MS, NMR of GSL; UV, MS, NMR of desGSL	332,350
62	Phe/Tyr	B	(2*S*)-2-Hydroxy-2(4-hydroxyphenyl)ethyl GSL	*p*-Hydroxy-glucobarbarin	UV, MS, NMR of desGSL	350
63	Phe/Tyr	B	(2*R*)-2-Hydroxy-2(4-methoxyphenyl)ethyl GSL		MS, NMR of GSL	351
64	Phe	B	2-(*α*-L-Rhamnopyranosyloxy)-benzyl GSL		MS of GSL and desGSL	327,348
65	Phe	B	4-(4′-*O*-Acetyl-*α*-L-4-rhamnopyranosyloxy)-benzyl GSL	4-Acetyl-glucomoringin	MS of GSL and ITC	311,352
66	Phe	B	2-(*α*-L-Arabinopyranosyloxy)-2phenylethyl GSL		NMR of GSL	353
67	Phe	B	6′-Isoferuloyl-2-phenylethyl GSL	6′-Isoferuloyl-gluconasturtiin	MS of GSL, UV, MS NMR of desGSL	339,340
68	Phe	B	6′-Isoferuloyl-(2*R*)-2-hydroxy-2phenylethyl GSL	6′-Isoferuloyl-epiglucobarbarin	MS, NMR of GSL; UV, MS, NMR of desGSL	340

Table A-2. Continued

No	Class	Index	Semi systematic Name	Trivial Name	Characterization Methods	Reference
69	Phe	B	6′-Isoferuloyl-(2*S*)-2-hydroxy-2phenylethyl GSL	6′-Isoferuloyl-glucobarbarin	MS, NMR of GSL; UV, MS, NMR of desGSL	340
70	Phe/Tyr	B	6′-Isoferuloyl-(*R*)-2-hydroxy-2(4-hydroxyphenyl)ethyl GSL		MS of GSL; UV, MS NMR of desGSL	340
71	Phe/Tyr	B	4-(*α*-L-Rhamnopyranosyloxy)-benzyl GSL	Glucomorinigin	MS, NMR of GSL and desGSL	246,354–356
72	Met	A	3-(Methylsulfanyl)propyl GSL	Glucoibervirin	MS, NMR of GSL	245
73	Met	A	4-Oxoheptyl GSL	Glucocapangulin	Deduction from IR, 5-oxooctanoic acid	321
74	Met	A	4-(Methylsulfanyl)butyl GSL	Glucoerucin	UV, IR, MS NMR of GSL	246,342
75	Met	A	5-(Methylsulfanyl)pentyl GSL	Glucoberteroin	UV, IR, MS, NMR of GSL; UV, MS, NMR of desGSL	357–359
76	Met	A	6-(Methylsulfanyl)heptyl GSL		UV, IR, MS, NMR of GSL	357,358
77	Met	A	6-(Methylsulfanyl)hexyl GSL	Glucolesquerellin	UV, IR, MS, NMR of GSL	357,358
78	Met	A	8-(Methylsulfanyl)-3-oxooctyl GSL		MS of GSL; MS, NMR of des GSL	250,327
79	Met	A	9-(Methylsulfanyl)nonyl GSL		MS of GSL	327
80	Met	A	10-(Methylsulfanyl)decyl GSL		MS of ITC	360
81	Met	A	2-Methylsulfinylethyl GSL		UV, MS, NMR of desGSL	361
82	Met	A	(*R*)-11-(Methylsulfinyl)-propyl glucosinolate	Glucoiberin	MS, NMR, X-Ray of GSL; UV, MS, NMR of desGSL	246,247,342

Table A-2. Continued

No	Class	Index	Semi systematic Name	Trivial Name	Characterization Methods	Reference
83	Met	A	(*R/S*)-4-(Methylsulfinyl)-butyl glucosinolate	Glucoraphanin	MS, NMR of GSL, UV, MS NMR of desGSL	242,246,342
84	Met	A	(*R/S*)-5-(Methylsulfinyl)pentyl GSL	Glucoalyssin	MS, NMR of GSL; MS of desGSL	342,362
85	Met	A	(*R/S*)-6-(Methylsulfinyl)-hexyl GSL	Glucohesperin	UV, IR, MS, NMR of GSL	342,357,358
86	Met	A	(*R/S*)-7-(Methylsulfinyl)-heptyl GSL		NMR of GSL; MS, NMR of desGSL	250,363
87	Met	A	(*R/S*)-8-(Methylsulfinyl)-octyl GSL	Glucohirsutin	UV, IR, MS, NMR of GSL; MS, NMR of desGSL	250,358
88	Met	A	(*R/S*)-9-(Methylsulfinyl)-nonyl GSL	Glucoarabin	UV, IR, MS, NMR of GSL; MS, NMR of desGSL	358,364
89	Met	A	(*R/S*)-10-(Methylsulfinyl)decyl GSL	Glucocamelinin	MS, NMR of GSL; MS of desGSL	250,365
90	Met	A	(*R/S*)-11-(Methylsulfinyl)undecyl GSL		MS of GSL	365
91	Met	A	3-(Methylsulfonyl)-propyl GSL	Glucocheirolin	MS of GSL; NMR of desGSL	312,366
92	Met	A	4-(Methylsulfonyl)butyl GSL	Glucoerysolin	MS of GSL; MS, NMR of desGSL	327,345,364
93	Met	A	6-(Methylsulfonyl)hexyl GSL		MS of GSL	327
94	Met	A	8-(Methylsulfonyl)octyl GSL		UV, IR, MS, NMR of GSL; MS, NMR of desGSL	250,364,367
95	Met	A	9-(Methylsulfonyl)nonyl GSL		UV, IR, MS, NMR of GSL; MS, NMR of desGSL	250,364,367
96	Met	A	10-(Methylsulfonyl)decyl GSL		MS, NMR of desGSL	345,364
97	Met	A	(3*E*)-4-(Methylsulfanyl)-but-3-enyl GSL		IR, MS, NMR of GSL; NMR of desGSL	246,342

Table A-2. Continued

No	Class	Index	Semi systematic Name	Trivial Name	Characterization Methods	Reference
98	Met	A	(*R/S,3E*)-4-(Methylsulfinyl)-but-3-enyl GSL	Glucoraphenin	MS, NMR of GSL; UV, NMR of desGSL	246,342,368
99	Met	A	3-Hydroxy-5-(methylsulfinyl)pentyl GSL		Deducted from tetrahydro-1,3-oxazine-2-thione	369
100	Met	A	3-Hydroxy-5-(methylsulfony)pentyl GSL		UV, IR, MS, NMR of ITC	369
101	Met	A	3-Hydroxy-6-(methylsulfanyl)hexyl GSL		Deducted from tetrahydro-1,3-oxazine-2-thione	370
102	Met	A	3-Hydroxy-6-(methylsufinyl)hexyl GSL		Deducted from ITC	370
103	Met	A	3-Hydroxy-5-(methylsulfinyl)pentyl GSL		Deducted from tetrahydro-1,3oxazine-2-thione and ITC	370
104	Met	A	8-(Methylsulfanyl)-3-oxooctyl GSL		Deducted from ITC	371
105	Met	A	(*R/S*)-8-(Methylsulfinyl)-3-oxooctyl GSL		Deducted from ITC	371
106	Met	A	4-Mercaptobutyl GSL		MS, NMR of GSL	372,373
107	Met	A	(*R*)-4-(Cystein-*S*-yl)butyl GSL	Glucorucolamine	MS, NMR of desGSL	374
108	Met	A	Dimeric 4-mercaptobutyl GSL		MS, NMR of GSL; MS of desGSL	372
109	Met	A	4-(*β*-D-Glucopyranosyl-disulfanyl)-butyl GSL	Diglucothiobeinin	MS of GSL; MS, NMR of desGSL	375,376
110	Met	A	6′-Benzoyl-4(methylsulfanyl) butyl GSL	6′-Benzoyl-glucoerucin	UV, MS, NMR of desGSL	361
111	Met	A	6′-Benzoyl-4(methylsulfinyl)butyl- GSL	6′-Benzoyl - glucopharanin	UV, MS, NMR of desGSL	361
112	Met	A	(*R/S*, *3E*)-6′-Sinapoyl-4-(methylsulfinyl)but-3-enyl GSL	6′-Sinapoyl-glucoraphenin	UV, IR, MS, NMR of desGSL	377

Table A-2. Continued

No	Class	Index	Semi systematic Name	Trivial Name	Characterization Methods	Reference
113	Se-Met	A	3-(Methylseleno)propyl GSL		Comparing MS with natural S-analogues	378
114	Se-Met	A	4-(Methylseleno)butyl GSL		Comparing MS with natural S-analogues	378
115	Se-Met	A	5-(Methylseleno)pentyl GSL		Comparing MS with natural S-analogues	378
116	Met	A	Allyl glucosinolate	Sinigrin	MS, NMR, X-Ray of GSL; UV, MS, NMR of desGSL	246,327
117	Met	A	But-3-enyl GSL	Gluconapin	MS, NMR of GSL; UV, MS, NMR of desGSL	246,250,342,362
118	Met	A	Pent-4-enyl GSL	Glucobrassicanapin	MS of GSL; MS, NMR of desGSL	250,362
119	Met	A	(*2S*)-2-Hydroxypent-4-enyl GSL	Gluconapoleiferin	MS of GSL	335
120	Met	A	(*2R*)-2-Hydroxybut-3-enyl GSL	Progoitrin	MS, NMR of GSL; UV, MS, NMR of desGSL	246,250,341,342,345
121	Met	A	(*2S*)-2-Hydroxybut-3-enyl GSL	Epiprogoitrin	MS, NMR of GSL; UV, MS, NMR of desGSL	246,250,335,341
122	Met	C	2′,3′-Dihydro-2′-oxoindol-3′-ylacetate ester at 2-OH of (*R*)-2-hydroxbut-3-enyl GSL	Glucoisatisin	UV, MS, NMR of GSL	379,380
123	Met	C	2′,3′-Dihydro-2′-oxoindol-3′-ylacetate of ester at 2-OH of (*S*)-2-hydroxbut-3-enyl GSL	Epiglucoisatisin	UV, MS, NMR of GSL	379,380
124	Met	C	2′,3′-Dihydro-3′-hydroxy-2′-oxoindol-3′-ylacetate ester at 2-OH of (*R*)-2-hydroxybut-3-enyl GSL	(*S*)-3′-Hydroxy-glucoisasitin	UV, MS, NMR of GSL	379

Table A-2. Continued

No	Class	Index	Semi systematic Name	Trivial Name	Characterization Methods	Reference
125	Met	C	2′,3′-Dihydro-3′-hydroxy-2′-oxoindol-3′-ylacetate ester at 2-OH of (*S*)-2-hydroxybut-3-enyl GSL	*(S)*-3′-Hydroxy-epiglucoisasitin	UV, MS, NMR of GSL	[379]
126	Met	B	(*2S*)-2-Benzoyloxybut-3-enyl GSL	2-*O*-Benzoyl-epiprogoitrin	MS of desGSL	[361]
127	Met	A	2-Hydroxyethyl GSL		NMR of GSL	[381]
128	Met	A	3-Hydroxypropyl GSL		MS, NMR of ITC	[382]
129	Met	A	4-Hydroxylbutyl GSL		MS of GSL	[383]
130	Met	A	3-Hydroxylbutyl GSL		Deducted from tetrahydro-1,3oxazine-2-thione	[318]
131	Met	B	2-(Benzoyloxy)ethyl GSL		MS of GSL	[383]
132	Met	B	3-(Benzoyloxy)propyl GSL	Glucomalcolmiin	MS of GSL; UV, MS of desGSL	[361,383,384]
133	Met	B	4-(Benzoyloxy)butyl GSL		MS of GSL; UV, MS, NMR of desGSL	[361,383]
134	Met	B	5-(Benzoyloxy)pentyl GSL		MS, NMR of desGSL	[361]
135	Met	B	6-(Benzoyloxy)hexyl GSL		Deducted from ITC	[384]
136	Met	B	3-Sinapoyloxypropyl GSL		MS, NMR of desGSL	[385]
137	Met	B	6′-Benzoyl-4-benzoyloxybutyl GSL		UV, MS, NMR of desGSL	[361]

desGSL: desfulfated Glucosinolates; IR: Infra-red; ITC: Isothiocyanates; MS: Mass Spectrometry; NMR: Nuclear Magnetic Resonance; Index: ?: Uncertain precursor.

APPENDIX B
SUPPLEMENTARY INFORMATION FOR CHAPTER 5

Table B-1. Protein concentration of AE and alkaline extracts.

Entries	%EtOH	T_e (°C)	Protein concentration of AE extracts (%)	Protein concentration of alkaline extracts (%)
0	0	25	-	59.22
1	70	50	41.3	64.26
2	20	25	48.5	65.75
3	70	50	42.5	64.9
4	20	50	46.5	67.3
5	45	50	48.7	63.8
6	20	75	47.2	58.7
7	70	25	42.3	67.2
8	70	50	46.9	62.7
9	90	25	44.4	63.6
10	20	25	48.3	67.3
11	90	50	44.5	63.8
12	45	75	54.5	58.1
13	70	75	51.3	55.7

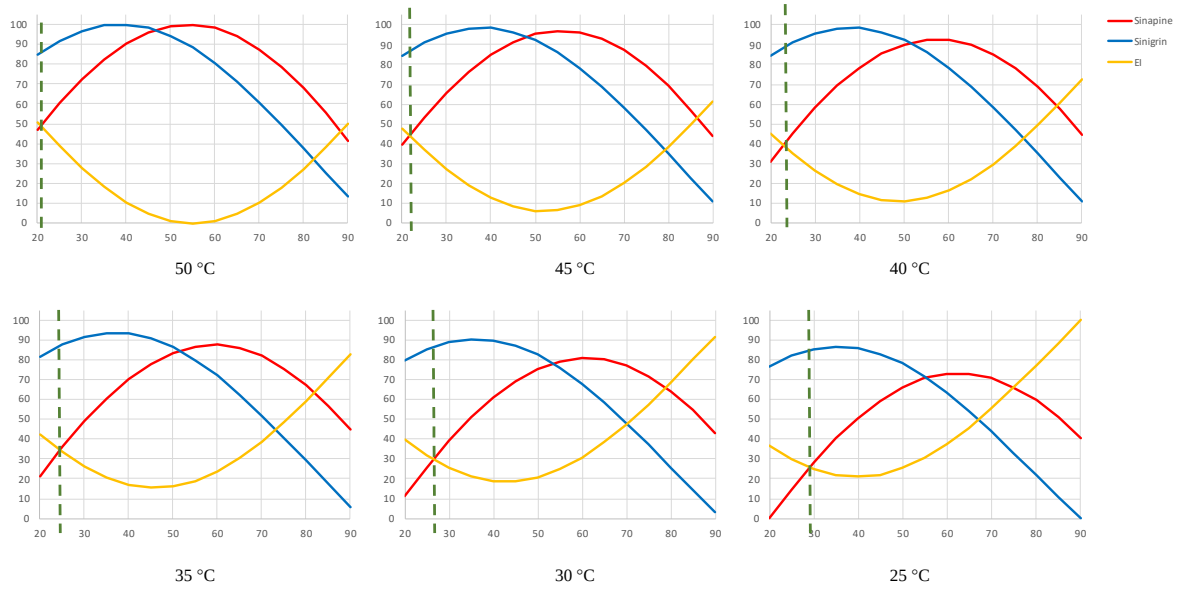

Figure B-1. Plotting chart to determine desired compromise at different temperature from 25 to 50°C. The response values were scaled where the minima and the maxima were set at 0 and 100%, respectively. The X axis presents %EtOH; and Y axis presents scaled responses.

Table B-2. Sinapine concentration of AE and alkaline extracts.

Entries	%EtOH	T_e (°C)	Sinapine concentration of AE extracts (mg/g_{DM})	Sinapine concentration of alkaline extracts (mg/g_{DM})
0	0	25	-	6.6723
1	70	50	10.3764	1.4336
2	20	25	8.0726	1.4033
3	70	50	9.8962	1.2599
4	20	50	8.6998	1.2901
5	45	50	11.3354	1.1287
6	20	75	10.0643	1.2110
7	70	25	10.4755	1.6094
8	70	50	10.3432	1.4518
9	90	25	8.6687	1.9641
10	20	25	7.2657	1.6398
11	90	50	9.4402	1.8860
12	45	75	10.2762	1.3258
13	70	75	9.7151	1.4688

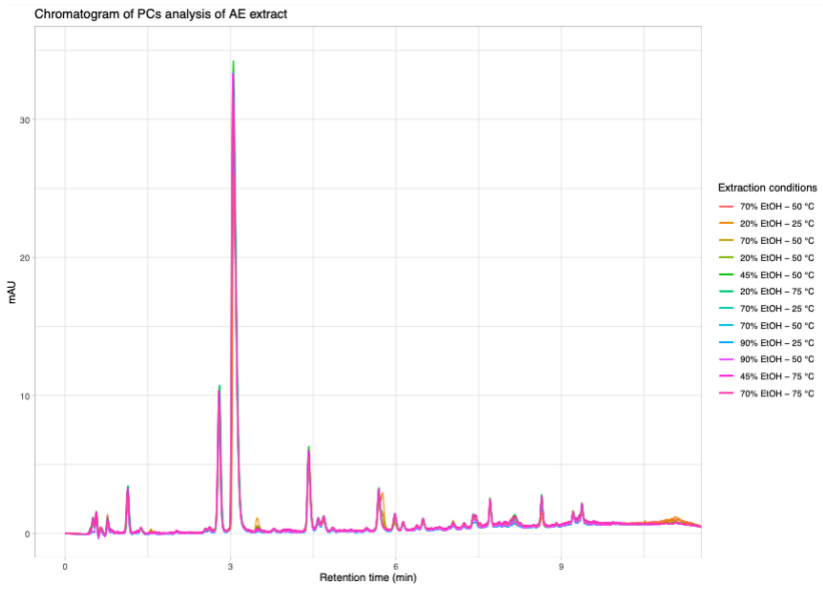

Figure B-2. PCs' analysis chromatograms of AE extracts. Chromatograms were recored at 320 nm.

Table B-3. Sinigrin concentration of AE and alkaline extracts.

Entries	%EtOH	T_e (°C)	Sinigrin concentration of AE extracts (µmol/g_{DM})	Sinigrin concentration of alkaline extracts (µmol/g_{DM})
0	0	25	-	70.7482
1	70	50	72.0563	13.3285
2	20	25	88.1575	7.6720
3	70	50	87.7529	12.3955
4	20	50	92.3045	12.6897
5	45	50	93.6177	2.0007
6	20	75	94.0140	-0.0395
7	70	25	74.3477	25.5384
8	70	50	32.5855	14.9310
9	90	25	42.5303	42.7234
10	20	25	79.1531	14.9071
11	90	50	47.6201	41.1014
12	45	75	91.6635	5.0773
13	70	75	83.1287	6.3332

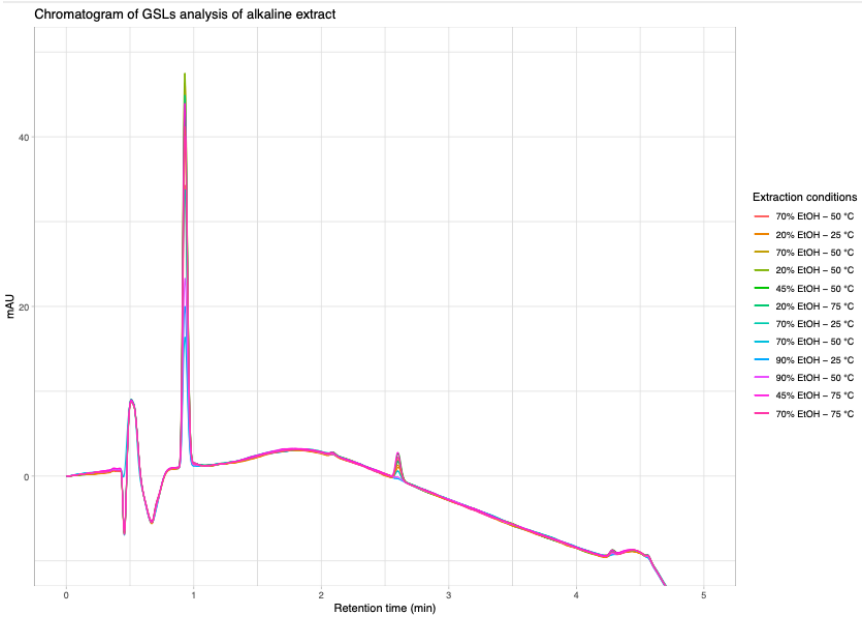

Figure B-3. GSLs' analysis chromatograms of AE extracts. Chromatograms were recorded at 229 nm

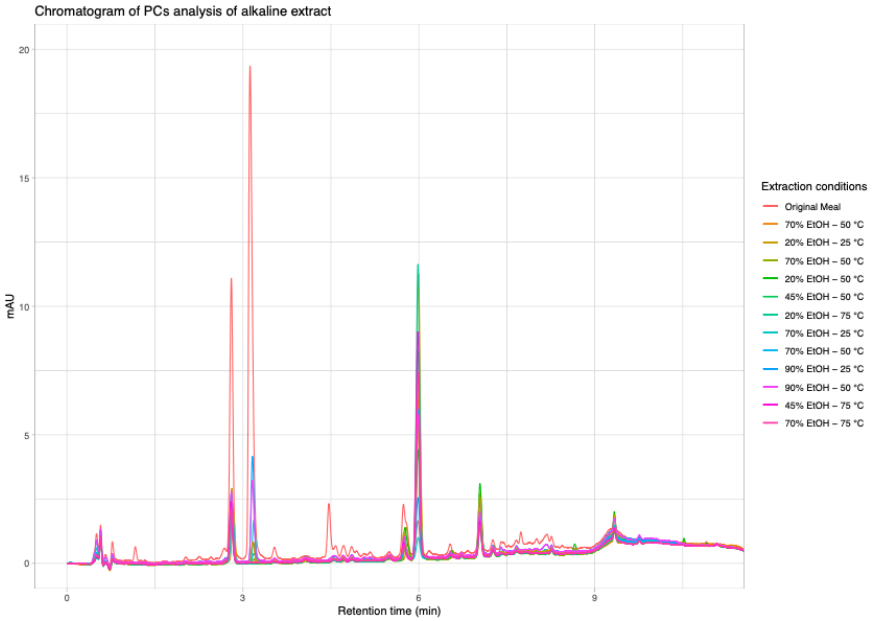

Figure B-4. PCs' analysis chromatograms of alkaline extracts. Chromatograms were recorded at 320 nm.

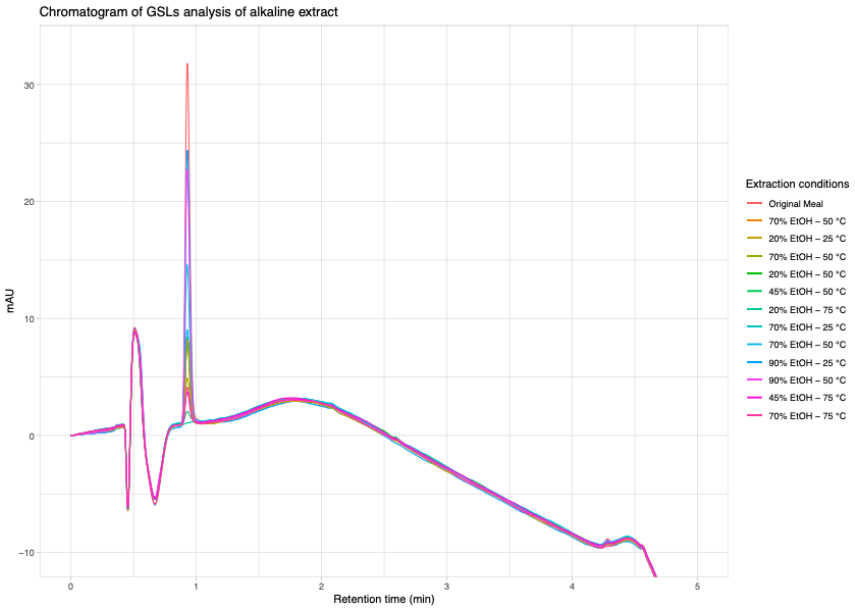

Figure B-5. GSLs' analysis chromatogram of alkaline extracts. Chromatogram were recorded at 229 nm

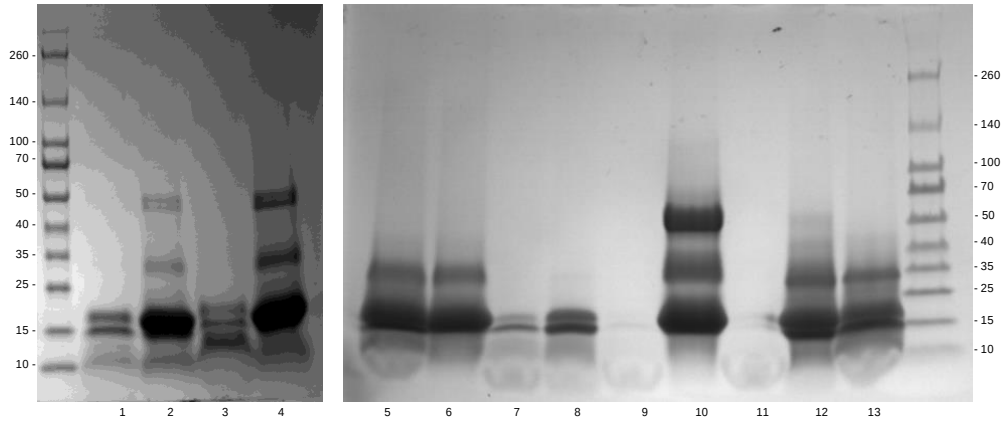

Figure B-6. SDS-PAGE under non reducing conditions of AE extracts.

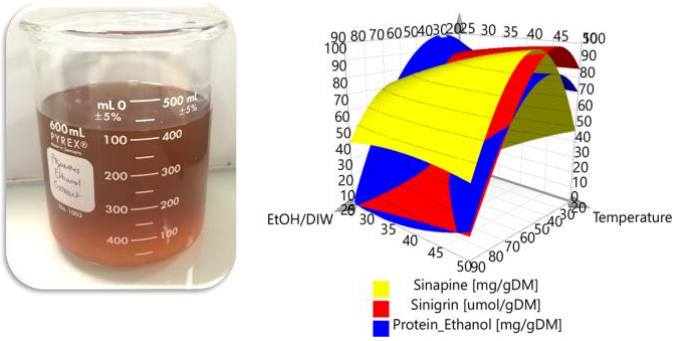

Figure B-7. (Left) Photograph of AE extracts from experimental design. (Right) Response Surface Plot of selected factors (%EtOH, T_e) and responses (Y_1, Y_2, Y_3).

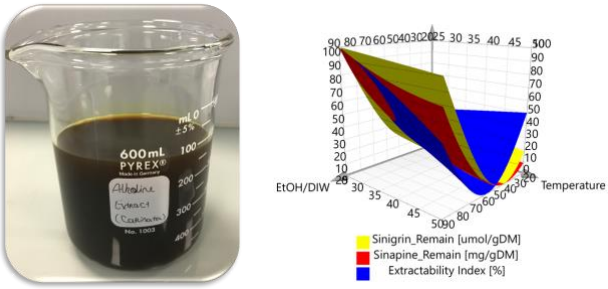

Figure B-8. (Left) Photograph of alkaline extracts from experimental design; (Right) Response Surface Plot of selected factors (%EtOH, T_e) and responses (Y_1, Y_2, Y_3).

APPENDIX C
SUPPLEMENTARY INFORMATION FOR CHAPTER 6

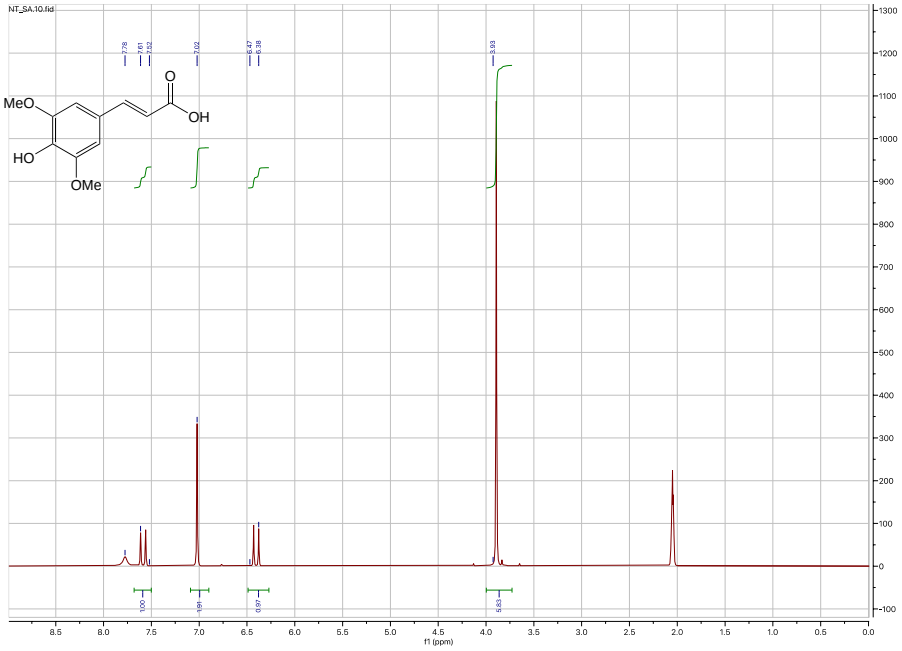

Figure C-1. ^{1}H NMR spectrum of SinA in acetone.

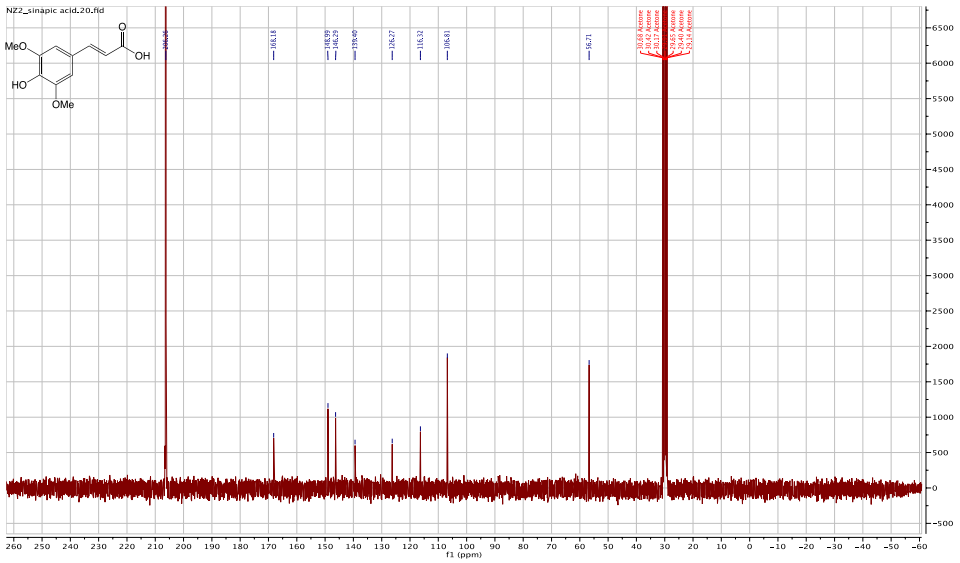

Figure C-2. ^{13}C NMR spectrum of SinA in acetone.

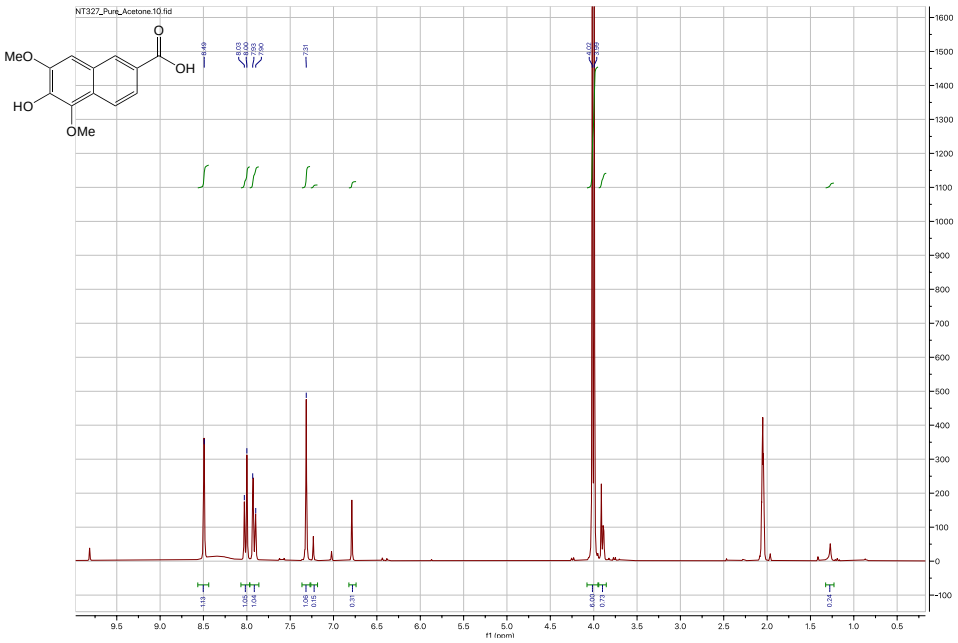

Figure C-3. ^{1}H NMR spectrum of DMNA in acetone.

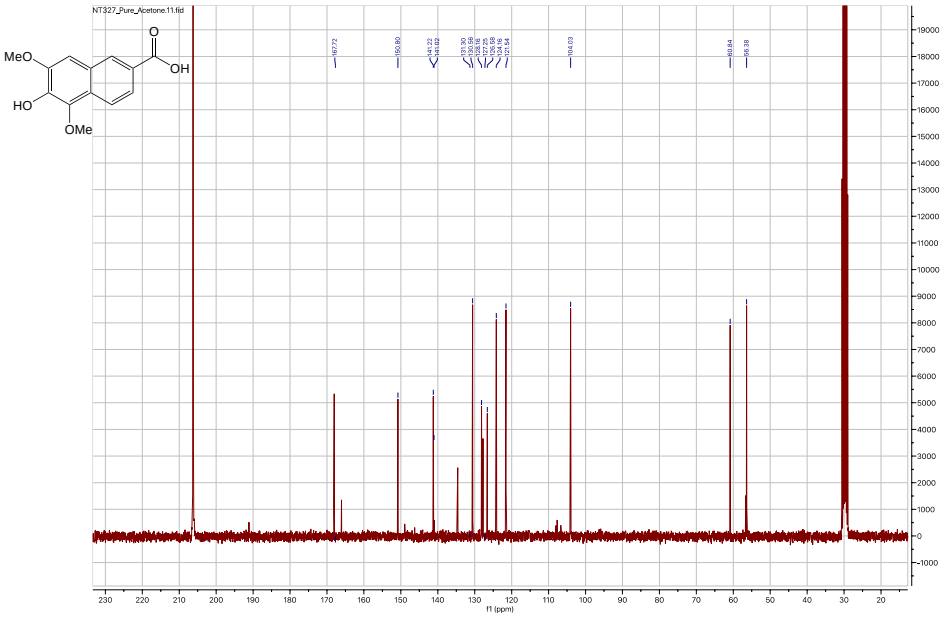

Figure C-4.^{13}C NMR spectrum of DMNA in acetone.

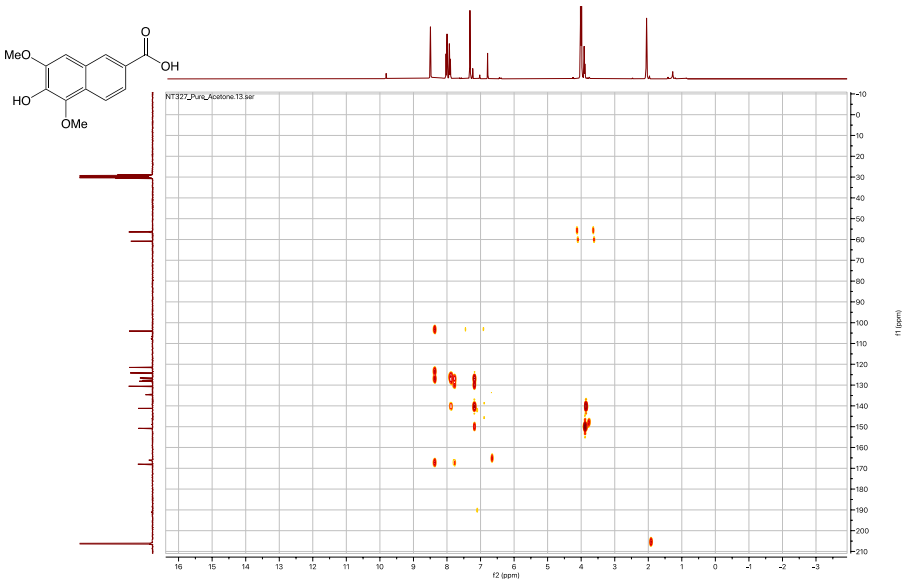

Figure C-5. 2D NMR (HSQC) of DMNA in acetone.

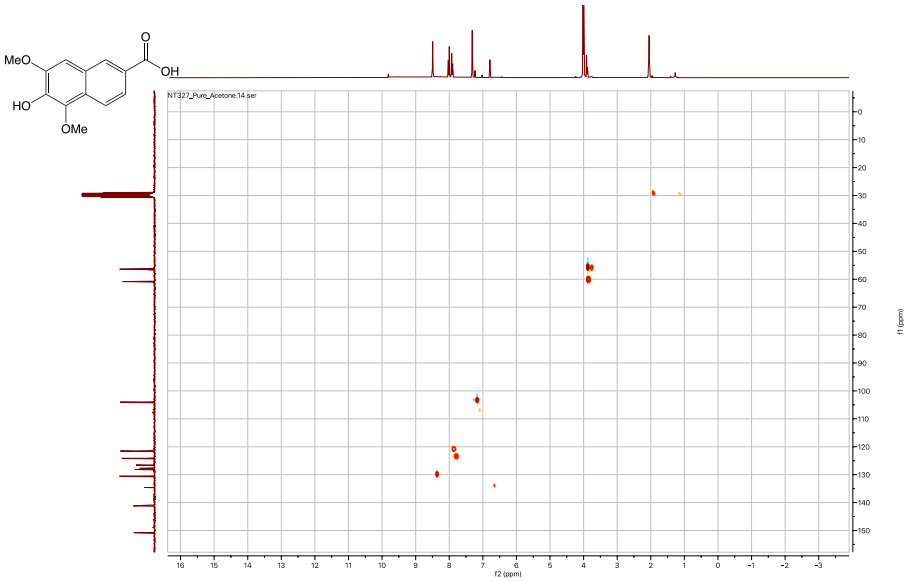

Figure C-6. 2D NMR (HMBC) of DMNA in acetone.

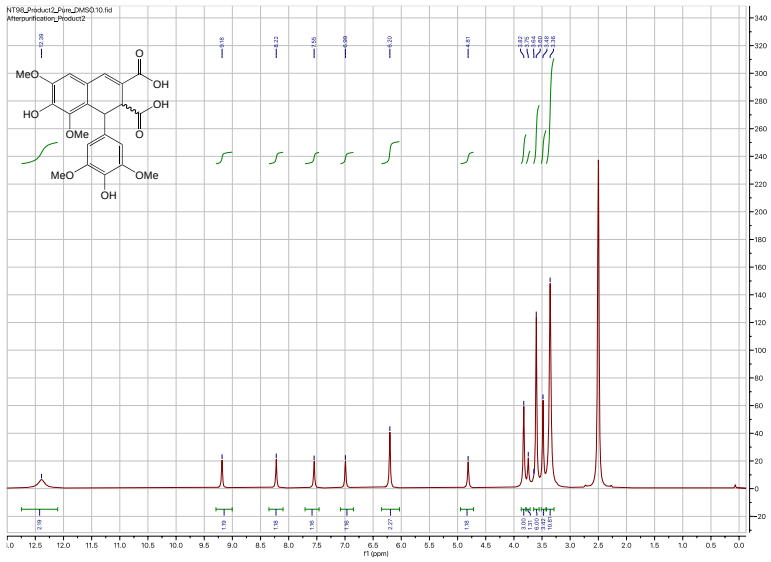

Figure C-7. ^{1}H NMR spectrum of ThoA in DMSO.

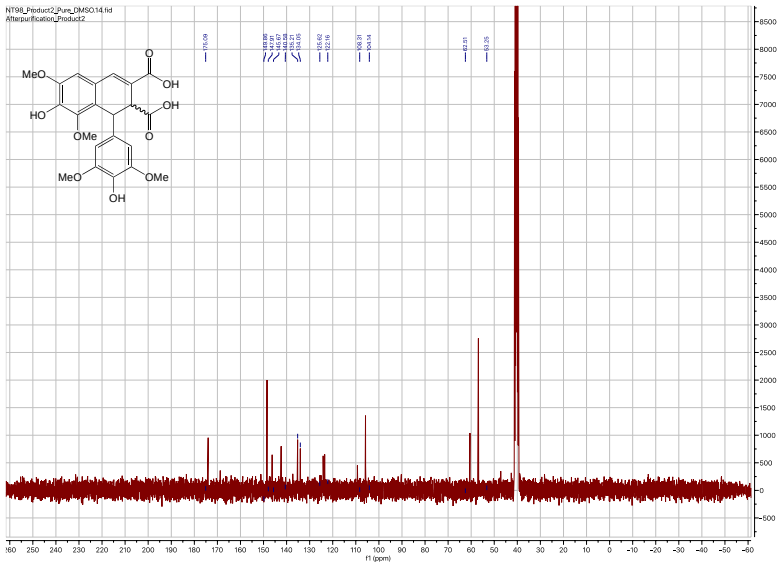

Figure C-8. ^{13}C NMR of ThoA in DMSO.

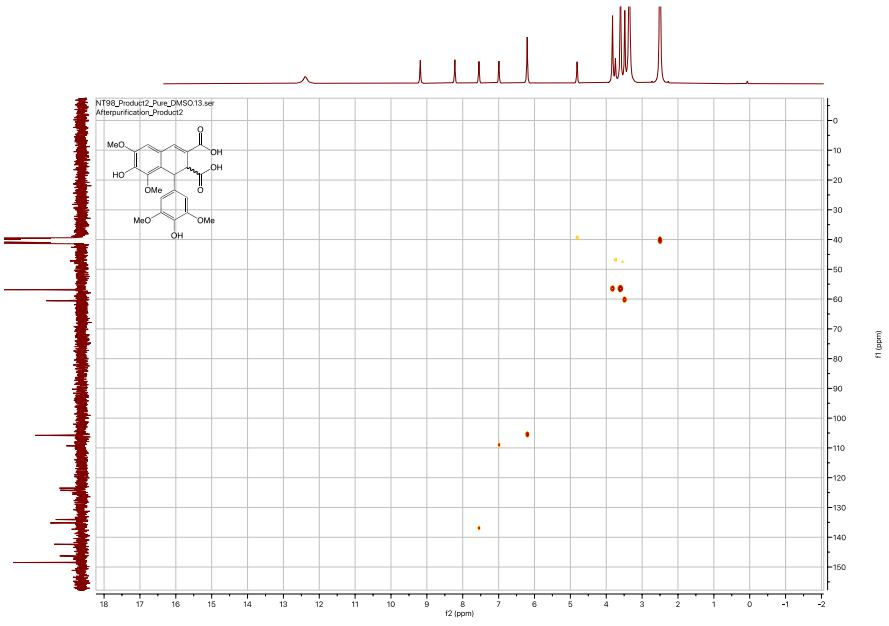

Figure C-9. 2D NMR (HSQC) of ThoA in DMSO.

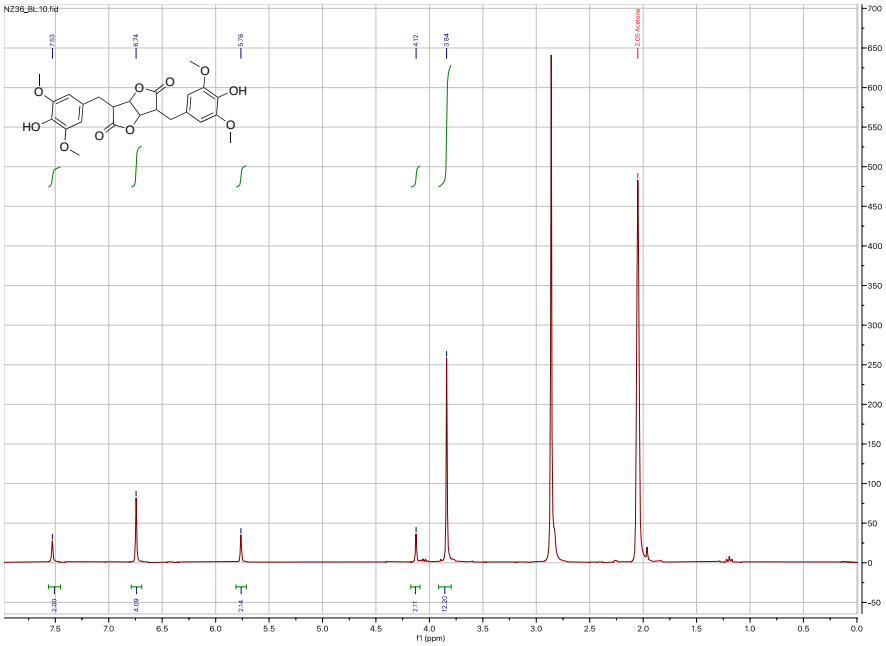

Figure C-10. ^{1}H NMR spectrum of bislactone in acetone.

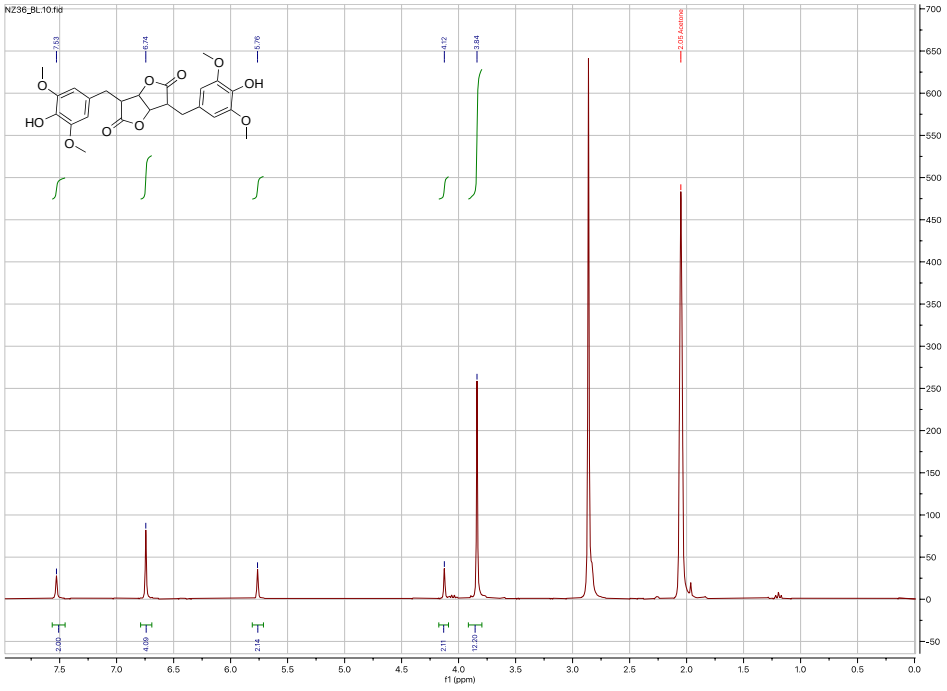

Figure C-11. ^{13}C NMR spectrum of bislactone in acetone.

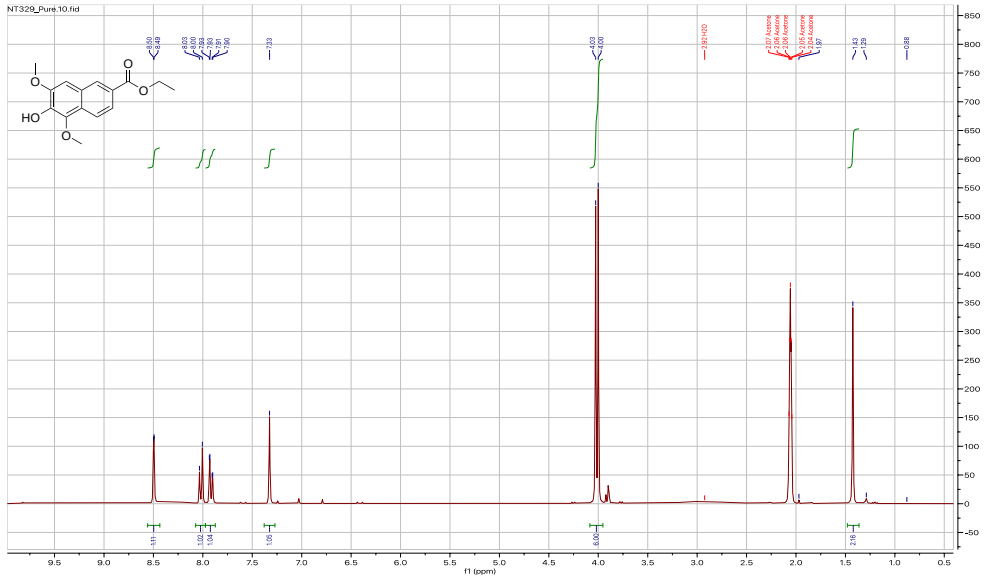

Figure C-12. ^{1}H NMR spectrum of ethyl-DMNA in acetone.

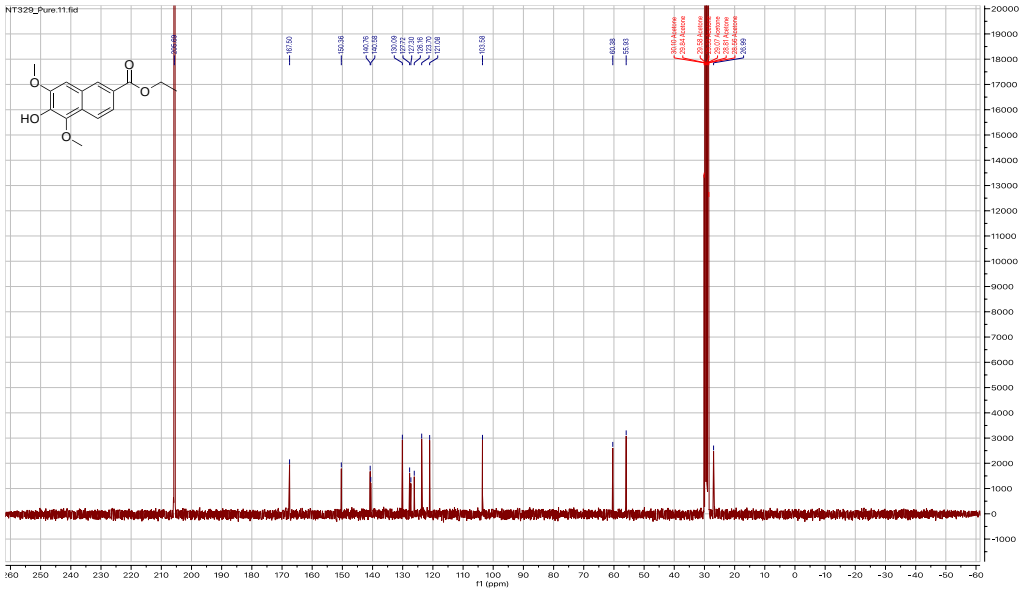

Figure C-13. ^{13}C NMR spectrum of ethyl-DMNA in acetone.

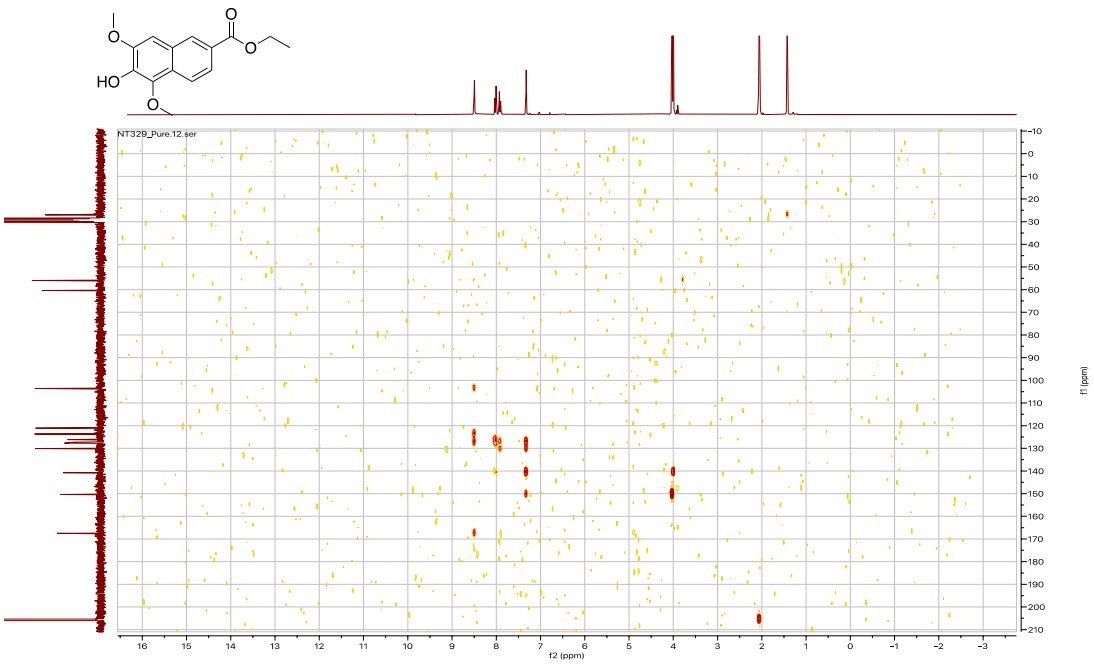

Figure C-14. 2D NMR (HSQC) of ethyl-DMNA in acetone.

SAPPENDIX D
SUPPLEMENTARY INFORMATION FOR CHAPTER 7

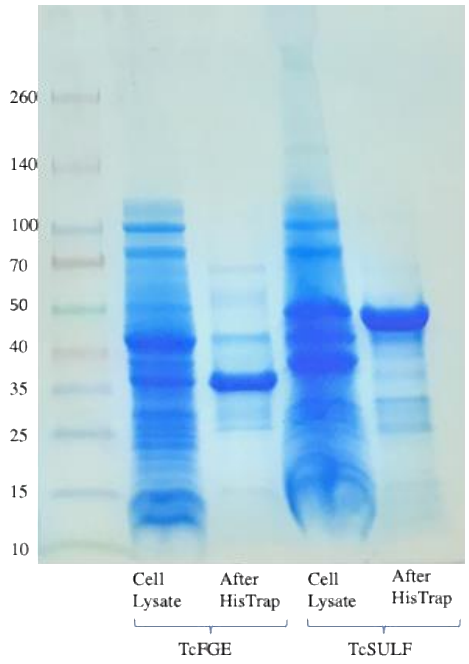

Figure D-1. SDS-PAGE gel analysis of cell lysate and concentrated fraction after purification using His-affinity chromatography.

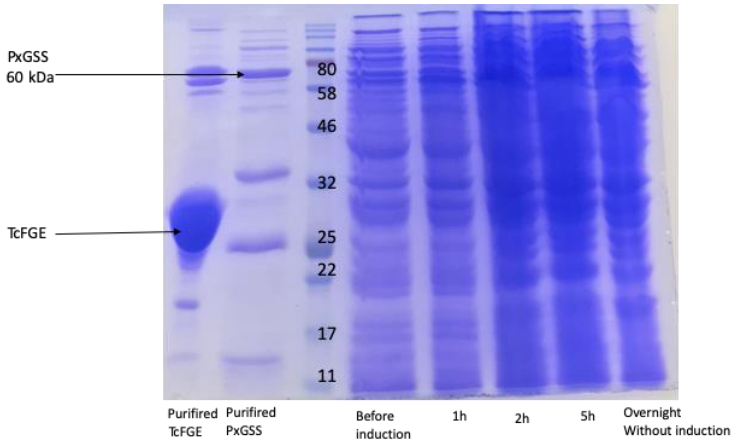

Figure D-2. SDS-PAGE analysis monitoring the growth of recombinant protein PxGSS by E. coli before and after induction with 0.5 mM IPTG.

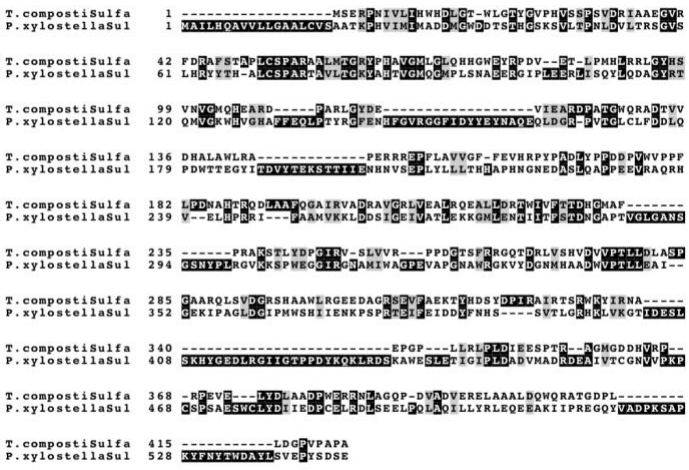

Figure D-3.Comparison of *P. xylostella* sulfatase and *T. composti* sulfatase protein sequences. The red box highlights the targeted area by FGE.

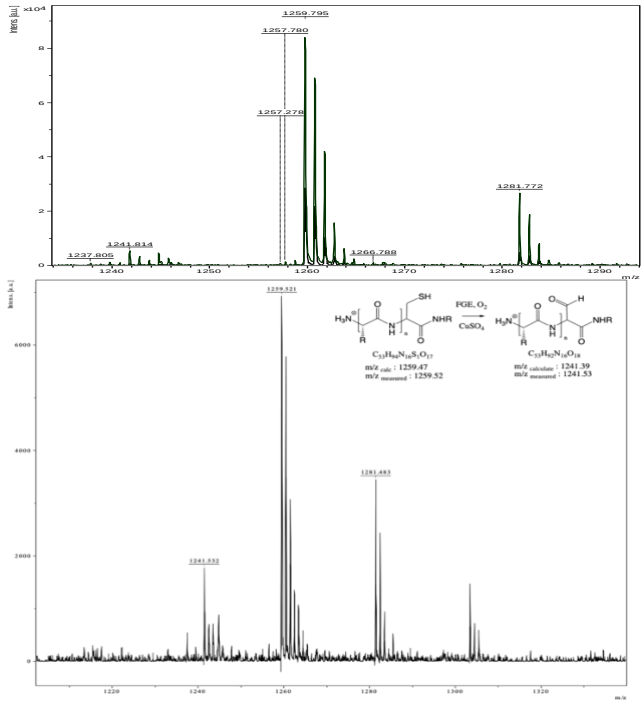

Figure D-4.Results of FGE assay characterized by MALDI-ToF-MS using sinapic acid as matrix. (Top) FGE assay results in the absence of Cu (I); (Bottom) FGE assay results with presence of Cu (I).

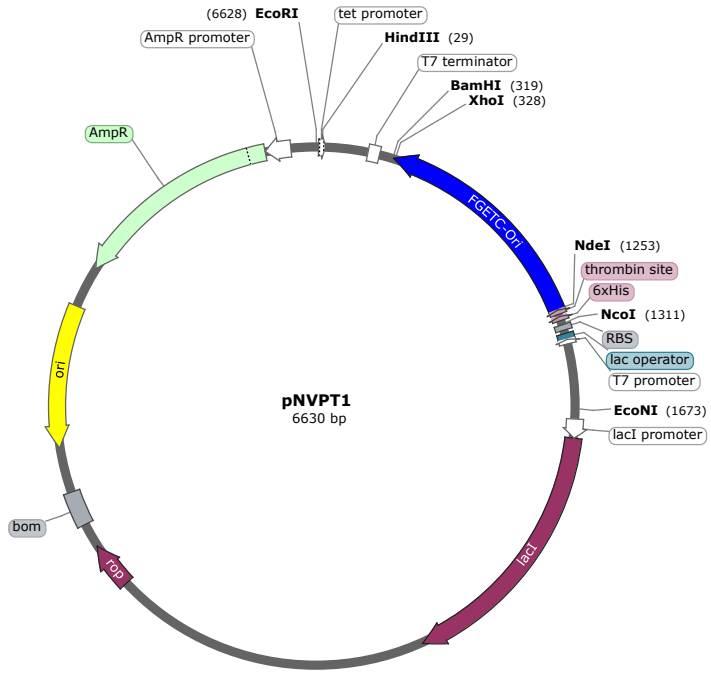

Figure D-5. Map of plasmid pNVPT1.

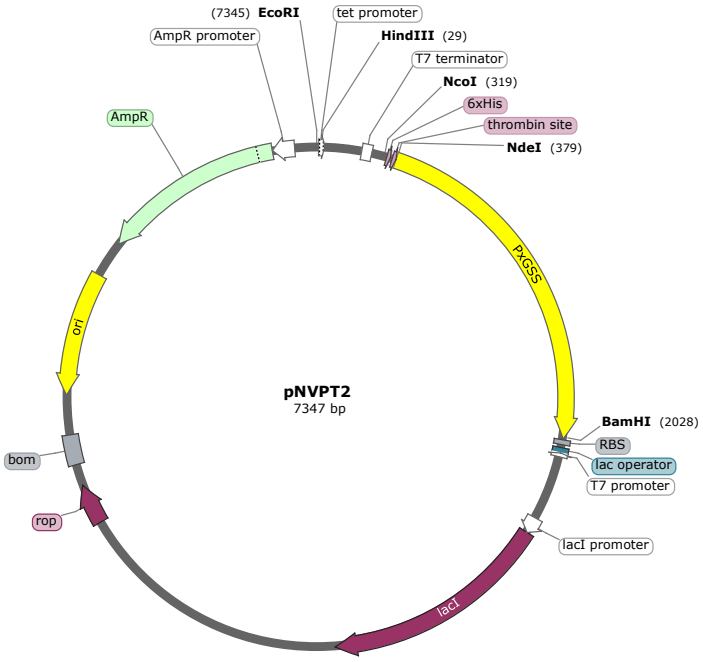

Figure D-6. Map of plasmid pNVPT2.

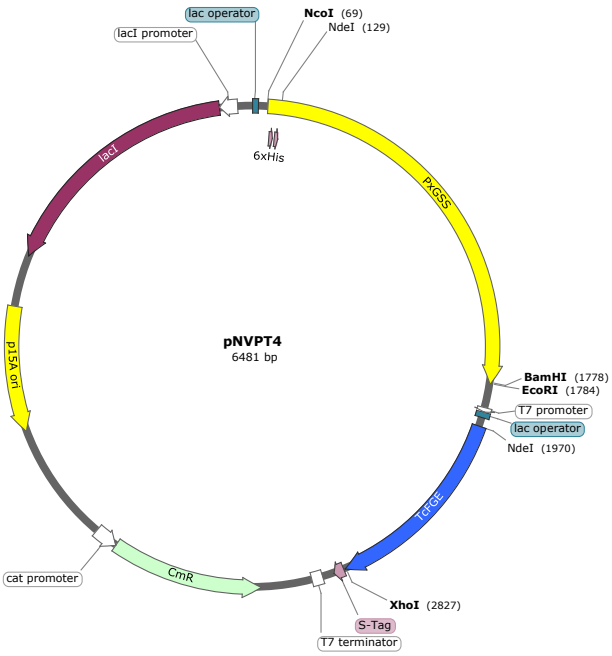

Figure D-7. Map of plasmid pNVPT4.

LIST OF REFERENCES

(1) International Energy Agency (IEA). Global Energy Review 2019. *IEA* **2020**.

(2) US Energy Information Administration. Renewable energy explained - https://www.eia.gov/energyexplained/renewable-sources/.

(3) Isahak, W. N. R. W.; Hisham, M. W. M.; Yarmo, M. A.; Yun Hin, T. Y. A Review on Bio-Oil Production from Biomass by Using Pyrolysis Method. *Renew. Sustain. Energy Rev.* **2012**, *16* (8), 5910–5923. https://doi.org/10.1016/j.rser.2012.05.039.

(4) Weiss, E. *Oilseed Crops*, 2nd ed.; Wiley-Blackwell, 2000.

(5) USDA. Oilseeds: World Markets and Trade - Report December 2019. **2019**.

(6) SPARC. Southeast Partnership for Advanced Renewables from Carinata - Https://Sparc-Cap.Org.

(7) Seepaul, R.; Small, I. M.; Mulvaney, M. J.; George, S.; Leon, R. G.; Geller, D.; Wright, D. L. Carinata , the Sustainable Crop for a Bio-Based Economy : 2018 – 2019 Production Recommendations for the Southeastern United States. **2019**, 1–12.

(8) Schulmeister, T. M.; Ruiz-Moreno, M.; Silva, G. M.; Garcia-Ascolani, M.; Ciriaco, F. M.; Henry, D. D.; Lamb, G. C.; Dubeux, J. C. B.; Dilorenzo, N. Evaluation of Brassica Carinata Meal on Ruminant Metabolism and Apparent Total Tract Digestibility of Nutrients in Beef Steers. *J. Anim. Sci.* **2019**, *97* (3), 1325–1334. https://doi.org/10.1093/jas/skz009.

(9) Downey, R. K.; Rimmer, S. R. *Agronomic Improvement in Oilseed Brassicas*; Elsevier Masson SAS, 1993; Vol. 50. https://doi.org/10.1016/S0065-2113(08)60831-7.

(10) Bouaid, A.; Diaz, Y.; Martinez, M.; Aracil, J. Pilot Plant Studies of Biodiesel Production Using Brassica Carinata as Raw Material. *Catal. Today* **2005**, *106* (1–4), 193–196. https://doi.org/10.1016/j.cattod.2005.07.163.

(11) George, S.; Seepaul, R.; Geller, D.; Dwivedi, P.; DiLorenzo, N.; Altman, R.; Coppola, E.; Miller, S. A.; Bennett, R.; Johnston, G.; Streit, L.; Csonka, S.; Field, J.; Marois, J.; Wright, D.; Small, I.; Philippidis, G. P. A Regional Inter-disciplinary Partnership Focusing on the Development of a Carinata-centered Bioeconomy. *GCB Bioenergy* **2021**, gcbb.12828. https://doi.org/10.1111/gcbb.12828.

(12) Kumar, S.; Seepaul, R.; Mulvaney, M. J.; Colvin, B.; George, S.; Marois, J. J.; Bennett, R.; Leon, R.; Wright, D. L.; Small, I. M. Brassica Carinata Genotypes Demonstrate Potential as a Winter Biofuel Crop in South East United States. *Ind. Crops Prod.* **2020**, *150* (October 2019), 112353. https://doi.org/10.1016/j.indcrop.2020.112353.

(13) Xin, H.; Yu, P. Chemical Profile, Energy Values, and Protein Molecular Structure Characteristics of Biofuel/Bio-Oil Co-Products (Carinata Meal) in Comparison with Canola Meal. *J. Agric. Food Chem.* **2013**, *61* (16), 3926–3933. https://doi.org/10.1021/jf400028n.

(14) Boot, A.; La Marta, J. The Safety and the Generally Recognized as Safe (GRAS) Status of the Proposed Uses of Canola/Rapeseed Protein Isolate in Human Food. **2016**, No. 683, 12–13.

(15) Tan, S. H.; Mailer, R. J.; Blanchard, C. L.; Agboola, S. O. Canola Proteins for Human Consumption: Extraction, Profile, and Functional Properties. *J. Food Sci.* **2011**, *76* (1), R16–R28. https://doi.org/10.1111/j.1750-3841.2010.01930.x.

(16) Pedroche, J.; Yust, M. M.; Lqari, H.; Girón-Calle, J.; Alaiz, M.; Vioque, J.; Millán, F. Brassica Carinata Protein Isolates: Chemical Composition, Protein Characterization and Improvement of Functional Properties by Protein Hydrolysis. *Food Chem.* **2004**, *88* (3), 337–346. https://doi.org/10.1016/j.foodchem.2004.01.045.

(17) Griffiths, D. W.; Birch, A. N. E.; Hillman, J. R. Antinutritional Compounds in the Brassicaceae: Analysis, Biosynthesis, Chemistry and Dietary Effects. *J. Hortic. Sci. Biotechnol.* **1998**, *73* (1), 1–18. https://doi.org/10.1080/14620316.1998.11510937.

(18) Wanasundara, J. P. D. Proteins of Brassicaceae Oilseeds and Their Potential as a Plant Protein Source. *Crit. Rev. Food Sci. Nutr.* **2011**, *51* (7), 635–677. https://doi.org/10.1080/10408391003749942.

(19) Arrutia, F.; Binner, E.; Williams, P.; Waldron, K. W. Oilseeds beyond Oil: Press Cakes and Meals Supplying Global Protein Requirements. *Trends Food Sci. Technol.* **2020**, *100* (March), 88–102. https://doi.org/10.1016/j.tifs.2020.03.044.

(20) Rubino, M. I.; Arntfield, S. D.; Nadon, C. A.; Bernatsky, A. Phenolic Protein Interactions in Relation to the Gelation Properties of Canola Protein. *Food Res. Int.* **1996**, *29* (7), 653–659. https://doi.org/10.1016/S0963-9969(97)89643-3.

(21) Sosulski, F. Organoleptic and Nutritional Effects of Phenolic Compounds on Oilseed Protein Products: A Review. *J. Am. Oil Chem. Soc.* **1979**, *56* (8), 711–715. https://doi.org/10.1007/BF02663047.

(22) Blažević, I.; Montaut, S.; Burčul, F.; Olsen, C. E.; Burow, M.; Rollin, P.; Agerbirk, N. Glucosinolate Structural Diversity, Identification, Chemical Synthesis and Metabolism in Plants. *Phytochemistry* **2020**, *169*, 112100. https://doi.org/10.1016/j.phytochem.2019.112100.

(23) Tripathi, M. K.; Mishra, A. S. Glucosinolates in Animal Nutrition: A Review. *Anim. Feed Sci. Technol.* **2007**, *132* (1–2), 1–27. https://doi.org/10.1016/j.anifeedsci.2006.03.003.

(24) Zhou, J. R.; Erdman, J. W. Phytic Acid in Health and Disease. *Crit. Rev. Food Sci. Nutr.* **1995**, *35* (6), 495–508. https://doi.org/10.1080/10408399509527712.

(25) Shamsuddin, A. M. A. M. Anti-Cancer Function of Phytic Acid. *Int. J. Food Sci. Technol.* **2002**, *37* (7), 769–782. https://doi.org/10.1046/j.1365-2621.2002.00620.x.

(26) Fox, C. H.; Eberl, M. Phytic Acid (IP6), Novel Broad Spectrum Anti-Neoplastic Agent: A Systematic Review. *Complement. Ther. Med.* **2002**, *10* (4), 229–234. https://doi.org/10.1016/S0965-2299(02)00092-4.

(27) Silva, E. O.; Bracarense, A. P. F. R. L. Phytic Acid: From Antinutritional to Multiple Protection Factor of Organic Systems. *J. Food Sci.* **2016**, *81* (6), R1357–R1362. https://doi.org/10.1111/1750-3841.13320.

(28) Vallejo, F.; Toms-Barbern, F. A.; Garca-Viguera, C. Potential Bioactive Compounds in Health Promotion from Broccoli Cultivars Grown in Spain. *J. Sci. Food Agric.* **2002**, *82* (11), 1293–1297. https://doi.org/10.1002/jsfa.1183.

(29) Nićiforović, N.; Abramovič, H. Sinapic Acid and Its Derivatives: Natural Sources and Bioactivity. *Compr. Rev. Food Sci. Food Saf.* **2014**, *13* (1), 34–51. https://doi.org/10.1111/1541-4337.12041.

(30) Pandey, K. B.; Rizvi, S. I. Plant Polyphenols as Dietary Antioxidants in Human Health and Disease. *Oxid. Med. Cell. Longev.* **2009**, *2* (5), 270–278. https://doi.org/10.4161/oxim.2.5.9498.

(31) Kensler, T. W. Chemoprevention by Inducers of Carcinogen Detoxication Enzymes. *Environ. Health Perspect.* **1997**, *105* (SUPPL. 4), 965–970. https://doi.org/10.2307/3433311.

(32) Dias, C.; Aires, A.; Saavedra, M. Antimicrobial Activity of Isothiocyanates from Cruciferous Plants against Methicillin-Resistant Staphylococcus Aureus (MRSA). *Int. J. Mol. Sci.* **2014**, *15* (11), 19552–19561. https://doi.org/10.3390/ijms151119552.

(33) Mazumder, A.; Dwivedi, A.; Plessis, J. Du. Sinigrin and Its Therapeutic Benefits. *Molecules* **2016**, *21* (4), 1–11. https://doi.org/10.3390/molecules21040416.

(34) Aider, M.; Barbana, C. Canola Proteins: Composition, Extraction, Functional Properties, Bioactivity, Applications as a Food Ingredient and Allergenicity – A Practical and Critical Review. *Trends Food Sci. Technol.* **2011**, *22* (1), 21–39. https://doi.org/10.1016/j.tifs.2010.11.002.

(35) FAO/WHO/UNU. *Energy and Protein Requirements*; 1985.

(36) Bhatla, S. C.; Kaushik, V.; Yadav, M. K. Use of Oil Bodies and Oleosins in Recombinant Protein Production and Other Biotechnological Applications. *Biotechnol. Adv.* **2010**, *28* (3), 293–300. https://doi.org/10.1016/j.biotechadv.2010.01.001.

(37) Wu, J.; Aluko, R. E.; Muir, A. D. Production of Angiotensin I-Converting Enzyme Inhibitory Peptides from Defatted Canola Meal. *Bioresour. Technol.* **2009**, *100* (21), 5283–5287. https://doi.org/10.1016/j.biortech.2009.03.090.

(38) Höglund, A. S.; Rödin, J.; Larsson, E.; Rask, L. Distribution of Napin and Cruciferin in Developing Rape Seed Embryos. *Plant Physiol.* **1992**, *98* (2), 509–515. https://doi.org/10.1104/pp.98.2.509.

(39) Shewry, P. R.; Napier, J. A.; Tatham, A. S. Seed Storage Proteins: Structures and Biosynthesis. *Plant Cell* **1995**, *7* (7), 945–956. https://doi.org/10.1105/tpc.7.7.945.

(40) Tandang-Silvas, M. R. G.; Fukuda, T.; Fukuda, C.; Prak, K.; Cabanos, C.; Kimura, A.; Itoh, T.; Mikami, B.; Utsumi, S.; Maruyama, N. Conservation and Divergence on Plant Seed 11S Globulins Based on Crystal Structures. *Biochim. Biophys. Acta - Proteins Proteomics* **2010**, *1804* (7), 1432–1442. https://doi.org/10.1016/j.bbapap.2010.02.016.

(41) Dalgalarrondo, M.; Robin, J.-M.; Azanza, J.-L. Subunit Composition of the Globulin Fraction of Rapeseed (Brassica Napus L.). *Plant Sci.* **1986**, *43* (2), 115–124. https://doi.org/10.1016/0168-9452(86)90151-2.

(42) Perera, S. P.; McIntosh, T. C.; Wanasundara, J. P. D. Structural Properties of Cruciferin and Napin of Brassica Napus (Canola) Show Distinct Responses to Changes in PH and Temperature. *Plants* **2016**, *5* (3), 64–74. https://doi.org/10.3390/plants5030036.

(43) Schwenke, K. D.; Linow, K.-J. A Reversible Dissociation of the 12 S Globulin from Rapeseed (Brassica Napus L.) Depending on Ionic Strength. *Food / Nahrung* **1982**, *26* (1), K5–K6. https://doi.org/10.1002/food.19820260139.

(44) Chabanon, G.; Chevalot, I.; Framboisier, X.; Chenu, S.; Marc, I. Hydrolysis of Rapeseed Protein Isolates: Kinetics, Characterization and Functional Properties of Hydrolysates. *Process Biochem.* **2007**, *42* (10), 1419–1428. https://doi.org/10.1016/j.procbio.2007.07.009.

(45) Fetzer, A.; Herfellner, T.; Stäbler, A.; Menner, M.; Eisner, P. Influence of Process Conditions during Aqueous Protein Extraction upon Yield from Pre-Pressed and Cold-Pressed Rapeseed Press Cake. *Ind. Crops Prod.* **2018**, *112* (December 2017), 236–246. https://doi.org/10.1016/j.indcrop.2017.12.011.

(46) Gorissen, S. H. M.; Crombag, J. J. R.; Senden, J. M. G.; Waterval, W. A. H.; Bierau, J.; Verdijk, L. B.; van Loon, L. J. C. Protein Content and Amino Acid Composition of Commercially Available Plant-Based Protein Isolates. *Amino Acids* **2018**, *50* (12), 1685–1695. https://doi.org/10.1007/s00726-018-2640-5.

(47) Bhatty, R. S.; McKenzie, S. L.; Finlayson, A. J. The Proteins of Rapeseed (Brassica Napus L.) Soluble in Salt Solutions. *Can. J. Biochem.* **1968**, *46* (10), 1191–1197. https://doi.org/10.1139/o68-178.

(48) Menéndez-Arias, L.; Monsalve, R. I.; Gavilanes, J. G.; Rodríguez, R. Molecular and Spectroscopic Characterisation of a Low Molecular Weight Seed Storage Protein from Yellow Mustard (Sinapis Alba L.). *Int. J. Biochem.* **1987**, *19* (10), 899–907. https://doi.org/10.1016/0020-711X(87)90170-4.

(49) Marambe, H. K.; McIntosh, T. C.; Cheng, B.; Wanasundara, J. P. D. Structural Stability and Sin a 1 Anti-Epitope Antibody Binding Ability of Yellow Mustard (Sinapis Alba L.) Napin during Industrial-Scale Myrosinase Inactivation Process. *Food Funct.* **2015**, *6* (7), 2384–2395. https://doi.org/10.1039/C4FO00806E.

(50) Pantoja-Uceda, D.; Palomares, O.; Bruix, M.; Villalba, M.; Rodríguez, R.; Rico, M.; Santoro, J. Solution Structure and Stability against Digestion of RproBnIb, a Recombinant 2S Albumin from Rapeseed: Relationship to Its Allergenic Properties. *Biochemistry* **2004**, *43* (51), 16036–16045. https://doi.org/10.1021/bi048069x.

(51) Pantoja-Uceda, D.; Bruix, M.; Giménez-Gallego, G.; Rico, M.; Santoro, J. Solution Structure of RicC3, a 2S Albumin Storage Protein from Ricinus Communis. *Biochemistry* **2003**, *42* (47), 13839–13847. https://doi.org/10.1021/bi0352217.

(52) Jyothi, T. C.; Sinha, S.; Singh, S. A.; Surolia, A.; Appu Rao, A. G. Napin from Brassica Juncea: Thermodynamic and Structural Analysis of Stability. *Biochim. Biophys. Acta - Proteins Proteomics* **2007**, *1774* (7), 907–919. https://doi.org/10.1016/j.bbapap.2007.04.008.

(53) Byczyńska, A.; Barciszewski, J. The Biosynthesis, Structure and Properties of Napin - The Storage Protein from Rape Seeds. *J. Plant Physiol.* **1999**, *154* (4), 417–425. https://doi.org/10.1016/S0176-1617(99)80277-6.

(54) Akbari, A.; Wu, J. An Integrated Method of Isolating Napin and Cruciferin from Defatted Canola Meal. *LWT - Food Sci. Technol.* **2015**, *64* (1), 308–315. https://doi.org/10.1016/j.lwt.2015.05.046.

(55) Rommi, K.; Hakala, T. K.; Holopainen, U.; Nordlund, E.; Poutanen, K.; Lantto, R. Effect of Enzyme-Aided Cell Wall Disintegration on Protein Extractability from Intact and Dehulled Rapeseed (Brassica Rapa L. and Brassica Napus L.) Press Cakes. *J. Agric. Food Chem.* **2014**, *62* (32), 7989–7997. https://doi.org/10.1021/jf501802e.

(56) Wang, B.; Meng, T.; Ma, H.; Zhang, Y.; Li, Y.; Jin, J.; Ye, X. Mechanism Study of Dual-Frequency Ultrasound Assisted Enzymolysis on Rapeseed Protein by Immobilized Alcalase. *Ultrason. Sonochem.* **2016**, *32*, 307–313. https://doi.org/10.1016/j.ultsonch.2016.03.023.

(57) Ugolini, L.; De Nicola, G.; Palmieri, S. Use of Reverse Micelles for the Simultaneous Extraction of Oil, Proteins, and Glucosinolates from Cruciferous Oilseeds. *J. Agric. Food Chem.* **2008**, *56* (5), 1595–1601. https://doi.org/10.1021/jf072582a.

(58) Bérot, S.; Compoint, J. P.; Larré, C.; Malabat, C.; Guéguen, J. Large Scale Purification of Rapeseed Proteins (Brassica Napus L.). *J. Chromatogr. B Anal. Technol. Biomed. Life Sci.* **2005**, *818* (1 SPEC. ISS.), 35–42. https://doi.org/10.1016/j.jchromb.2004.08.001.

(59) Wu, J.; Muir, A. D. Comparative Structural, Emulsifying, and Biological Properties of 2 Major Canola Proteins, Cruciferin and Napin. *J. Food Sci.* **2008**, *73* (3). https://doi.org/10.1111/j.1750-3841.2008.00675.x.

(60) Akbari, A.; Lavasanifar, A.; Wu, J. Interaction of Cruciferin-Based Nanoparticles with Caco-2 Cells and Caco-2/HT29-MTX Co-Cultures. *Acta Biomater.* **2017**, *64*, 249–258. https://doi.org/10.1016/j.actbio.2017.10.017.

(61) Wang, F.; Yang, Y.; Ju, X.; Udenigwe, C. C.; He, R. Polyelectrolyte Complex Nanoparticles from Chitosan and Acylated Rapeseed Cruciferin Protein for Curcumin Delivery. *J. Agric. Food Chem.* **2018**, *66* (11), 2685–2693. https://doi.org/10.1021/acs.jafc.7b05083.

(62) Akbari, A.; Wu, J. Cruciferin Nanoparticles: Preparation, Characterization and Their Potential Application in Delivery of Bioactive Compounds. *Food Hydrocoll.* **2016**, *54*, 107–118. https://doi.org/10.1016/j.foodhyd.2015.09.017.

(63) Pinterits, A.; Arntfield, S. D. Improvement of Canola Protein Gelation Properties through Enzymatic Modification with Transglutaminase. *LWT - Food Sci. Technol.* **2008**, *41* (1), 128–138. https://doi.org/10.1016/j.lwt.2007.01.011.

(64) Schwenke, K. D.; Dahme, A.; Wolter, T. Heat-Induced Gelation of Rapeseed Proteins: Effect of Protein Interaction and Acetylation. *JAOCS, J. Am. Oil Chem. Soc.* **1998**, *75* (1), 83–87. https://doi.org/10.1007/s11746-998-0015-x.

(65) Palomares, O.; Cuesta-Herranz, J.; Vereda, A.; Sirvent, S.; Villalba, M.; Rodríguez, R. Isolation and Identification of an 11S Globulin as a New Major Allergen in Mustard Seeds. *Ann. Allergy, Asthma Immunol.* **2005**, *94* (5), 586–592. https://doi.org/10.1016/S1081-1206(10)61138-6.

(66) Monsalve, R. I.; Villalba, M.; Rodríguez, R. Allergy to Mustard Seeds: The Importance of 2S Albumins as Food Allergens. *Internet Symp. Food Allergens* **2001**, *3* (2), 57–69.

(67) Terras, F.; Schoofs, H.; Thevissen, K.; Osborn, R. W.; Vanderleyden, J.; Cammue, B.; Broekaert, W. F. Synergistic Enhancement of the Antifungal Activity of Wheat and Barley Thionins by Radish and Oilseed Rape 2S Albumins and by Barley Trypsin Inhibitors. *Plant Physiol.* **1993**, *103* (4), 1311–1319.

(68) Neumann, G. M.; Condron, R.; Thomas, I.; Polya, G. M. Purification and Sequencing of Multiple Forms of Brassica Napus Seed Napin Large Chains That Are Calmodulin Antagonists and Substrates for Plant Calcium-Dependent Protein Kinase. *Biochim. Biophys. Acta - Protein Struct. Mol. Enzymol.* **1996**, *1295* (1), 34–43. https://doi.org/10.1016/0167-4838(96)00007-6.

(69) Cocucci, M.; Negrini, N. Changes in the Levels of Calmodulin and of a Calmodulin Inhibitor in the Early Phases of Radish (Raphanus Sativus L.) Seed Germination. *Plant Physiol.* **1988**, *88* (3), 910–914. https://doi.org/10.1104/pp.88.3.910.

(70) Siloto, R. M. P.; Findlay, K.; Lopez-Villalobos, A.; Yeung, E. C.; Nykiforuk, C. L.; Moloney, M. M. The Accumulation of Oleosins Determines the Size of Seed Oilbodies in Arabidopsis. *Plant Cell* **2006**, *18* (8), 1961–1974. https://doi.org/10.1105/tpc.106.041269.

(71) Chen, K.; Yin, Y.; Liu, S.; Guo, Z.; Zhang, K.; Liang, Y.; Zhang, L.; Zhao, W.; Chao, H.; Li, M. Genome-Wide Identification and Functional Analysis of Oleosin Genes in Brassica Napus L. *BMC Plant Biol.* **2019**, *19* (1), 1–20. https://doi.org/10.1186/s12870-019-1891-y.

(72) Koiwa, H.; Bressan, R. A.; Hasegawa, P. M. Regulation of Protease Inhibitors and Plant Defense. *Trends Plant Sci.* **1997**, *2* (10), 379–384. https://doi.org/10.1016/S1360-1385(97)90052-2.

(73) Cipollini, D. F.; Bergelson, J. Environmental and Developmental Regulation of Trypsin Inhibitor Activity in Brassica Napus. *J. Chem. Ecol.* **2000**, *26* (6), 1411–1422. https://doi.org/10.1023/A:1005540107957.

(74) Huang, A. H. C. Plant Lipid Droplets and Their Associated Proteins: Potential for Rapid Advances. *Plant Physiol.* **2018**, *176* (3), 1894–1918. https://doi.org/10.1104/pp.17.01677.

(75) Tzen, J. T. C.; Lie, G. C.; Huang, A. H. C. Characterization of the Charged Components and Their Topology on the Surface of Plant Seed Oil Bodies. *J. Biol. Chem.* **1992**, *267* (22), 15626–15634.

(76) Huang, A. H. C. Oil Bodies and Oleosins in Seeds. *Annu. Rev. Plant Physiol. Plant Mol. Biol.* **1992**, *43* (1), 177–200. https://doi.org/10.1146/annurev.pp.43.060192.001141.

(77) Murphy, D. J. Structure, Function and Biogenesis of Storage Lipid Bodies and Oleosins in Plants. *Prog. Lipid Res.* **1993**, *32* (3), 247–280. https://doi.org/10.1016/0163-7827(93)90009-L.

(78) Svendsen, I.; Nicolova, D.; Goshev, I.; Genov, N. Isolation and Characterization of a Trypsin Inhibitor from the Seeds of Kohlrabi (Brassica Napus Var. Rapifera) Belonging to the Napin Family of Storage Proteins. *Carlsberg Res. Commun.* **1989**, *54* (6), 231–239. https://doi.org/10.1007/BF02910458.

(79) D'Andréa, S.; Jolivet, P.; Boulard, C.; Larré, C.; Froissard, M.; Chardot, T. Selective One-Step Extraction of Arabidopsis Thaliana Seed Oleosins Using Organic Solvents. *J. Agric. Food Chem.* **2007**, *55* (24), 10008–10015. https://doi.org/10.1021/jf0717079.

(80) Dastranj, M.; Borzoui, E.; Bandani, A. R.; Franco, O. L. Inhibitory Effects of an Extract from Non-Host Plants on Physiological Characteristics of Two Major Cabbage Pests. *Bull. Entomol. Res.* **2018**, *108* (3), 370–379. https://doi.org/10.1017/S0007485317000864.

(81) Duong-Ly, K. C.; Gabelli, S. B. *Salting out of Proteins Using Ammonium Sulfate Precipitation*, 1st ed.; Elsevier Inc., 2014; Vol. 541. https://doi.org/10.1016/B978-0-12-420119-4.00007-0.

(82) Vargo, K. B.; Sood, N.; Moeller, T. D.; Heiney, P. A.; Hammer, D. A. Spherical Micelles Assembled from Variants of Recombinant Oleosin. *Langmuir* **2014**, *30* (38), 11292–11300. https://doi.org/10.1021/la502664e.

(83) Nouri-Ganbalani, G.; Borzoui, E.; Shahnavazi, M.; Nouri, A. Induction of Resistance against Plutella Xylostella (L.) (Lep.: Plutellidae) by Jasmonic Acid and Mealy Cabbage Aphid Feeding in Brassica Napus L. *Front. Physiol.* **2018**, *9* (JUL), 1–11. https://doi.org/10.3389/fphys.2018.00859.

(84) Nicholson, R. L.; Hammerschmidt, R. Phenolic Compounds and Their Role in Disease Resistance. *Annu. Rev. Phytopathol. Vol. 30* **1992**, 369–389. https://doi.org/10.1146/annurev.py.30.090192.002101.

(85) Beckman, C. H. Phenolic-Storing Cells: Keys to Programmed Cell Death and Periderm Formation in Wilt Disease Resistance and in General Defence Responses in Plants? *Physiol. Mol. Plant Pathol.* **2000**, *57* (3), 101–110. https://doi.org/10.1006/pmpp.2000.0287.

(86) Maddox, C. E.; Laur, L. M.; Tian, L. Antibacterial Activity of Phenolic Compounds against the Phytopathogen Xylella Fastidiosa. *Curr. Microbiol.* **2010**, *60* (1), 53–58. https://doi.org/10.1007/s00284-009-9501-0.

(87) Engels, C.; Schieber, A.; Gänzle, M. G. Sinapic Acid Derivatives in Defatted Oriental Mustard (Brassica Juncea L.) Seed Meal Extracts Using UHPLC-DAD-ESI-MS n and Identification of Compounds with Antibacterial Activity. *Eur. Food Res. Technol.* **2012**, *234* (3), 535–542. https://doi.org/10.1007/s00217-012-1669-z.

(88) Yun, K. J.; Koh, D. J.; Kim, S. H.; Park, S. J.; Ryu, J. H.; Kim, D. G.; Lee, J. Y.; Lee, K. T. Anti-Inflammatory Effects of Sinapic Acid through the Suppression of Inducible Nitric Oxide Synthase, Cyclooxygase-2, and Proinflammatory Cytokines Expressions via Nuclear Factor-KB Inactivation. *J. Agric. Food Chem.* **2008**, *56* (21), 10265–10272. https://doi.org/10.1021/jf802095g.

(89) Oueslati, S.; Ksouri, R.; Falleh, H.; Pichette, A.; Abdelly, C.; Legault, J. Phenolic Content, Antioxidant, Anti-Inflammatory and Anticancer Activities of the Edible Halophyte Suaeda Fruticosa Forssk. *Food Chem.* **2012**, *132* (2), 943–947. https://doi.org/10.1016/j.foodchem.2011.11.072.

(90) Raj Preeth, D.; Shairam, M.; Suganya, N.; Hootan, R.; Kartik, R.; Pierre, K.; Suvro, C.; Rajalakshmi, S. Green Synthesis of Copper Oxide Nanoparticles Using Sinapic Acid: An Underpinning Step towards Antiangiogenic Therapy for Breast Cancer. *J. Biol. Inorg. Chem.* **2019**, *24* (5), 633–645. https://doi.org/10.1007/s00775-019-01676-z.

(91) Boeing, J. S.; Barizão, É. O.; Rotta, E. M.; Volpato, H.; Nakamura, C. V.; Maldaner, L.; Visentainer, J. V. Phenolic Compounds from Butia Odorata (Barb. Rodr.) Noblick Fruit and Its Antioxidant and Antitumor Activities. *Food Anal. Methods* **2020**, *13* (1), 61–68. https://doi.org/10.1007/s12161-019-01515-6.

(92) Yoon, B. H.; Jung, J. W.; Lee, J. J.; Cho, Y. W.; Jang, C. G.; Jin, C.; Oh, T. H.; Ryu, J. H. Anxiolytic-like Effects of Sinapic Acid in Mice. *Life Sci.* **2007**, *81* (3), 234–240. https://doi.org/10.1016/j.lfs.2007.05.007.

(93) Jaufurally, A. S.; Teixeira, A. R. S.; Hollande, L.; Allais, F.; Ducrot, P.-H. Optimization of the Laccase-Catalyzed Synthesis of (+/-)-Syringaresinol and Study of Its Thermal and Antiradical Activities. *ChemistrySelect* **2016**, *1* (16), 5165–5171. https://doi.org/10.1002/slct.201600543.

(94) Janvier, M.; Hollande, L.; Jaufurally, A. S.; Pernes, M.; Ménard, R.; Grimaldi, M.; Beaugrand, J.; Balaguer, P.; Ducrot, P. H.; Allais, F. Syringaresinol: A Renewable and Safer Alternative to Bisphenol A for Epoxy-Amine Resins. *ChemSusChem* **2017**, *10* (4), 738–746. https://doi.org/10.1002/cssc.201601595.

(95) Hollande, L.; Do Marcolino, I.; Balaguer, P.; Domenek, S.; Gross, R. A.; Allais, F. Preparation of Renewable Epoxy-Amine Resins with Tunable Thermo-Mechanical Properties, Wettability and Degradation Abilities from Lignocellulose- and Plant Oils-Derived Components. *Front. Chem.* **2019**, *7* (MAR), 1–11. https://doi.org/10.3389/fchem.2019.00159.

(96) Lin, L.-Z.; Harnly, J. M. Phenolic Component Profiles of Mustard Greens, Yu Choy, and 15 Other Brassica Vegetables. *J. Agric. Food Chem.* **2010**, *58* (11), 6850–6857. https://doi.org/10.1021/jf1004786.

(97) Cartea, M. E.; Francisco, M.; Soengas, P.; Velasco, P. Phenolic Compounds in Brassica Vegetables. *Molecules* **2011**, *16* (1), 251–280. https://doi.org/10.3390/molecules16010251.

(98) Thiel, A.; Muffler, K.; Tippkötter, N.; Suck, K.; Sohling, U.; Hruschka, S. M.; Ulber, R. A Novel Integrated Downstream Processing Approach to Recover Sinapic Acid, Phytic Acid and Proteins from Rapeseed Meal. *J. Chem. Technol. Biotechnol.* **2015**, *90* (11), 1999–2006. https://doi.org/10.1002/jctb.4664.

(99) Odinot, E.; Fine, F.; Sigoillot, J.-C.; Navarro, D.; Laguna, O.; Bisotto, A.; Peyronnet, C.; Ginies, C.; Lecomte, J.; Faulds, C.; Lomascolo, A. A Two-Step Bioconversion Process for Canolol Production from Rapeseed Meal Combining an Aspergillus Niger Feruloyl Esterase and the Fungus Neolentinus Lepideus. *Microorganisms* **2017**, *5* (4), 67. https://doi.org/10.3390/microorganisms5040067.

(100) Reungoat, V.; Gaudin, M.; Flourat, A. L.; Isidore, E.; Mouterde, L. M. M.; Allais, F.; Ducatel, H.; Ioannou, I. Optimization of an Ethanol/Water-Based Sinapine Extraction from Mustard Bran Using Response Surface Methodology. *Food Bioprod. Process.* **2020**, *122*, 322–331. https://doi.org/10.1016/j.fbp.2020.06.001.

(101) Fernandes, F.; Valentão, P.; Sousa, C.; Pereira, J. A.; Seabra, R. M.; Andrade, P. B. Chemical and Antioxidative Assessment of Dietary Turnip (Brassica Rapa Var. Rapa L.). *Food Chem.* **2007**, *105* (3), 1003–1010. https://doi.org/10.1016/j.foodchem.2007.04.063.

(102) Harbaum, B.; Hubbermann, E. M.; Zhu, Z.; Schwarz, K. Free and Bound Phenolic Compounds in Leaves of Pak Choi (Brassica Campestris L. Ssp. Chinensis Var. Communis) and Chinese Leaf Mustard (Brassica Juncea Coss). *Food Chem.* **2008**, *110* (4), 838–846. https://doi.org/10.1016/j.foodchem.2008.02.069.

(103) Laguna, O.; Odinot, E.; Bisotto, A.; Baréa, B.; Villeneuve, P.; Sigoillot, J. C.; Record, E.; Faulds, C. B.; Fine, F.; Lesage-Meessen, L.; Lomascolo, A.; Lecomte, J. Release of Phenolic Acids from Sunflower and Rapeseed Meals Using Different Carboxylic Esters Hydrolases from Aspergillus Niger. *Ind. Crops Prod.* **2019**, *139* (April), 111579. https://doi.org/10.1016/j.indcrop.2019.111579.

(104) Sharma, A.; Thakur, S.; Kumar, V.; Kanwar, M. K.; Kesavan, A. K.; Thukral, A. K.; Bhardwaj, R.; Alam, P.; Ahmad, P. Pre-Sowing Seed Treatment with 24-Epibrassinolide Ameliorates Pesticide Stress in Brassica Juncea L. Through the Modulation of Stress Markers. *Front. Plant Sci.* **2016**, *7* (NOVEMBER2016), 1–12. https://doi.org/10.3389/fpls.2016.01569.

(105) Gunnaiah, R.; Kushalappa, A. C.; Duggavathi, R.; Fox, S.; Somers, D. J. Integrated Metabolo-Proteomic Approach to Decipher the Mechanisms by Which Wheat Qtl (Fhb1) Contributes to Resistance against Fusarium Graminearum. *PLoS One* **2012**, *7* (7). https://doi.org/10.1371/journal.pone.0040695.

(106) Moreno, D. A.; Víllora, G.; Ruiz, J. M.; Romero, L. Growth Conditions, Elemental Accumulation and Induced Physiological Changes in Chinese Cabbage. *Chemosphere* **2003**, *52* (6), 1031–1040. https://doi.org/10.1016/S0045-6535(03)00330-8.

(107) Blokhina, O.; Virolainen, E.; Fagerstedt, K. V. Antioxidants, Oxidative Damage and Oxygen Deprivation Stress: A Review. *Ann. Bot.* **2003**, *91*, 179–194. https://doi.org/10.1093/aob/mcf118.

(108) Toscano, S.; Trivellini, A.; Cocetta, G.; Bulgari, R.; Francini, A.; Romano, D.; Ferrante, A. Effect of Preharvest Abiotic Stresses on the Accumulation of Bioactive Compounds in Horticultural Produce. *Front. Plant Sci.* **2019**, *10* (October), 1–17. https://doi.org/10.3389/fpls.2019.01212.

(109) Vogt, T. Phenylpropanoid Biosynthesis. *Mol. Plant* **2010**, *3* (1), 2–20. https://doi.org/10.1093/mp/ssp106.

(110) Fraser, C. M.; Chapple, C. The Phenylpropanoid Pathway in Arabidopsis. *Arab. B.* **2011**, *9*, e0152. https://doi.org/10.1199/tab.0152.

(111) Schmid, J.; Amrhein, N. Molecular Organization of the Shikimate Pathway in Higher Plants. *Phytochemistry* **1995**, *39* (4), 737–749. https://doi.org/10.1016/0031-9422(94)00962-S.

(112) Herrmann, K. M.; Weaver, L. M. The Shikimate Pathway. *Annu. Rev. Plant Biol.* **1999**, *50*, 473–503. https://doi.org/10.1146/annurev.arplant.50.1.473.

(113) Maeda, H.; Dudareva, N. The Shikimate Pathway and Aromatic Amino Acid Biosynthesis in Plants. *Annu. Rev. Plant Biol.* **2012**, *63*, 73–105. https://doi.org/10.1146/annurev-arplant-042811-105439.

(114) Koukol, J.; Conn, E. E. The Metabolism of Aromatic Compounds in Higher Plants. IV. Purification and Properties of the Phenylalanine Deaminase of Hordeum Vulgare. *J. Biol. Chem.* **1961**, *236* (10), 2692–2698.

(115) MacDonald, M. J.; D'Cunha, G. B. A Modern View of Phenylalanine Ammonia Lyase. *Biochem. Cell Biol.* **2007**, *85* (3), 273–282. https://doi.org/10.1139/O07-018.

(116) Jun, S. Y.; Sattler, S. A.; Cortez, G. S.; Vermerris, W.; Sattler, S. E.; Kang, C. H. Biochemical and Structural Analysis of Substrate Specificity of a Phenylalanine Ammonia-Lyase. *Plant Physiol.* **2018**, *176* (2), 1452–1468. https://doi.org/10.1104/pp.17.01608.

(117) Werck-Reichhart, D.; Feyereisen, R. Cytochromes P450 A Success Story. *Genome Biol.* **2000**, *1* (6), 1–9.

(118) Zhang, Z.; He, S.; Liu, H.; Sun, X.; Ye, Y.; Cao, X.; Wu, Z.; Sun, H. Effect of PH Regulation on the Components and Functional Properties of Proteins Isolated from Cold-Pressed Rapeseed Meal through Alkaline Extraction and Acid Precipitation. *Food Chem.* **2020**, *327* (May), 126998. https://doi.org/10.1016/j.foodchem.2020.126998.

(119) Knobloch, K.; Hahlbrock, K. Isoenzymes of P-Coumarate: CoA Ligase from Cell Suspension Cultures of Glycine Max. *Eur. J. Biochem.* **1975**, *52* (2), 311–320. https://doi.org/10.1111/j.1432-1033.1975.tb03999.x.

(120) Lindermayr, C.; Fliegmann, J.; Ebel, J. Deletion of a Single Amino Acid Residue from Different 4-Coumarate:CoA Ligases from Soybean Results in the Generation of New Substrate Specificities. *J. Biol. Chem.* **2003**, *278* (5), 2781–2786. https://doi.org/10.1074/jbc.M202632200.

(121) Li, Z.; Nair, S. K. Structural Basis for Specificity and Flexibility in a Plant 4-Coumarate:CoA Ligase. *Structure* **2015**, *23* (11), 2032–2042. https://doi.org/10.1016/j.str.2015.08.012.

(122) Goujon, T.; Sibout, R.; Pollet, B.; Maba, B.; Nussaume, L.; Bechtold, N.; Lu, F.; Ralph, J.; Mila, I.; Barrière, Y.; Lapierre, C.; Jouanin, L. A New Arabidopsis Thaliana Mutant Deficient in the Expression of O-Methyltransferase Impacts Lignins and Sinapoyl Esters. *Plant Mol. Biol.* **2003**, *51* (6), 973–989. https://doi.org/10.1023/A:1023022825098.

(123) Soubeyrand, E.; Kelly, M.; Keene, S. A.; Bernert, A. C.; Latimer, S.; Johnson, T. S.; Elowsky, C.; Colquhoun, T. A.; Block, A. K.; Basset, G. J. Arabidopsis 4-COUMAROYL-COA LIGASE 8 Contributes to the Biosynthesis of the Benzenoid Ring of Coenzyme Q in Peroxisomes. *Biochem. J.* **2019**, *476* (22), 3521–3532. https://doi.org/10.1042/BCJ20190688.

(124) Boerjan, W.; Ralph, J.; Baucher, M. Lignin Biosynthesis. *Annu. Rev. Plant Biol.* **2003**, *54*, 519–546. https://doi.org/10.1146/annurev.arplant.54.031902.134938.

(125) Matsuno, M.; Compagnon, V.; Schoch, G. A.; Schmitt, M.; Debayle, D.; Bassard, J. E.; Pollet, B.; Hehn, A.; Heintz, D.; Ullmann, P.; Lapierre, C.; Bernier, F.; Ehlting, J.; Werck-Reichhart, D. Evolution of a Novel Phenolic Pathway for Pollen Development. *Science (80-.).* **2009**, *325* (5948), 1688–1692. https://doi.org/10.1126/science.1174095.

(126) Wang, M.; Zhu, X.; Wang, K.; Lu, C.; Luo, M.; Shan, T.; Zhang, Z. A Wheat Caffeic Acid 3-O-Methyltransferase TaCOMT-3D Positively Contributes to Both Resistance to Sharp Eyespot Disease and Stem Mechanical Strength. *Sci. Rep.* **2018**, *8* (1), 1–14. https://doi.org/10.1038/s41598-018-24884-0.

(127) Nair, R. B.; Bastress, K. L.; Ruegger, M. O.; Denault, J. W.; Chapple, C. The Arabidopsis Thaliana Reduced Epidermal Fluorescence1 Gene Encodes an Aldehyde Dehydrogenase Involved in Ferulic Acid and Sinapic Acid Biosynthesis. *Plant Cell* **2004**, *16* (2), 544–554. https://doi.org/10.1105/tpc.017509.

(128) Lorenzen, M.; Racicot, V.; Strack, D.; Chapple, C. Sinapic Acid Ester Metabolism in Wild Type and a Sinapoylglucose-Accumulating Mutant of Arabidopsis. *Plant Physiol.* **1996**, *112* (4), 1625–1630. https://doi.org/10.1104/pp.112.4.1625.

(129) Vogt, T.; Aebershold, R.; Ellis, B. Purification and Characterization of Sinapine Synthase from Seeds of Brassica Napus. *Arch. Biochem. Biophys.* **1993**, *300* (2), 622–628. https://doi.org/10.1006/abbi.1993.1086.

(130) Clauß, K.; von Roepenack-Lahaye, E.; Böttcher, C.; Roth, M. R.; Welti, R.; Erban, A.; Kopka, J.; Scheel, D.; Milkowski, C.; Strack, D. Overexpression of Sinapine Esterase Bnsce3 in Oilseed Rape Seeds Triggers Global Changes in Seed Metabolism. *Plant Physiol.* **2011**, *155* (3), 1127–1145. https://doi.org/10.1104/pp.110.169821.

(131) Horbury, M. D.; Flourat, A. L.; Greenough, S. E.; Allais, F.; Stavros, V. G. Investigating Isomer Specific Photoprotection in a Model Plant Sunscreen. *Chem. Commun.* **2018**, *54* (8), 936–939. https://doi.org/10.1039/C7CC09061G.

(132) Mouterde, L. M. M.; Allais, F. Microwave-Assisted Knoevenagel-Doebner Reaction: An Efficient Method for Naturally Occurring Phenolic Acids Synthesis. *Front. Chem.* **2018**, *6* (September), 1–7. https://doi.org/10.3389/fchem.2018.00426.

(133) Peyrot, C.; Peru, A. A. M.; Mouterde, L. M. M.; Allais, F. Proline-Mediated Knoevenagel–Doebner Condensation in Ethanol: A Sustainable Access to p -Hydroxycinnamic Acids. *ACS Sustain. Chem. Eng.* **2019**, *7* (10), 9422–9427. https://doi.org/10.1021/acssuschemeng.9b00624.

(134) Clausen, S.; Olsen, O.; Sorensen, H. 4-Hydroxybenzoylcholine: A Natural Product Present in Sinapis Alba. *Phytochemistry* **1982**, *21* (4), 917–922. https://doi.org/10.1016/0031-9422(82)80093-9.

(135) Clausen, S.; Olsen, O.; Sørensen, H. Separation of Aromatic Choline Esters by High-Performance Liquid Chromatography. *J. Chromatogr. A* **1983**, *260*, 193–199. https://doi.org/10.1016/0021-9673(83)80026-0.

(136) Mouterde, L. M. M.; Peru, A. A. M.; Mention, M. M.; Brunissen, F.; Allais, F. Sustainable Straightforward Synthesis and Evaluation of the Antioxidant and Antimicrobial Activity of Sinapine and Analogues. *J. Agric. Food Chem.* **2020**, *68* (26), 6998–7004. https://doi.org/10.1021/acs.jafc.0c02183.

(137) Matsuba, Y.; Okuda, Y.; Abe, Y.; Kitamura, Y.; Terasaka, K.; Mizukami, H.; Kamakura, H.; Kawahara, N.; Goda, Y.; Sasaki, N.; Ozeki, Y. Enzymatic Preparation of 1-O-Hydroxycinnamoyl-β-D-Glucoses and Their Application to the Study of 1-O-Hydroxycinnamoyl-β-D-Glucose-Dependent Acyltransferase in Anthocyanin-Producing Cultured Cells of Daucus Carota and Glehnia Littoralis. *Plant Biotechnol.* **2008**, *25* (4), 369–375. https://doi.org/10.5511/plantbiotechnology.25.369.

(138) Zhu, Y.; Ralph, J. Stereoselective Synthesis of 1-O-β-Feruloyl and 1-O-β-Sinapoyl Glucopyranoses. *Tetrahedron Lett.* **2011**, *52* (29), 3729–3731. https://doi.org/10.1016/j.tetlet.2011.05.038.

(139) Allais, F.; Martinet, S.; Ducrot, P. H. Straightforward Total Synthesis of 2-O-Feruloyl-L-Malate, 2-O-Sinapoyl-L-Malate and 2-O-5-Hydroxyferuloyl-L-Malate. *Synthesis (Stuttg).* **2009**, No. 21, 3571–3578. https://doi.org/10.1055/s-0029-1216983.

(140) Peyrot, C.; Mention, M. M.; Fournier, R.; Brunissen, F.; Couvreur, J.; Balaguer, P.; Allais, F. Expeditious and Sustainable Two-Step Synthesis of Sinapoyl- l -Malate and Analogues: Towards Non-Endocrine Disruptive Bio-Based and Water-Soluble Bioactive Compounds . *Green Chem.* **2020**, *22* (19), 6510–6518. https://doi.org/10.1039/d0gc02763d.

(141) Dean, J. C.; Kusaka, R.; Walsh, P. S.; Allais, F.; Zwier, T. S. Plant Sunscreens in the UV-B: Ultraviolet Spectroscopy of Jet-Cooled Sinapoyl Malate, Sinapic Acid, and Sinapate Ester Derivatives. *J. Am. Chem. Soc.* **2014**, *136* (42), 14780–14795. https://doi.org/10.1021/ja5059026.

(142) Baker, L. A.; Staniforth, M.; Flourat, A. L.; Allais, F.; Stavros, V. G. Gas-Solution Phase Transient Absorption Study of the Plant Sunscreen Derivative Methyl Sinapate. *ChemPhotoChem* **2018**, *2* (8), 743–748. https://doi.org/10.1002/cptc.201800060.

(143) Peyrot, C.; Mention, M. M.; Brunissen, F.; Allais, F. Sinapic Acid Esters: Octinoxate Substitutes Combining Suitable Uv Protection and Antioxidant Activity. *Antioxidants* **2020**, *9* (9), 782-. https://doi.org/10.3390/antiox9090782.

(144) Chuo, S. C.; Nasir, H. M.; Mohd-Setapar, S. H.; Mohamed, S. F.; Ahmad, A.; Wani, W. A.; Muddassir, M.; Alarifi, A. A Glimpse into the Extraction Methods of Active Compounds from Plants. *Crit. Rev. Anal. Chem.* **2020**, *0* (0), 1–30. https://doi.org/10.1080/10408347.2020.1820851.

(145) Flourat, A. L.; Combes, J.; Bailly-Maitre-Grand, C.; Magnien, K.; Haudrechy, A.; Renault, J.-H.; Allais, F. Accessing P-Hydroxycinnamic Acids: Chemical Synthesis, Biomass Recovery or Engineered Microbial Production? *ChemSusChem* **2020**, 1–13. https://doi.org/10.1002/cssc.202002141.

(146) Prapakornwiriya, N.; Diosady, L. L. Recovery of Sinapic Acid from the Waste Effluent of Mustard Protein Isolation by Ion Exchange Chromatography. *JAOCS, J. Am. Oil Chem. Soc.* **2014**, *91* (2), 357–362. https://doi.org/10.1007/s11746-013-2366-1.

(147) Flourat, A. L.; Willig, G.; Teixeira, A. R. S.; Allais, F. Eco-Friendly Extraction of Sinapine From Residues of Mustard Production. *Front. Sustain. Food Syst.* **2019**, *3*. https://doi.org/10.3389/fsufs.2019.00012.

(148) Laguna, O.; Barakat, A.; Alhamada, H.; Durand, E.; Baréa, B.; Fine, F.; Villeneuve, P.; Citeau, M.; Dauguet, S.; Lecomte, J. Production of Proteins and Phenolic Compounds Enriched Fractions from Rapeseed and Sunflower Meals by Dry Fractionation Processes. *Ind. Crops Prod.* **2018**, *118*, 160–172. https://doi.org/10.1016/j.indcrop.2018.03.045.

(149) Moreno-González, M.; Girish, V.; Keulen, D.; Wijngaard, H.; Lauteslager, X.; Ferreira, G.; Ottens, M. Recovery of Sinapic Acid from Canola/Rapeseed Meal Extracts by Adsorption. *Food Bioprod. Process.* **2020**, *120*, 69–79. https://doi.org/10.1016/j.fbp.2019.12.002.

(150) Li, J.; Guo, Z. Complete Utilization of Rapeseed Meal to Produce Lipophilic Antioxidants, Protein, and Monosugars in a Concordant Manner. *ACS Sustain. Chem. Eng.* **2017**, *5* (7), 6218–6226. https://doi.org/10.1021/acssuschemeng.7b01171.

(151) Dubie, J.; Stancik, A.; Morra, M.; Nindo, C. Antioxidant Extraction from Mustard (Brassica Juncea) Seed Meal Using High-Intensity Ultrasound. *J. Food Sci.* **2013**, *78* (4), 542–548. https://doi.org/10.1111/1750-3841.12085.

(152) Sparr Eskilsson, C.; Björklund, E. Analytical-Scale Microwave-Assisted Extraction. *J. Chromatogr. A* **2000**, *902* (1), 227–250. https://doi.org/10.1016/S0021-9673(00)00921-3.

(153) Nandasiri, R.; Eskin, N. A. M.; Thiyam-Höllander, U. Antioxidative Polyphenols of Canola Meal Extracted by High Pressure: Impact of Temperature and Solvents. *J. Food Sci.* **2019**, *84* (11), 3117–3128. https://doi.org/10.1111/1750-3841.14799.

(154) Li, H.; Wu, J.; Rempel, C. B.; Thiyam, U. Effect of Operating Parameters on Oil and Phenolic Extraction Using Supercritical CO2. *JAOCS, J. Am. Oil Chem. Soc.* **2010**, *87* (9), 1081–1089. https://doi.org/10.1007/s11746-010-1594-x.

(155) Szydlowska-Czerniak, A.; Tulodziecka, A. Application of Response Surface Methodology to Optimize Ultrasound-Assisted Extraction of Total Antioxidants from Brassica Napus Cultivars. *Eur. J. Lipid Sci. Technol.* **2015**, *117* (4), 491–502. https://doi.org/10.1002/ejlt.201400310.

(156) Yu, X.; Gouyo, T.; Grimi, N.; Bals, O.; Vorobiev, E. Ultrasound Enhanced Aqueous Extraction from Rapeseed Green Biomass for Polyphenol and Protein Valorization. *Comptes Rendus Chim.* **2016**, *19* (6), 766–777. https://doi.org/10.1016/j.crci.2016.03.007.

(157) Jokić, S.; Cvjetko, M.; Božić, D.; Fabek, S.; Toth, N.; Vorkapić-Furač, J.; Redovniković, I. R. Optimisation of Microwave-Assisted Extraction of Phenolic Compounds from Broccoli and Its Antioxidant Activity. *Int. J. Food Sci. Technol.* **2012**, *47* (12), 2613–2619. https://doi.org/10.1111/j.1365-2621.2012.03143.x.

(158) Yang, M.; Zheng, C.; Zhou, Q.; Liu, C.; Li, W.; Huang, F. Influence of Microwaves Treatment of Rapeseed on Phenolic Compounds and Canolol Content. *J. Agric. Food Chem.* **2014**, *62* (8), 1956–1963. https://doi.org/10.1021/jf4054287.

(159) Zago, E.; Lecomte, J.; Barouh, N.; Aouf, C.; Carré, P.; Fine, F.; Villeneuve, P. Influence of Rapeseed Meal Treatments on Its Total Phenolic Content and Composition in Sinapine, Sinapic Acid and Canolol. *Ind. Crops Prod.* **2015**, *76*, 1061–1070. https://doi.org/10.1016/j.indcrop.2015.08.022.

(160) Yu, G.; Guo, T.; Huang, Q. Preparation of Rapeseed Oil with Superhigh Canolol Content and Superior Quality Characteristics by Steam Explosion Pretreatment Technology. *Food Sci. Nutr.* **2020**, *8* (5), 2271–2278. https://doi.org/10.1002/fsn3.1502.

(161) Khoddami, A.; Wilkes, M. A.; Roberts, T. H. Techniques for Analysis of Plant Phenolic Compounds. *Molecules* **2013**, *18* (2), 2328–2375. https://doi.org/10.3390/molecules18022328.

(162) Mohn, T.; Cutting, B.; Ernst, B.; Hamburger, M. Extraction and Analysis of Intact Glucosinolates-A Validated Pressurized Liquid Extraction/Liquid Chromatography-Mass Spectrometry Protocol for Isatis Tinctoria, and Qualitative Analysis of Other Cruciferous Plants. *J. Chromatogr. A* **2007**, *1166* (1–2), 142–151. https://doi.org/10.1016/j.chroma.2007.08.028.

(163) Nguyen, V. P. T.; Stewart, J.; Lopez, M.; Ioannou, I.; Allais, F. Glucosinolates: Natural Occurrence, Biosynthesis, Accessibility, Isolation, Structures, and Biological Activities. *Molecules* **2020**, *25* (19), 4537. https://doi.org/10.3390/molecules25194537.

(164) Li, J.; Guo, Z. Concurrent Extraction and Transformation of Bioactive Phenolic Compounds from Rapeseed Meal Using Pressurized Solvent Extraction System. *Ind. Crops Prod.* **2016**, *94*, 152–159. https://doi.org/10.1016/j.indcrop.2016.08.045.

(165) Huynh, N. T.; Smagghe, G.; Gonzales, G. B.; Van Camp, J.; Raes, K. Enzyme-Assisted Extraction Enhancing the Phenolic Release from Cauliflower (Brassica Oleracea L. Var. Botrytis) Outer Leaves. *J. Agric. Food Chem.* **2014**, *62* (30), 7468–7476. https://doi.org/10.1021/jf502543c.

(166) Neelam, K. A.; Sharma, K. K. Phenylpropanoids and Its Derivatives: Biological Activities and Its Role in Food, Pharmaceutical and Cosmetic Industries. *Crit. Rev. Food Sci. Nutr.* **2020**, *60* (16), 2655–2675. https://doi.org/10.1080/10408398.2019.1653822.

(167) Sova, M.; Saso, L. Natural Sources, Pharmacokinetics, Biological Activities and Health Benefits of Hydroxycinnamic Acids and Their Metabolites. *Nutrients* **2020**, *12* (8), 2190. https://doi.org/10.3390/nu12082190.

(168) Nenadis, N.; Tsimidou, M. Observations on the Estimation of Scavenging Activity of Phenolic Compounds Using Rapid 1,1-Diphenyl-2-Picrylhydrazyl (DPPH.) Tests. *JAOCS, J. Am. Oil Chem. Soc.* **2002**, *79* (12), 1191–1195. https://doi.org/10.1007/s11746-002-0626-z.

(169) Kikuzaki, H.; Hisamoto, M.; Hirose, K.; Akiyama, K.; Taniguchi, H. Antioxidant Properties of Ferulic Acid and Its Related Compounds. *J. Agric. Food Chem.* **2002**, *50* (7), 2161–2168. https://doi.org/10.1021/jf011348w.

(170) Thiyam, U.; Stöckmann, H.; Zum Felde, T.; Schwarz, K. Antioxidative Effect of the Main Sinapic Acid Derivatives from Rapeseed and Mustard Oil By-Products. *Eur. J. Lipid Sci. Technol.* **2006**, *108* (3), 239–248. https://doi.org/10.1002/ejlt.200500292.

(171) Horbury, M. D.; Holt, E. L.; Mouterde, L. M. M.; Balaguer, P.; Cebrián, J.; Blasco, L.; Allais, F.; Stavros, V. G. Towards Symmetry Driven and Nature Inspired UV Filter Design. *Nat. Commun.* **2019**, *10* (1), 1–8. https://doi.org/10.1038/s41467-019-12719-z.

(172) Sharma, A.; Bányiová, K.; Babica, P.; El Yamani, N.; Collins, A. R.; Čupr, P. Different DNA Damage Response of Cis and Trans Isomers of Commonly Used UV Filter after the Exposure on Adult Human Liver Stem Cells and Human Lymphoblastoid Cells. *Sci. Total Environ.* **2017**, *593–594*, 18–26. https://doi.org/10.1016/j.scitotenv.2017.03.043.

(173) Burnett, M. E.; Wang, S. Q. Current Sunscreen Controversies: A Critical Review. *Photodermatol. Photoimmunol. Photomed.* **2011**, *27* (2), 58–67. https://doi.org/10.1111/j.1600-0781.2011.00557.x.

(174) Krause, M.; Klit, A.; Blomberg Jensen, M.; Søeborg, T.; Frederiksen, H.; Schlumpf, M.; Lichtensteiger, W.; Skakkebaek, N. E.; Drzewiecki, K. T. Sunscreens: Are They Beneficial for Health? An Overview of Endocrine Disrupting Properties of UV-Filters. *Int. J. Androl.* **2012**, *35* (3), 424–436. https://doi.org/10.1111/j.1365-2605.2012.01280.x.

(175) Lyon, G. D.; McGill, F. M. Inhibition of Polygalacturonase and Polygalacturonic Acid Lyase from Erwinia Carotovora Subsp. Carotovora by Phenolics in Vitro. *Potato Res.* **1989**, *32* (3), 267–274. https://doi.org/10.1007/BF02357838.

(176) Nowak, H.; Kujawa, K.; Zadernowski, R.; Roczniak, B.; KozŁowska, H. Antioxidative and Bactericidal Properties of Phenolic Compounds in Rapeseeds. *Fett Wiss. Technol. Sci. Technol.* **1992**, *94* (4), 149–152. https://doi.org/10.1002/lipi.19920940406.

(177) Calabriso, N.; Massaro, M.; Scoditti, E.; Pasqualone, A.; Laddomada, B.; Carluccio, M. A. Phenolic Extracts from Whole Wheat Biofortified Bread Dampen Overwhelming Inflammatory Response in Human Endothelial Cells and Monocytes: Major Role of VCAM-1 and CXCL-10. *Eur. J. Nutr.* **2019**. https://doi.org/10.1007/s00394-019-02109-y.

(178) Singh, P. P.; Jha, S.; Irchhaiya, R. Antidiabetic and Antioxidant Activity of Hydroxycinnamic Acids from Calamintha Officinalis Moench. *Med. Chem. Res.* **2012**, *21* (8), 1717–1721. https://doi.org/10.1007/s00044-011-9690-5.

(179) Adisakwattana, S. Cinnamic Acid and Its Derivatives: Mechanisms for Prevention and Management of Diabetes and Its Complications. *Nutrients* **2017**, *9* (2). https://doi.org/10.3390/nu9020163.

(180) Najmanová, I.; Pourová, J.; Vopršalová, M.; Pilařová, V.; Semecký, V.; Nováková, L.; Mladěnka, P. Flavonoid Metabolite 3-(3-Hydroxyphenyl)Propionic Acid Formed by Human Microflora Decreases Arterial Blood Pressure in Rats. *Mol. Nutr. Food Res.* **2016**, *60* (5), 981–991. https://doi.org/10.1002/mnfr.201500761.

(181) Wittstock, U.; Halkier, B. A. Cytochrome P450 CYP79A2 from Arabidopsis Thaliana L. Catalyzes the Conversion of L-Phenylalanine to Phenylacetaldoxime in the Biosynthesis of Benzylglucosinolate. *J. Biol. Chem.* **2000**, *275* (19), 14659–14666. https://doi.org/10.1074/jbc.275.19.14659.

(182) Borgen, B. H.; Thangstad, O. P.; Ahuja, I.; Rossiter, J. T.; Bones, A. M. Removing the Mustard Oil Bomb from Seeds: Transgenic Ablation of Myrosin Cells in Oilseed Rape (Brassica Napus) Produces MINELESS Seeds. *J. Exp. Bot.* **2010**, *61* (6), 1683–1697. https://doi.org/10.1093/jxb/erq039.

(183) Martínez-Ballesta, M.; Moreno-Fernández, D. A.; Castejón, D.; Ochando, C.; Morandini, P. A.; Carvajal, M. The Impact of the Absence of Aliphatic Glucosinolates on Water Transport under Salt Stress in Arabidopsis Thaliana. *Front. Plant Sci.* **2015**, *6* (JULY), 1–12. https://doi.org/10.3389/fpls.2015.00524.

(184) Borek, V.; Morra, M. J.; Brown, P. D.; McCaffrey, J. P. Allelochemicals Produced during Sinigrin Decomposition in Soil. *J. Agric. Food Chem.* **1994**, *42* (4), 1030–1034. https://doi.org/10.1021/jf00040a037.

(185) Bednarek, P.; Pislewska-Bednarek, M.; Svatos, A.; Schneider, B.; Doubsky, J.; Mansurova, M.; Humphry, M.; Consonni, C.; Panstruga, R.; Sanchez-Vallet, A.; Molina, A.; Schulze-Lefert, P. A Glucosinolate Metabolism Pathway in Living Plant Cells Mediates Broad-Spectrum Antifungal Defense. *Science (80-.).* **2009**, *323* (5910), 101–106. https://doi.org/10.1126/science.1163732.

(186) Benn, M. H.; Ettlinger, M. G. The Synthesis of Sinigrin. *Chem. Commun.* **1965**, No. 19, 445–447. https://doi.org/10.1039/C19650000445.

(187) Cassel, S.; Casenave, B.; Déléris, G.; Latxague, L.; Rollin, P. Exploring an Alternative Approach to the Synthesis of Arylalkyl and Indolylmethyl Glucosinolates. *Tetrahedron* **1998**, *54* (29), 8515–8524. https://doi.org/10.1016/S0040-4020(98)00465-7.

(188) Rollin, P.; Tatibouët, A. Glucosinolates: The Synthetic Approach. *Comptes Rendus Chim.* **2011**, *14* (2–3), 194–210. https://doi.org/10.1016/j.crci.2010.05.002.

(189) Kushad, M. M.; Brown, A. F.; Kurilich, A. C.; Juvik, J. A.; Klein, B. P.; Wallig, M. A.; Jeffery, E. H. Variation of Glucosinolates in Vegetable Crops of Brassica Oleracea. *J. Agric. Food Chem.* **1999**, *47* (4), 1541–1548. https://doi.org/10.1021/jf980985s.

(190) Barba, F. J.; Nikmaram, N.; Roohinejad, S.; Khelfa, A.; Zhu, Z.; Koubaa, M. Bioavailability of Glucosinolates and Their Breakdown Products: Impact of Processing. *Front. Nutr.* **2016**, *3*, 24. https://doi.org/10.3389/fnut.2016.00024.

(191) Hanschen, F. S. Domestic Boiling and Salad Preparation Habits Affect Glucosinolate Degradation in Red Cabbage (Brassica Oleracea Var. Capitata f. Rubra). *Food Chem.* **2020**, *321* (March), 126694. https://doi.org/10.1016/j.foodchem.2020.126694.

(192) Crocoll, C.; Halkier, B. A.; Burow, M. Analysis and Quantification of Glucosinolates. *Curr. Protoc. Plant Biol.* **2016**, *1* (2), 385–409. https://doi.org/10.1002/cppb.20027.

(193) Fahey, J. W.; Zalcmann, A. T.; Talalay, P. The Chemical Diversity and Distribution of Glucosinolates and Isothiocyanates among Plants. *Phytochemistry* **2001**, *56* (1), 5–51. https://doi.org/10.1016/S0031-9422(00)00316-2.

(194) Agerbirk, N.; Olsen, C. E. Glucosinolate Structures in Evolution. *Phytochemistry* **2012**, *77*, 16–45. https://doi.org/10.1016/j.phytochem.2012.02.005.

(195) Munday, R.; Munday, C. M. Induction of Phase II Detoxification Enzymes in Rats by Plant-Derived Isothiocyanates: Comparison of Allyl Isothiocyanate with Sulforaphane and Related Compounds. *J. Agric. Food Chem.* **2004**, *52* (7), 1867–1871. https://doi.org/10.1021/jf030549s.

(196) Dinkova-Kostova, A. T.; Kostov, R. V. Glucosinolates and Isothiocyanates in Health and Disease. *Trends Mol. Med.* **2012**, *18* (6), 337–347. https://doi.org/10.1016/j.molmed.2012.04.003.

(197) Liu, S.; Huang, H.; Yi, X.; Zhang, Y.; Yang, Q.; Zhang, C.; Fan, C.; Zhou, Y. Dissection of Genetic Architecture for Glucosinolate Accumulations in Leaves and Seeds of Brassica Napus by Genome-wide Association Study. *Plant Biotechnol. J.* **2020**, *18* (6), 1472–1484. https://doi.org/10.1111/pbi.13314.

(198) Velasco, P.; Soengas, P.; Vilar, M.; Cartea, M. E.; del Rio, M. Comparison of Glucosinolate Profiles in Leaf and Seed Tissues of Different Brassica Napus Crops. *J. Am. Soc. Hortic. Sci.* **2008**, *133* (4), 551–558. https://doi.org/10.21273/JASHS.133.4.551.

(199) Troufflard, S.; Mullen, W.; Larson, T. R.; Graham, I. A.; Crozier, A.; Amtmann, A.; Armengaud, P. Potassium Deficiency Induces the Biosynthesis of Oxylipins and Glucosinolates in Arabidopsis Thaliana. *BMC Plant Biol.* **2010**, *10*. https://doi.org/10.1186/1471-2229-10-172.

(200) Martínez-Ballesta, M. del C.; Moreno, D. A.; Carvajal, M. The Physiological Importance of Glucosinolates on Plant Response to Abiotic Stress in Brassica. *Int. J. Mol. Sci.* **2013**, *14* (6), 11607–11625. https://doi.org/10.3390/ijms140611607.

(201) Márquez-Lema, A.; Fernández-Martínez, J. M.; Pérez-Vich, B.; Velasco, L. Transgressive Segregation for Reduced Glucosinolate Content in Brassica Carinata A. Braun. *Plant Breed.* **2006**, *125* (4), 400–402. https://doi.org/10.1111/j.1439-0523.2006.01240.x.

(202) Márquez-Lema, A.; Fernández-Martínez, J. M.; Pérez-Vich, B.; Velasco, L. Inheritance of Very High Glucosinolate Content in Ethiopian Mustard Seeds. *Plant Breed.* **2009**, *128* (3), 278–281. https://doi.org/10.1111/j.1439-0523.2008.01563.x.

(203) Chodur, G. M.; Olson, M. E.; Wade, K. L.; Stephenson, K. K.; Nouman, W.; Garima; Fahey, J. W. Wild and Domesticated Moringa Oleifera Differ in Taste, Glucosinolate Composition, and Antioxidant Potential, but Not Myrosinase Activity or Protein Content. *Sci. Rep.* **2018**, *8* (1), 1–10. https://doi.org/10.1038/s41598-018-26059-3.

(204) Ishida, M.; Nagata, M.; Ohara, T.; Kakizaki, T.; Hatakeyama, K.; Nishio, T. Small Variation of Glucosinolate Composition in Japanese Cultivars of Radish (Raphanus Sativus L.) Requires Simple Quantitative Analysis for Breeding of Glucosinolate Component. *Breed. Sci.* **2012**, *62* (1), 63–70. https://doi.org/10.1270/jsbbs.62.63.

(205) Halkier, B. A.; Du, L. The Biosynthesis of Glucosinolates. *Trends Plant Sci.* **1997**, *2* (11), 425–431. https://doi.org/10.1016/S1360-1385(97)01128-X.

(206) Halkier, B. A.; Gershenzon, J. Biology and Biochemistry of Glucosinolates. *Annu. Rev. Plant Biol.* **2006**, *57* (1), 303–333. https://doi.org/10.1146/annurev.arplant.57.032905.105228.

(207) Chisholm, M. D.; Wetter, L. R. Biosynthesis of Mustard Oil Glucosides: IV. The Administration of Methionine-C14 and Related Compounds to Horseradish. *Can. J. Biochem.* **1964**, *42* (7), 1033–1040. https://doi.org/10.1139/o64-114.

(208) Graser, G.; Schneider, B.; Oldham, N. J.; Gershenzon, J. The Methionine Chain Elongation Pathway in the Biosynthesis of Glucosinolates in Eruca Sativa (Brassicaceae). *Arch. Biochem. Biophys.* **2000**, *378* (2), 411–419. https://doi.org/10.1006/abbi.2000.1812.

(209) Graser, G.; Oldham, N. J.; Brown, P. D.; Temp, U.; Gershenzon, J. The Biosynthesis of Benzoic Acid Glucosinolate Esters in Arabidopsis Thaliana. *Phytochemistry* **2001**, *57* (1), 23–32. https://doi.org/10.1016/S0031-9422(00)00501-X.

(210) Sønderby, I. E.; Geu-Flores, F.; Halkier, B. A. Biosynthesis of Glucosinolates - Gene Discovery and Beyond. *Trends Plant Sci.* **2010**, *15* (5), 283–290. https://doi.org/10.1016/j.tplants.2010.02.005.

(211) Czerniawski, P.; Bednarek, P. Glutathione S-Transferases in the Biosynthesis of Sulfur-Containing Secondary Metabolites in Brassicaceae Plants. *Front. Plant Sci.* **2018**, *871* (November), 1–8. https://doi.org/10.3389/fpls.2018.01639.

(212) Piotrowski, M.; Schemenewitz, A.; Lopukhina, A.; Müller, A.; Janowitz, T.; Weiler, E. W.; Oecking, C. Desulfoglucosinolate Sulfotransferases from Arabidopsis Thaliana Catalyze the Final Step in the Biosynthesis of the Glucosinolate Core Structure. *J. Biol. Chem.* **2004**, *279* (49), 50717–50725. https://doi.org/10.1074/jbc.M407681200.

(213) Grubb, C. D.; Zipp, B. J.; Ludwig-Müller, J.; Masuno, M. N.; Molinski, T. F.; Abel, S. Arabidopsis Glucosyltransferase UGT74B1 Functions in Glucosinolate Biosynthesis and Auxin Homeostasis. *Plant J.* **2004**, *40* (6), 893–908. https://doi.org/10.1111/j.1365-313X.2004.02261.x.

(214) Grubb, C. D.; Abel, S. Glucosinolate Metabolism and Its Control. *Trends Plant Sci.* **2006**, *11* (2), 89–100. https://doi.org/10.1016/j.tplants.2005.12.006.

(215) Mikkelsen, M. D.; Petersen, B. L.; Olsen, C. E.; Halkier, B. A. Biosynthesis and Metabolic Engineering of Glucosinolates. *Amino Acids* **2002**, *22* (3), 279–295. https://doi.org/10.1007/s007260200014.

(216) Wittstock, U.; Halkier, B. A. Glucosinolate Research in the Arabidopsis Era. *Trends Plant Sci.* **2002**, *7* (6), 263–270. https://doi.org/10.1016/S1360-1385(02)02273-2.

(217) Mackay, T. F. C. Quantitative Trait Loci in Drosophila. *Nat. Rev. Genet.* **2001**, *2* (1), 11–20. https://doi.org/10.1038/35047544.

(218) Kliebenstein, D. J.; Kroymann, J.; Brown, P.; Figuth, A.; Pedersen, D.; Gershenzon, J.; Mitchell-Olds, T. Genetic Control of Natural Variation in Arabidopsis Glucosinolate Accumulation. *Plant Physiol.* **2001**, *126* (2), 811–825. https://doi.org/10.1104/pp.126.2.811.

(219) Pfalz, M.; Vogel, H.; Kroymann, J. The Gene Controlling the Indole Glucosinolate Modifier1 Quantitative Trait Locus Alters Indole Glucosinolate Structures and Aphid Resistance in Arabidopsis. *Plant Cell* **2009**, *21* (3), 985–999. https://doi.org/10.1105/tpc.108.063115.

(220) Wentzell, A. M.; Rowe, H. C.; Hansen, B. G.; Ticconi, C.; Halkier, B. A.; Kliebenstein, D. J. Linking Metabolic QTLs with Network and Cis-EQTLs Controlling Biosynthetic Pathways. *PLoS Genet.* **2007**, *3* (9), 1687–1701. https://doi.org/10.1371/journal.pgen.0030162.

(221) Kroymann, J.; Textor, S.; Tokuhisa, J. G.; Falk, K. L.; Bartram, S.; Gershenzon, J.; Mitchell-Olds, T. A Gene Controlling Variation in Arabidopsis Glucosinolate Composition Is Part of the Methionine Chain Elongation Pathway. *Plant Physiol.* **2001**, *127* (3), 1077–1088. https://doi.org/10.1104/pp.010416.

(222) Li, J.; Hansen, B. G.; Ober, J. A.; Kliebenstein, D. J.; Halkier, B. A. Subclade of Flavin-Monooxygenases Involved in Aliphatic Glucosinolate Biosynthesis. *Plant Physiol.* **2008**, *148* (3), 1721–1733. https://doi.org/10.1104/pp.108.125757.

(223) Hirani, A. H.; Zelmer, C. D.; McVetty, P. B. E.; Daayf, F.; Li, G. Homoeologous GSL-ELONG Gene Replacement for Manipulation of Aliphatic Glucosinolates in Brassica Rapa L. by Marker Assisted Selection. *Front. Plant Sci.* **2013**, *4* (MAR), 1–12. https://doi.org/10.3389/fpls.2013.00055.

(224) Ettlinger, M. G.; Lundeen, A. J. First Synthesis of a Mustard Oil Glucoside; The Enzymatic Lossen Rearrangement. *J. Am. Chem. Soc.* **1957**, *79* (7), 1764–1765. https://doi.org/10.1021/ja01564a066.

(225) Benn, M. H. A New Mustard Oil Glucoside Synthesis: The Synthesis of Glucotropaeolin. *Can. J. Chem.* **1963**, *41* (11), 2836–2838. https://doi.org/10.1139/v63-415.

(226) Kumaran, G.; Kulkarni, G. H. Synthesis of α-Functionalized and Nonfunctionalized Hydroximoyl Chlorides from Conjugated Nitroalkenes and Nitroalkanes. *J. Org. Chem.* **1997**, *62* (5), 1516–1520. https://doi.org/10.1021/jo961553o.

(227) MacLeod, A. J.; Rossiter, J. T. Synthesis of 2-Hydroxybut-3-Enylglucosinolate (Progoitrin). *J. Chem. Soc. Perkin Trans. 1* **1983**, *53* (9), 717. https://doi.org/10.1039/p19830000717.

(228) Keller, T. H.; Yelland, L. J.; Benn, M. H. A New Glucosinolate Synthesis. *Can. J. Chem.* **1984**, *62* (3), 437–440. https://doi.org/10.1139/v84-075.

(229) Szmigielska, A. M.; Schoenau, J. J.; Levers, V. Determination of Glucosinolates in Canola Seeds Using Anion Exchange Membrane Extraction Combined with the High-Pressure Liquid Chromatography Detection. *J. Agric. Food Chem.* **2000**, *48* (10), 4487–4491. https://doi.org/10.1021/jf000477u.

(230) Grosser, K.; van Dam, N. M. A Straightforward Method for Glucosinolate Extraction and Analysis with High-Pressure Liquid Chromatography (HPLC). *J. Vis. Exp.* **2017**, No. 121, 55425. https://doi.org/10.3791/55425.

(231) Blažević, I.; Dulović, A.; Čikeš Čulić, V.; Popović, M.; Guillot, X.; Burčul, F.; Rollin, P. Microwave-Assisted versus Conventional Isolation of Glucosinolate Degradation Products from Lunaria Annua L. and Their Cytotoxic Activity. *Biomolecules* **2020**, *10* (2), 215. https://doi.org/10.3390/biom10020215.

(232) Popović, M.; Maravić, A.; Čulić, V. Č.; Dulović, A.; Burčul, F.; Blažević, I. Biological Effects of Glucosinolate Degradation Products from Horseradish: A Horse That Wins the Race. *Biomolecules* **2020**, *10* (2), 1–15. https://doi.org/10.3390/biom10020343.

(233) Doheny-Adams, T.; Redeker, K.; Kittipol, V.; Bancroft, I.; Hartley, S. E. Development of an Efficient Glucosinolate Extraction Method. *Plant Methods* **2017**, *13* (1), 17. https://doi.org/10.1186/s13007-017-0164-8.

(234) Thies, W. Isolation of Sinigrin and Glucotropaeolin from Cruciferous Seeds. *Fett Wiss. Technol. Sci. Technol.* **1988**, *90* (8), 311–314. https://doi.org/10.1002/lipi.19880900806.

(235) Förster, N.; Ulrichs, C.; Schreiner, M.; Müller, C. T.; Mewis, I. Development of a Reliable Extraction and Quantification Method for Glucosinolates in Moringa Oleifera. *Food Chem.* **2015**, *166*, 456–464. https://doi.org/10.1016/j.foodchem.2014.06.043.

(236) Wang, T.; Liang, H.; Yuan, Q. Optimization of Ultrasonic-Stimulated Solvent Extraction of Sinigrin from Indian Mustard Seed (Brassica Juncea L.) Using Response Surface Methodology. *Phytochem. Anal.* **2011**, *22* (3), 205–213. https://doi.org/10.1002/pca.1266.

(237) Sut, S.; Boschiero, I.; Solana, M.; Malagoli, M.; Bertucco, A.; Dall'Acqua, S. Supercritical CO2 Extraction of Eruca Sativa Using Cosolvents: Phytochemical Composition by LC-MS Analysis. *Molecules* **2018**, *23* (12), 6–10. https://doi.org/10.3390/molecules23123240.

(238) Richter, B. E.; Jones, B. A.; Ezzell, J. L.; Porter, N. L.; Avdalovic, N.; Pohl, C. Accelerated Solvent Extraction: A Technique for Sample Preparation. *Anal. Chem.* **1996**, *68* (6), 1033–1039. https://doi.org/10.1021/ac9508199.

(239) Rafińska, K.; Pomastowski, P.; Rudnicka, J.; Krakowska, A.; Maruśka, A.; Narkute, M.; Buszewski, B. Effect of Solvent and Extraction Technique on Composition and Biological Activity of Lepidium Sativum Extracts. *Food Chem.* **2019**, *289* (March), 16–25. https://doi.org/10.1016/j.foodchem.2019.03.025.

(240) Wang, T.; Liang, H.; Yuan, Q. Separation of Sinigrin from Indian Mustard (Brassica Juncea L.) Seed Using Macroporous Ion-Exchange Resin. *Korean J. Chem. Eng.* **2012**, *29* (3), 396–403. https://doi.org/10.1007/s11814-011-0175-5.

(241) Charpentier, N.; Bostyn, S.; Coïc, J. P. Isolation of a Rich Glucosinolate Fraction by Liquid Chromatography from an Aqueous Extract Obtained by Leaching Dehulled Rapeseed Meal (Brassica Napus L.). *Ind. Crops Prod.* **1998**, *8* (2), 151–158. https://doi.org/10.1016/S0926-6690(97)10020-6.

(242) Rochfort, S.; Caridi, D.; Stinton, M.; Trenerry, V. C.; Jones, R. The Isolation and Purification of Glucoraphanin from Broccoli Seeds by Solid Phase Extraction and Preparative High Performance Liquid Chromatography. *J. Chromatogr. A* **2006**, *1120* (1–2), 205–210. https://doi.org/10.1016/j.chroma.2006.01.046.

(243) Ito, Y. High-Speed Countercurrent Chromatography. *Nature* **1987**, *326* (6111), 419–420. https://doi.org/10.1038/326419a0.

(244) Fahey, J. W.; Wade, K. L.; Stephenson, K. K.; Chou, F. E. Separation and Purification of Glucosinolates from Crude Plant Homogenates by High-Speed Counter-Current Chromatography. *J. Chromatogr. A* **2003**, *996* (1–2), 85–93. https://doi.org/10.1016/S0021-9673(03)00607-1.

(245) Chidewe, C.; Castillo, U. F.; Sem, D. S. Structural Analysis and Antimicrobial Activity of Chromatographically Separated Fractions of Leaves of Sesamum Angustifolium (Oliv.) Engl. *J. Biol. Act. Prod. from Nat.* **2017**, *7* (6), 463–474. https://doi.org/10.1080/22311866.2017.1417057.

(246) Ibrahim, N.; Allart-Simon, I.; De Nicola, G. R.; Iori, R.; Renault, J. H.; Rollin, P.; Nuzillard, J. M. Advanced NMR-Based Structural Investigation of Glucosinolates and Desulfoglucosinolates. *J. Nat. Prod.* **2018**, *81* (2), 323–334. https://doi.org/10.1021/acs.jnatprod.7b00776.

(247) Jaki, B.; Sticher, O.; Veit, M.; Fröhlich, R.; Pauli, G. F. Evaluation of Glucoiberin Reference Material from Iberis Amara by Spectroscopic Fingerprinting. *J. Nat. Prod.* **2002**, *65* (4), 517–522. https://doi.org/10.1021/np0100800.

(248) Marsh, R. E.; Waser, J. Refinement of the Crystal Structure of Sinigrin. *Acta Crystallogr. Sect. B Struct. Crystallogr. Cryst. Chem.* **1970**, *26* (7), 1030–1037. https://doi.org/10.1107/s0567740870003539.

(249) Montaut, S.; Bleeker, R. S.; Jacques, C. Phytochemical Constituents of Cardamine Diphylla. *Can. J. Chem.* **2010**, *88* (1), 50–55. https://doi.org/10.1139/V09-153.

(250) Olsen, C. E.; Huang, X. C.; Hansen, C. I. C.; Cipollini, D.; Ørgaard, M.; Matthes, A.; Geu-Flores, F.; Koch, M. A.; Agerbirk, N. Glucosinolate Diversity within a Phylogenetic Framework of the Tribe Cardamineae (Brassicaceae) Unraveled with HPLC-MS/MS and NMR-Based Analytical Distinction of 70 Desulfoglucosinolates. *Phytochemistry* **2016**, *132*, 33–56. https://doi.org/10.1016/j.phytochem.2016.09.013.

(251) Jing, B.; Guo, R.; Wang, M.; Zhang, L.; Yu, X. Influence of Seed Roasting on the Quality of Glucosinolate Content and Flavor in Virgin Rapeseed Oil. *Lwt* **2020**, *126* (March), 109301. https://doi.org/10.1016/j.lwt.2020.109301.

(252) Song, L.; Thornalley, P. J. Effect of Storage, Processing and Cooking on Glucosinolate Content of Brassica Vegetables. *Food Chem. Toxicol.* **2007**, *45* (2), 216–224. https://doi.org/10.1016/j.fct.2006.07.021.

(253) Hanschen, F. S.; Lamy, E.; Schreiner, M.; Rohn, S. Reactivity and Stability of Glucosinolates and Their Breakdown Products in Foods. *Angew. Chemie - Int. Ed.* **2014**, *53* (43), 11430–11450. https://doi.org/10.1002/anie.201402639.

(254) Lazzeri, L.; Curto, G.; Leoni, O.; Dallavalle, E. Effects of Glucosinolates and Their Enzymatic Hydrolysis Products via Myrosinase on the Root-Knot Nematode Meloidogyne Incognita (Kofoid et White) Chitw. *J. Agric. Food Chem.* **2004**, *52* (22), 6703–6707. https://doi.org/10.1021/jf030776u.

(255) Buskov, S.; Serra, B.; Rosa, E.; Sørensen, H.; Sørensen, J. C. Effects of Intact Glucosinolates and Products Produced from Glucosinolates in Myrosinase-Catalyzed Hydrolysis on the Potato Cyst Nematode (Globodera Rostochiensis Cv. Woll). *J. Agric. Food Chem.* **2002**, *50* (4), 690–695. https://doi.org/10.1021/jf010470s.

(256) Burmeister, W. P.; Cottaz, S.; Driguez, H.; Iori, R.; Palmieri, S.; Henrissat, B. The Crystal Structures of Sinapis Alba Myrosinase and a Covalent Glycosyl–Enzyme Intermediate Provide Insights into the Substrate Recognition and Active-Site Machinery of an S-Glycosidase. *Structure* **1997**, *5* (5), 663–676. https://doi.org/10.1016/S0969-2126(97)00221-9.

(257) Cottaz, S.; Henrissat, B.; Driguez, H. Mechanism-Based Inhibition and Stereochemistry of Glucosinolate Hydrolysis by Myrosinase. *Biochemistry* **1996**, *35* (48), 15256–15259. https://doi.org/10.1021/bi9622480.

(258) Burmeister, W. P.; Cottaz, S.; Rollin, P.; Vasella, A.; Henrissat, B. High Resolution X-Ray Crystallography Shows That Ascorbate Is a Cofactor for Myrosinase and Substitutes for the Function of the Catalytic Base. *J. Biol. Chem.* **2000**, *275* (50), 39385–39393. https://doi.org/10.1074/jbc.M006796200.

(259) Ettlinger, M. G.; Dateo, G. P.; Harrison, B. W.; Mabry, T. J.; Thompson, C. P. Vitamin C As A Coenzyme: The Hydrolysis of Mustard Oil Glucosides. *Proc. Natl. Acad. Sci.* **1961**, *47* (12), 1875–1880. https://doi.org/10.1073/pnas.47.12.1875.

(260) Ratzka, A.; Vogel, H.; Kliebenstein, D. J.; Mitchell-Olds, T.; Kroymann, J. Disarming the Mustard Oil Bomb. *Proc. Natl. Acad. Sci.* **2002**, *99* (17), 11223–11228. https://doi.org/10.1073/pnas.172112899.

(261) Falk, K. L.; Gershenzon, J. The Desert Locust, Schistocerca Gregaria, Detoxifies the Glucosinolates of Schouwia Purpurea by Desulfation. *J. Chem. Ecol.* **2007**, *33* (8), 1542–1555. https://doi.org/10.1007/s10886-007-9331-0.

(262) Heidel-Fischer, H. M.; Kirsch, R.; Reichelt, M.; Ahn, S.-J.; Wielsch, N.; Baxter, S. W.; Heckel, D. G.; Vogel, H.; Kroymann, J. An Insect Counteradaptation against Host Plant Defenses Evolved through Concerted Neofunctionalization. *Mol. Biol. Evol.* **2019**, *36* (5), 930–941. https://doi.org/10.1093/molbev/msz019.

(263) Ahn, S.-J.; Betzin, F.; Gikonyo, M. W.; Yang, Z.-L.; Köllner, T. G.; Beran, F. Identification and Evolution of Glucosinolate Sulfatases in a Specialist Flea Beetle. *Sci. Rep.* **2019**, *9* (1), 15725. https://doi.org/10.1038/s41598-019-51749-x.

(264) Wittstock, U.; Burow, M. Glucosinolate Breakdown in Arabidopsis: Mechanism, Regulation and Biological Significance. *Arab. B.* **2010**, *8* (8), e0134. https://doi.org/10.1199/tab.0134.

(265) Eisenschmidt-Bönn, D.; Schneegans, N.; Backenköhler, A.; Wittstock, U.; Brandt, W. Structural Diversification during Glucosinolate Breakdown: Mechanisms of Thiocyanate, Epithionitrile and Simple Nitrile Formation. *Plant J.* **2019**, *99* (2), tpj.14327. https://doi.org/10.1111/tpj.14327.

(266) Aumaitre, A.; Bourdon, D.; Peiniau, J.; Freire, J. B. Effect of Graded Levels of Raw and Processed Rapeseed on Feed Digestibility and Nutrient Utilization in Young Pigs. *Anim. Feed Sci. Technol.* **1989**, *24* (3–4), 275–287. https://doi.org/10.1016/0377-8401(89)90149-1.

(267) Mabon, N.; Mandiki, S. N. M.; Derycke, G.; Bister, J. L.; Wathelet, J. P.; Marlier, M.; Paquay, R. Chemical Changes and Influences of Rapeseed Antinutritional Factors on Lamb Physiology and Performance. 3. Antinutritional Factors in Plasma and Organs. *Anim. Feed Sci. Technol.* **2000**, *85* (1–2), 111–120. https://doi.org/10.1016/S0377-8401(00)00122-X.

(268) Hanschen, F. S.; Yim, B.; Winkelmann, T.; Smalla, K.; Schreiner, M. Degradation of Biofumigant Isothiocyanates and Allyl Glucosinolate in Soil and Their Effects on the Microbial Community Composition. *PLoS One* **2015**, *10* (7), 1–18. https://doi.org/10.1371/journal.pone.0132931.

(269) Kuchernig, J. C.; Burow, M.; Wittstock, U. Evolution of Specifier Proteins in Glucosinolate-Containing Plants. *BMC Evol. Biol.* **2012**, *12* (1). https://doi.org/10.1186/1471-2148-12-127.

(270) Mumm, R.; Burow, M.; Bukovinszkine'Kiss, G.; Kazantzidou, E.; Wittstock, U.; Dicke, M.; Gershenzon, J. Formation of Simple Nitriles upon Glucosinolate Hydrolysis Affects Direct and Indirect Defense against the Specialist Herbivore, Pieris Rapae. *J. Chem. Ecol.* **2008**, *34* (10), 1311–1321. https://doi.org/10.1007/s10886-008-9534-z.

(271) Christ, B.; Bartels, W. L.; Broughton, D.; Seepaul, R.; Geller, D. In Pursuit of a Homegrown Biofuel: Navigating Systems of Partnership, Stakeholder Knowledge, and Adoption of Brassica Carinata in the Southeast United States. *Energy Res. Soc. Sci.* **2020**, *70* (June). https://doi.org/10.1016/j.erss.2020.101665.

(272) Chen, R.; Wang, X.-J.; Zhang, Y.-Y.; Xing, Y.; Yang, L.; Ni, H.; Li, H.-H. Simultaneous Extraction and Separation of Oil, Proteins, and Glucosinolates from Moringa Oleifera Seeds. *Food Chem.* **2019**, *300* (5), 125162. https://doi.org/10.1016/j.foodchem.2019.125162.

(273) Fang, J.; Reichelt, M.; Kai, M.; Schneider, B. Metabolic Profiling of Lignans and Other Secondary Metabolites from Rapeseed (Brassica Napus L.). *J. Agric. Food Chem.* **2012**, *60* (42), 10523–10529. https://doi.org/10.1021/jf303907b.

(274) Kalaydzhiev, H.; Ivanova, P.; Stoyanova, M.; Pavlov, A.; Rustad, T.; Silva, C. L. M.; Chalova, V. I. Valorization of Rapeseed Meal: Influence of Ethanol Antinutrients Removal on Protein Extractability, Amino Acid Composition and Fractional Profile. *Waste and Biomass Valorization* **2020**, *11* (6), 2709–2719. https://doi.org/10.1007/s12649-018-00553-1.

(275) *AOAC Official Methods for Analysis - Association of Official Analytical Chemists*; 2000.

(276) DuBois, M.; Gilles, K. A.; Hamilton, J. K.; Rebers, P. A.; Smith, F. Colorimetric Method for Determination of Sugars and Related Substances. *Anal. Chem.* **1956**, *28* (3), 350–356. https://doi.org/10.1021/ac60111a017.

(277) Reichwald, K.; Hatzack, F. Application of a Modified Haug and Lantzsch Method for the Rapid and Accurate Photometrical Phytate Determination in Soybean, Wheat, and Maize Meals. *J. Agric. Food Chem.* **2008**, *56* (9), 2888–2891. https://doi.org/10.1021/jf0730690.

(278) Aluko, R. E.; McIntosh, T. Polypeptide Profile and Functional Properties of Defatted Meals and Protein Isolates of Canola Seeds. *J. Sci. Food Agric.* **2001**, *81* (4), 391–396. https://doi.org/10.1002/1097-0010(200103)81:4<391::AID-JSFA823>3.0.CO;2-S.

(279) Pearce, K. N.; Kinsella, J. E. Emulsifying Properties of Proteins: Evaluation of a Turbidimetric Technique. *J. Agric. Food Chem.* **1978**, *26* (3), 716–723. https://doi.org/10.1021/jf60217a041.

(280) Hostettler, F. D.; Seikel, M. K. Lignans of Ulmus Thomasii Heartwood-II. Lignans Related to Thomasic Acid. *Tetrahedron* **1969**, *25* (11), 2325–2337. https://doi.org/10.1016/S0040-4020(01)82782-4.

(281) Charlton, J. L.; Lee, K. A. Thomasidioic Acid and 6-Hydroxy-5,7-Dimethoxy-2-Naphthoic Acid: Are They Really Natural Products? *Tetrahedron Lett.* **1997**, *38* (42), 7311–7312. https://doi.org/10.1016/S0040-4039(97)01775-9.

(282) Lukacs, S. J.; Cohen, S. M.; Long, F. H. Optical Properties of a Liquid-Crystalline Random Copolyester. *J. Phys. Chem. B* **1999**, *103* (32), 6648–6652. https://doi.org/10.1021/jp984785v.

(283) Gutierrez, G. A.; Chivers, R. A.; Blackwell, J.; Stamatoff, J. B.; Yoon, H. The Structure of Liquid Crystalline Aromatic Copolyesters Prepared from 4-Hydroxybenzoic Acid and 2-Hydroxy-6-Naphthoic Acid. *Polymer (Guildf).* **1983**, *24* (8), 937–942. https://doi.org/10.1016/0032-3861(83)90141-6.

(284) Heifferon, K. V.; Spiering, G. A.; Talley, S. J.; Hegde, M.; Moore, R. B.; Turner, S. R.; Long, T. E. Synthesis and Characterization of a Nematic Fully Aromatic Polyester Based on Biphenyl 3,4′-Dicarboxylic Acid. *Polym. Chem.* **2019**, *10* (31), 4287–4296. https://doi.org/10.1039/c9py00683d.

(285) Gershon, H.; Parmegiani, R. Antimicrobial Activity of 8-Quinolinols, Salicylic Acids, Hydroxynaphthoic Acids, and Salts of Selected Quinolinols with Selected Hydroxy-Acids. *Appl. Microbiol.* **1962**, *10*, 348–353. https://doi.org/10.1128/aem.10.4.348-353.1962.

(286) Dogan, H. N.; Rollas, S.; Erdeniz, H. Synthesis, Structure Elucidation and Antimicrobial Activity of Some 3- Hydroxy-2-Naphthoic Acid Hydrazide Derivatives. *Farmaco* **1998**, *53* (7), 462–467. https://doi.org/10.1016/S0014-827X(98)00049-4.

(287) Lee, K.-A. S. Oxidative Coupling of Sinapic Acid, University of Manitoba, Winnipeg, Manitoba, Canada, 1997.

(288) Mention, M. M.; Flourat, A. L.; Peyrot, C.; Allais, F. Biomimetic Regioselective and High-Yielding Cu(i)-Catalyzed Dimerization of Sinapate Esters in Green Solvent Cyrene™: Towards Sustainable Antioxidant and Anti-UV Ingredients. *Green Chem.* **2020**, *22* (6), 2077–2085. https://doi.org/10.1039/d0gc00122h.

(289) Rubino, M. I.; Arntfield, S. D.; Charlton, J. L. Conversion of Phenolics to Lignans: Sinapic Acid to Thomasidioic Acid. *J. Am. Oil Chem. Soc.* **1995**, *72* (12), 1465–1470. https://doi.org/10.1007/BF02577839.

(290) Rubino, M. I.; Arntfield, S. D.; Charlton, J. L. Evaluation of Alkaline Conversion of Sinapic Acid to Thomasidioic Acid. *J. Agric. Food Chem.* **1996**, *44* (6), 1399–1402. https://doi.org/10.1021/jf950431e.

(291) Cai, R. C.; Arntfield, S. D.; Charlton, J. L. Structural Changes of Sinapic Acid during Alkali-Induced Air Oxidation and the Development of Colored Substances. *JAOCS, J. Am. Oil Chem. Soc.* **1999**, *76* (6), 757–764. https://doi.org/10.1007/s11746-999-0172-6.

(292) Bunzel, M.; Ralph, J.; Kim, H.; Lu, F.; Ralph, S. A.; Marita, J. M.; Hatfield, R. D.; Steinhart, H. Sinapate Dehydrodimers and Sinapat-Ferulate Heterodimers in Cereal Dietary Fiber. *J. Agric. Food Chem.* **2003**, *51* (5), 1427–1434. https://doi.org/10.1021/jf020910v.

(293) Fuganti, C.; Serra, S. Studies on the Synthesis of Highly Substituted Naphthol: Preparation of 6-Hydroxy-5,7-Dimethoxy-2-Naphthoic Acid, Isolated from Ulmus Thomasii. *J. Chem. Res. - Part S* **1998**, No. 10, 638–639. https://doi.org/10.1039/a803651i.

(294) Tranchimand, S.; Tron, T.; Gaudin, C.; Iacazio, G. Synthesis of Bis-Lactone Lignans through Laccase Catalysis. *J. Mol. Catal. B Enzym.* **2006**, *42* (1–2), 27–31. https://doi.org/10.1016/j.molcatb.2006.06.003.

(295) Hanson, S. R.; Best, M. D.; Wong, C.-H. Sulfatases: Structure, Mechanism, Biological Activity, Inhibition, and Synthetic Utility. *Angew. Chemie Int. Ed.* **2004**, *43* (43), 5736–5763. https://doi.org/10.1002/anie.200300632.

(296) Appel, M. J.; Bertozzi, C. R. Formylglycine, a Post-Translationally Generated Residue with Unique Catalytic Capabilities and Biotechnology Applications. *ACS Chem. Biol.* **2015**, *10* (1), 72–84. https://doi.org/10.1021/cb500897w.

(297) Knop, M.; Engi, P.; Lemnaru, R.; Seebeck, F. P. In Vitro Reconstitution of Formylglycine-Generating Enzymes Requires Copper(I). *ChemBioChem* **2015**, *16* (15), 2147–2150. https://doi.org/10.1002/cbic.201500322.

(298) Laemmli, U. K. Cleavage of Structural Proteins during the Assembly of the Head of Bacteriophage T4. *Nature* **1970**, *227* (5259), 680–685.

(299) Jonas, S.; van Loo, B.; Hyvönen, M.; Hollfelder, F. A New Member of the Alkaline Phosphatase Superfamily with a Formylglycine Nucleophile: Structural and Kinetic Characterisation of a Phosphonate Monoester Hydrolase/Phosphodiesterase from Rhizobium Leguminosarum. *J. Mol. Biol.* **2008**, *384* (1), 120–136. https://doi.org/10.1016/j.jmb.2008.08.072.

(300) Amyot, L.; McDowell, T.; Martin, S. L.; Renaud, J.; Gruber, M. Y.; Hannoufa, A. Assessment of Antinutritional Compounds and Chemotaxonomic Relationships between Camelina Sativa and Its Wild Relatives. *J. Agric. Food Chem.* **2019**, *67* (3), 796–806. https://doi.org/10.1021/acs.jafc.8b04724.

(301) Moshgani, M.; Kolvoort, E.; de Jong, T. J. Pronounced Effects of Slug Herbivory on Seedling Recruitment of Brassica Cultivars and Accessions, Especially Those with Low Levels of Aliphatic Glucosinolates. *Basic Appl. Ecol.* **2014**, *15* (7), 607–615. https://doi.org/10.1016/j.baae.2014.08.011.

(302) Baaij, B. M.; Kim, H. K.; Grosser, K.; Worrich, A.; de Jong, T. J. Slug Herbivory on Hybrids of the Crop Brassica Napus and Its Wild Relative B. Rapa. *Basic Appl. Ecol.* **2018**, *31*, 52–60. https://doi.org/10.1016/j.baae.2018.06.001.

(303) Gupta, S.; Sangha, M.; Kaur, G.; Atwal, A.; Banga, S.; Banga, S. Variability for Leaf and Seed Glucosinolate Contents and Profiles in a Germplasm Collection of the Brassica Juncea. *Biochem. Anal. Biochem.* **2012**, *01* (07), 1–5. https://doi.org/10.4172/2161-1009.1000120.

(304) Zhao, Y.; Yue, Z.; Zhong, X.; Lei, J.; Tao, P.; Li, B. Distribution of Primary and Secondary Metabolites among the Leaf Layers of Headed Cabbage (Brassica Oleracea Var. Capitata). *Food Chem.* **2020**, *312* (December 2019), 126028. https://doi.org/10.1016/j.foodchem.2019.126028.

(305) Wei, L.; Liu, C.; Zheng, H.; Zheng, L. Melatonin Treatment Affects the Glucoraphanin-Sulforaphane System in Postharvest Fresh-Cut Broccoli (Brassica Oleracea L.). *Food Chem.* **2020**, *307* (August 2019), 125562. https://doi.org/10.1016/j.foodchem.2019.125562.

(306) Döring, A.; Ulber, B. Performance of Cabbage Stem Flea Beetle Larvae (Psylliodes Chrysocephala) in Brassicaceous Plants and the Effect of Glucosinolate Profiles. *Entomol. Exp. Appl.* **2020**, *168* (3), 200–208. https://doi.org/10.1111/eea.12891.

(307) Badenes-Perez, F. R.; Reichelt, M.; Gershenzon, J.; Heckel, D. G. Interaction of Glucosinolate Content of Arabidopsis Thaliana Mutant Lines and Feeding and Oviposition by Generalist and Specialist Lepidopterans. *Phytochemistry* **2013**, *86*, 36–43. https://doi.org/10.1016/j.phytochem.2012.11.006.

(308) Yi, G.; Lim, S.; Chae, W. B.; Park, J. E.; Park, H. R.; Lee, E. J.; Huh, J. H. Root Glucosinolate Profiles for Screening of Radish (Raphanus Sativus L.) Genetic Resources. *J. Agric. Food Chem.* **2016**, *64* (1), 61–70. https://doi.org/10.1021/acs.jafc.5b04575.

(309) Tetteh, O. N. A.; Ulrichs, C.; Huyskens-Keil, S.; Mewis, I.; Amaglo, N. K.; Oduro, I. N.; Adarkwah, C.; Obeng-Ofori, D.; Förster, N. Effects of Harvest Techniques and Drying Methods on the Stability of Glucosinolates in Moringa Oleifera Leaves during Post-Harvest. *Sci. Hortic. (Amsterdam).* **2019**, *246* (October 2018), 998–1004. https://doi.org/10.1016/j.scienta.2018.11.089.

(310) Mekonnen, Y.; Dräger, B. Glucosinolates in Moringa Stenopetala. *Planta Med.* **2003**, *69* (4), 380–382. https://doi.org/10.1055/s-2003-38881.

(311) Bennett, R. N.; Mellon, F. A.; Foidl, N.; Pratt, J. H.; Dupont, M. S.; Perkins, L.; Kroon, P. A. Profiling Glucosinolates and Phenolics in Vegetative and Reproductive Tissues of the Multi-Purpose Trees Moringa Oleifera L. (Horseradish Tree) and Moringa Stenopetala L. *J. Agric. Food Chem.* **2003**, *51* (12), 3546–3553. https://doi.org/10.1021/jf0211480.

(312) Bojesen, G.; Larsen, E. Characterization of Five Glucosinolates by Fast Atom Bombardment Mass Spectrometry and Collision Activation of [M-H]-1. *Biol. Mass Spectrom.* **1991**, *20* (5), 286–288. https://doi.org/10.1002/bms.1200200508.

(313) Mahamat Nour Adam Sakine. In Vitro Anti-Hyperglycaemic Effect of Glucocapparin Isolated from the Seeds of Boscia Senegalensis (Pers.) Lam. Ex Poiret Parasuis. *African J. Biotechnol.* **2012**, *11* (23), 6345–6349. https://doi.org/10.5897/ajb11.3445.

(314) Kjær, A.; Christensen, B. W.; Larsen, P. O. IsoThiocyanates. XXXIX. Glucobenzosisymbrin, a New Glucoside Present in Seeds of Sisymbrium Austriacum Jacq.. *Acta Chem. Scand.* **1961**, *15*, 1477–1484. https://doi.org/10.3891/acta.chem.scand.15-1477.

(315) Radulović, N.; Dekić, M.; Stojanović-Radić, Z. A New Antimicrobial Glucosinolate Autolysis Product, 4- Isothiocyanatobutanoic Acid, from the Diffuse Wallflower (Erysimum Diffusum): Methyl 4-Isothiocyanatobutanoate, a Long Unrecognized Artifact of the Isolation Procedure? *Food Chem.* **2011**, *129* (1), 125–130. https://doi.org/10.1016/j.foodchem.2011.04.043.

(316) Chisholm, M. D. Biosynthesis of 3-Methoxycarbonylpropylglucosinolate in an Erysimum Species. *Phytochemistry* **1973**, *12* (3), 605–608. https://doi.org/10.1016/S0031-9422(00)84451-9.

(317) Kjær, A.; Larsen, I.; Tjus, E.; Burris, R. H. IsoThiocyanates. IX. The Occurrence of Ethyl IsoThiocyanate in Nature. *Acta Chemica Scandinavica*. 1954, pp 699–701. https://doi.org/10.3891/acta.chem.scand.08-0699.

(318) Kjær, A.; Schuster, A. Glucosinolates in Capparis Flexuosa of Jamaican Origin. *Phytochemistry* **1971**, *10* (12), 3155–3160. https://doi.org/10.1016/S0031-9422(00)97368-0.

(319) Kojima, M.; Uchida, Mi.; Akahori, Y. Studies on the Volatile Components of Wasabia Japonica, Brassica Juncea and Cochlearia Armoracia by Gas Chromatography-Mass Spectrometry. I. Determination of Low Mass Volatile Components. *YAKUGAKU ZASSHI* **1973**, *93* (4), 453–459. https://doi.org/10.1248/yakushi1947.93.4_453.

(320) Grob, K.; Matile, P. Capillary GC of Glucosinolate-Derived Horseradish Constituents. *Phytochemistry* **1980**, *19* (8), 1789–1793. https://doi.org/10.1016/S0031-9422(00)83814-5.

(321) Kjær, A.; Thomsen, H.; Hansen, S. E.; Levitin, N. E.; Westin, G. IsoThiocyanates XXXVIII. Glucocapangulin, a Novel IsoThiocyanate-Producing Glucoside. *Acta Chem. Scand.* **1960**, *14*, 1226–1227. https://doi.org/10.3891/acta.chem.scand.14-1226.

(322) Kjær, A.; Thomsen, H.; Edman, P.; Kvande, P. C.; Meisingseth, E. Gluconorcappasalin, a Thioglucoside Producing 5-Oxoheptyl Isothiocyanate on Enzymic Hydrolysis. *Acta Chem. Scand.* **1963**, *17*, 561–562. https://doi.org/10.3891/acta.chem.scand.17-0561.

(323) Kjær, A.; Thomsen, H.; Lipschitz, L.; Nielsen, J. T. Isothiocyanates. XLVI. Glucocappasalin, a New Naturally Occurring Thioglucoside. *Acta Chem. Scand.* **1962**, *16*, 2065–2066. https://doi.org/10.3891/acta.chem.scand.16-2065.

(324) Gaind, K. N.; Gandhi, K. S.; Junega, T. R.; Kjær, A.; Juhl Nielsen, B. 4,5,6,7-Tetrahydroxydecyl Isothiocyanate Derived from a Glucosinolate in Capparis Grandis. *Phytochemistry* **1975**, *14* (5–6), 1415–1418. https://doi.org/10.1016/S0031-9422(00)98640-0.

(325) El-Migirab, S.; Berger, Y.; Jadot, J. Isothiocyanates, Thiourees et Thiocarbamates Isoles de Pentadiplandra Brazzeana. *Phytochemistry* **1977**, *16* (11), 1719–1721. https://doi.org/10.1016/0031-9422(71)85078-1.

(326) Sirinut, P.; Petchkongkeaw, A.; Romsaiyud, J.; Prateeptongkum, S.; Thongyoo, P. Phytochemical Constituents from the Root of Luvunga Scandens and Biological Activity Evaluation. *Nat. Prod. Commun.* **2017**, *12* (9), 1483–1484. https://doi.org/10.1177/1934578x1701200926.

(327) Bennett, R. N.; Mellon, F. A.; Kroon, P. A. Screening Crucifer Seeds as Sources of Specific Intact Glucosinolates Using Ion-Pair High-Performance Liquid Chromatography Negative Ion Electrospray Mass Spectrometry. *J. Agric. Food Chem.* **2004**, *52* (3), 428–438. https://doi.org/10.1021/jf030530p.

(328) Kjær, A.; Wagnières, W. 3-Methyl-3-Butenylglucosinolate, a New Isothiocyanate-Producing Thioglucoside. *Acta Chem. Scand.* **1965**, *19*, 1989–1991. https://doi.org/10.3891/acta.chem.scand.19-1989.

(329) Blažević, I.; Mastelić, J. Glucosinolate Degradation Products and Other Bound and Free Volatiles in the Leaves and Roots of Radish (Raphanus Sativus L.). *Food Chem.* **2009**, *113* (1), 96–102. https://doi.org/10.1016/j.foodchem.2008.07.029.

(330) Dauvergne, X.; Cérantola, S.; Salaün, S.; Magné, C.; Kervarec, N.; Bessières, M. A.; Deslandes, E. General Occurrence of the Glucosinolate Glucocochlearin within the Cochlearia Genus. *Carbohydr. Res.* **2006**, *341* (12), 2166–2169. https://doi.org/10.1016/j.carres.2006.05.014.

(331) Kjær, A.; Christensen, B. W.; Krohn, C.; Motzfeldt, K.; Theander, O.; Flood, H. Isothiocyanates. XLI. Glucobenzsisaustricin, a New Glucoside Present in Seeds of Sisymbrium Austriacum Jacq. *Acta Chem. Scand.* **1962**, *16*, 83–86. https://doi.org/10.3891/acta.chem.scand.16-0083.

(332) Agerbirk, N.; Olsen, C. E.; Chew, F. S.; Ørgaard, M. Variable Glucosinolate Profiles of Cardamine Pratensis (Brassicaceae) with Equal Chromosome Numbers. *J. Agric. Food Chem.* **2010**, *58* (8), 4693–4700. https://doi.org/10.1021/jf904362m.

(333) Pedras, M. S. C.; Zheng, Q. A.; Gadagi, R. S. The First Naturally Occurring Aromatic Isothiocyanates, Rapalexins A and B, Are Cruciferous Phytoalexins. *Chem. Commun.* **2007**, No. 4, 368–370. https://doi.org/10.1039/b615424g.

(334) Pfalz, M.; Mukhaimar, M.; Perreau, F.; Kirk, J.; Hansen, C. I. C.; Olsen, C. E.; Agerbirk, N.; Kroymann, J. Methyl Transfer in Glucosinolate Biosynthesis Mediated by Indole Glucosinolate O-Methyltransferase 5. *Plant Physiol.* **2016**, *172* (4), 2190–2203. https://doi.org/10.1104/pp.16.01402.

(335) Millán, S.; Sampedro, M. C.; Gallejones, P.; Castellón, A.; Ibargoitia, M. L.; Goicolea, M. A.; Barrio, R. J. Identification and Quantification of Glucosinolates in Rapeseed Using Liquid Chromatography-Ion Trap Mass Spectrometry. *Anal. Bioanal. Chem.* **2009**, *394* (6), 1661–1669. https://doi.org/10.1007/s00216-009-2823-8.

(336) Agerbirk, N.; Petersen, B. L.; Olsen, C. E.; Halkier, B. A.; Nielsen, J. K. 1,4-Dimethoxyglucobrassicin in Barbarea and 4-Hydroxyglucobrassicin in Arabidopsis and Brassica. *J. Agric. Food Chem.* **2001**, *49* (3), 1502–1507. https://doi.org/10.1021/jf001256r.

(337) Schraudolf, H.; Bäuerle, R. 1N-Acetyl-3-Indolylmethylglucosinolate in Seedlings of Tovaria Pendula Ruiz et Pav. *Zeitschrift fur Naturforsch. - Sect. C J. Biosci.* **1986**, *41* (5–6), 526–528. https://doi.org/10.1515/znc-1986-5-605.

(338) Elliott, M. C.; Stowe, B. B. A Novel Sulphonated Natural Indole. *Phytochemistry* **1970**, *9* (7), 1629–1632. https://doi.org/10.1016/S0031-9422(00)85287-5.

(339) Bianco, G.; Agerbirk, N.; Losito, I.; Cataldi, T. R. I. Acylated Glucosinolates with Diverse Acyl Groups Investigated by High Resolution Mass Spectrometry and Infrared Multiphoton Dissociation. *Phytochemistry* **2014**, *100*, 92–102. https://doi.org/10.1016/j.phytochem.2014.01.010.

(340) Agerbirk, N.; Olsen, C. E. Isoferuloyl Derivatives of Five Seed Glucosinolates in the Crucifer Genus Barbarea. *Phytochemistry* **2011**, *72* (7), 610–623. https://doi.org/10.1016/j.phytochem.2011.01.034.

(341) Kusznierewicz, B.; Iori, R.; Piekarska, A.; Namieśnik, J.; Bartoszek, A. Convenient Identification of Desulfoglucosinolates on the Basis of Mass Spectra Obtained during Liquid Chromatography-Diode Array-Electrospray Ionisation Mass Spectrometry Analysis: Method Verification for Sprouts of Different Brassicaceae Species Extract. *J. Chromatogr. A* **2013**, *1278*, 108–115. https://doi.org/10.1016/j.chroma.2012.12.075.

(342) Maldini, M.; Foddai, M.; Natella, F.; Petretto, G. L.; Rourke, J. P.; Chessa, M.; Pintore, G. Identification and Quantification of Glucosinolates in Different Tissues of Raphanus Raphanistrum by Liquid Chromatography Tandem-Mass Spectrometry. *J. Food Compos. Anal.* **2017**, *61*, 20–27. https://doi.org/10.1016/j.jfca.2016.06.002.

(343) Pagnotta, E.; Agerbirk, N.; Olsen, C. E.; Ugolini, L.; Cinti, S.; Lazzeri, L. Hydroxyl and Methoxyl Derivatives of Benzylglucosinolate in Lepidium Densiflorum with Hydrolysis to Isothiocyanates and Non-Isothiocyanate Products: Substitution Governs Product Type and Mass Spectral Fragmentation. *J. Agric. Food Chem.* **2017**, *65* (15), 3167–3178. https://doi.org/10.1021/acs.jafc.7b00529.

(344) De Nicola, G. R.; Nyegue, M.; Montaut, S.; Iori, R.; Menut, C.; Tatibouët, A.; Rollin, P.; Ndoyé, C.; Zollo, P. H. A. Profile and Quantification of Glucosinolates in Pentadiplandra Brazzeana Baillon. *Phytochemistry* **2012**, *73*, 51–56. https://doi.org/10.1016/j.phytochem.2011.09.006.

(345) Agerbirk, N.; Warwick, S. I.; Hansen, P. R.; Olsen, C. E. Sinapis Phylogeny and Evolution of Glucosinolates and Specific Nitrile Degrading Enzymes. *Phytochemistry* **2008**, *69* (17), 2937–2949. https://doi.org/10.1016/j.phytochem.2008.08.014.

(346) Montaut, S.; Zhang, W. D.; Nuzillard, J. M.; De Nicola, G. R.; Rollin, P. Glucosinolate Diversity in Bretschneidera Sinensis of Chinese Origin. *J. Nat. Prod.* **2015**, *78* (8), 2001–2006. https://doi.org/10.1021/acs.jnatprod.5b00338.

(347) Agerbirk, N.; Olsen, C. E. Glucosinolate Hydrolysis Products in the Crucifer Barbarea Vulgaris Include a Thiazolidine-2-One from a Specific Phenolic Isomer as Well as Oxazolidine-2-Thiones. *Phytochemistry* **2015**, *115* (1), 143–151. https://doi.org/10.1016/j.phytochem.2014.11.002.

(348) Agerbirk, N.; Matthes, A.; Erthmann, P.; Ugolini, L.; Cinti, S.; Lazaridi, E.; Nuzillard, J. M.; Müller, C.; Bak, S.; Rollin, P.; Lazzeri, L. Glucosinolate Turnover in Brassicales Species to an Oxazolidin-2-One, Formed via the 2-Thione and without Formation of Thioamide. *Phytochemistry* **2018**, *153*, 79–93. https://doi.org/10.1016/j.phytochem.2018.05.006.

(349) Dekić, M. S.; Radulović, N. S.; Stojanović, N. M.; Randjelović, P. J.; Stojanović-Radić, Z. Z.; Najman, S.; Stojanović, S. Spasmolytic, Antimicrobial and Cytotoxic Activities of 5-Phenylpentyl Isothiocyanate, a New Glucosinolate Autolysis Product from Horseradish (Armoracia Rusticana P. Gaertn., B. Mey. & Scherb., Brassicaceae). *Food Chem.* **2017**, *232*, 329–339. https://doi.org/10.1016/j.foodchem.2017.03.150.

(350) Agerbirk, N.; Olsen, C. E.; Nielsen, J. K. Seasonal Variation in Leaf Glucosinolates and Insect Resistance in Two Types of Barbarea Vulgaris Ssp. Arcuata. *Phytochemistry* **2001**, *58* (1), 91–100. https://doi.org/10.1016/S0031-9422(01)00151-0.

(351) Agerbirk, N.; Olsen, C. E.; Poulsen, E.; Jacobsen, N.; Hansen, P. R. Complex Metabolism of Aromatic Glucosinolates in Pieris Rapae Caterpillars Involving Nitrile Formation, Hydroxylation, Demethylation, Sulfation, and Host Plant Dependent Carboxylic Acid Formation. *Insect Biochem. Mol. Biol.* **2010**, *40* (2), 126–137. https://doi.org/10.1016/j.ibmb.2010.01.003.

(352) Waterman, C.; Cheng, D. M.; Rojas-Silva, P.; Poulev, A.; Dreifus, J.; Lila, M. A.; Raskin, I. Stable, Water Extractable Isothiocyanates from Moringa Oleifera Leaves Attenuate Inflammation in Vitro. *Phytochemistry* **2014**, *103*, 114–122. https://doi.org/10.1016/j.phytochem.2014.03.028.

(353) Olsen, O.; Rasmussen, K. W.; Sørensen, H. Glucosinolates in Sesamoides Canescens and S. Pygmaea: Identification of 2-(α-l-Arabinopyranosyloxy)-2-Phenylethylglucosinolate. *Phytochemistry* **1981**, *20* (8), 1857–1861. https://doi.org/10.1016/0031-9422(81)84021-6.

(354) Gueyrard, D.; Barillari, J.; Iori, R.; Palmieri, S.; Rollin, P. First Synthesis of an O-Glycosylated Glucosinolate Isolated from Moringa Oleifera. *Tetrahedron Lett.* **2000**, *41* (43), 8307–8309. https://doi.org/10.1016/S0040-4039(00)01466-0.

(355) Maldini, M.; Maksoud, S. A.; Natella, F.; Montoro, P.; Petretto, G. L.; Foddai, M.; De Nicola, G. R.; Chessa, M.; Pintore, G. Moringa Oleifera: Study of Phenolics and Glucosinolates by Mass Spectrometry. *J. Mass Spectrom.* **2014**, *49* (9), 900–910. https://doi.org/10.1002/jms.3437.

(356) de Graaf, R. M.; Krosse, S.; Swolfs, A. E. M.; te Brinke, E.; Prill, N.; Leimu, R.; van Galen, P. M.; Wang, Y.; Aarts, M. G. M.; van Dam, N. M. Isolation and Identification of 4-α-Rhamnosyloxy Benzyl Glucosinolate in Noccaea Caerulescens Showing Intraspecific Variation. *Phytochemistry* **2015**, *110*, 166–171. https://doi.org/10.1016/j.phytochem.2014.11.016.

(357) Montaut, S.; Grandbois, J.; Righetti, L.; Barillari, J.; Iori, R.; Rollin, P. Updated Glucosinolate Profile of Dithyrea Wislizenii. *J. Nat. Prod.* **2009**, *72* (5), 889–893. https://doi.org/10.1021/np800738w.

(358) Montaut, S.; Montagut-Romans, A.; Chiari, L.; Benson, H. J. Glucosinolates in Draba Borealis DC. (Brassicaceae) in a Taxonomic Perspective. *Biochem. Syst. Ecol.* **2018**, *78*, 31–34. https://doi.org/10.1016/j.bse.2018.03.003.

(359) Denicola, G. R.; Blažević, I.; Montaut, S.; Rollin, P.; Mastelić, J.; Iori, R.; Tatibouët, A. Glucosinolate Distribution in Aerial Parts of Degenia Velebitica. *Chem. Biodivers.* **2011**, *8* (11), 2090–2096. https://doi.org/10.1002/cbdv.201100114.

(360) Daxenbichler, M. E.; Spencer, G. F.; Carlson, D. G.; Rose, G. B.; Brinker, A. M.; Powell, R. G. Glucosinolate Composition of Seeds from 297 Species of Wild Plants. *Phytochemistry* **1991**, *30* (8), 2623–2638. https://doi.org/10.1016/0031-9422(91)85112-D.

(361) Reichelt, M.; Brown, P. D.; Schneider, B.; Oldham, N. J.; Stauber, E.; Tokuhisa, J.; Kliebenstein, D. J.; Mitchell-Olds, T.; Gershenzon, J. Benzoic Acid Glucosinolate Esters and Other Glucosinolates from Arabidopsis Thaliana. *Phytochemistry* **2002**, *59* (6), 663–671. https://doi.org/10.1016/S0031-9422(02)00014-6.

(362) Zimmermann, N. S.; Gerendás, J.; Krumbein, A. Identification of Desulphoglucosinolates in Brassicaceae by LC/MS/MS: Comparison of ESI and Atmospheric Pressure Chemical Ionisation-MS. *Mol. Nutr. Food Res.* **2007**, *51* (12), 1537–1546. https://doi.org/10.1002/mnfr.200700103.

(363) Agerbirk, N.; Olsen, C. E.; Cipollini, D.; Ørgaard, M.; Linde-Laursen, I.; Chew, F. S. Specific Glucosinolate Analysis Reveals Variable Levels of Epimeric Glucobarbarins, Dietary Precursors of 5-Phenyloxazolidine-2-Thiones, in Watercress Types with Contrasting Chromosome Numbers. *J. Agric. Food Chem.* **2014**, *62* (39), 9586–9596. https://doi.org/10.1021/jf5032795.

(364) Yamane, A.; Fujikura, J.; Ogawa, H.; Mizutani, J. Isothiocyanates as Alleopathic Compounds from Rorippa Indica Hiern. (Cruciferae) Roots. *J. Chem. Ecol.* **1992**, *18* (11), 1941–1954. https://doi.org/10.1007/BF00981918.

(365) Berhow, M. A.; Polat, U.; Glinski, J. A.; Glensk, M.; Vaughn, S. F.; Isbell, T.; Ayala-Diaz, I.; Marek, L.; Gardner, C. Optimized Analysis and Quantification of Glucosinolates from Camelina Sativa Seeds by Reverse-Phase Liquid Chromatography. *Ind. Crops Prod.* **2013**, *43* (1), 119–125. https://doi.org/10.1016/j.indcrop.2012.07.018.

(366) Huang, X.; Renwick, J. A. A.; Sachdev-Gupta, K. A Chemical Basis for Differential Acceptance of Erysimum Cheiranthoides by Two Pieris Species. *J. Chem. Ecol.* **1993**, *19* (2), 195–210. https://doi.org/10.1007/BF00993689.

(367) Fabre, N.; Bon, M.; Moulis, C.; Fouraste, I.; Stanislas, E. Three Glucosinolates from Seeds of Brassica Juncea. *Phytochemistry* **1997**, *45* (3), 525–527. https://doi.org/10.1016/S0031-9422(96)00765-0.

(368) Iori, R.; Barillari, J.; Gallienne, E.; Bilardo, C.; Tatibouët, A.; Rollin, P. Thio-Functionalised Glucosinolates: Unexpected Transformation of Desulfoglucoraphenin. *Tetrahedron Lett.* **2008**, *49* (2), 292–295. https://doi.org/10.1016/j.tetlet.2007.11.059.

(369) Kjær, A.; Schuster, A.; Miksche, G. E.; Liaaen-Jensen, S.; Lamvik, A.; Sunde, E.; Sørensen, N. A. Glucosinolates in Erysimum Hieracifolium L.; Three New, Naturally Occurring Glucosinolates. *Acta Chem. Scand.* **1970**, *24*, 1631–1638. https://doi.org/10.3891/acta.chem.scand.24-1631.

(370) Kjaer, A.; Schuster, A. ω-Methylthioalkylglucosinolates and Some Oxidized Congeners in Seeds of Erysimum Rhaeticum. *Phytochemistry* **1973**, *12* (4), 929–933. https://doi.org/10.1016/0031-9422(73)80705-8.

(371) Kjær, A.; Schuster, A.; Vestersjø, E.; Andresen, A. F.; Pearson, W. B.; Meisalo, V. Glucosinolates in Seeds of Arabis Hirsuta (L.) Scop.: Some New, Naturally Derived Isothiocyanates. *Acta Chem. Scand.* **1972**, *26*, 8–14. https://doi.org/10.3891/acta.chem.scand.26-0008.

(372) Bennett, R. N.; Mellon, F. A.; Botting, N. P.; Eagles, J.; Rosa, E. A. S.; Williamson, G. Identification of the Major Glucosinolate (4-Mercaptobutyl Glucosinolate) in Leaves of Eruca Sativa L. (Salad Rocket). *Phytochemistry* **2002**, *61* (1), 25–30. https://doi.org/10.1016/S0031-9422(02)00203-0.

(373) Cataldi, T. R. I.; Rubino, A.; Lelario, F.; Bufo, S. A. Naturally Occurring Glucosinolates in Plant Extracts of Rocket Salad (Eruca Sativa L.) Identified by Liquid Chromatography Coupled with Negative Ion Electrospray Ionization and Quadrupole Ion-Trap Mass Spectrometry. *Rapid Commun. Mass Spectrom.* **2007**, *21* (14), 2374–2388. https://doi.org/10.1002/rcm.3101.

(374) Kim, J. H.; Jander, G. Myzus Persicae (Green Peach Aphid) Feeding on Arabidopsis Induces the Formation of a Deterrent Indole Glucosinolate. *Plant J.* **2007**, *49* (6), 1008–1019. https://doi.org/10.1111/j.1365-313X.2006.03019.x.

(375) KIM, S.-J.; JIN, S.; ISHII, G. Isolation and Structural Elucidation of 4-(β-<scp>D</Scp> -Glucopyranosyldisulfanyl)Butyl Glucosinolate from Leaves of Rocket Salad (*Eruca Sativa* L.) and Its Antioxidative Activity. *Biosci. Biotechnol. Biochem.* **2004**, *68* (12), 2444–2450. https://doi.org/10.1271/bbb.68.2444.

(376) Lelario, F.; Bianco, G.; Bufo, S. A.; Cataldi, T. R. I. Establishing the Occurrence of Major and Minor Glucosinolates in Brassicaceae by LC-ESI-Hybrid Linear Ion-Trap and Fourier-Transform Ion Cyclotron Resonance Mass Spectrometry. *Phytochemistry* **2012**, *73*, 74–83. https://doi.org/10.1016/j.phytochem.2011.09.010.

(377) Kim, K. H.; Moon, E.; Kim, S. Y.; Choi, S. U.; Lee, J. H.; Lee, K. R. 4-Methylthio-Butanyl Derivatives from the Seeds of Raphanus Sativus and Their Biological Evaluation on Anti-Inflammatory and Antitumor Activities. *J. Ethnopharmacol.* **2014**, *151* (1), 503–508. https://doi.org/10.1016/j.jep.2013.11.003.

(378) Matich, A. J.; McKenzie, M. J.; Lill, R. E.; Brummell, D. A.; McGhie, T. K.; Chen, R. K. Y.; Rowan, D. D. Selenoglucosinolates and Their Metabolites Produced in Brassica Spp. Fertilised with Sodium Selenate. *Phytochemistry* **2012**, *75*, 140–152. https://doi.org/10.1016/j.phytochem.2011.11.021.

(379) Fréchard, A.; Fabre, N.; Péan, C.; Montaut, S.; Fauvel, M.-T.; Rollin, P.; Fourasté, I. Novel Indole-Type Glucosinolates from Woad (Isatis Tinctoria L.). *Tetrahedron Lett.* **2001**, *42* (51), 9015–9017. https://doi.org/10.1016/S0040-4039(01)02015-9.

(380) Mohn, T.; Hamburger, M. Glucosinolate Pattern in Isatis Tinctoria and I. Indigotica Seeds. *Planta Med.* **2008**, *74* (8), 885–888. https://doi.org/10.1055/s-2008-1074554.

(381) Hu, Z.; Lewis, J. A.; Hanley, A. B.; Fenwick, G. R. 2-Hydroxyethyl Glucosinolate from Capparis Masaikai of Chinese Origin. *Phytochemistry* **1989**, *28* (4), 1252–1254. https://doi.org/10.1016/0031-9422(89)80221-3.

(382) Daxenbichler, M. E.; Spencer, G. F.; Schroeder, W. P. 3-Hydroxypropylglucosinolate, a New Glucosinolate in Seeds of Erysimum Hieracifolium and Malcolmia Maritima. *Phytochemistry* **1980**, *19* (5), 813–815. https://doi.org/10.1016/0031-9422(80)85117-X.

(383) Bringmann, G.; Kajahn, I.; Nuesuüß, C.; Pelzing, M.; Laug, S.; Unger, M.; Holzgrabe, U. Analysis of the Glucosinolate Pattern of Arabidopsis Thaliana Seeds by Capillary Zone Electrophoresis Coupled to Electrospray Ionization-Mass Spectrometry. *Electrophoresis* **2005**, *26* (7–8), 1513–1522. https://doi.org/10.1002/elps.200410255.

(384) Hogge, L. R.; Reed, D. W.; Underhill, E. W.; Haughn, G. W. Hplc Separation of Glucosinolates from Leaves and Seeds of Arabidopsls Thaliana and Their Identification Using Thermospray Liquid Chromatography/Mass Spectrometry. *J. Chromatogr. Sci.* **1988**, *26* (11), 551–556. https://doi.org/10.1093/chromsci/26.11.551.

(385) Kliebenstein, D. J.; D'Auria, J. C.; Behere, A. S.; Kim, J. H.; Gunderson, K. L.; Breen, J. N.; Lee, G.; Gershenzon, J.; Last, R. L.; Jander, G. Characterization of Seed-Specific Benzoyloxyglucosinolate Mutations in Arabidopsis Thaliana. *Plant J.* **2007**, *51* (6), 1062–1076. https://doi.org/10.1111/j.1365-313X.2007.03205.x.

(386) Nguyen, V. P. T.; Stewart, J. D.; Ioannou, I.; Allais, F. Sinapic Acid and Sinapate Esters in Brassica: Innate Accumulation, Biosynthesis, Accessibility via Chemical Synthesis or Recovery From Biomass, and Biological Activities. *Front. Chem.* **2021**, *9* (May), 664602. https://doi.org/10.3389/fchem.2021.664602.

BIOGRAPHICAL SKETCH

Vinh Phuc Thinh (Thinh) Nguyen was born in 1991, in Ho Chi Minh city, Vietnam. After graduated from high school (Nguyen Thi Minh Khai in Ho Chi Minh City) in 2009, he left his hometown to study biology at the University of Reims Champagne-Ardenne in France. After the first year, he decided to switch his major to chemistry-physics and obtained his bachelor's degree in chemistry in 2014. During the last year of his bachelor studies, he began undergraduate level research in the lab of Dr. Gilles Lemercier in coordination chemistry (ICMR, University of Reims Champagne-Ardenne). This experience encouraged him to pursue his master's degree in molecular chemistry at the same school. He has conducted two master's level research projects in organometallic chemistry under the supervision of Dr. Florian Jaroschik (ICMR, University of Reims Champagne-Ardenne, France) and Dr. Jan Cermak (ICPF, Prague, Czech Republic) in 2015 and 2016, respectively.

Thinh was selected for the joint doctoral program between AgroParisTech, France and University of Florida, USA, under supervision of Dr. Florent Allais (URD ABI, France) and Dr. Jon Stewart (Department of Chemistry, UF) starting in fall 2016. Having been given the opportunity, he began the doctoral research on the valorization of Carinata meal, a non-food biomass issued from aviation biofuel production, as a renewable resource of biobased chemicals funded by the Southeast Partnership for Advanced Renewable Carinata (NIFA-USDA).

In 2020, he published his first research article titled, "Glucosinolates: Natural Occurrence, Biosynthesis, Accessibility, Isolation, Structures, and Biological Activities" in Molecules. He was also selected to co-chair of the inaugural Gordon Research Seminar 2021 Biomass to Biobased Chemicals and Materials, which was expected to

be conducted in 2021. Due to the global Covid-19 crisis, the occurrence of the seminar, however, was postponed in 2023. Thinh received his Doctor of Philosophy in chemistry from the University of Florida in august 2021 and moved to Saint-Louis, Haut-Rhin, France, for his professional career.